약학박사 학위논문

Research on the functional role of epidermal keratinocytes in inflammatory responses to skin toxicants

피부독성물질에 대한 표피각질형성세포의 염증 반응 연구

2020 년 8 월

서울대학교 대학원

약학과 천연물과학전공

이 은 영

Research on the functional role of epidermal keratinocytes in inflammatory responses to skin toxicants

피부독성물질에 대한 표피각질형성세포의
염증 반응 연구

지도 교수 노 민 수

이 논문을 약학박사 학위논문으로 제출함
2020 년 8 월

서울대학교 대학원
약학과 천연물과학전공
이 은 영

이은영의 약학박사 학위논문을 인준함
2020 년 7 월

위 원 장 이 상 국 (인)

부위원장 박 성 혁 (인)

위 원 강 건 욱 (인)

위 원 임 경 민 (인)

위 원 노 민 수 (인)

ABSTRACT

The skin has been extensively investigated as a physical and immunological barrier tis-sue to diverse harmful external effects, including ultraviolet (UV) radiation, microorganisms, and xenobiotic chemicals such as drugs, pesticides, cosmetics, industrial chemicals, and environmental pollutants. Using normal human keratinocytes (NHKs), we investigated the role of epidermal keratinocytes (KCs) in sensing responses to common xenobiotic chemicals in contact with the skin, including formaldehyde, sensitizers, and sunscreen agents, to elucidate molecular pathways of skin responses, as well as identify novel biomarkers in KCs to regulate and ameliorate skin inflammation. It is crucial to understand toxicological mechanisms underlying sub-cytotoxic formaldehyde, widely present in various types of products at low levels, to investigate the role of NHKs in xenobiotic sensing responses under normal living conditions. In the cellular transsulfuration pathway, sub-cytotoxic formaldehyde upregulated two enzymes, cystathionine γ-lyase (CTH) and cystathionine-β-synthase (CBS). We proposed that CTH and CBS may play a role in the resolution of inflammation by suppressing the early pro-inflammatory responses mediated by sub-cytotoxic formaldehyde in NHKs. Allergic contact dermatitis (ACD) and irritant contact dermatitis (ICD) are common inflammatory skin disorders. Although ACD and ICD are differentiated based on pathophysiological backgrounds, both can present similar clinical aspects and histopathologies. In this study, to elucidate the roles of NHKs in toxicological molecular mechanisms responsible for the pathogenesis of ACD and ICD, we demonstrated that interleukin-8 (IL-8, CXCL8) and C-X-C motif chemokine ligand 14 (CXCL14) were commonly altered by both sodium lauryl sulfate (SLS) and urushiol. IL-8 was upregulated in response to both SLS and urushiol but CXCL14 was

down-regulated in NHKs. In a validation study performed using NHKs with OECD TG429 reference chemicals for skin sensitization, 87.5% of the reference sensitizing chemicals significantly induced either CXCL8 upregulation or CXCL14 downregulation, and 62.5% of reference sensitizers downregulated CXCL14 expression. In NHKs, the downregulation of constitutively expressed CXCL14 was regulated by both the mitogen-activated protein kinase (MAPK)/ERK and Janus kinase 3 (JAK3)/signal transducer and activator of transcription 6 (STAT6) pathways. Additionally, CXCL14 in NHKs may play important roles in the skin allergic response and could be used as a mechanism-based biomarker to improve the distinction between allergenic sensitizers and non-sensitizers during in vitro skin sensitization test. Furthermore, we investigated whether phosphodiesterase 4B (PDE4B), playing a well-established role in inflammatory responses in immune cells, has a role in the mechanism of BP-3-induced phototoxicity in NHKs. UVB-irradiated BP-3 significantly upregulated PDE4B and pro-inflammatory mediators and downregulated the level of cornified envelope associated proteins.

In conclusion, we proposed novel mechanism-based biomarkers in the xenobiotic sensing response; (1) role of ER-UPR-associated genes and CTB/CTH in inflammation resolution, (2) CXCL14 in the STAT6-dependent pathway as a novel biomarker for the in vitro sensitization test, and (3) PDE4B-related phototoxic mechanism for investigating the structure-toxicity relationship.

Keywords: Human keratinocytes, Gene Ontology (GO) enrichment analysis, Cystathionine γ-lyase (CTH), Cystathionine-β-synthase (CBS), CXCL14, Inflammation resolution, Allergic contact dermatitis (ACD)

***Student number*:** 2015-31191

TABLE OF CONTENTS

LIST OF FIGURES

LIST OF TABLES

I. INTRODUCTION

1. Molecular response of epidermal keratinocytes to environmental toxicants

Investigations regarding biological mechanisms in the skin have increased across various fields, including pharmaceutical, dermatological, cosmetic, and medical aesthetic device companies. The epidermal tissue forms a physical and immunological barrier structure, which preserves water, protects against various environmental insults such as ultraviolet (UV) radiation, microorganisms, and xenobiotic chemicals, including drugs, pesticides, cosmetics, industrial chemicals, and environmental pollutants, and helps maintain homeostasis (Fig. 1). The skin has three main layers, the epidermis, dermis, and the hypodermis, differing significantly in their anatomy and functions. The epidermis is the outer layer of the skin, mainly consisting of differentiated keratinocytes (KCs). KCs constitute 90-95% of the epidermis and are well known to have an important role in the initiation and progression, as well as persistence, of skin inflammation and immune responses (Albanesi et al., 2005). In response to stimuli, KCs express and release various cytokines and immune mediators (Steinhoff et al., 2001). In several different skin disorders such as allergic contact dermatitis (ACD) and irritant contact dermatitis (ICD), phototoxicity, atopic dermatitis, and psoriasis, serious defects such as dysfunctions of the epidermal barrier and abnormalities in intercellular communication in KCs have been observed (Suter et al., 2009; Hanel et al., 2013).

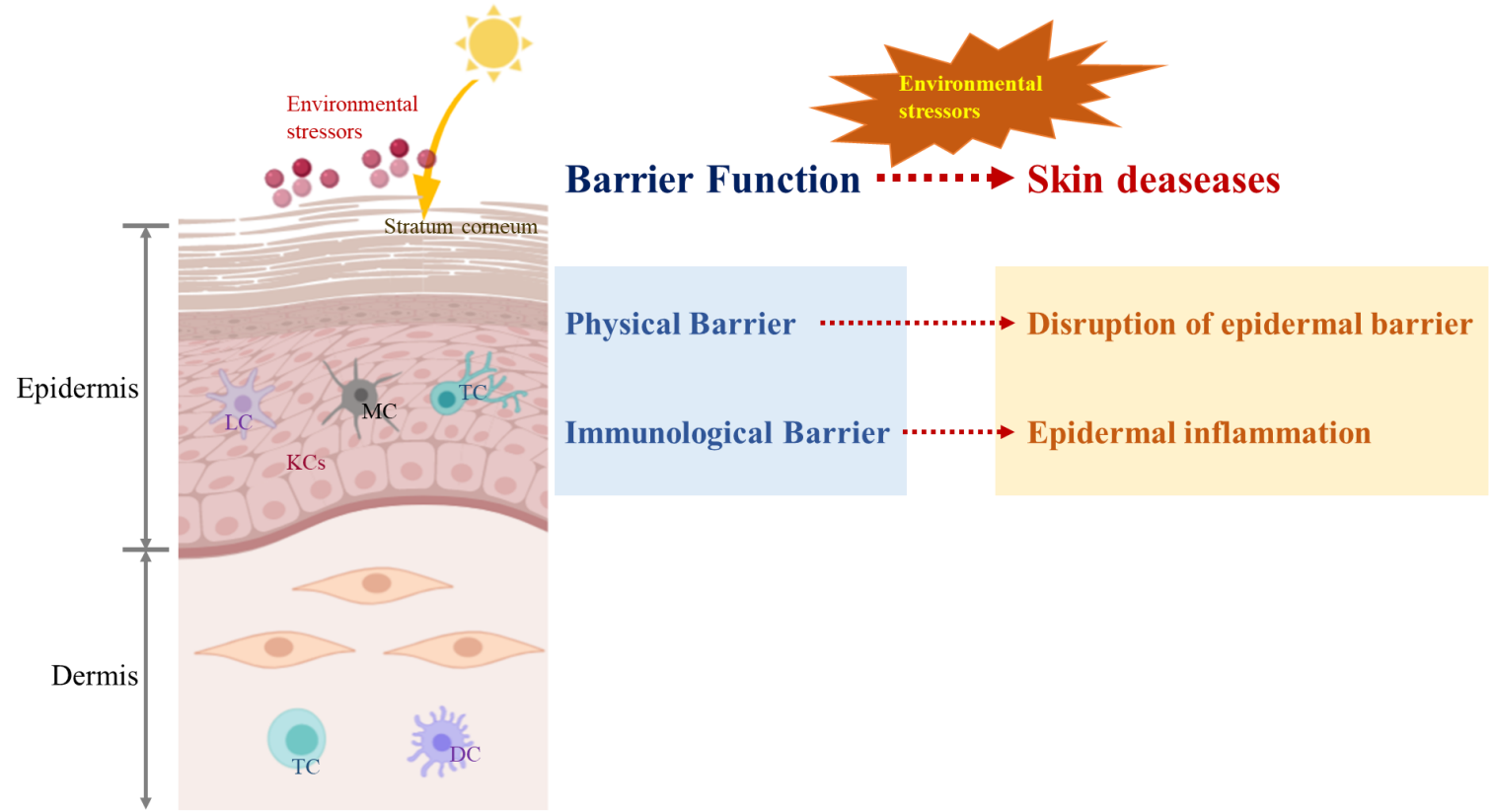

Fig. 1. Skin barrier and epidermal inflammation.

Furthermore, Asian dust storm particles (ADSPs) are known to induce severe adverse health effects such as asthma, contact dermatitis, and conjunctivitis (Ichinose et al., 2008). Interleukin (IL)-8 is a major mediator of the inflammatory response (Barker et al., 1991), produced by various cell types, including KCs, and functioning as a chemoattractant or mitogenic factor. Additionally, it is similar to IL-6 but has a longer half-life. Furthermore, IL-6 is produced in the dermis and epidermis from several cell types, including KCs, during various dermatological disorders (Sugawara et al., 2001). Moreover, it is not only involved in inflammatory responses, but also the regulation of metabolic, regenerative, and neural processes (Scheller et al., 2011). IL-8 and IL-6 can induce inflammatory skin diseases, including contact dermatitis and atopic dermatitis (Reich et al., 2003). Granulocyte-macrophage colony-stimulating factor (GM-CSF) is a major mediator of tissue inflammation, that serves as a communication conduit in various cell types, including KCs (Becher et al., 2016). Furthermore, GM-CSF is an important immune modulator in Langerhans cell (LC) maturation (Jux et al., 2009). In a previous study evaluating the effects of ADSPs containing various environmental pollutants, ADSPs significantly upregulated gene transcription of *IL*-8, *IL-6,* and *GM-CSF* (Choi et al., 2011). ADSPs upregulated mRNA levels of cytochrome P450 1A1 (*CYP1A1*), *CYP1A2,* and *CYP1B1,* indicators of aryl hydrocarbon receptor (AHR) activation, with AHR regulating the transcription of several key enzymes in xenobiotic metabolism (Monk et al., 2003). Caspase 14 is involved in KC terminal differentiation and regulates the metabolism of filaggrin (Hoste et al., 2011). Furthermore, gene transcription of *caspase 14*, which affects KC differentiation, was increased in human epidermal KCs by ADSPs (Choi et al., 2011). In human skin, ADSPs can stimulate toxicological processes by upregulating AHR activation, as

well as the production of pro-inflammatory cytokines and immune modulators, and altering normal epidermal differentiation (Fig. 2).

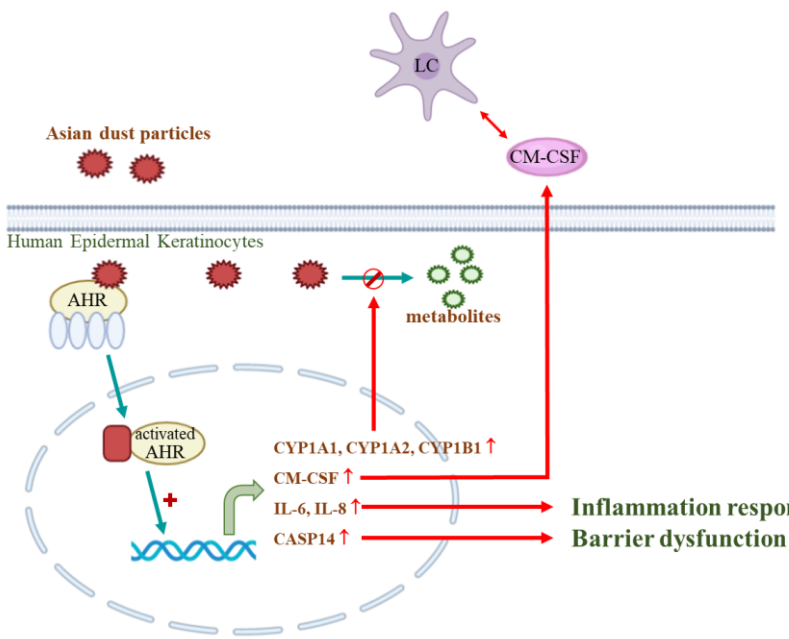

Fig. 2. Summary scheme for inflammatory response and dysfunction of epidermal in NHKs by barrier in Asian dust storm particles.

Numerous inflammatory skin diseases such as ACD, atopic dermatitis, and psoriasis are characterized by their CD4-positive (CD4+) T helper (Th) cell responses (Lowes et al., 2008; Eyerich et al., 2011). Based on their cytokine expression profiles, Th cells can differentiate into several subtypes, including Th1, Th2, Th17, and Th22 (Eyerich et al., 2009). ACD is a specific immune response to various contact allergens. After a first exposure, the allergen sensitizes the cutaneous immune system in the human skin. Following subsequent exposure, the allergen elicits a T cell-mediated immune process triggering ACD (Kaplan et al., 2012; McFadden et al., 2013). During the sensitization phase, LCs or dendritic cells (DCs) present contact allergens to T cells in local lymph nodes, following migra-

tion from the epidermis to local lymph nodes via the cutaneous lymphatic system (Kimber et al., 2012). Both angiogenesis and inflammation may be associated with chronic skin inflammation pathologies, including atopic dermatitis (Zhang et al., 2006; Huggenberger and Detmar, 2011; Thairu et al., 2011). Increased angiogenesis and lymphangiogenesis are important features of chronic inflammation. The vascular endothelial growth factor (VEGF) is produced by cells stimulating the formation of blood vessels and is involved in both angiogenesis and lymphangiogenesis (Ferrara et al., 2003). Interferon γ (IFNγ) is mainly produced by Th1 cells and is associated with allergic-related immunopathologies (Teixeira et al., 2005). IL-4 is a cytokine produced mainly by Th2 cells, IL-17 is a pro-inflammatory cytokine produced by Th17 cells, and IL-22 is produced by several populations of immune cells, including Th22 and Th17 cells at the site of inflammation (Eyerich et al., 2017). Tumor necrosis factor α (TNFα) and IL-1α are well known as principal pro-inflammatory cytokines expressed in several cell types, including activated macrophages, neutrophils, dendritic cells, and KCs (Noske, 2018). In a previous study investigating the allergen contact response of NHKs, it has been demonstrated that the major pro-inflammatory cytokines, TNF-α, IFNγ, IL-4, IL-6, IL-17, IL-22, and IL-1α, stimulate a significant increase in VEGF in NHKs (Bae et al., 2015a). Especially, chemical allergens formaldehyde, 2,4-dinitrochlorobenzene (DNCB), and urushiol increased the gene transcription of lymphangiogenic *VEGF-C*, but not that of *VEGF-A* and *VEGF-B*. It has been suggested that most chemical allergens increase the production of VEGF in NHKs, and VEGF in KCs regulated the lymphangiogenic process through VEGF-C during the skin sensitization process (Fig. 3).

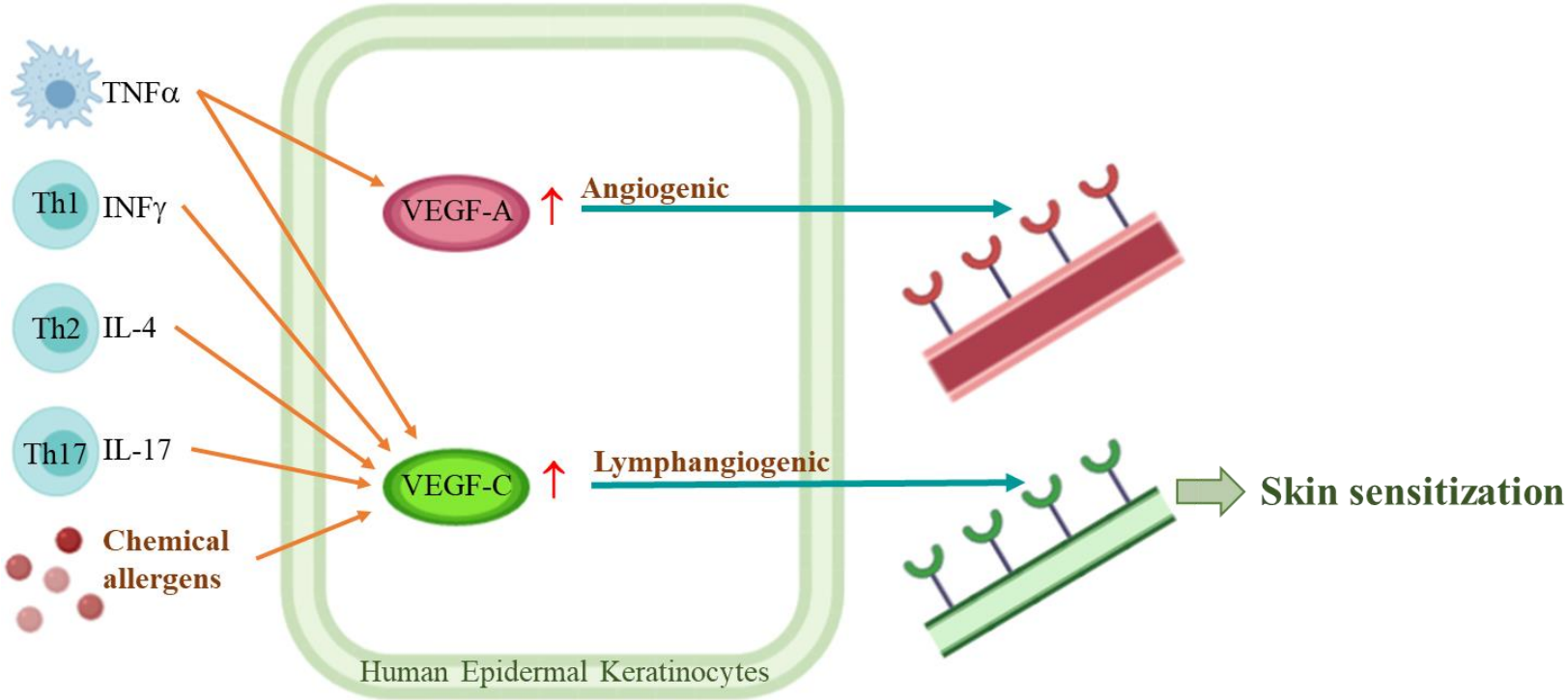

Fig. 3. Stimulation of VEGFC by pro-inflammatory cytokines and chemical allergens in NHKs

Previously, a whole-genome microarray analysis has revealed that IL-24 is significantly upregulated in NHKs treated with pro-inflammatory cytokines IL-1β, IL-6, and TNF-α, and with Th cell-derived cytokines, IFNγ, IL-4, IL-17a, and IL-22, which are major cytokines of Th1, Th 2, Th 17, or Th 22 cells (Jin et al., 2014). In differentially expressed genes (DEGs) selected in response to at least three interleukins among IFNγ, IL-4, IL-17a, IL-22, and IL-6, non-coding RNA H19, CXCL14, and filaggrin were downregulated in NHKs. Environmental toxic stimuli, including SLS and UVB irradiation, stimulated the upregulation of IL-24 in NHKs. IL-24 can stimulate major pro-inflammatory mediators such as IL-8, prostaglandin E2 (PGE_2), and matrix metalloproteinase 1 (MMP1), and activates the Janus kinase (JAK) 1- signal transducer and activator of transcription (STAT) 3 and mitogen-activated protein kinase (MAPK) pathways in NHKs. Reportedly, IL-24 derived from KCs plays a role in the positive response regulation of cutaneous inflammation induced by environmental and endogenous toxic stimuli (Fig. 4).

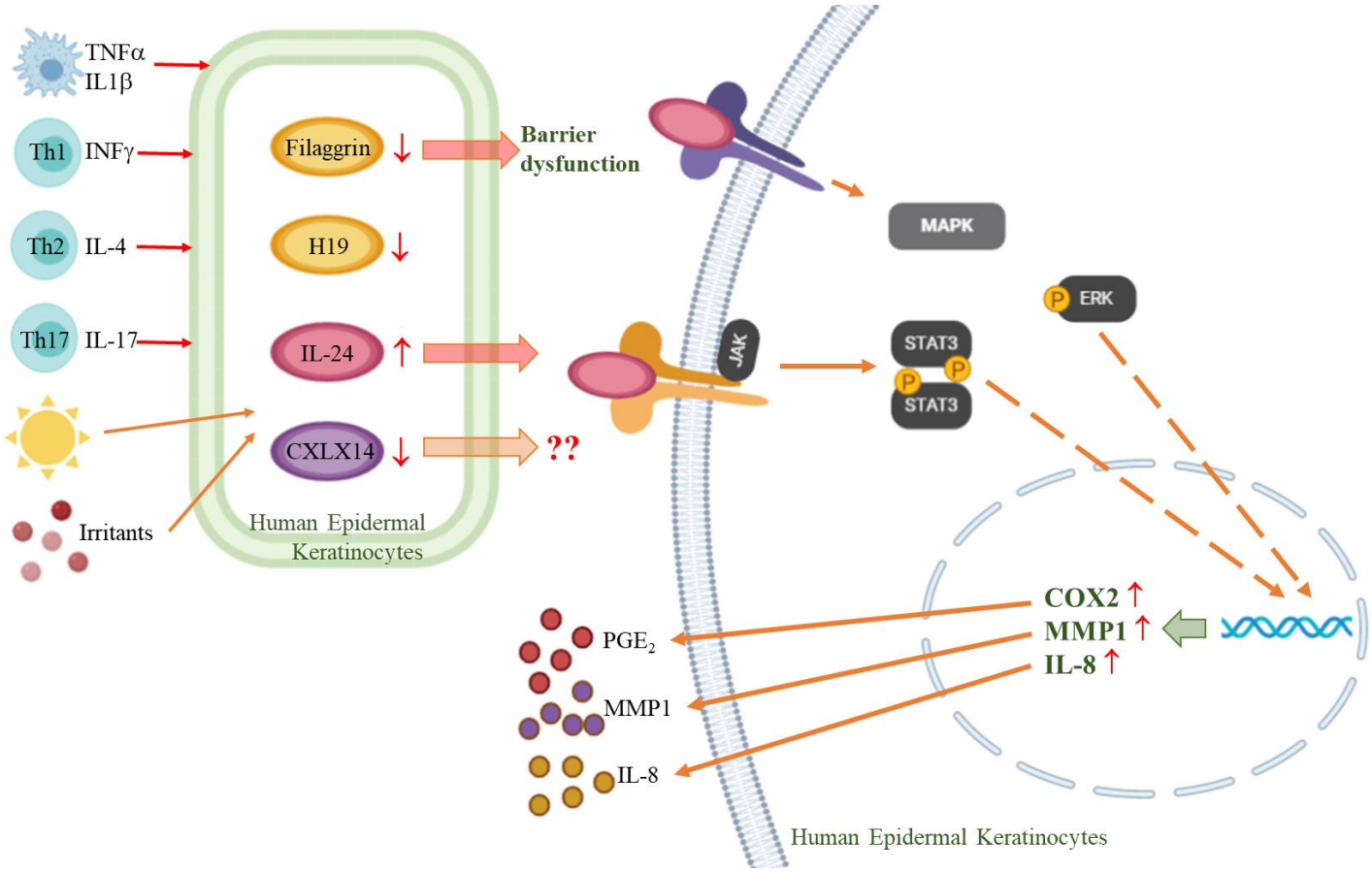

Fig. 4. Roles of IL24 induced by pro-inflammatory cytokines and environmental toxic stressors in NHKs

2. Environmental toxic stimuli on the skin

Skin inflammation may occur in response to physical injury or exposure to hazardous agents such as chemical allergens, irritants, UV irradiation, and infection. Formaldehyde is one of the main external hazardous agents threatening human health. Since the early 1900s, formaldehyde and formaldehyde releasers have been extensively used in various industrial products, including household products, occupational products, and cosmetics (Flyvholm and Andersen, 1993; Lundov et al., 2010). Notably, the annual European industrial production of formaldehyde is estimated at over 1000,000 tons (ECHA, 2020). Epidemiological studies have revealed that formaldehyde is related with an increased risk of leukemia, nasopharyngeal cancer (Bachand et al., 2010), childhood asthma (Garrett et al., 1999), and ACD (Lundov et al., 2010). In toxicological studies, formaldehyde has been identified as a human carcinogen (Cogliano et al., 2005). Furthermore, formaldehyde exposure can cause various dermatological and respiratory problems in humans, including allergic and irritation reactions in the skin, eyes, and respiratory tract (De Jong et al., 2009). Therefore, investigations into gene expression profiles induced by formaldehyde have been performed in various mammalian cells, including human nasal epithelial cells and human tracheal fibroblasts (Li et al., 2007; Neuss et al., 2010). However, few studies have investigated the effects of formaldehyde on human epidermal cells. In the cosmetic industry, ACD induced by formaldehyde has been reported since the 1960s (Thyssen et al., 2007). Notably, patients with formaldehyde-induced ACD (3.9%) have increased in the USA and Europe (de Groot et al., 2010; Fasth et al., 2018). In a recent study, formaldehyde significantly upregulated IL-8, VEGF, and IL-24 in human KCs (Bae et al., 2015a). Genome-wide transcription profile studies have mainly been conducted utilizing respiratory

epithelial cells to elucidate molecular mechanisms of formaldehyde-induced toxicity (Li et al., 2007; Neuss et al., 2010). Additionally, formaldehyde is mainly present at low levels in both indoor and outdoor air (Gustafson et al., 2005; Rovira et al., 2016). Consumer products may contain extremely low levels of formaldehyde as a fumigant, fertilizer, preservative, or contaminant (Lefebvre et al., 2012; Jeong et al., 2015). Additionally, molecular biology studies have demonstrated that substances such as formaldehyde, presenting a high frequency of exposure and potentially harmful effects in human skin, significantly contribute to the mechanism of skin inflammation. However, most molecular profile studies have investigated high formaldehyde concentrations, which are cytotoxic to target cells and stimulate the expression of genes related to cell death-related biological pathways, including apoptosis (Szende and Tyihak, 2010). It is crucial to investigate the toxicological effects of sub-cytotoxic formaldehyde exposure encountered during normal living conditions, to elucidate molecular mechanisms of skin inflammation induced by typical hazardous agents.

Contact dermatitis is an inflammatory skin response to various contact hazards. ACD and ICD are two major clinical problems resulting from contact conditions and be differentiated based on pathophysiological presentations. Despite differing pathogenesis, ACD and ICD can demonstrate similar clinical manifestations such as erythema, edema, and even vesicle formation. Some irritants may induce weak allergic-like stimuli and activate cellular responses similar to allergens (Fluhr et al., 2008; Park et al., 2018). However, the molecular differentiation between mechanisms mediating irritation and allergic responses remain unknown. Various skin irritants and sensitizers may induce KC stimulation, generating pro-inflammatory cytokines such as IL-1α, TNF-α, IFNγ, VEGF, and IL-8 (Coquette et al., 2003; Bae

et al., 2015a; Kim et al., 2018). Thus, the characterization and identification of cytokines derived by KCs are necessary to elucidate the difference in molecular mechanisms associated with distinct pathogenic responses between ACD and ICD. A previous study has revealed that 14 of 16 reference human sensitizers from the OECD Test Guideline (TG) 429 reference chemicals significantly increased either C-X-C motif chemokine ligand 8 (CXCL8, IL-8) or VEGF in KCs (Bae et al., 2015a). In contrast, chemical non-sensitizers, except SLS, upregulated only CXCL8. Hence, there exists a need for novel biomarkers to distinguish between sensitizers and irritant non-sensitizers.

Benzophenone-3 (BP-3; oxybenzone), a broad-spectrum UV protective agent, is extensively used as an organic sunscreen for protecting the skin against UV-induced damage (Calafat et al., 2008). Despite the health benefits of organic sunscreen agents, BP-3 has been known to induce adverse toxic effects such as contact allergy and phototoxicity (Calafat et al., 2008). Phototoxicity is a toxic response to a substance excited after subsequent exposure to UV irradiation (Gaspar et al., 2013). A phototoxic substance is excited following the absorption of excessive solar radiation energy, inducing pro-inflammatory reactions, and causing direct cellular skin damage (Kim et al., 2015).

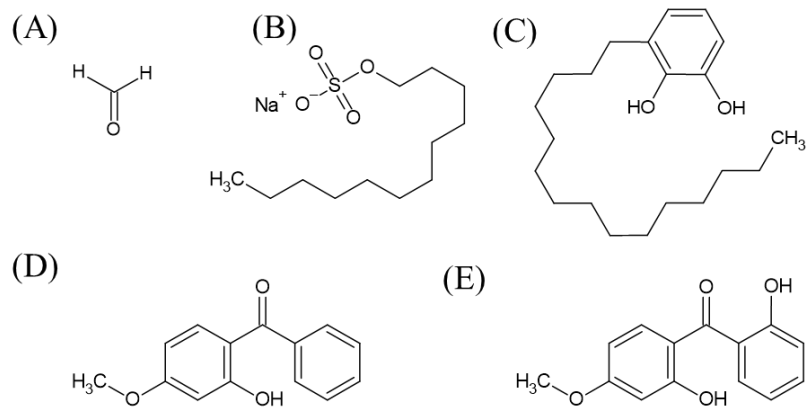

Fig. 5. Chemical structure of (A) formaldehyde, (B) sodium lauryl sulfate (SLS), (C) urushiol, (D) benzophenone (BP-3), and (E) benzophenone-8 (BP-8).

II. RESULTS

Chapter 1. Effects of formaldehyde in NHKs

1. Genome-wide transcription profile in sub-cytotoxic formaldehyde-treated NHKs

To investigate a genome-wide transcription profile data of NHKs after exposure to formaldehyde at sub-cytotoxic concentration, which not cause significant cell death, as the level of formaldehyde exposure in daily life conditions, we first determined noncytotoxic concentration of formaldehyde. Cell viability was assessed by WST-8-based cytotoxicity test 24 h after formaldehyde treatment (Fig. 6). The cell viability of the 300 μM formaldehyde-treated NHKs was 44% lower that of the vehicle-treated control. No difference in cell viability was detected treated with 200 μM formaldehyde for 24 h in culture compared to that of the control. Therefore, the whole genome-scale transcription profile study was performed in 200 μM formaldehyde-treated NHKs.

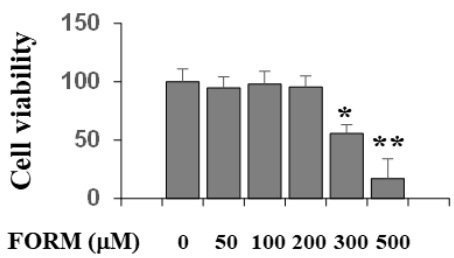

Fig. 6. Cytotoxic effects of formaldehyde on NHKs. Cell viability was evaluated in formaldehyde-treated NHKs by the WST8-based cytotoxicity tests as described in the Materials and Methods section. Values represent the mean ± standard deviation (SD) (n = 3). *$p < 0.05$ and **$p < 0.01$ were considered statistically significant compared to the controls.

The raw microarray data (n = 4) can be accessed from the National center for Biotechnology Information gene Expression Omnibus (NCBI GEO) database as raw data by dataset ID GSE76446. 175 upregulated and 116 downregulated DEGs were identified as results of comparing expression data between formaldehyde-treated and control NHKs (Table 1 and 2).

Table 1. Upregulated 175 DEGs

Probe Set ID (Gene Symbol)	Mean fold change
204475_at (MMP1)	8.19
205828_at (MMP3)	7.98
221565_s_at (CALHM2)	6.65
219563_at (LINC00341)	5.89
209114_at (TSPAN1)	5.48
203234_at (UPP1)	5.36
218843_at (FNDC4)	5.11
217127_at (CTH)	4.93
239045_at (N/A)	4.77
212419_at (ZCCHC24)	4.62
209611_s_at (SLC1A4)	4.56
218000_s_at (PHLDA1)	4.38
208161_s_at (ABCC3)	4.33
212816_s_at (CBS)	4.28
226028_at (ROBO4)	4.25
226769_at (FIBIN)	4.09
241994_at (XDH)	4.07
212190_at (SERPINE2)	4.03
234699_at (RNASE7)	4.00
236423_at (N/A)	3.97
209949_at (NCF2)	3.97
242993_at (N/A)	3.88
1555788_a_at (TRIB3)	3.85
209383_at (DDIT3)	3.85
219256_s_at (SH3TC1)	3.84
203349_s_at (ETV5)	3.83
208891_at (DUSP6)	3.82
221541_at (CRISPLD2)	3.66
214452_at (BCAT1)	3.61
224009_x_at (DHRS9)	3.60
203304_at (BAMBI)	3.57
243222_at (ALPK1)	3.51
1558392_at (SYNE2)	3.41
219181_at (LIPG)	3.39
210511_s_at (INHBA)	3.38
207345_at (FST)	3.36
209369_at (ANXA3)	3.35
1558212_at (LOC101930048)	3.35
206710_s_at (EPB41L3)	3.27
229070_at (ADTRP)	3.27
233011_at (ANXA1)	3.25
203817_at (GUCY1B3)	3.24
217494_s_at (N/A)	3.23
224143_at (TTTY8)	3.23
210895_s_at (CD86)	3.23
206101_at (ECM2)	3.22
208937_s_at (ID1)	3.19
214088_s_at (FUT3)	3.18
204827_s_at (CCNF)	3.16
207419_s_at (RAC2)	3.13

Probe Set ID (Gene Symbol)	Mean fold change
202847_at (PCK2)	3.08
204748_at (PTGS2)	3.07
211719_x_at (FN1)	3.06
203438_at (STC2)	3.04
239331_at (N/A)	3.01
232150_at (N/A)	2.99
236429_at (ZNF83)	2.97
238450_at (PFKFB2)	2.96
1563296_at (LINC00572)	2.93
210042_s_at (CTSZ)	2.92
211130_x_at (EDA)	2.92
231202_at (ALDH1L2)	2.87
222223_s_at (IL36RN)	2.87
206084_at (PTPRR)	2.86
242391_at (N/A)	2.85
230574_at (LOC100130938)	2.85
240552_at (N/A)	2.85
202267_at (LAMC2)	2.81
221539_at (EIF4EBP1)	2.80
233296_x_at (N/A)	2.78
206584_at (LY96)	2.78
222858_s_at (DAPP1)	2.77
205627_at (CDA)	2.77
214682_at (PKD1P1)	2.76
1570490_at (RP11-646E18.4)	2.75
226886_at (GFPT1)	2.73
223082_at (SH3KBP1)	2.72
241695_s_at (N/A)	2.70
201481_s_at (PYGB)	2.70
207717_s_at (PKP2)	2.70
211603_s_at (ETV4)	2.69
213524_s_at (G0S2)	2.69
1560760_s_at (LOC101927988)	2.68
203889_at (SCG5)	2.67
205047_s_at (ASNS)	2.66

Probe Set ID (Gene Symbol)	Mean fold change
204257_at (FADS3)	2.64
209683_at (FAM49A)	2.63
219836_at (ZBED2)	2.63
228646_at (PPP1R1C)	2.61
217966_s_at (FAM129A)	2.61
202014_at (PPP1R15A)	2.60
201169_s_at (BHLHE40)	2.58
228275_at (LINC00888)	2.58
210474_s_at (CDK11A)	2.54
232434_at (DIRC3)	2.54
38037_at (HBEGF)	2.53
1556267_at (MYRFL)	2.52
243117_at (N/A)	2.49
205046_at (CENPE)	2.48
231697_s_at (N/A)	2.48
222221_x_at (EHD1)	2.47
223235_s_at (SMOC2)	2.47
229441_at (PRSS23)	2.46
204669_s_at (RNF24)	2.44
201340_s_at (ENC1)	2.44
220122_at (MCTP1)	2.44
210999_s_at (GRB10)	2.42
211053_at (KCNG1)	2.41
202627_s_at (SERPINE1)	2.41
204088_at (P2RX4)	2.40
238133_at (N/A)	2.40
1558871_at (BC016361)	2.39
207381_at (ALOX12B)	2.39
234994_at (TMEM200A)	2.36
244494_at (N/A)	2.33
1554310_a_at (EIF4G3)	2.31
205376_at (INPP4B)	2.29
203946_s_at (ARG2)	2.29
1552777_a_at (RAET1E)	2.28
240259_at (FLRT2)	2.28
244041_at (STX6)	2.28

Probe Set ID (Gene Symbol)	Mean fold change
1554835_a_at (B3GNT5)	2.28
1562245_a_at (ZNF578)	2.27
202558_s_at (HSPA13)	2.27
238534_at (LRRFIP1)	2.26
230134_s_at (RC3H2)	2.25
240549_at (LOC100507459)	2.25
218651_s_at (LARP6)	2.24
219773_at (NOX4)	2.24
240991_at (N/A)	2.24
1560208_at (LOC101930593)	2.24
202499_s_at (SLC2A3)	2.23
209738_x_at (PSG6)	2.22
209822_s_at (VLDLR)	2.22
235737_at (TSLP)	2.22
202241_at (TRIB1)	2.21
220575_at (FAM106A)	2.21
1557389_at (SH3PXD2A-AS1)	2.20
235745_at (ERN1)	2.20
223688_s_at (LY6K)	2.20
218692_at (SYBU)	2.19
239704_at (RNF144B)	2.18
203706_s_at (FZD7)	2.18
209210_s_at (FERMT2)	2.17
214599_at (IVL)	2.17
204802_at (RRAD)	2.17
219387_at (CCDC88A)	2.16
205547_s_at (TAGLN)	2.16
219155_at (PITPNC1)	2.16

Probe Set ID (Gene Symbol)	Mean fold change
235094_at (N/A)	2.15
1566901_at (TGIF1)	2.14
1552620_at (SPRR4)	2.13
1560853_x_at (ZNF826P)	2.13
207076_s_at (ASS1)	2.12
207463_x_at (PRSS3)	2.11
217315_s_at (KLK13)	2.10
213572_s_at (SERPINB1)	2.10
213116_at (NEK3)	2.10
220153_at (ENTPD7)	2.09
228298_at (PCED1B)	2.08
223315_at (NTN4)	2.08
232676_x_at (MYEF2)	2.08
236930_at (LOC101928143)	2.06
238780_s_at (KCNJ5)	2.06
223195_s_at (SESN2)	2.05
218368_s_at (TNFRSF12A)	2.04
203423_at (RBP1)	2.04
238482_at (KLF7)	2.03
211782_at (IDS)	2.03
207064_s_at (AOC2)	2.03
1554594_at (ARHGAP27)	2.02
205067_at (IL1B)	2.02
41856_at (UNC5B)	2.02
227806_at (C16orf74)	2.01
212171_x_at (VEGFA)	2.04

N/A; not available

Table 2. Downregulated 116 DEGs

Probe Set ID (Gene Symbol)	Mean fold change
203708_at (PDE4B)	0.11
209821_at (IL33)	0.21
214821_at (SLC25A4)	0.24
232628_at (N/A)	0.25
204457_s_at (GAS1)	0.26
228262_at (MAP7D2)	0.26
206149_at (CHP2)	0.27
219893_at (CCDC71)	0.27
230905_at (N/A)	0.27
230560_at (STXBP6)	0.27
241416_at (LOC101928806)	0.28
214598_at (CLDN8)	0.30
1560305_x_at (FKBP4)	0.30
239817_at (N/A)	0.31
229390_at (FAM26F)	0.32
220263_at (SMAD5-AS1)	0.33
204519_s_at (PLLP)	0.35
235006_at (CDKN2AIPNL)	0.36
226539_s_at (CCDC42B)	0.36
228062_at (NAP1L5)	0.37
237386_at (LOC100129361)	0.37
242627_at (N/A)	0.37
216532_x_at (RP3-406P24.1)	0.37
229290_at (DAPL1)	0.38
1553111_a_at (KBTBD6)	0.38
214456_x_at (SAA1)	0.38
209732_at (CLEC2B)	0.38
242281_at (GLUL)	0.39
1552359_at (MCMDC2)	0.39
204821_at (BTN3A3)	0.40
239796_x_at (TIRAP)	0.40
219800_s_at (THNSL1)	0.40
37512_at (HSD17B6)	0.40
206561_s_at (AKR1B10)	0.40

Probe Set ID (Gene Symbol)	Mean fold change
242907_at (GBP2)	0.41
217651_at (N/A)	0.41
239900_x_at (RP11-379F4.6)	0.41
243326_at (N/A)	0.41
205623_at (ALDH3A1)	0.42
235438_at (N/A)	0.42
1566324_a_at (MAF)	0.42
226852_at (MTA3)	0.42
217019_at (RPS4XP3)	0.42
231195_at (KLRG2)	0.42
219488_at (A4GALT)	0.42
1557322_at (ZNF230)	0.42
218858_at (DEPTOR)	0.42
231089_at (LOC100505664)	0.43
208606_s_at (WNT4)	0.43
204430_s_at (SLC2A5)	0.43
229720_at (BAG1)	0.44
1560826_at (N/A)	0.44
226066_at (MITF)	0.44
1562428_at (LOC654780)	0.44
233937_at (GGNBP2)	0.44
208607_s_at (SAA1)	0.44
239423_at (RP11-251G23.5)	0.45
242053_at (N/A)	0.45
210643_at (TNFSF11)	0.45
214826_at (PDE12)	0.45
226923_at (SCFD2)	0.45
223290_at (PDXP)	0.45
232533_at (METTL8)	0.45
1560011_at (AX747544)	0.45
214930_at (SLITRK5)	0.45
1556667_at (FTCDNL1)	0.45
225767_at (RNA45S5)	0.45
240013_at (N/A)	0.45

Probe Set ID (Gene Symbol)	Mean fold change
222121_at (ARHGEF26)	0.45
1557066_at (LUC7L)	0.45
228766_at (CD36)	0.46
228449_at (MORC2)	0.46
208588_at (TPT1P8)	0.46
240806_at (RPL15)	0.46
222802_at (EDN1)	0.46
1557398_at (N/A)	0.46
200799_at (HSPA1A)	0.46
208078_s_at (SIK1)	0.46
1554360_at (FCHSD2)	0.47
224370_s_at (CAPS2)	0.47
240391_at (NDUFB2)	0.47
239447_at (TRA2B)	0.47
213283_s_at (SALL2)	0.47
238755_at (RASSF10)	0.47
230209_at (ZXDC)	0.47
219077_s_at (WWOX)	0.47
209243_s_at (PEG3)	0.47
221232_s_at (ANKRD2)	0.47
230003_at (SLC16A7)	0.48
230748_at (SLC16A6)	0.48
225564_at (SPATA13)	0.48
240413_at (PYHIN1)	0.48
207826_s_at (ID3)	0.48
242528_at (HOXA-AS2)	0.48
232528_at (N/A)	0.48
239066_at (N/A)	0.48
215491_at (MYCL)	0.48
216384_x_at (LOC100506248)	0.48
230057_at (LOC285178)	0.48
1552705_at (DUSP19)	0.48
209094_at (DDAH1)	0.49
211658_at (PRDX2)	0.49
232060_at (ROR1)	0.49
228671_at (TMEM201)	0.49
218927_s_at (CHST12)	0.49
1564876_s_at (FOXP2)	0.49
1569086_at (C19orf83)	0.49
219498_s_at (BCL11A)	0.49
242979_at (IRS1)	0.49
218500_at (THEM6)	0.50
222663_at (RIOK2)	0.50
229455_at (AC083843.1)	0.50
61732_r_at (IFT74)	0.50
229298_at (KBTBD7)	0.50
235654_at (TMEM218)	0.50
214762_at (ATP6V1G2)	0.50

N/A; not available

2. Analysis of DEGs using Gene Ontology (GO) Biological Process (BP) enrichment analysis

We compared the frequency of GO BP terms in the DEGs with the total gene set to identify significant biological phenotype in the formaldehyde-induced DEGs (Table 3). The topmost GO BP term among upregulated formaldehyde-induced DEGs is endoplasmic reticulum (ER) unfolded protein response (UPR) (GO:0030968). The biological phenotype of ER UPR is related to cell death mechanism (Sano and Reed, 2013). The other GO BP enrichment analysis listed the cellular pathway related to cell death in sub-cytotoxic formaldehyde-induced NHKs. In addition, cellular pathways associated with inflammatory response were significantly enriched in the upregulated DEGs including positive regulation of the nitric oxide biosynthetic process (GO:0045429), cell migration (GO:0016477), positive regulation of fever generation (GO:0031622), positive regulation of the prostaglandin biosynthetic process (GO:0031394), and positive regulation of interleukin (IL)-8 production (GO:0032757).

Table 3. Top 20 GO BP terms in sub-cytotoxic formaldehyde-induced upregulated DEGs

GO Code	Up DEGs	Total	Gene Ontology Biological Process Term	Gene symbol
GO:0030968	7	99	endoplasmic reticulum unfolded protein response	CTH (4.93), DDIT3 (3.85), STC2 (3.04), GFPT1 (2.73), ASNS (2.66), PPP1R15A (2.6), ERN1 (2.2)
GO:0008652	5	41	cellular amino acid biosynthetic process	CTH (4.93), CBS (4.28), BCAT1 (3.61), ASNS (2.66), ASS1 (2.12)
GO:0018149	4	23	peptide cross-linking	ANXA1 (3.25), FN1 (3.06), IVL (2.17), SPRR4 (2.13)
GO:0008360	7	116	regulation of cell shape	LINC00341 (5.89), BAMBI (3.57), EPB41L3 (3.27), FN1 (3.06), SH3KBP1 (2.72), FERMT2 (2.17), VEGFA (2.04)
GO:0019346	2	2	transsulfuration	CTH (4.93), CBS (4.28)
GO:0045429	4	35	positive regulation of nitric oxide biosynthetic process	PTGS2 (3.07), P2RX4 (2.4), ASS1 (2.12), IL1B (2.02)
GO:0070814	2	3	hydrogen sulfide biosynthetic process	CTH (4.93), CBS (4.28)
GO:0030949	3	16	positive regulation of vascular endothelial growth factor receptor signaling pathway	GRB10 (2.42), IL1B (2.02), VEGFA (2.04)
GO:0016477	7	174	cell migration	TSPAN1 (5.48), BAMBI (3.57), FN1 (3.06), SH3KBP1 (2.72), HBEGF (2.53), CCDC88A (2.16), VEGFA (2.04)
GO:0007179	6	136	transforming growth factor beta receptor signaling pathway	BAMBI (3.57), ID1 (3.19), PPP1R15A (2.6), SERPINE1 (2.41), FERMT2 (2.17), TGIF1 (2.14)
GO:0010757	2	5	negative regulation of plasminogen activation	SERPINE2 (4.03), SERPINE1 (2.41)
GO:0031622	2	5	positive regulation of fever generation	PTGS2 (3.07), IL1B (2.02)
GO:0031394	2	5	positive regulation of prostaglandin biosynthetic process	ANXA1 (3.25), PTGS2 (3.07)
GO:0046882	2	5	negative regulation of follicle-stimulating hormone secretion	INHBA (3.38), FST (3.36)
GO:0032757	3	23	positive regulation of interleukin-8 production	DDIT3 (3.85), SERPINE1 (2.41), IL1B (2.02)
GO:0042346	3	24	positive regulation of NF-kappaB import into nucleus	PTGS2 (3.07), EDA (2.92), IL1B (2.02)
GO:0006801	3	24	superoxide metabolic process	CBS (4.28), NCF2 (3.97), NOX4 (2.24)
GO:0030198	9	325	extracellular matrix organization	MMP1 (8.19), MMP3 (7.98), CRISPLD2 (3.66), ECM2 (3.22), FN1 (3.06), LAMC2 (2.81), SMOC2 (2.47), SERPINE1 (2.41), NTN4 (2.08)
GO:0034976	4	55	response to endoplasmic reticulum stress	TRIB3 (3.85), DDIT3 (3.85), STC2 (3.04), FAM129A (2.61)
GO:0050667	2	6	homocysteine metabolic process	CBS (4.28), NOX4 (2.24)

3. Validation of DEGs in formaldehyde-treated NHKs

DEGs selected by microarray results were validated by independent measurement, Q-RT-PCR and Western blotting. mRNA levels of *MMP1, MMP3, CBS* and *CTH* were confirmed by Q-RT-PCR in the independently prepared NHKs treated with formaldehyde (Fig. 7A and B). The transcriptions of *MMP1, MMP3, CBS* and *CTH* were significantly upregulated in a concentration -dependent manner (Fig. 7C and D). The mRNA levels of asparagine synthetase (*ASNS*) was also upregulated in the formaldehyde-treated NHKs than in that of the control by Q-RT-PCR (Fig. 7E). Fibronectin, involucrin (IVL), and small proline rich protein 4 (*SPRR4*) were upregulated in formaldehyde-treated NHKs (Fig. 7F-H). In addition, DEGs associated with the major pro-inflammatory mediators, PTGS2, VEGF-A, and CXCL8/IL8 were confirmed by Q-RT-PCR (Fig. 7I-K). Among the validated DEGs in the Q-RT-PCR, the protein expression levels of CBS, CTH, and fibronectin were further confirmed by Western blotting (Fig. 8A). In the supernatants of the cell culture, the levels of MMP1, prostaglandin E2 (PGE_2), VEGF-A, and CXCL8/IL-8 were validated by ELISA (Fig. 8B-E).

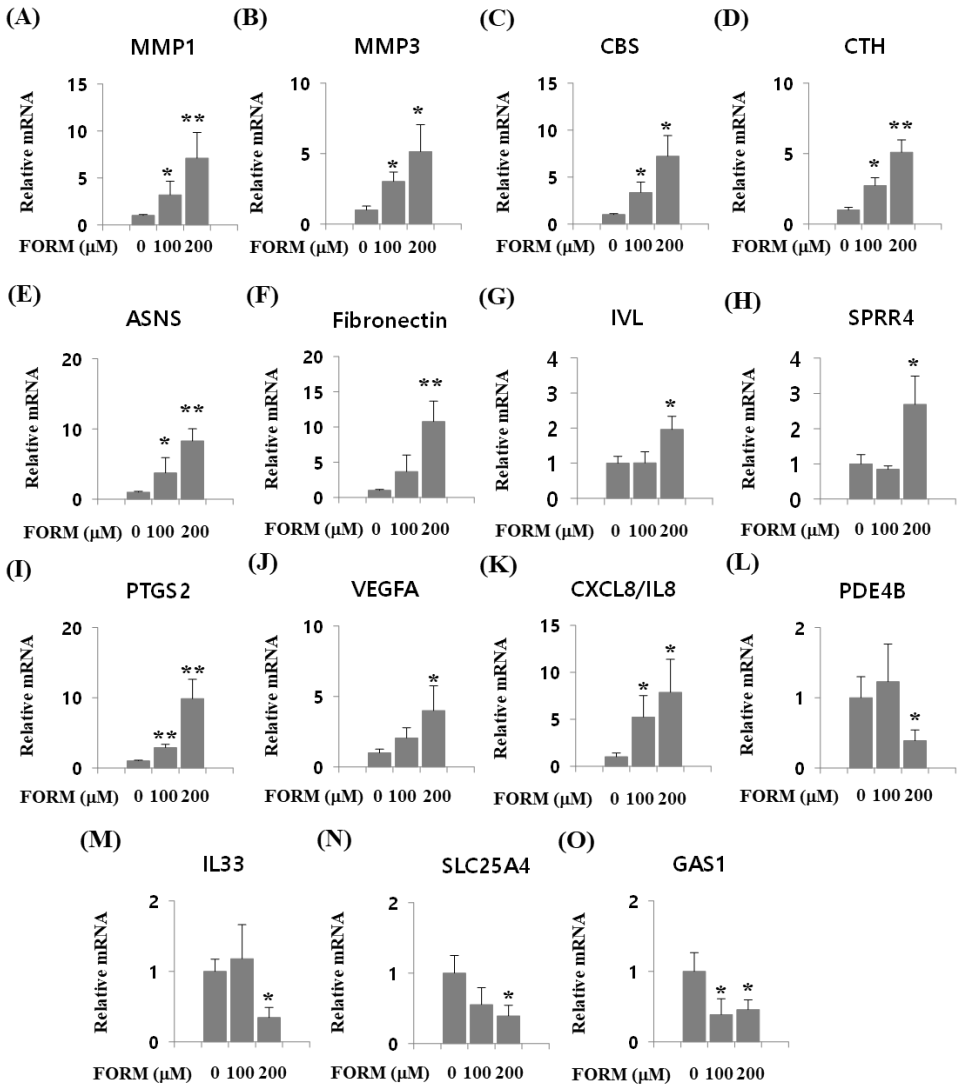

Fig. 7. Validation of the microarray results by Q-RT-PCR. To confirmed the mRNA levels of MMP1 (A), MMP3 (B), CBS (C), CTH (D), ASNS (E), Fibronectin (F), IVL (G), SPRR4 (H), PTGS2 (I), VEGF-A (J), CXCL8/IL-8 (K), PDE4B (L), IL-33 (M), SLC25A4 (N) and GAS1 (O), total RNA samples were extracted from confluently cultured NHKs treated with formaldehyde (FORM) for 24 h. Values represent the mean ± SD of the mRNA of the various genes relative to human GAPDH expression. Error bars represent SD of three independent measurements (n=3). *$p < 0.05$ and **$p < 0.01$.

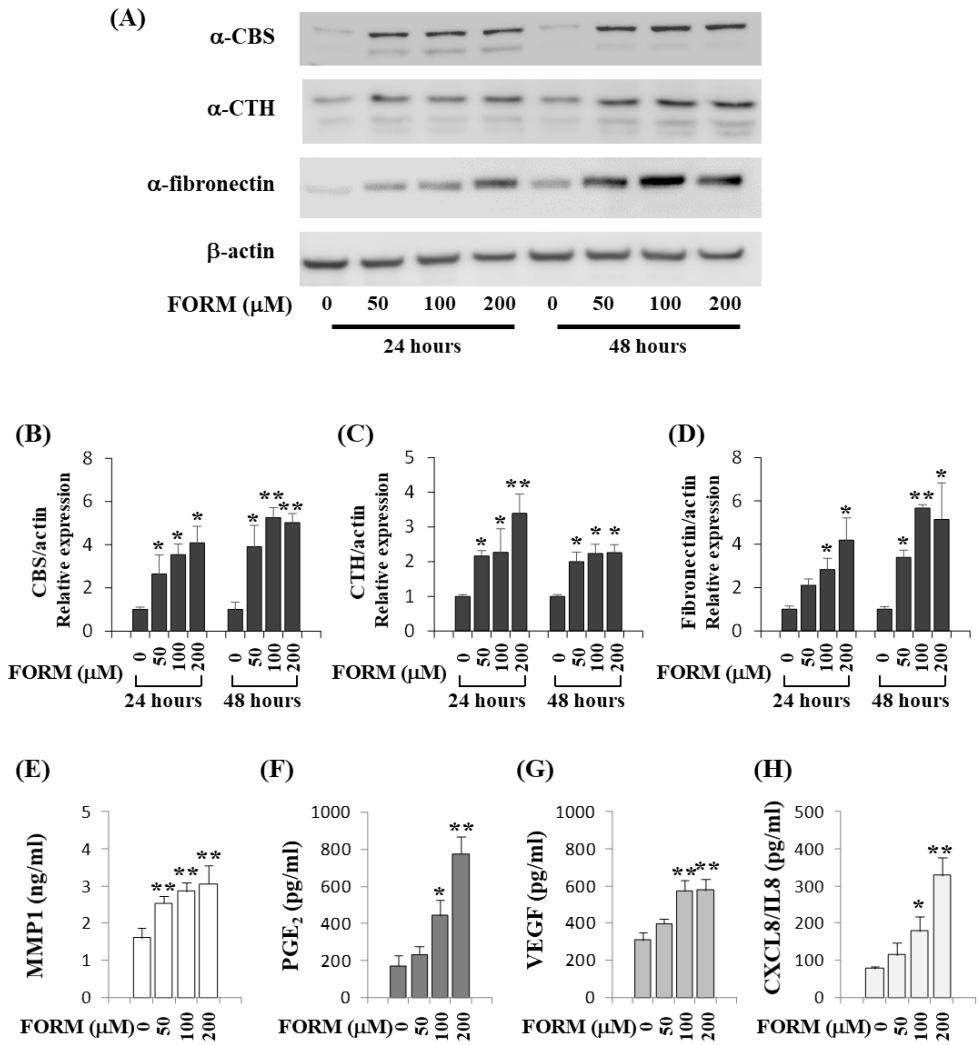

Fig. 8. The effects of formaldehyde on the protein expression of validated DEGs in NHKs. Protein samples from formaldehyde-treated NHKs were prepared for western blotting analysis of CBS, CTH and fibronectin (A). Three independent Western blotting results were quantified against β-actin level for CBS (B), CTH (C) and fibronectin (D). The protein levels of MMP1 (E), PGE_2 (F), VEGF (G), and CXCL8/IL-8 (H) in the culture supernatants of NHKs were measured by ELISA. Values represent the mean ± SD (n= 3). *$p < 0.05$ and **$p < 0.01$.

4. Time course expression profile of *CBS*, *CTH* and pro-inflammatory cytokines

In the study of temporal expression profile of DEGs, the *PGS2* mRNA increased after 2 h of formaldehyde treatment and *IL-8* mRNA increased at 6 h. In contrast, gene transcriptions of *CBS*, *CTH* and *VEGF* were induced at 24 h after formaldehyde treatment (Fig. 9). The sub-cytotoxic formaldehyde affects NHKs not only to induce pro-inflammatory DEGs, *PTGS2* and *CXCL8/IL-8*, but also to increase DEGs associated with anti-inflammatory or cytoprotective response, such as CBS and CTH (Wang et al., 2014), suggesting that these two conflicting biological reactions proceed simultaneously.

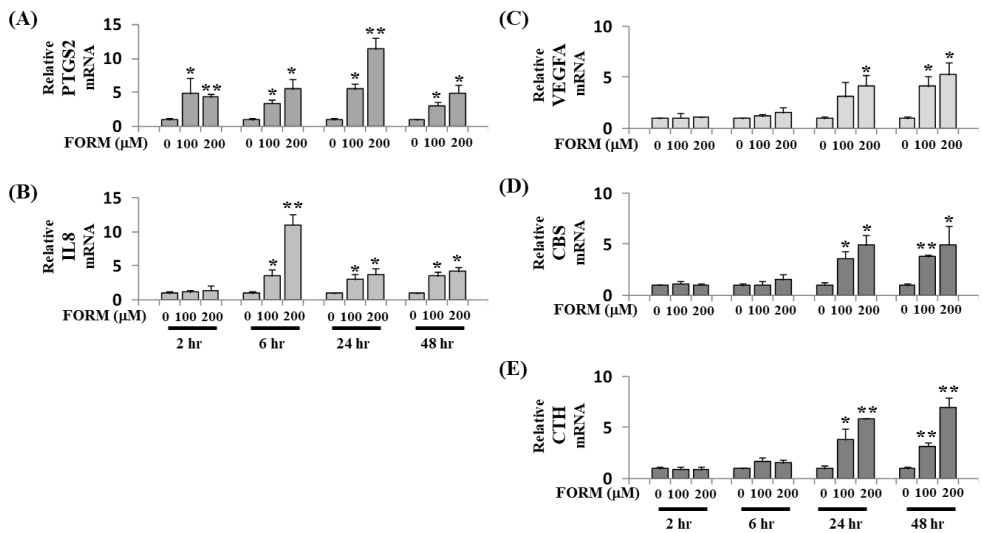

Fig. 9. Time course expression profile in the sub-cytotoxic formaldehyde-treated NHKs. Q-RT-PCR was performed to detect the mRNA levels of *PTGS2* (A), *CXCL8/IL-8* (B), *VEGF-A* (C), *CBS* (D), and *CTH* (E). Values represent the mean ± SD of the mRNA of the various genes relative to human *GAPDH* expression (n= 3). *$p < 0.05$ and **$p < 0.01$.

5. Biological reaction associated with CBS and CTH in the formaldehyde-induced inflammation

L-cystathionine and L-cysteine, key intermediates in the metabolic pathways mediated with CBS and CTH, significantly antagonized the production of MMP1, PGE_2, CXCL8/IL-8, and VEGF in 100 μM formaldehyde-treated NHKs (Fig. 10A-C). VEGF upregulation induced by formaldehyde was significantly suppressed by L-cysteine (Fig. 10D).

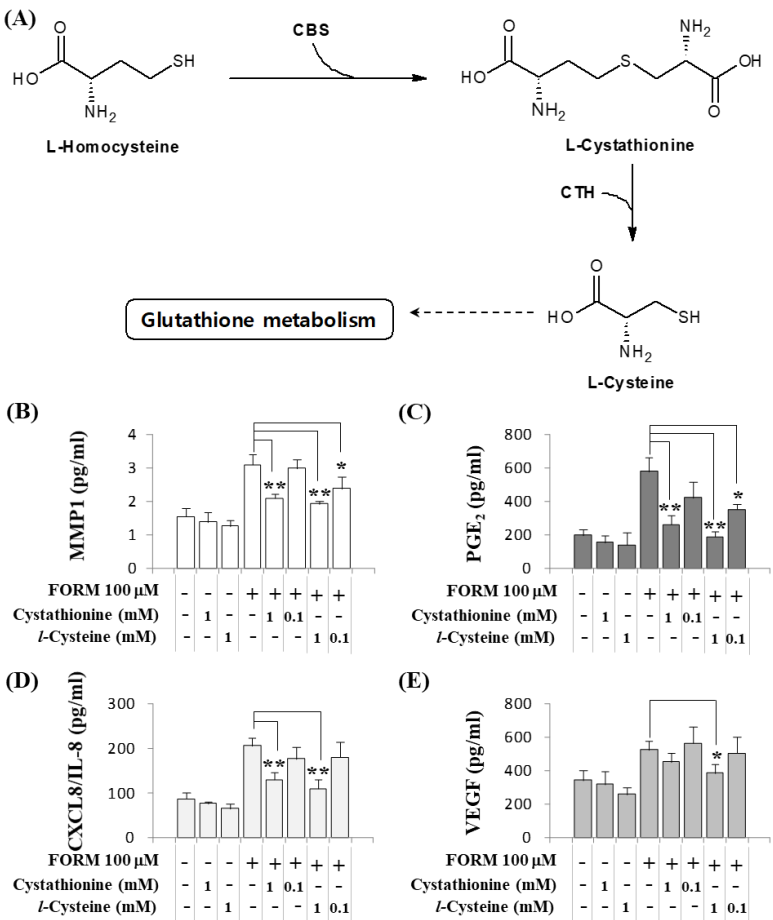

Fig. 10. The effects of L-cystathionine and L-cysteine in NHKs on pro-inflammatory responses. CBS and CTH-mediated transsulfuration pathway associated with L-cystathionine and L-cysteine (A). The protein levels of MMP1 (B), PGE_2 (C), CXCL8/IL-8 (D) and VEGF (F) measured by ELISA in the culture supernatants. Values represent the mean ± SD (n= 3). *$p < 0.05$ and **$p < 0.01$.

6. Effects of immune cytokines on CBS and CTH transcription

We investigated whether formaldehyde-induced upregulation of *CBS* and *CTH* is valid in other cutaneous inflammatory response in NHKs. TNFα, associated with acute inflammation state, did not significantly change the mRNA levels of both *CBS* and *CTH*. Among the major T helper cell cytokines such as IFNγ, IL-4, IL-17, and IL-11 associated chronic states, IFNγ and IL4 significantly increased the gene transcription of *CBS* and *CTH* in NHKs (Fig. 11).

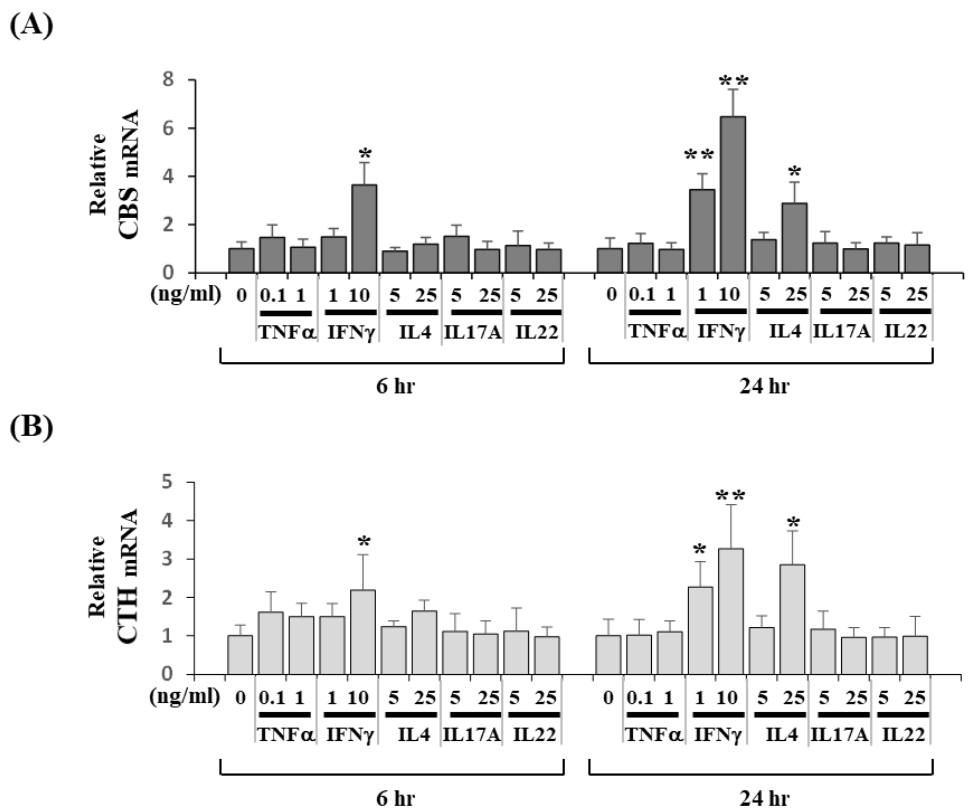

Fig. 11. The effects of pro-inflammatory cytokines on the gene transcription of CBS and CTH in NHKs. Total RNA samples in NKHs treated with TNFα, IFNγ, IL-4, IL-17A, or IL-22 were extracted and Q-RT-PCR was performed for determining the CBS (A) and CTH (B) mRNA levels. Values represent the mean ± SD (n= 3). *$p < 0.05$ and **$p < 0.01$.

Chapter 2. Effects of sensitizers and non-sensitizers in NHKs

1. Genome-wide transcription profile in SLS- or urushiol-treated NHKs

Noncytotoxic concentrations for SLS or urushiol were determined to rule out the possibility that the genes associated with cell death. Cell viability was assessed by a WST-8-based cytotoxicity test 24 h after chemical treatment (Fig. 12). Whole genome-scale transcription data were determined in NHKs treated with 10 μM SLS or 5 μM urushiol for 24 h. The raw microarray data can be accessed from the NCBI GEO database under accession number GSE126354. 259 upregulated and 193 downregulated DEGs were selected in the SLS-treated NHKs according to three selection criteria, data variability among samples, fold expression changes, and statistical *p* for each probe set, (Table 4 and 5). For the urushiol-treated NHKs, 173 upregulated and 124 downregulated DEGs were identified (Table 6 and 7). We summarized these results with Venn diagrams showing the DEGs overlapping in response to both SLS and urushiol. Among selected DEGs in SLS- or Urushiol-treated NHKs, 9 DEGs were commonly increased in response to SLS and urushiol, ATP12A, CXCL8, DEFB103A, MAP3K8, MMP10, SNORA68, TAC1, TM4SF1 and UCA1 (Fig. 13A). Commonly downregulated DEGs by both SLS and urushiol were ARFGAP2, CLK3, CXCL14, H19, HERC6 and MIR302B (Fig. 13B).

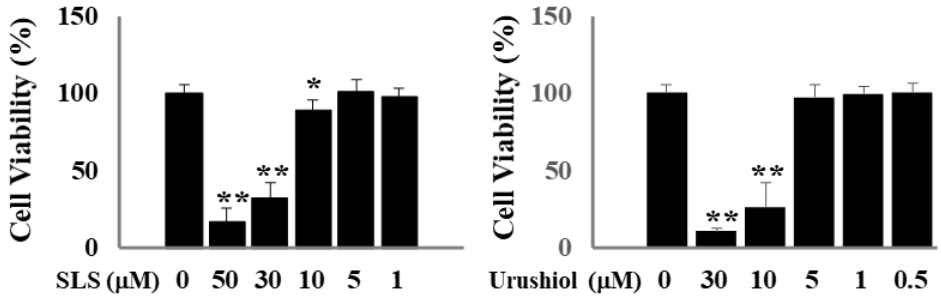

Fig. 12. Effects of SLS and urushiol on the cell viability of NHKs. Values represent the mean ± standard deviation (SD) (n = 3). *$p < 0.05$ and **$p < 0.01$.

Table 4. Upregulated DEGs in the SLS-treated NHKs

Probe Set ID (Gene Symbol)	Mean fold change
202859_x_at (CXCL8)	6.21
213524_s_at (G0S2)	4.82
235102_x_at (SNORD3A)	4.41
221525_at (ZMIZ2)	3.81
207113_s_at (TNF)	3.81
244861_at (ZNF527)	3.77
205896_at (SLC22A4)	3.69
207710_at (LCE2B)	3.65
209237_s_at (SLC23A2)	3.63
221009_s_at (ANGPTL4)	3.54
244168_s_at (ULK4)	3.42
206914_at (CRTAM)	3.33
1553534_at (NLRP10)	3.32
219500_at (CLCF1)	3.21
218358_at (CRELD2)	3.21
214502_at (HIST1H2BJ)	3.2
237439_at (USP43)	3.14
208161_s_at (ABCC3)	3.12
205619_s_at (MEOX1)	3.09
210056_at (RND1)	3.09
214285_at (FABP3)	3.07
231416_at (DHDH)	3.05
209189_at (FOS)	3.03

Probe Set ID (Gene Symbol)	Mean fold change
223720_at (SPINK7)	3.01
238885_at (KIAA1549)	2.94
205818_at (BRINP1)	2.94
203634_s_at (CPT1A)	2.93
207649_at (KRT37)	2.93
200644_at (MARCKSL1)	2.86
204470_at (CXCL1)	2.84
205476_at (CCL20)	2.8
211924_s_at (PLAUR)	2.8
1405_i_at (CCL5)	2.75
218681_s_at (SDF2L1)	2.73
231412_at (LOC101929709)	2.73
207980_s_at (CITED2)	2.71
206157_at (PTX3)	2.7
241592_at (RP11-567C2.1)	2.69
235835_at (CTD-2619J13.17)	2.68
222772_at (MYEF2)	2.65
44783_s_at (HEY1)	2.63
204695_at (CDC25A)	2.61
204174_at (ALOX5AP)	2.61
203665_at (HMOX1)	2.59
209101_at (CTGF)	2.58
225634_at (ZC3HAV1)	2.55

Probe Set ID (Gene Symbol)	Mean fold change
204472_at (GEM)	2.54
233057_at (HSPB8)	2.54
219916_s_at (RNF39)	2.51
208577_at (HIST1H3C)	2.5
1569003_at (VMP1)	2.49
212771_at (FAM171A1)	2.46
232047_at (LOC102725383)	2.45
222802_at (EDN1)	2.44
214913_at (ADAMTS3)	2.41
218906_x_at (KLC2)	2.41
238308_at (RP11-343H5.6)	2.4
1555976_s_at (MYL12A)	2.39
244849_at (SEMA3A)	2.37
235437_at (LA16c-380H5.5)	2.36
239532_at (RP11-559M23.1)	2.35
231589_at (LOC101928917)	2.34
207466_at (GAL)	2.33
214469_at (HIST1H2AE)	2.32
231236_at (ZFP57)	2.31
205680_at (MMP10)	2.31
203710_at (ITPR1)	2.3
202957_at (HCLS1)	2.29
226961_at (PRR15)	2.29
206683_at (ZNF165)	2.28
217039_x_at (ELK2AP)	2.28
206632_s_at (APOBEC3B)	2.26
225822_at (TMEM125)	2.26
226264_at (SUSD1)	2.25
213182_x_at (CDKN1C)	2.25
242808_at (LOC101060510)	2.25
220322_at (IL36G)	2.25
216556_x_at (SUMO1P2)	2.24
222783_s_at (SMOC1)	2.24
1557666_s_at (AK8)	2.24
206172_at (IL13RA2)	2.22
206002_at (GPR64)	2.22

Probe Set ID (Gene Symbol)	Mean fold change
204836_at (GLDC)	2.22
1554520_at (LOC283861)	2.21
219270_at (CHAC1)	2.2
230574_at (LOC100130938)	2.2
218573_at (MAGEH1)	2.2
240101_at (STAM-AS1)	2.2
209356_x_at (EFEMP2)	2.19
215285_s_at (PHTF1)	2.18
226047_at (MRVI1)	2.18
219118_at (FKBP11)	2.17
1557321_a_at (CAPN14)	2.17
201596_x_at (KRT18)	2.17
231468_at (SH3BP4)	2.16
241746_at (CUL7)	2.15
202910_s_at (CD97)	2.14
205159_at (CSF2RB)	2.14
201289_at (CYR61)	2.13
230203_at (FLJ46875)	2.13
227345_at (TNFRSF10D)	2.12
229578_at (JPH2)	2.12
232833_at (RP6-201G10.2)	2.12
228177_at (CREBBP)	2.11
208180_s_at (HIST1H4H)	2.11
219987_at (ERVMER34-1)	2.1
242957_at (VWCE)	2.1
203718_at (PNPLA6)	2.1
209304_x_at (GADD45B)	2.1
235826_at (LOC101928954)	2.1
220193_at (SH3D21)	2.09
230729_at (RP11-355B11.2)	2.09
201081_s_at (PIP4K2B)	2.09
229690_at (FAM109A)	2.09
219634_at (CHST11)	2.09
1558345_a_at (LOC439911)	2.09
225557_at (CSRNP1)	2.08
221646_s_at (ZDHHC11)	2.08

Probe Set ID (Gene Symbol)	Mean fold change
209851_at (ZC3H13)	2.08
209499_x_at (TNFSF12-TNFSF13)	2.07
240633_at (DOK7)	2.07
201702_s_at (PPP1R10)	2.07
204794_at (DUSP2)	2.06
219697_at (HS3ST2)	2.06
201693_s_at (EGR1)	2.06
230660_at (SERTAD4)	2.06
202790_at (CLDN7)	2.06
200762_at (DPYSL2)	2.05
221042_s_at (CLMN)	2.04
1552309_a_at (NEXN)	2.04
236119_s_at (SPRR2G)	2.04
206247_at (MICB)	2.04
230166_at (KIAA1958)	2.04
224239_at (DEFB103A)	2.04
212531_at (LCN2)	2.04
213629_x_at (MT1F)	2.04
229963_at (BEX5)	2.03
1554730_at (MCTP1)	2.03
225548_at (SHROOM3)	2.03
206155_at (ABCC2)	2.02
220375_s_at (C5orf66)	2.02
213435_at (SATB2)	2.01
238756_at (GAS2L3)	2.01
37892_at (COL11A1)	2.01
230934_at (LOC102724967)	2
244519_at (ASXL1)	2
1556148_s_at (RP11-16N11.2)	2
230222_at (RP11-456H18.2)	2
201006_at (PRDX2)	2
1553973_a_at (SPINK6)	1.99
209355_s_at (PPAP2B)	1.99
1564796_at (EMP1)	1.99
206969_at (KRT34)	1.99

Probe Set ID (Gene Symbol)	Mean fold change
238491_at (TAF1A-AS1)	1.99
40284_at (FOXA2)	1.98
1557070_at (TFAP2A-AS1)	1.98
1554170_a_at (MBLAC1)	1.98
1568605_at (JRK)	1.98
244126_at (PEX11G)	1.97
239303_at (PIWIL2)	1.97
226912_at (ZDHHC23)	1.96
236059_at (LOC100130428)	1.96
210761_s_at (GRB7)	1.96
205451_at (FOXO4)	1.95
226728_at (SLC27A1)	1.95
1568640_at (PCBP1-AS1)	1.95
222223_s_at (IL36RN)	1.95
215495_s_at (SAMD4A)	1.95
218676_s_at (PCTP)	1.95
205462_s_at (HPCAL1)	1.95
201473_at (JUNB)	1.94
242963_at (SGMS2)	1.94
230307_at (SLC25A21-AS1)	1.94
202525_at (PRSS8)	1.94
219918_s_at (ASPM)	1.93
203068_at (KLHL21)	1.93
218421_at (CERK)	1.93
220620_at (CRCT1)	1.92
207582_at (PIN1P1)	1.92
226838_at (TTC32)	1.92
231895_at (SASS6)	1.91
207367_at (ATP12A)	1.91
218723_s_at (RGCC)	1.91
236193_at (HIST1H2BC)	1.91
204958_at (PLK3)	1.9
208138_at (GAST)	1.9
1554522_at (CNNM2)	1.9
211263_s_at (PCSK6)	1.9
215779_s_at (HIST1H2BG)	1.9

Probe Set ID (Gene Symbol)	Mean fold change
1557383_a_at (RP5-1092A3.4)	1.9
200035_at (CTDNEP1)	1.9
1565681_s_at (DIP2C)	1.9
239852_at (MMAA)	1.89
223680_at (ZNF607)	1.89
202083_s_at (SEC14L1)	1.89
227775_at (CELF6)	1.89
231095_at (LOC101928045)	1.88
224328_s_at (LCE3D)	1.88
211899_s_at (TRAF4)	1.88
210147_at (ART3)	1.88
228433_at (NFYA)	1.88
204856_at (B3GNT3)	1.88
212013_at (PXDN)	1.88
202644_s_at (TNFAIP3)	1.88
229227_at (DICER1-AS1)	1.87
228563_at (GJC1)	1.87
206039_at (RAB33A)	1.87
221035_s_at (TEX14)	1.87
207348_s_at (LIG3)	1.87
1569052_at (RP11-288H12.4)	1.87
215150_at (YOD1)	1.87
238168_at (TM4SF1)	1.86
239144_at (B3GAT2)	1.86
206552_s_at (TAC1)	1.86
230494_at (SLC20A1)	1.86
225655_at (UHRF1)	1.86
1556158_at (FAM154B)	1.86
212185_x_at (MT2A)	1.86
218121_at (HMOX2)	1.86
205145_s_at (MYL5)	1.86
232853_at (RP11-552M11.8)	1.86
1569121_at (SLC25A24)	1.86
216005_at (TNC)	1.86
213241_at (PLXNC1)	1.86

Probe Set ID (Gene Symbol)	Mean fold change
218309_at (CAMK2N1)	1.85
237732_at (PRR9)	1.85
204533_at (CXCL10)	1.85
219990_at (E2F8)	1.85
222139_at (ERV3-2)	1.85
206752_s_at (DFFB)	1.85
211527_x_at (VEGFA)	1.85
232306_at (CDH26)	1.85
207526_s_at (IL1RL1)	1.84
1558304_s_at (TSEN54)	1.84
230187_s_at (LOC101929855)	1.84
1556784_at (RP1-178F10.1)	1.84
202708_s_at (HIST2H2BE)	1.84
205027_s_at (MAP3K8)	1.84
235365_at (DFNB59)	1.83
212759_s_at (TCF7L2)	1.83
41469_at (PI3)	1.83
201489_at (PPIF)	1.83
223929_s_at (RP11-533E19.7)	1.83
205691_at (SYNGR3)	1.83
209278_s_at (TFPI2)	1.83
235771_at (LINC00472)	1.83
220174_at (LRRC8E)	1.82
227919_at (UCA1)	1.82
239056_at (SEC22C)	1.82
215499_at (LOC100996792)	1.82
202626_s_at (LYN)	1.82
1554327_a_at (CANT1)	1.82
230815_at (LOC389765)	1.81
202627_s_at (SERPINE1)	1.81
229047_at (PLEKHB1)	1.81
1556051_a_at (BICD1)	1.8
207908_at (KRT2)	1.8
1566402_at (SNORA68)	1.8
228394_at (STK10)	1.8

Table 5. Downregulated DEGs in the SLS-treated NHKs

Probe Set ID (Gene Symbol)	Mean fold change
222484_s_at (CXCL14)	0.08
204942_s_at (ALDH3B2)	0.12
224646_x_at (H19)	0.18
229290_at (DAPL1)	0.21
1553454_at (RPTN)	0.25
207324_s_at (DSC1)	0.27
231771_at (GJB6)	0.28
235533_at (COX19)	0.29
213075_at (OLFML2A)	0.29
209383_at (DDIT3)	0.3
206642_at (DSG1)	0.31
244264_at (KLRG2)	0.32
201892_s_at (IMPDH2)	0.32
202847_at (PCK2)	0.34
228879_at (SNORA76C)	0.34
202295_s_at (CTSH)	0.34
207455_at (P2RY1)	0.34
202350_s_at (LOC100506558)	0.34
203585_at (ZNF185)	0.35
219358_s_at (ADAP2)	0.35
244289_at (ZNF300P1)	0.36
210145_at (PLA2G4A)	0.36
204542_at (ST6GALNAC2)	0.36
205433_at (BCHE)	0.36
209160_at (AKR1C3)	0.37
229886_at (C5orf34)	0.37
226226_at (TMEM45B)	0.38
205235_s_at (KIF20B)	0.38
225541_at (RPL22L1)	0.38
229130_at (AX746755)	0.39
1554447_at (JPX)	0.39
222940_at (SULT1E1)	0.39
204908_s_at (BCL3)	0.39
209596_at (MXRA5)	0.39

Probe Set ID (Gene Symbol)	Mean fold change
226448_at (FAM89A)	0.39
225731_at (ANKRD50)	0.39
225220_at (SNHG8)	0.39
212977_at (ACKR3)	0.4
231849_at (KRT80)	0.4
204469_at (PTPRZ1)	0.4
225386_s_at (HNRNPLL)	0.4
1556064_at (LOC284926)	0.4
228990_at (SNHG12)	0.4
227162_at (ZBTB26)	0.4
206023_at (NMU)	0.4
217497_at (TYMP)	0.41
224610_at (SNHG1)	0.41
1557126_a_at (PLD1)	0.41
218986_s_at (DDX60)	0.41
218377_s_at (RWDD2B)	0.41
1563805_a_at (FAM83C)	0.42
209821_at (IL33)	0.42
217693_x_at (MAGOH2)	0.42
219538_at (WDR5B)	0.42
223541_at (HAS3)	0.43
232434_at (DIRC3)	0.43
207469_s_at (PIR)	0.43
219477_s_at (LOC101930578)	0.43
238510_at (LOC101928852)	0.43
226755_at (MIR205HG)	0.43
231925_at (RP11-38P22.2)	0.44
206445_s_at (PRMT1)	0.44
240420_at (AADACL2)	0.44
228152_s_at (DDX60L)	0.44
239136_at (UNC5B-AS1)	0.44
221081_s_at (DENND2D)	0.44
226122_at (PLEKHG1)	0.44
203705_s_at (FZD7)	0.44

Probe Set ID (Gene Symbol)	Mean fold change
225505_s_at (PCED1A)	0.45
1560011_at (AX747544)	0.45
242578_x_at (SLC22A3)	0.46
205900_at (KRT1)	0.46
235857_at (KCTD11)	0.46
218897_at (TMEM177)	0.46
242998_at (RDH12)	0.46
1555942_a_at (MIR205)	0.46
219571_s_at (ZNF12)	0.46
213776_at (LOC157562)	0.46
204279_at (PSMB9)	0.46
222830_at (GRHL1)	0.47
218773_s_at (MSRB2)	0.47
225651_at (UBE2E2)	0.47
229927_at (LEMD1)	0.47
214605_x_at (GPR1)	0.48
1557192_at (COX10-AS1)	0.48
219299_at (TRMT12)	0.48
228628_at (SRGAP2C)	0.48
216532_x_at (RP3-406P24.1)	0.48
229252_at (ATG9B)	0.48
1558687_a_at (FOXN1)	0.48
201667_at (GJA1)	0.48
227791_at (SLC9A9)	0.48
229493_at (HOXD-AS2)	0.48
202687_s_at (TNFSF10)	0.48
205756_s_at (F8)	0.48
226060_at (RFT1)	0.49
215011_at (SNHG3)	0.49
229638_at (IRX3)	0.49
223496_s_at (CCDC8)	0.49
203192_at (ABCB6)	0.49
210970_s_at (IBTK)	0.49
234949_at (FRG1B)	0.49
228280_at (ZC3HAV1L)	0.49

Probe Set ID (Gene Symbol)	Mean fold change
207291_at (PRRG4)	0.49
231061_at (MIR302B)	0.49
209154_at (P2RX5-TAX1BP3)	0.49
231148_at (IGFL2)	0.5
209417_s_at (IFI35)	0.5
203132_at (RB1)	0.5
1554897_s_at (RHBDL2)	0.5
225103_at (MRPL38)	0.5
218992_at (PLGRKT)	0.5
201816_s_at (GBAS)	0.5
236500_at (RP11-285J16.1)	0.5
230281_at (C16orf46)	0.51
234863_x_at (FBXO5)	0.51
229090_at (ZEB1-AS1)	0.51
212067_s_at (C1R)	0.51
226488_at (RCCD1)	0.51
242835_s_at (LOC728730)	0.52
217973_at (DCXR)	0.52
230266_at (RAB7B)	0.52
219352_at (HERC6)	0.52
1554253_a_at (CERS3)	0.52
225836_s_at (RHNO1)	0.52
235099_at (CMTM8)	0.52
229533_x_at (ZNF680)	0.52
239151_at (BMS1P5)	0.52
217736_s_at (EIF2AK1)	0.52
219041_s_at (REPIN1)	0.52
209301_at (CA2)	0.52
232095_at (SRGAP2B)	0.52
209250_at (DEGS1)	0.52
211975_at (ARFGAP2)	0.52
1562474_at (LOC101929147)	0.52
202659_at (PSMB10)	0.53
202862_at (FAH)	0.53
205759_s_at (SULT2B1)	0.53

Probe Set ID (Gene Symbol)	Mean fold change
1557113_at (LOC283588)	0.53
1559078_at (AL833181)	0.53
220352_x_at (FLJ42627)	0.53
222016_s_at (ZSCAN31)	0.53
218383_at (HAUS4)	0.53
202575_at (CRABP2)	0.53
233013_x_at (WAC-AS1)	0.53
1552777_a_at (RAET1E)	0.53
218349_s_at (ZWILCH)	0.53
244835_at (AF086126)	0.53
228925_at (ADAM1A)	0.53
1553775_at (FLJ31715)	0.54
207345_at (FST)	0.54
221761_at (ADSS)	0.54
228531_at (SAMD9)	0.54
218686_s_at (RHBDF1)	0.54
224735_at (CYB561A3)	0.54
202820_at (AHR)	0.54
202201_at (BLVRB)	0.54
234985_at (LDLRAD3)	0.54
206539_s_at (CYP4F12)	0.54
224013_s_at (SOX7)	0.54
205047_s_at (ASNS)	0.54
222931_s_at (THNSL1)	0.54
218397_at (FANCL)	0.54
239644_at (ZC3H8)	0.54
212841_s_at (PPFIBP2)	0.54
225457_s_at (LINC00263)	0.55

Probe Set ID (Gene Symbol)	Mean fold change
206170_at (ADRB2)	0.55
204070_at (RARRES3)	0.55
219079_at (CYB5R4)	0.55
236166_at (LOC285147)	0.55
202934_at (HK2)	0.55
231886_at (LOC100134822)	0.55
223832_s_at (CAPNS2)	0.55
223168_at (RHOU)	0.55
223526_at (C18orf21)	0.55
217850_at (GNL3)	0.55
1557411_s_at (SLC25A43)	0.55
227238_at (MUC15)	0.56
244424_at (LOC439938)	0.56
234594_at (ITPK1-AS1)	0.56
205251_at (PER2)	0.56
201505_at (LAMB1)	0.56
205569_at (LAMP3)	0.56
223599_at (TRIM6)	0.56
202140_s_at (CLK3)	0.56
1552794_a_at (ZNF547)	0.56
213492_at (COL2A1)	0.56
228495_at (GPATCH11)	0.56
219905_at (ERMAP)	0.56
223647_x_at (HSCB)	0.56
209792_s_at (KLK10)	0.56
210278_s_at (AP4S1)	0.56
207463_x_at (PRSS3)	0.56

Table 6. Upregulated DEGs in the urushiol-treated NHKs

Probe Set ID (Gene Symbol)	Mean fold change
217127_at (CTH)	3.47
224239_at (DEFB103A)	3.34
226980_at (DEPDC1B)	3.03
205828_at (MMP3)	2.87
218513_at (TMA16)	2.85
236948_x_at (SRSF11)	2.85
220945_x_at (MANSC1)	2.76
244828_x_at (NAF1)	2.69
234875_at (RPL7AP10)	2.64
1561330_at (DSG4)	2.62
232056_at (SCEL)	2.55
1555382_at (POF1B)	2.54
231489_x_at (CREG2)	2.53
236129_at (GALNT5)	2.49
227919_at (UCA1)	2.49
207345_at (FST)	2.48
208257_x_at (PSG1)	2.44
214682_at (PKD1P1)	2.42
235834_at (CALD1)	2.42
210219_at (SP100)	2.38
206214_at (PLA2G7)	2.37
232071_at (MRPL19)	2.37
210282_at (ZMYM2)	2.36
212981_s_at (FAM115A)	2.36
1568955_at (SRGAP2)	2.35
205220_at (HCAR3)	2.33
207367_at (ATP12A)	2.32
229566_at (WFDC21P)	2.3
1557285_at (AREG)	2.3
227386_s_at (TMEM200B)	2.26
206170_at (ADRB2)	2.26
205367_at (SH2B2)	2.24
204935_at (PTPN2)	2.23
205718_at (ITGB7)	2.23

Probe Set ID (Gene Symbol)	Mean fold change
230127_at (RP6-99M1.2)	2.19
217144_at (UBBP1)	2.16
201110_s_at (THBS1)	2.15
235050_at (SLC2A12)	2.15
208607_s_at (SAA1)	2.15
239650_at (NCKAP5)	2.14
219795_at (SLC6A14)	2.14
230927_at (CTD-3025N20.3)	2.12
202859_x_at (CXCL8)	2.12
206192_at (CDSN)	2.12
232360_at (EHF)	2.11
211445_x_at (NACAP1)	2.1
204567_s_at (ABCG1)	2.09
223484_at (C15orf48)	2.09
223608_at (EFCAB2)	2.08
206392_s_at (RARRES1)	2.08
219280_at (BRWD1)	2.08
209387_s_at (TM4SF1)	2.08
217092_x_at (RP6-11O7.2)	2.07
222187_x_at (G3BP1)	2.07
1566402_at (SNORA68)	2.06
226908_at (LRIG3)	2.06
243188_at (ZNF283)	2.05
239478_x_at (GPATCH2L)	2.05
236488_s_at (CTD-3092A11.2)	2.05
236170_x_at (RP11-379H18.1)	2.04
242280_x_at (CPEB4)	2.04
216348_at (RPS17P5)	2.03
228283_at (CMC1)	2.03
231054_at (SPACA4)	2.02
210001_s_at (SOCS1)	2.02
1559867_at (AK056982)	2.01
217497_at (TYMP)	2.01
210876_at (ANXA2P1)	2.01

Probe Set ID (Gene Symbol)	Mean fold change
203840_at (BLZF1)	2.01
230774_at (PTGR2)	2
226402_at (CYP2U1)	2
217019_at (RPS4XP3)	1.99
244835_at (AF086126)	1.99
1557636_a_at (C7orf57)	1.98
214186_s_at (HCG26)	1.98
204444_at (KIF11)	1.98
236128_at (ZNF91)	1.98
227570_at (TMEM86A)	1.98
242458_at (RALGPS2)	1.98
205680_at (MMP10)	1.97
217205_at (AL590762.11)	1.97
203779_s_at (MPZL2)	1.97
218397_at (FANCL)	1.97
235114_x_at (HOOK3)	1.97
221100_at (C6orf15)	1.97
222297_x_at (RPL18P10)	1.96
219532_at (ELOVL4)	1.95
243550_at (ZDHHC21)	1.94
220465_at (CEBPA-AS1)	1.94
1553574_at (IFNE)	1.94
242979_at (IRS1)	1.94
227099_s_at (C11orf96)	1.94
225385_s_at (HNRNPLL)	1.93
242773_at (SLC5A1)	1.93
233252_s_at (STRBP)	1.93
224329_s_at (CNFN)	1.92
1557166_at (PDCD4)	1.92
214698_at (PTBP3)	1.92
1557236_at (APOL6)	1.92
206662_at (GLRX)	1.92
220123_at (SLC35F5)	1.92
1566140_at (HOPX)	1.92
1554314_at (C6orf141)	1.91
206595_at (CST6)	1.91

Probe Set ID (Gene Symbol)	Mean fold change
227399_at (VGLL3)	1.91
244486_at (PINK1-AS)	1.91
205027_s_at (MAP3K8)	1.91
217313_at (AC004692.5)	1.91
216650_at (RP1-130G2.1)	1.9
236396_at (LOC101927263)	1.9
210057_at (BOLA2)	1.9
243818_at (SFTA1P)	1.9
211756_at (PTHLH)	1.89
206295_at (IL18)	1.89
217379_at (RP11-209A2.1)	1.89
1561530_at (LOC101927164)	1.89
226261_at (ZNRF2)	1.89
1553454_at (RPTN)	1.89
204363_at (F3)	1.88
204120_s_at (ADK)	1.88
211361_s_at (SERPINB13)	1.87
224262_at (IL1F10)	1.87
219009_at (C14orf93)	1.87
238793_at (TIGD7)	1.87
1553605_a_at (ABCA13)	1.87
227391_x_at (LRRFIP1)	1.87
207002_s_at (PLAGL1)	1.87
237159_x_at (AP1S3)	1.87
219094_at (ARMC8)	1.87
228600_x_at (FAM221A)	1.87
230379_x_at (NDUFAF7)	1.86
224397_s_at (TMTC1)	1.86
232291_at (MIR17)	1.86
214801_at (TOR1AIP2)	1.86
228047_at (SNORA72)	1.86
1553995_a_at (NT5E)	1.86
243792_x_at (PTPN13)	1.86
210293_s_at (SEC23B)	1.86
1552532_a_at (ATP6V1C2)	1.85

Probe Set ID (Gene Symbol)	Mean fold change
230209_at (ZXDC)	1.85
218182_s_at (CLDN1)	1.85
207096_at (SAA2-SAA4)	1.85
209738_x_at (PSG6)	1.85
1567107_s_at (TPM4)	1.84
230005_at (SVIP)	1.83
206115_at (EGR3)	1.83
1552301_a_at (CORO6)	1.83
209720_s_at (SERPINB3)	1.83
1561884_at (CEPT1)	1.83
206552_s_at (TAC1)	1.83
243386_at (CASZ1)	1.82
216387_x_at (NPM1P22)	1.82
1554177_a_at (ATP5S)	1.81
235388_at (CHD9)	1.81
212824_at (FUBP3)	1.81

Probe Set ID (Gene Symbol)	Mean fold change
212364_at (MYO1B)	1.81
228397_at (TUG1)	1.81
231277_x_at (DTWD2)	1.81
219294_at (CENPQ)	1.81
215930_s_at (CTAGE5)	1.81
206188_at (ZNF623)	1.8
1553749_at (FAM76B)	1.8
244669_at (SNORD50A)	1.8
1566764_at (MACC1)	1.8
228823_at (POLR2J2)	1.8
239697_x_at (C3orf67)	1.8
1557309_at (DENND1B)	1.8
231821_x_at (LINC01061)	1.8
233011_at (ANXA1)	1.8
217125_at (UBBP2)	1.8

Table 7. Downregulated DEGs in the urushiol-treated NHKs

Probe Set ID (Gene Symbol)	Mean fold change
224646_x_at (H19)	0.25
201703_s_at (PPP1R10)	0.35
213390_at (ZC3H4)	0.36
227582_at (KLHDC9)	0.36
1568906_at (LOC728196)	0.41
227445_at (ZNF689)	0.41
227538_at (MED26)	0.42
203094_at (MAD2L1BP)	0.42
223346_at (VPS18)	0.42
202386_s_at (KIAA0430)	0.43
205094_at (PEX12)	0.43
209497_s_at (RBM4B)	0.44
214717_at (PKI55)	0.44
206914_at (CRTAM)	0.44
211975_at (ARFGAP2)	0.44
224870_at (DANCR)	0.44
219368_at (NAP1L2)	0.45
204247_s_at (CDK5)	0.45
219281_at (MSRA)	0.46
221215_s_at (RIPK4)	0.46
228855_at (NUDT7)	0.46
225557_at (CSRNP1)	0.46
205826_at (MYOM2)	0.46
224185_at (RP11-199F11.2)	0.46
204805_s_at (H1FX)	0.47
235896_s_at (MIEF2)	0.47
219885_at (SLFN12)	0.47
206587_at (CCT6B)	0.47
231858_x_at (AP5B1)	0.47
205541_s_at (GSPT2)	0.47
218248_at (FAM111A)	0.47
219773_at (NOX4)	0.47
212803_at (NAB2)	0.48
205652_s_at (TTLL1)	0.48
235532_at (RP11-226L15.5)	0.48
207068_at (ZFP37)	0.48
209182_s_at (C10orf10)	0.48
228550_at (RTN4R)	0.48
210515_at (HNF1A)	0.48
227665_at (BC062753)	0.48
227098_at (DUSP18)	0.49
210239_at (IRX5)	0.49
223630_at (C7orf13)	0.49
237048_at (RP11-66N11.8)	0.49
222484_s_at (CXCL14)	0.49
209565_at (RNF113A)	0.49
230860_at (CEP19)	0.49
204012_s_at (LCMT2)	0.5
231906_at (HOXD8)	0.5
201767_s_at (ELAC2)	0.5
227599_at (MB21D2)	0.51
218959_at (HOXC10)	0.51
1569077_x_at (ZNF836)	0.51
221135_s_at (ASTE1)	0.51
227345_at (TNFRSF10D)	0.51
202140_s_at (CLK3)	0.52
224759_s_at (TMEM263)	0.52
217796_s_at (NPLOC4)	0.52
235411_at (PGBD1)	0.52
235407_at (RABGEF1)	0.52
219730_at (LOC100996782)	0.52
209111_at (RNF5)	0.52
219352_at (HERC6)	0.52
215779_s_at (HIST1H2BG)	0.52
201341_at (ENC1)	0.53
214522_x_at (HIST1H2AD)	0.53
206515_at (CYP4F3)	0.53
235747_at (LINC00849)	0.53

Probe Set ID (Gene Symbol)	Mean fold change
222075_s_at (OAZ3)	0.53
235176_at (ZFP82)	0.53
203342_at (TIMM17B)	0.53
243179_at (RP1-151F17.2)	0.53
228208_x_at (ZNF354C)	0.53
225621_at (ALG2)	0.53
1553881_at (MGC16142)	0.53
218559_s_at (MAFB)	0.54
209732_at (CLEC2B)	0.54
203474_at (IQGAP2)	0.54
204436_at (PLEKHO2)	0.54
214965_at (SPATA2L)	0.54
229796_at (SIX4)	0.54
204768_s_at (FEN1)	0.54
207740_s_at (NUP62)	0.54
223378_at (GLIS2)	0.54
206182_at (ZNF134)	0.54
219394_at (PGS1)	0.54
223394_at (SERTAD1)	0.54
212838_at (DNMBP)	0.54
227379_at (MBOAT1)	0.55
1568932_at (BC034636)	0.55
214910_s_at (APOM)	0.55
244758_at (ZBED9)	0.55
224509_s_at (RTN4IP1)	0.55
219303_at (RNF219)	0.55
241602_at (ZNF582)	0.55
228769_at (ZSCAN22)	0.55

Probe Set ID (Gene Symbol)	Mean fold change
218735_s_at (ZNF544)	0.55
231815_at (PHF12)	0.55
214469_at (HIST1H2AE)	0.55
213041_s_at (ATP5D)	0.55
230598_at (RP11-554J4.1)	0.55
203062_s_at (MDC1)	0.55
229449_at (CTA-445C9.15)	0.56
225804_at (CYB5D2)	0.56
226800_at (EFCAB7)	0.56
242625_at (RSAD2)	0.56
220786_s_at (SLC38A4)	0.56
241827_at (ZNF615)	0.56
202492_at (ATG9A)	0.56
231061_at (MIR302B)	0.56
222760_at (ZNF703)	0.56
213407_at (PHLPP2)	0.56
231832_at (GALNT4)	0.56
1560503_a_at (TFAP2A-AS1)	0.56
209179_s_at (MBOAT7)	0.56
204420_at (FOSL1)	0.56
226891_at (XXYLT1)	0.56
218993_at (RNMTL1)	0.56
203139_at (DAPK1)	0.56
219123_at (ZNF232)	0.56
226515_at (CCDC127)	0.56
219063_at (C1orf35)	0.56
235230_at (PLCXD2)	0.56
213043_s_at (MED24)	0.56

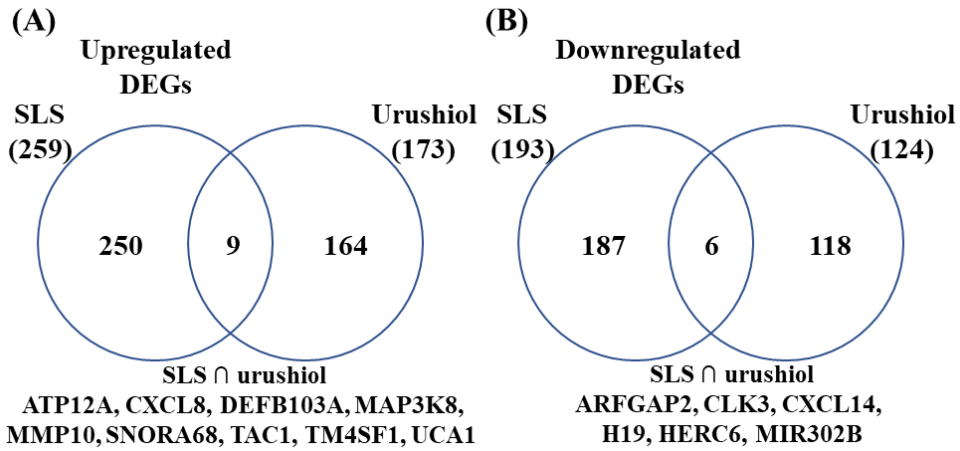

Fig. 13. Venn diagrams for DEGs in SLS- or urushiol-treated NHKs. The Venn diagrams show numbers of selected DEGs in SLS- or urushiol-treated NHKs. Commonly upregulated (A) and downregulated (B) DEGs were shown in Gene Symbol.

2. GO BP enrichment analysis in SLS-induced or urushiol-induced DEGs

As shown in the table 8, SLS-induced upregulated DEGs were significantly enriched in pro-inflammatory response, such as the inflammatory response (GO:0006954), cellular response to calcium ion (GO:0071277), immune response (GO:0006955), and cellular response to lipopolysaccharide (GO:0071222). The significant enriched in the urushiol-induced upregulated DEGs also pro-inflammatory biological process, including cytokine-mediated signaling pathway (GO:0019221) and inflammatory response (GO:0006954). In the SLS-induced downregulated DEGs, GO BPs such as chemotaxis (GO: 0006935), oxidation-reduction process (GO:0055114), cornification (GO:0070268), G1/S transition of the mitotic cell cycle (GO:0000082), keratinization (GO:0031424), and cellular protein metabolic process (GO:0044267) were significantly suppressed in NHKs. Only three GO BP terms, nervous system development (GO:0007399), positive regulation of cell proliferation (GO:0008284), and cellular protein metabolic process (GO:0044267) were significantly downregulated in urushiol-treated NHKs.

Table 8. Enriched Gene Ontology biological processes in the SLS- or urushiol-induced DEGs in NHKs

		GO Term ID	GO BP Terms	P value (*chi* test)	Gene symbol (fold change)
Up	SLS-enriched GO BPs in 259 DEGs	GO:0006954	inflammatory response	<0.0001	CXCL8 (6.21), TNF (3.81), FOS (3.03), CXCL1 (2.84), CCL20 (2.80), CCL5 (2.75), PTX3 (2.7), GAL (2.33), IL36G (2.25), CD97 (2.14), TNFRSF10D (2.12), IL36RN (1.95), TNFAIP3 (1.88), TAC1 (1.86), CXCL10 (1.85), LYN (1.82)
		GO:0070268	cornification	<0.0001	KRT37 (2.93), KRT18 (2.17), SPRR2G (2.04), SPINK6 (1.99), PRSS8 (1.94), PCSK6 (1.9), LCE3D (1.88), PI3 (1.83), KRT2 (1.8)
		GO:0018149	peptide cross-linking	<0.0001	LCE2B (3.65), SPRR2G (2.04), CRCT1 (1.92), LCE3D (1.88), PRR9 (1.85), PI3 (1.83), KRT2 (1.80)
		GO:0071277	cellular response to calcium ion	<0.0001	FOS (3.03), ALOX5AP (2.61), EDN1 (2.44), JUNB (1.94), SLC25A24 (1.86), PPIF (1.83)
		GO:0006955	immune response	<0.0001	CXCL8 (6.21), TNF (3.81), CXCL1 (2.84), CCL20 (2.8), CCL5 (2.75), GEM (2.54), CD97 (2.14), TNFRSF10D (2.12), MICB (2.04), PXDN (1.88), TNFAIP3 (1.88), CXCL10 (1.85), IL1RL1 (1.84)
		GO:0071222	cellular response to lipopoly-saccharide	<0.0001	CXCL8 (6.21), CCL20 (2.8), CCL5 (2.75), LCN2 (2.04), ABCC2 (2.02), TNFAIP3 (1.88), CXCL10 (1.85), SERPINE1 (1.81)
		GO:0032868	response to insulin	<0.0001	FABP3 (3.07), CCL5 (2.75), GAL (2.33), EGR1 (2.06), SLC27A1 (1.95), LYN (1.82)
	Urushiol-enriched GO BPs in 173 DEGs	GO:0043434	response to peptide hormone	0.0002	AREG (2.3), SOCS1 (2.02), IRS1 (1.94) ANXA1 (1.8)
		GO:0030216	keratinocyte differentiation	0.0003	DSG4 (2.62), SCEL (2.55), CDSN (2.12), ANXA1 (1.8)
		GO:0008544	epidermis development	0.0007	SCEL (2.55), CDSN (2.12), CST6 (1.91), PTHLH (1.89)
		GO:0019221	cytokine-mediated signaling pathway	0.0008	SP100 (2.38), SH2B2 (2.24), PTPN2 (2.23), SOCS1 (2.02), IFNE (1.94), F3 (1.88), IL1F10 (1.87)
		GO:0006928	movement of cell or subcellular component	0.0011	CALD1 (2.42), CXCL8 (2.12), TPM4 (1.84), ANXA1 (1.8)
		GO:0055086	nucleobase-containing small molecule metabolic process		TYMP (2.01), GLRX (1.92), ADK (1.88), NT5E (1.86)
		GO:0007565	female pregnancy	0.0019	PSG1 (2.44), ADRB2 (2.26), PTHLH (1.89), PSG6 (1.85)
		GO:0006954	inflammatory response	0.0131	SP100 (2.38), THBS1 (2.15), CXCL8 (2.12), IL18 (1.89), IL1F10 (1.87), TAC1 (1.83), ANXA1 (1.8)
Down	SLS-enriched GO BPs in 193 DEGs	GO:0006935	chemotaxis	0.0001	CXCL14 (0.04), ACKR3 (0.40), TYMP (0.41), PLD1 (0.41), PLGRKT (0.5), CMTM8 (0.52)
		GO:0055114	oxidation-reduction process	0.0001	ALDH3B2 (0.12), IMPDH2 (0.32), AKR1C3 (0.37), PIR (0.43), RDH12 (0.46), MSRB2 (0.47), F8 (0.48), DCXR (0.52), DEGS1 (0.52), CYB561A3 (0.54), BLVRB (0.54), CYP4F12 (0.54), CYB5R4 (0.55)
		GO:0070268	cornification	0.0003	RPTN (0.25), DSC1 (0.27), DSG1 (0.31), KRT80 (0.4), KRT1 (0.46)
		GO:0000082	G1/S transition of mitotic cell cycle	0.0030	PSMB9 (0.46), RB1 (0.5), FBXO5 (0.51), PSMB10 (0.53), RHOU (0.55)
		GO:0031424	keratinization	0.0054	DSC1 (0.27), DSG1 (0.31), KRT80 (0.4), KRT1 (0.46)
		GO:0044267	cellular protein metabolic pro-cess	0.0137	COX19 (0.29), DDIT3 (0.3), CTSH (0.34), ST6GALNAC2 (0.36), BCHE (0.36), MSRB2 (0.47), F8 (0.48), RFT1 (0.49), ARFGAP2 (0.52), ASNS (0.54), MUC15 (0.56)
	Urushiol-enriched GO BPs in 127 DEGs	GO:0007399	nervous system development	0.0384	NAB2 (0.48), ENC1 (0.53), MAFB (0.54), GLIS2 (0.54)
		GO:0008284	positive regulation of cell pro-liferation	0.0425	CTGF (0.24), HOXC10 (0.51), SERTAD1 (0.54), ZNF703 (0.56), FOSL1 (0.56)
		GO:0044267	cellular protein metabolic pro-cess	0.0478	ARFGAP2 (0.44), MSRA (0.46), GSPT2 (0.47), TIMM17B (0.53), ALG2 (0.53), NUP62 (0.54), MDC1 (0.55)

* '#' denotes 'number'

3. Validation of DEGs in formaldehyde-treated NHKs

DEGs selected by microarray results were validated by independent measurement, Q-RT-PCR and Western blotting. For the SLS-upregulated DEGs, the transcription of *CXCL8*, *TNF*, *CCL5*, *JUNB*, *FOS*, and *SPRR2G* and the SLS-downregulated DEGs, *CXCL14* and *H19*, were confirmed with independently prepared NHKs (Fig. 14).

The transcriptions of *CXCL8*, *SP100*, *SOCS1*, *THBS1*, *ANXA1*, and *DSG4* were confirmed by Q-RT-PCR in urushiol-upregulated DEGs, because they were significantly associated with enriched GO BPs (Fig. 15). In the inflammatory response-associated DEGs, the *CXCL8*, *SOCS1* and *THBS1* upregulated by urushiol were validated in NHKs, but microarray expression of *SP100* was not confirmed by Q-RT-PCR (Fig. 15B). The mRNA levels of keratinocyte differentiation-associated DEGs, *ANXA1* and *DSG4*, were significantly upregulated by urushiol in NHKs (Fig. 15E and F). The gene transcriptions of *CXCL14* and *H19* were also significantly downregulated in urushiol-treated NHKs (Fig. 15G and H). Although the gene transcription of SP100 was not validated in urushiol-treated NHKs, the microarray expression of DEGs associated with inflammation and epidermal differentiation was confirmed for both SLS- and urushiol treated NHKs.

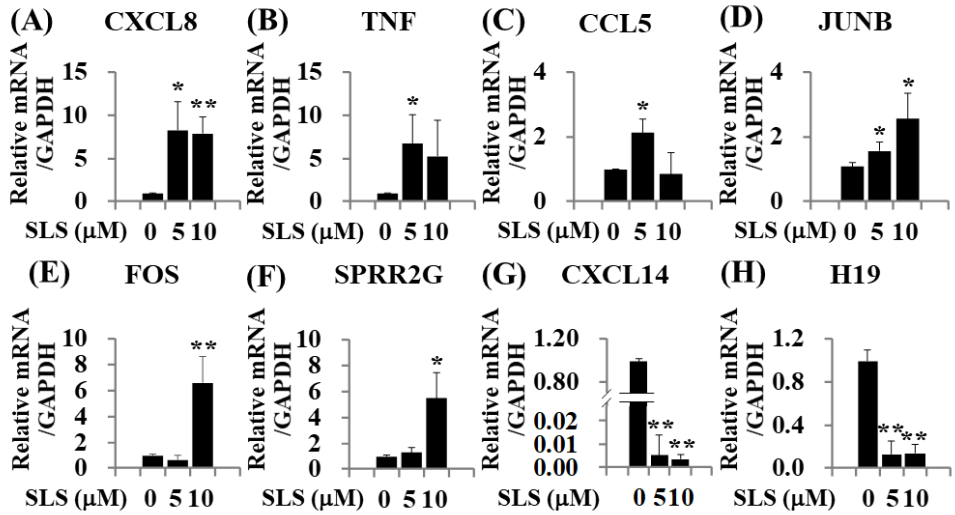

Fig. 14. Validation of the microarray results in response to SLS using Q-RT-PCR. To determine the mRNA levels of CXCL8 (A), TNF (B), CCL5 (C), JUNB (D), FOS (E), SPRR2G (F), CXCL14 (G) and H19 (H). Values represent the mean ± SD of the mRNA of the various genes relative to human GAPDH expression (n = 3). *$p < 0.05$ and **$p < 0.01$.

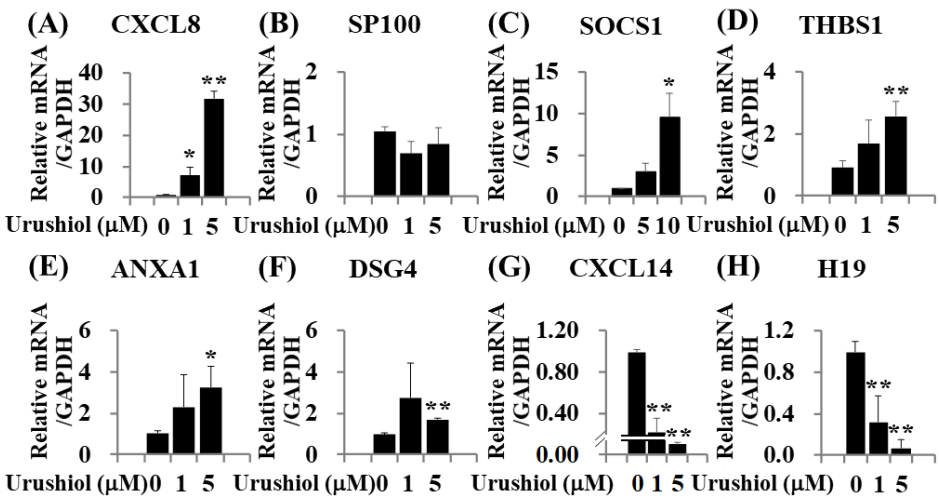

Fig. 15. Validation of the microarray results in response to urushiol using Q-RT-PCR. To determine the mRNA levels of CXCL8 (A), SP100 (B), SOCS1 (C), THBS1 (D), ANXA1 (E), DSG4 (F), CXCL14 (G) and H19 (H). Values represent the mean ± SD of the mRNA of the various genes relative to human GAPDH expression (n = 3). *$p < 0.05$ and **$p < 0.01$.

4. Temporal expression profile of DEGs in NHKs treated with sensitizers and non-sensitizers

The transcription levels of two chemokines, *CXCL8/IL-8* and *CXCL14*, were affected on SLS- or urushiol-induced NHKs. *CXCL8/IL-8* upregulation in KCs and dendritic cells (DC) has been well known as an essential biomarker for *in vitro* skin sensitization tests (Coquette et al., 2003; Bae et al., 2015a). However, *CXCL14* has not been studied much as an *in vitro* toxicity test. SLS, methyl salicylate, urushiol and 2-mercaptobenzothiazole significantly increased *CXCL8/IL-8* in NHKs (Fig. 16A-D). In contrast, *CXCL14* was significantly decreased by SLS, urushiol, and 2-mercaptobenzothiazole but methyl salicylate did not affect *CXCL14* gene transcription in NHKs (Fig. 16E-H). IFNγ, IL-4 and IL-22 downregulated the constitutive *CXCL14* expression (Jin et al., 2014), suggesting that the downregulation of *CXCL14* have an important role in epidermal immune response such as allergenic reaction in NHKs.

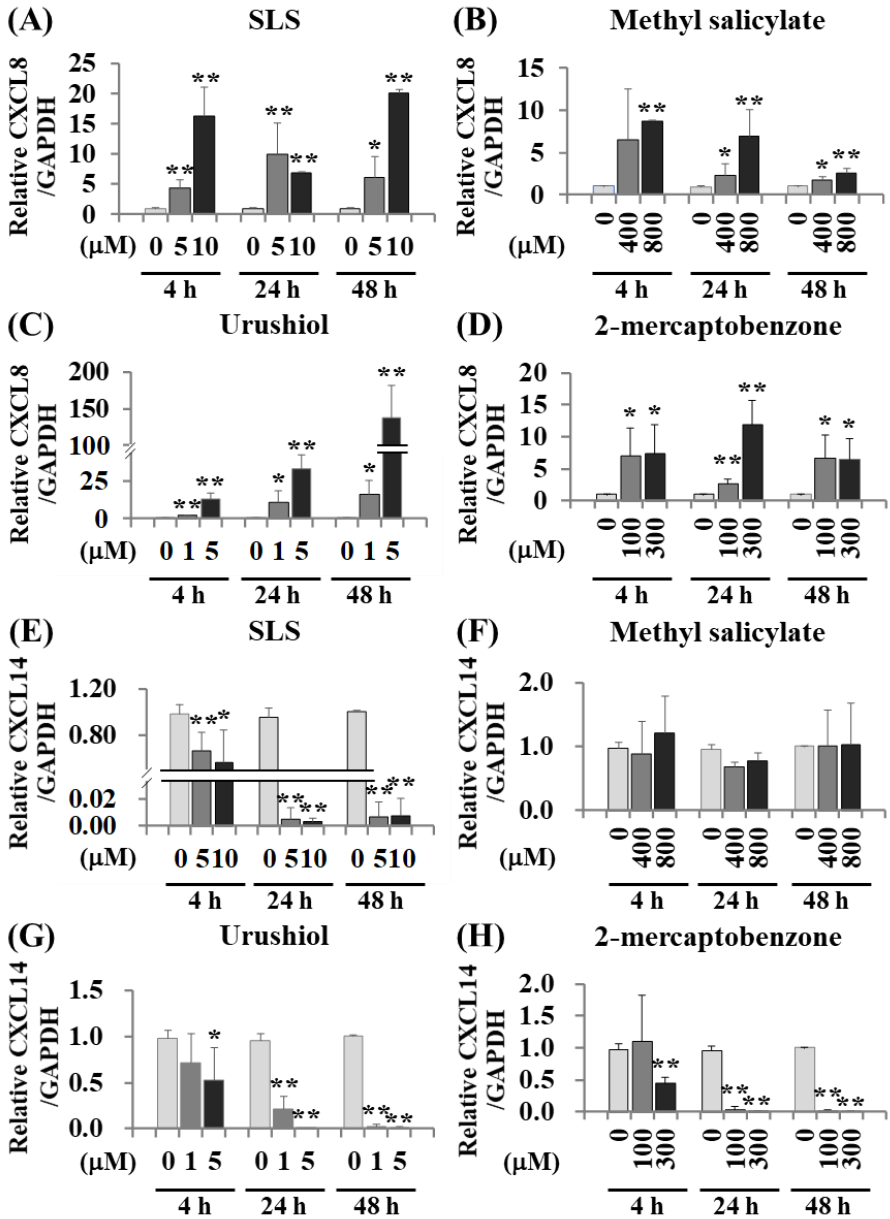

Fig. 16. Temporal expression profile in NHKs treated with non-sensitizers or sensitizers using Q-RT-PCR. CXCL8 mRNA levels in NHKs treated with SLS (A), methyl salicylate (B), urushiol (C) and 2-mercaptobenzothiazole (D), and CXCL14 mRNA levels in NHKs treated with SLS (E), methyl salicylate (F), urushiol (G) and 2-mercaptobenzothiazole (H) were measured. Values represent the mean ± SD of the mRNA of the various genes relative to human GAPDH expression (n = 3). *$p < 0.05$ and **$p < 0.01$.

5. Effects of non-sensitizers and sensitizers on expression of CXCL8 and CXCL14

As shown in the table 9, Among sixteen OECD TG 429 reference sensitizers, 10 sensitizers, including isoeugenol, citral, cinnamic alcohol, imidazolidinyl urea, cobalt chloride, DNCB, 4-phenylene diamine, 2-mercaptobenzothiazole, phenyl benzoate, and methyl methacrylate significantly increased CXCL8 protein expression in NHKs (Fig. 17A). In contrast, ten sensitizers, cobalt chloride, DNCB, 4-phenylene diamine, 2-mercaptobenzothiazole, phenyl benzoate, methyl methacrylate, CMI/MI, HCA, nickel chloride, and ethylene glycol dimethacrylate significantly decreased protein expression level of CXCL14 in NHKs (Fig. 17A). In addition, six sensitizers, cobalt chloride, DNCB, 4-phenylene diamine, 2-mercaptobenzothiazole, phenyl benzoate, and methyl methacrylate significantly influenced protein expression of both CXCL8/IL-8 and CXCL14 in NHKs (Fig. 17A). Among the TG429 reference non-sensitizers, only SLS significantly decreased CXCL14 (Table 10, Fig. 17B). The downregulation of CXCL14 as a biomarker increased the specificity and accuracy for the predictive performance (Fig. 17C). Therefore, CXCL14 may be a more selective biomarker than CXCL8 to distinguish between human sensitizers and human skin non-sensitizers.

Table 9. Effects of human skin sensitizers in NHKs

OECD TG429 substances (CAS number)					
CMI/MI (26172-55-4) /	Chemical concentration (μm)	0 (vehicle)	50	10	2
human sensitizer (+), LLNA (+)	Cell survival (%)	100 ± 9	37 ± 12**	103 ± 8	95 ± 7
	CXCL14 (pg/ml)	130 ± 19	9 ± 5**	30 ± 24**	52 ± 34**
	IL-8 (pg/ml)	12 ± 8	20 ± 17	15 ± 5	22 ± 12*
DNCB (97-00-7)	Chemical concentration (μm)	0 (vehicle)	10	2	0.4
human sensitizer (+), LLNA (+)	Cell survival (%)	100 ± 7	6 ± 4**	61 ± 18**	84 ± 6*
	CXCL14 (pg/ml)	146 ± 33	55 ± 14**	25 ± 24**	136 ± 67
	IL-8 (pg/ml)	15 ± 1	26 ± 10	13 ± 1	16 ± 4
4-phenylene diamine (106-50-3)	Chemical concentration (μm)	0 (vehicle)	10	2	0.4
human sensitizer (+), LLNA (+)	Cell survival (%)	100 ± 8	22 ± 7**	68 ± 18*	98 ± 8
	CXCL14 (pg/ml)	141 ± 17	23 ± 5**	18 ± 18**	135 ± 36
	IL-8 (pg/ml)	16 ± 8	87 ± 26**	81 ± 36*	15 ± 13
Cobalt chloride (7646-79-9)	Chemical concentration (μm)	0 (vehicle)	50	10	2
human sensitizer (+), LLNA (+)	Cell survival (%)	100 ± 8	56 ± 18**	90 ± 6	97 ± 2
	CXCL14 (pg/ml)	117 ± 42	41 ± 15*	48 ± 21*	105 ± 38
	IL-8 (pg/ml)	13 ± 11	386 ± 27**	88 ± 33**	13 ± 5
Nickel chloride (7718-54-9)	Chemical concentration (μm)	0 (vehicle)	50	10	2
human sensitizer (+), LLNA (-)	Cell survival (%)	100 ± 8	26 ± 8**	100 ± 8	102 ± 8
	CXCL14 (pg/ml)	139 ± 19	36 ± 8**	76 ± 16**	93 ± 28*
	IL-8 (pg/ml)	15 ± 3	14 ± 2	13 ± 2	15 ± 3
Isoeugenol (97-54-1)	Chemical concentration (μm)	0 (vehicle)	10	2	0.4
human sensitizer (+), LLNA (+)	Cell survival (%)	100 ± 8	16 ± 8**	59 ± 19**	92 ± 8
	CXCL14 (pg/ml)	130 ± 32	180 ± 39	104 ± 39	143 ± 59
	IL-8 (pg/ml)	17 ± 8	45 ± 18*	5 ± 4	7 ± 2
2-Mercaptobenzothiazole (149-30-4)	Chemical concentration (μm)	0 (vehicle)	50	10	2
human sensitizer (+), LLNA (+)	Cell survival (%)	100 ± 8	99 ± 8	102 ± 8	99 ± 7
	CXCL14 (pg/ml)	128 ± 22	15 ± 5**	50 ± 20**	138 ± 29
	IL-8 (pg/ml)	12 ± 11	749 ± 45**	576 ± 174**	35 ± 11*
Citral (5392-40-5)	Chemical concentration (μm)	0 (vehicle)	10	2	0.4
human sensitizer (+), LLNA (+)	Cell survival (%)	100 ± 8	11 ± 5**	91 ± 8	98 ± 3
	CXCL14 (pg/ml)	133 ± 16	194 ± 18**	133 ± 22	133 ± 20
	IL-8 (pg/ml)	16 ± 4	130 ± 27**	15 ± 4	15 ± 3

OECD TG429 substances (CAS number)					
HCA (101-86-0)	Chemical concentration (μm)	0 (vehicle)	10	2	0.4
human sensitizer (+), LLNA (+)	Cell survival (%)	100 ± 10	50 ± 18**	103 ± 9	106 ± 11
	CXCL14 (pg/ml)	126 ± 24	80 ± 14*	102 ± 42	119 ± 22
	IL-8 (pg/ml)	16 ± 3	14 ± 1	13 ± 2	14 ± 2
Eugenol (97-53-0)	Chemical concentration (μm)	0 (vehicle)	10	2	0.4
human sensitizer (+), LLNA (+)	Cell survival (%)	100 ± 8	9 ± 1**	76 ± 6**	96 ± 8
	CXCL14 (pg/ml)	137 ± 18	111 ± 44	105 ± 29	119 ± 30
	IL-8 (pg/ml)	15 ± 2	19 ± 3	12 ± 2	13 ± 2
phenyl benzoate (93-99-2)	Chemical concentration (μm)	0 (vehicle)	50	10	2
human sensitizer (+), LLNA (+)	Cell survival (%)	100 ± 10	86 ± 9	106 ± 8	105 ± 7
	CXCL14 (pg/ml)	130 ± 23	96 ± 16	97 ± 10*	120 ± 36
	IL-8 (pg/ml)	14 ± 6	23 ± 8	13 ± 1	13 ± 2
Cinnamic alcohol (104-54-1)	Chemical concentration (μm)	0 (vehicle)	10	2	0.4
human sensitizer (+), LLNA (+)	Cell survival (%)	100 ± 10	51 ± 5**	104 ± 8	107 ± 10
	CXCL14 (pg/ml)	135 ± 22	157 ± 16	112 ± 14	114 ± 21
	IL-8 (pg/ml)	15 ± 1	176 ± 33**	16 ± 2	17 ± 1*
Imidazolidinyl urea (39236-46-9)	Chemical concentration (μm)	0 (vehicle)	10	2	0.4
human sensitizer (+), LLNA (+)	Cell survival (%)	100 ± 8	34 ± 13**	100 ± 8	98 ± 8
	CXCL14 (pg/ml)	128 ± 25	115 ± 27	116 ± 26	137 ± 33
	IL-8 (pg/ml)	15 ± 3	169 ± 15**	18 ± 3	16 ± 2
Methyl methacrylate (80-62-6)	Chemical concentration (μm)	0 (vehicle)	50	10	2
human sensitizer (+), LLNA (+)	Cell survival (%)	100 ± 10	69 ± 5**	106 ± 9	103 ± 12
	CXCL14 (pg/ml)	127 ± 17	68 ± 14**	80 ± 8**	120 ± 39
	IL-8 (pg/ml)	14 ± 7	34 ± 8*	16 ± 10	14 ± 10
Isopropanol (67-63-0)	Chemical concentration (μm)	0 (vehicle)	50	10	2
human sensitizer (+), LLNA (-)	Cell survival (%)	100 ± 8	99 ± 7	95 ± 7	100 ± 8
	CXCL14 (pg/ml)	144 ± 25	176 ± 35	158 ± 23	147 ± 22
	IL-8 (pg/ml)	14 ± 6	17 ± 4	23 ± 14	16 ± 4
Ethylene glycol dimethacrylate (97-90-54)	Chemical concentration (μm)	0 (vehicle)	50	10	2
human sensitizer (+), LLNA (+)	Cell survival (%)	100 ± 7	17 ± 3**	82 ± 8*	99 ± 7
	CXCL14 (pg/ml)	127 ± 12	30 ± 17**	51 ± 4**	114 ± 12
	IL-8 (pg/ml)	15 ± 3	20 ± 5	8 ± 5*	7 ± 1**

CMI/MI = 5-chloro-2-methyl-4-isothiazolin-3-one/2-methyl-4-isothiazolin-3-one, DNCB = 2,4dinitrochlorobenzene, HCA= hexyl cinnamic alcohol. * Denotes $p < 0.05$ (n = 3). ** Denotes $p < 0.01$ (n = 3), when compared to the values of vehicle-treated samples.

Table 10. Effects of human skin non-sensitizers in NHKs

OECD TG429 substances (CAS number)					
Chlorobenzene (108-90-7)	Chemical concentration (μm)	0 (vehicle)	50	10	2
human sensitizer (-), LLNA (-)	Cell survival (%)	100 ± 7	100 ± 7	95 ± 8	95 ± 7
	CXCL14 (pg/ml)	118 ± 36	100 ± 8	100 ± 9	114 ± 10
	IL-8 (pg/ml)	15 ± 2	44 ± 17*	24 ± 4**	36 ± 8**
Lactic acid (50-21-5)	Chemical concentration (μm)	0 (vehicle)	50	10	2
human sensitizer (-), LLNA (-)	Cell survival (%)	100 ± 10	23 ± 4**	97 ± 12	100 ± 11
	CXCL14 (pg/ml)	127 ± 12	136 ± 31	118 ± 36	126 ± 23
	IL-8 (pg/ml)	15 ± 6	9 ± 1	16 ± 6	19 ± 2
Methyl salicylate (119-36-8)	Chemical concentration (μm)	0 (vehicle)	50	10	2
human sensitizer (-), LLNA (-)	Cell survival (%)	100 ± 9	17 ± 4**	93 ± 9	99 ± 9
	CXCL14 (pg/ml)	126 ± 26	113 ± 37	100 ± 46	121 ± 45
	IL-8 (pg/ml)	16 ± 4	26 ± 10	93 ± 25**	26 ± 6*
Salicylic acid (69-72-7)	Chemical concentration (μm)	0 (vehicle)	50	10	2
human sensitizer (-), LLNA (-)	Cell survival (%)	100 ± 7	23 ± 2**	92 ± 7	98 ± 8
	CXCL14 (pg/ml)	130 ± 21	144 ± 49	146 ± 39	145 ± 42
	IL-8 (pg/ml)	15 ± 1	94 ± 26**	40 ± 8**	29 ± 3**
Sodium lauryl sulfate (151-21-3)	Chemical concentration (μm)	0 (vehicle)	10	2	0.4
human sensitizer (-), LLNA (+)	Cell survival (%)	100 ± 7	18 ± 3**	85 ± 10	103 ± 8
	CXCL14 (pg/ml)	140 ± 18	29 ± 3**	55 ± 8**	139 ± 21
	IL-8 (pg/ml)	21 ± 3	278 ± 55**	2 ± 2**	4 ± 1**
Xylene (1330-20-7)	Chemical concentration (μm)	0 (vehicle)	50	10	2
human sensitizer (-), LLNA (+)	Cell survival (%)	100 ± 8	18 ± 3**	98 ± 7	104 ± 7
	CXCL14 (pg/ml)	135 ± 34	166 ± 56	133 ± 15	133 ± 20
	IL-8 (pg/ml)	15 ± 1	25 ± 9	24 ± 5**	28 ± 5**

* Denotes $p < 0.05$ (n = 3). ** Denotes $p < 0.01$ (n = 3), when compared to the values of vehicle-treated samples.

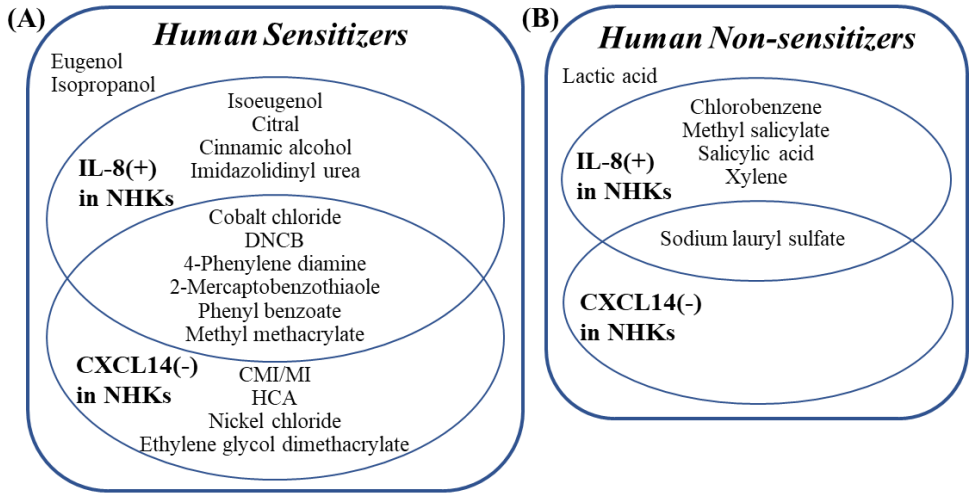

(C)

Human	CXCL8/IL-8		CXCL14	
	Positive	Negative	Positive	Negative
16 sensitizers	10	6	10	6
6 non-sensitizers	5	1	1	5
Sensitivity (%)	62.5		62.5	
Specificity (%)	16.7		83.3	
Accuracy (%)	66.7		90.9	

Fig. 17. Venn diagram representing the effect of human sensitizers and non-sensitizers on CXCL8 and/or CXCL14 production in NHKs. The effects of sixteen reference sensitizers (A) in Table 9, and six reference non-sensitizers (B) in Table 10 were classified in the Venn diagram according to the significant upregulation of CXCL8 or the downregulation of CXCL14 in NHKs. The predictive performance was calculated as sensitivity, specificity and accuracy (C).

6. Downregulation of CXCL14 related to the JAK/STAT and MAPK signaling pathways in NHKs

The SLS-induced CXCL14 downregulation was significantly suppressed by the MAPK/ERK inhibitor PD98059 and the JAK3 inhibitor WHI-P131 (Fig. 18A). JAK1 inhibitor piceatannol and the JAK2 inhibitor AG490 had no effect on down-regulation of the SLS-induced CXCL14 (Fig. 18A). Both PD98059 and WHI-P131 significantly decreased CXCL14 in a dose-dependent manner (Fig. 18B). SLS up-regulated the phosphorylation of ERK and STAT6 in NHKs. The MAPK/ERK inhibitor PD9805 significantly inhibited the phosphorylation of ERK by SLS and the JAK3 inhibitor WHI-P131 significantly inhibited the phosphorylation of the SLS-induced STAT6 (Fig. 18C-F).

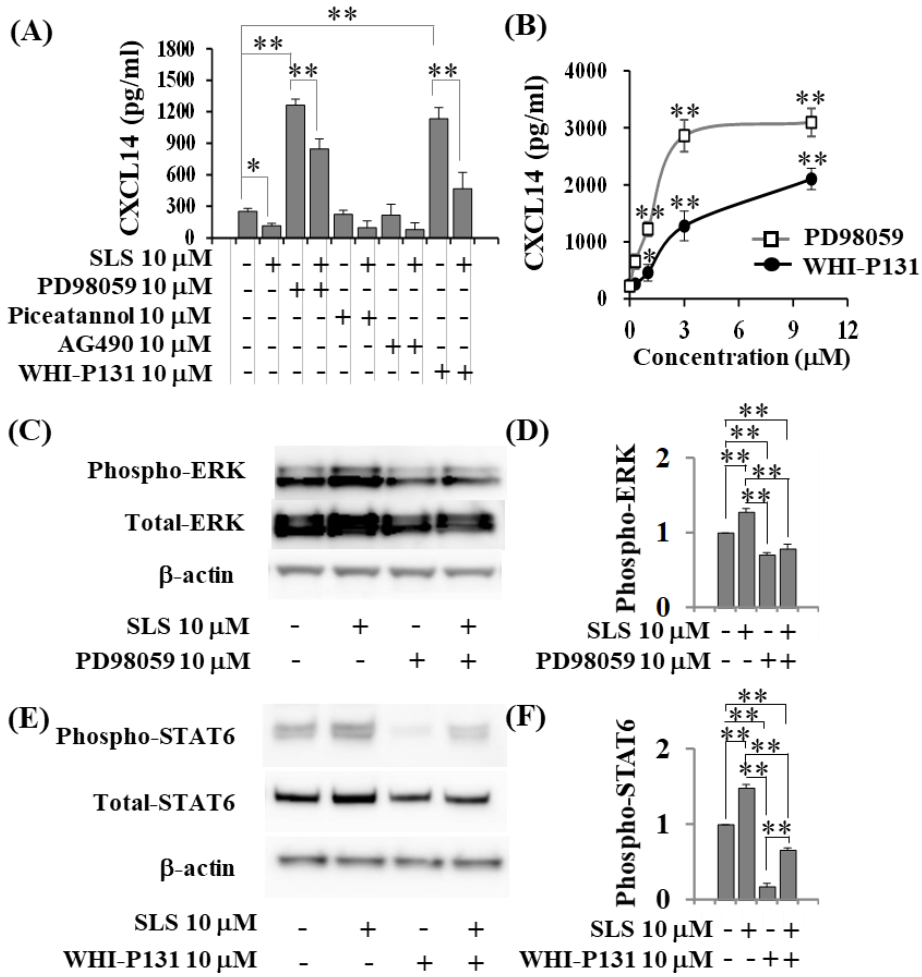

Fig. 18. Effects of SLS on MAPK and STAT6 signaling pathways in NHKs. (A) the expression levels of CXCL14 protein expression by PD98059 and WHI-P131 using ELISA, (B) Results of phospho-ERK by PD98059 (C and D), phospho-STAT6 by WHI-P131 (E and F) in SLS-treated NHKs compared to β-actin levels (n=3, independent experiments). Values represent the mean ± SD. *$p < 0.05$ and **$p < 0.01$.

Chapter 3. Effects of photoactivated BP-3 in NHKs

1. Effects of BP-3 in *PDE4B* gene transcription by in UVB-irradiated NHKs

In this study, we investigated the effects to PDE4B with 17 commercially available sunscreen agents (Fig. 19). When NHKs were treated with 10 μM of each sunscreen agent for 24 h, BP-3 and BP-8 significantly upregulated *PDE4B* transcription by 4.71 and 2.27 folds respectively, compared with vehicle control. Avobenzone and octocrylene upregulated *PDE4B* by 1.85- and 1.88-fold, although the increases were not statistically significant. Therefore, we selected BP-3 to study the role of PDE4B in the phototoxic responses in NHKs caused by organic sunscreen agents.

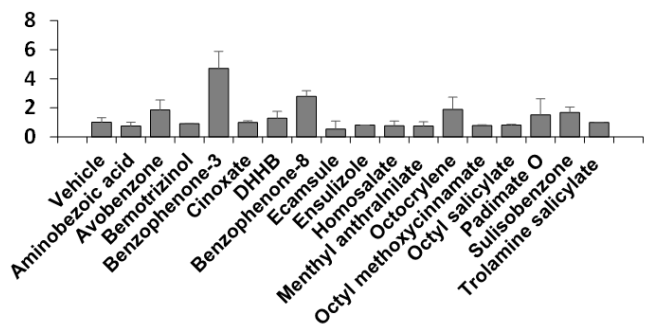

Fig. 19. Effects of *PDE4B* gene transcription by commercial sunscreen agents in NHKs. mRNA levels of *PDE4B* in NHKs after treatment with commercially available sunscreen agents by Q-RT-PCR. Values represent the mean ± SD. *$p < 0.05$ and **$p < 0.01$.

We determined the cell culture conditions may not cause significant cell death to study the toxicological mechanisms of BP-3-induced phototoxicity in NHKs. No

difference in cell viability was detected in NHKs irradiated with 20 mJ/cm^2 UVB for 24 h in culture compared to that of the control (Fig. 20A). No apparent cytotoxicity was observed in culture up to a dose of 25 μM BP-3 (Fig. 20B). To investigate UVB-irradiated BP-3 under non-cytotoxic conditions, we evaluated the concentration-dependent cytotoxic effects of BP-3 on NHKs under a fixed dose of UVB irradiation (Fig. 20C). After 20 mJ/cm^2 UVB, 20 μM BP-3 decreased the viability of NHKs compared to the vehicle treatment. Therefore, we selected 20 mJ/cm^2 UVB and 10 μM BP-3 as the maximum treatment doses to investigate their combined effects on phototoxicity in NHKs. The treatment with only UVB increased the gene transcription of *PDE4B* in a dose-dependent manner in NHKs (Fig. 20D). mRNA levels of *PDE4B* were additively upregulated in NHKs co-treated with UVB and BP-3 (Fig. 20D). In addition, PDE4B protein levels were synergistically upregulated in NHKs by both UVB and BP-3 (Fig. 20E and F).

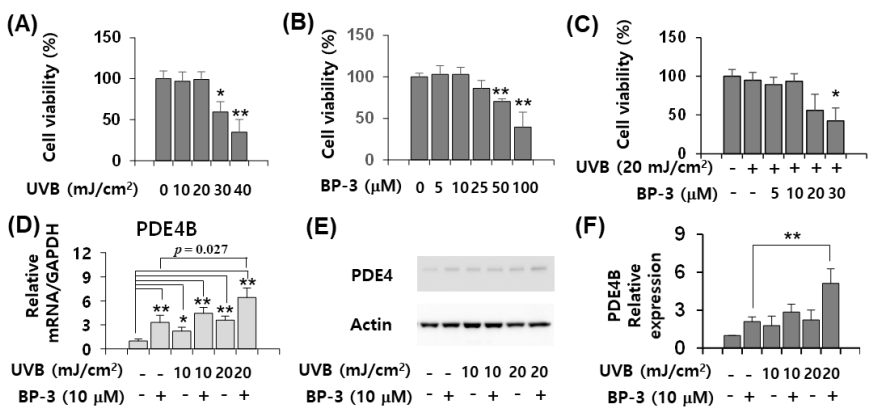

Fig. 20. *PDE4B* gene transcription by UVB, BP-3 or UVB-activated BP-3 in NHKs. (A) Cell viability was evaluated 24 h after treatment of UVB (B), BP-3 (C), or both UVB and BP-3 (D). *PDE4B* mRNA (E) and protein levels (F) were measured respectively, 24 h after NHKs were treated individually or with a combination of BP-3 and UVB. (G) Three independent PDE4 Western blotting results were quantified against β-actin using ImageJ software. Values represent the mean ± SD (n = 3). *$p < 0.05$ and **$p < 0.01$.

2. Downregulation of intracellular cAMP signaling in UVB-irradiated NHKs by BP-3

UVB-irradiation induced the phosphorylation of CREB and ATF1 than non-irradiation in NHKs. However, BP-3 decreased both CREB phosphorylation and ATF1 phosphorylation regardless of UVB irradiation in NHKs (Fig. 21A and B), suggesting that BP-3-induced PDE4B production suppresses the activation of cAMP-dependent transcription factors. The treatment of only BP-3 stimulated H2AX phosphorylation and BRCA1 phosphorylation and showed the difference compared to the effect on CREB phosphorylation (Fig. 21C and D). The treatment with both BP-3 and UVB did not affect H2AX phosphorylation and BRCA1 phosphorylation compared to the treatment with only UVB in NHKs (Fig. 21C and D).

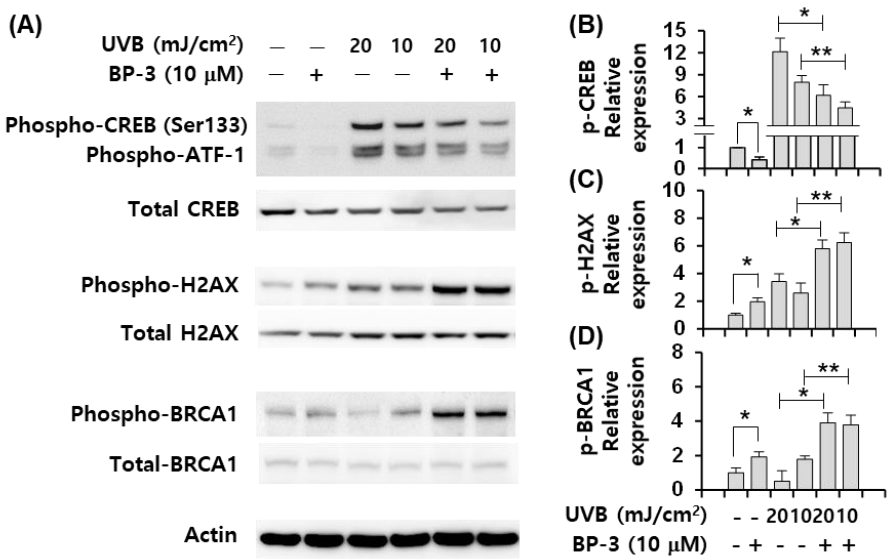

Fig. 21. Effects of phosphorylation of cAMP-dependent transcription factors and UVB-dependent DNA damage biomarkers after BP-3 and/or UVB irradiation. (A) protein levels phospho-CREB, phospho-ATF-1, total CREB, phospho-H2AX, total H2AX, phospho-BRCA1, and total BRCA1 using Western blotting. Results of phospho-CREB (B), phospho-H2AX (C), and phospho-BRCA1 (D) using ImageJ software Values represent the mean ± SD. *$p < 0.05$, **$p < 0.01$.

3. BP-3 and UVB upregulated PGE_2, TNFα, and IL8 in NHKs

To study the additive effect of BP-3 and UVB-irradiation on NHKs, we measured the mRNA levels of major proinflammatory factors such as PTGS2, TNFα, CXCL8/IL-8 and lymphangiogenic VEGF-C (Fig. 22). Twenty-four hours after treatment with only 10 μM BP-3 significantly increased the mRNA levels of *PTGS2*, *CXCL8/IL-8*, and *VEGF-C*. *TNFα* gene was not affected by the only BP-3 treatment (Fig. 22B). UVB-irradiated BP-3 additively upregulated the gene transcription of *PTGS2* in NHKs. The BP-3-dependent synergistic upregulation of TNFα and CXCL8/IL-8 mRNA levels was observed in NHKs (Fig. 22C). Additive or synergistic upregulation of VEGFC transcription was not observed (Fig. 22D). Next, the PGE_2, TNFα, IL-8, and VEGF, accumulated in the cell culture supernatants, were measured over 24 h after treatment with BP-3 and UVB. PGE_2 was significantly increased by single or co-treatment with BP-3 and UVB in NHKs (Fig. 22E). The protein levels of TNFα, IL-8, and VEGF in NHKs treated with 20 mJ/cm^2 UVB-irradiation were significantly higher than the control (Fig. 22F–H). The protein levels of TNFα and IL-8 were synergistically upregulated in the culture supernatants of NHKs induced by 20 mJ/cm^2 UVB-irradiated BP-3, whereas the effect on PGE_2 was additive by BP-3 and UVB. However, BP-3 did not additively increase VEGF production in UVB-irradiated NHKs (Fig. 22H). BP-3 may differentially affect the UVB-irradiated NHKs in the early and delayed stages of inflammatory response.

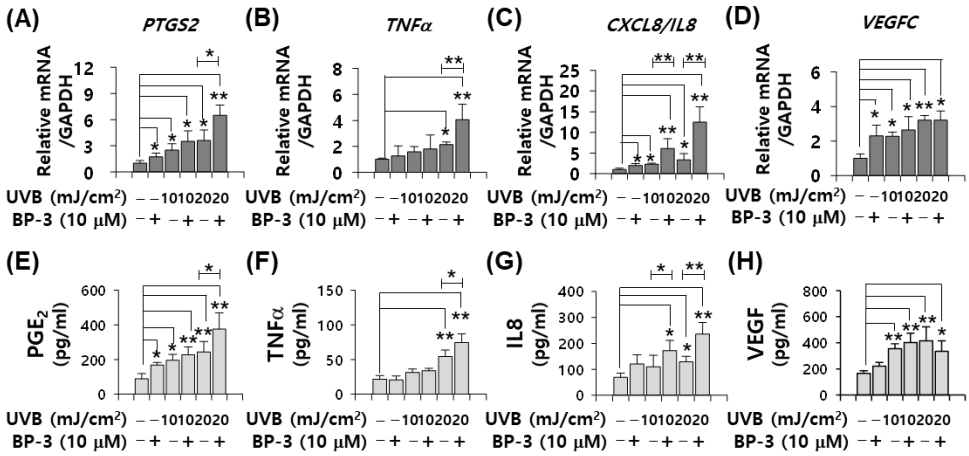

Fig. 22. The effects of UVB and BP-3 on NHK pro-inflammatory cytokine responses. The mRNA levels of *PTGS*$_2$ (A), *TNF*α (B), *CXCL8/IL-8* (C) and *VEGF-C* (D) were measured by Q-RT-PCR. Values represent the mean ± SD of the genes of interest relative to that of human GAPDH. In parallel, the protein levels of PGE_2 (E), TNFα (F), IL-8 (G) and VEGF (H) were measured by ELISA in the cell culture supernatants of NHKs. Values is mean ± SD (n =3). *$p < 0.05$, **$p < 0.01$.

4. Effects of BP-3 and UVB irradiation to the epidermal differentiation markers expression in NHKs

In NHKs treated with 20 mJ/cm^2 UVB-irradiation, the epidermal permeability barrier-associated proteins, such as keratin 1, keratin 10, loricrin and involucrin, were decreased in response to BP-3 (Fig. 23A–E). These results indicated that BP-3 and UVB changed skin barrier integrity. Although only BP-3 did not change the protein levels of S100A7 in NHKs, BP-3 and UVB co-treatment synergistically increased S100A7 protein levels in NHKs compared to only UVB treatment (Fig. 23F). Notably, UVB-irradiated BP-3 synergistically downregulated the expression of loricrin and involucrin, major cornified envelope-associated proteins. In parallel, the additive upregulation of PDE4B protein expression levels was confirmed by BP-3 and UVB stimulation (Fig. 23G) and the phosphorylation of both CREB and ATF-1 (Fig. 23A).

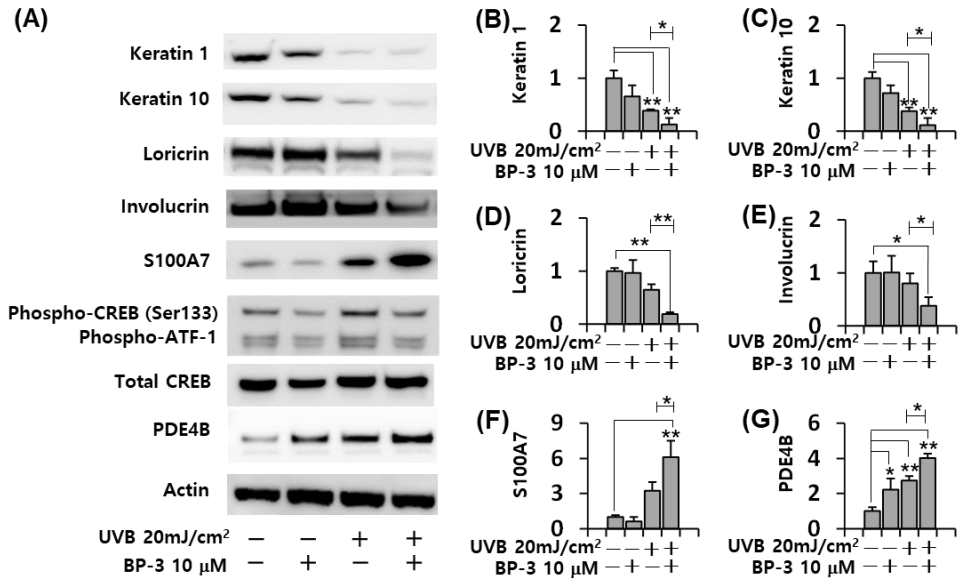

Fig. 23. The effects of UVB and BP-3 on the expression of cornified envelope-associated proteins in NHKs. (A) the protein levels of keratin 1, keratin 10, loricrin, involucrin, S100A7, phospho-CREB, phospho-ATF-1, total CREB and PDE4B in NHKs treated with BP-3 and UVB. Three independent results for keratin 1 (B), keratin 10 (C), loricrin (D), involucrin (E), S100A7 (F) and PDE4B (G) were quantified relative to β-actin levels by using ImageJ software. Values represent the mean ± SD (n =3). *$p < 0.05$, **$p < 0.01$.

5. The effects of BP-3 in UVB-irradiated NHKs were mediated by PDE4B

The BP-3-induced downregulation of the skin barrier function-related epidermal differentiation markers, keratin 1, keratin 10, and loricrin by a pharmacological inhibitor of PDE4B rolipram was observed in UVB-irradiated NHKs (Fig. 24A–D). These results indicated that BP-3-induced PDE4B upregulation is associated with the regulation of pro-inflammatory factors and epidermal differentiation markers. The UVB-irradiated BP-3-dependent upregulation of S100A7 in NHKs was also antagonized by rolipram (Fig. 24A and E). Furthermore, the association of PDE4B with the effects of BP-3 and UVB on both the upregulation of pro-inflammatory mediators and the downregulation of epidermal differentiation markers, was confirmed using a reconstituted 3D human epidermis model, EpiDerm™. In reconstituted 3D human epidermis model, the pro-inflammatory mediators, PGE_2, TNFα, and IL-8, additively increased by UVB-irradiated BP-3, and the upregulation was inhibited by the PDE4 inhibitor rolipram (Fig. 25A–C). Additive downregulation of keratin 1 and keratin 10 by BP-3 and UVB co-treatment was observed using immunohistochemistry (Fig. 25D). Rolipram also attenuated the decrease in keratin 1 and keratin 10 in the 3D human epidermis co-treated with BP-3 and UVB (Fig. 25E and F). These results showed that BP-3 induced PDE4B upregulation was related to changes in the expression of pro-inflammatory and epidermal differentiation markers in NHKs.

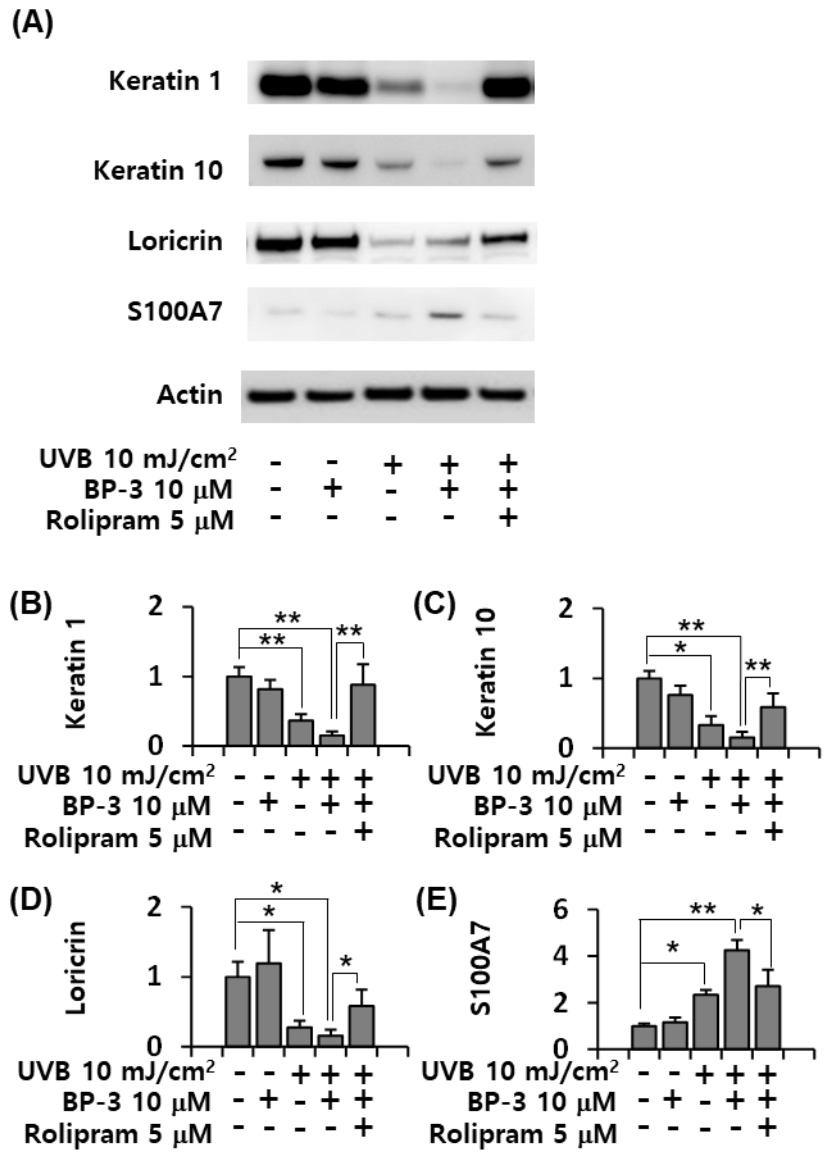

Fig. 24. The effects of PDE4 inhibitor rolipram on UVB-stimulated BP-3-induced responses in NHKs. NHKs were pre-treated with rolipram for 30 min before combined BP-3 and UVB treatment. Cells were treated or co-treated with UVB and BP-3 for 24 h. (A) Protein expression levels of keratin 1, keratin 10, loricrin, and S100A7. Three independent results for keratin 1 (B), keratin 10 (C), loricrin (D) and S100A7 (E) quantified relative to β-actin levels by using ImageJ software. Values represent the mean ± SD (n =3). *$p < 0.05$, **$p < 0.01$.

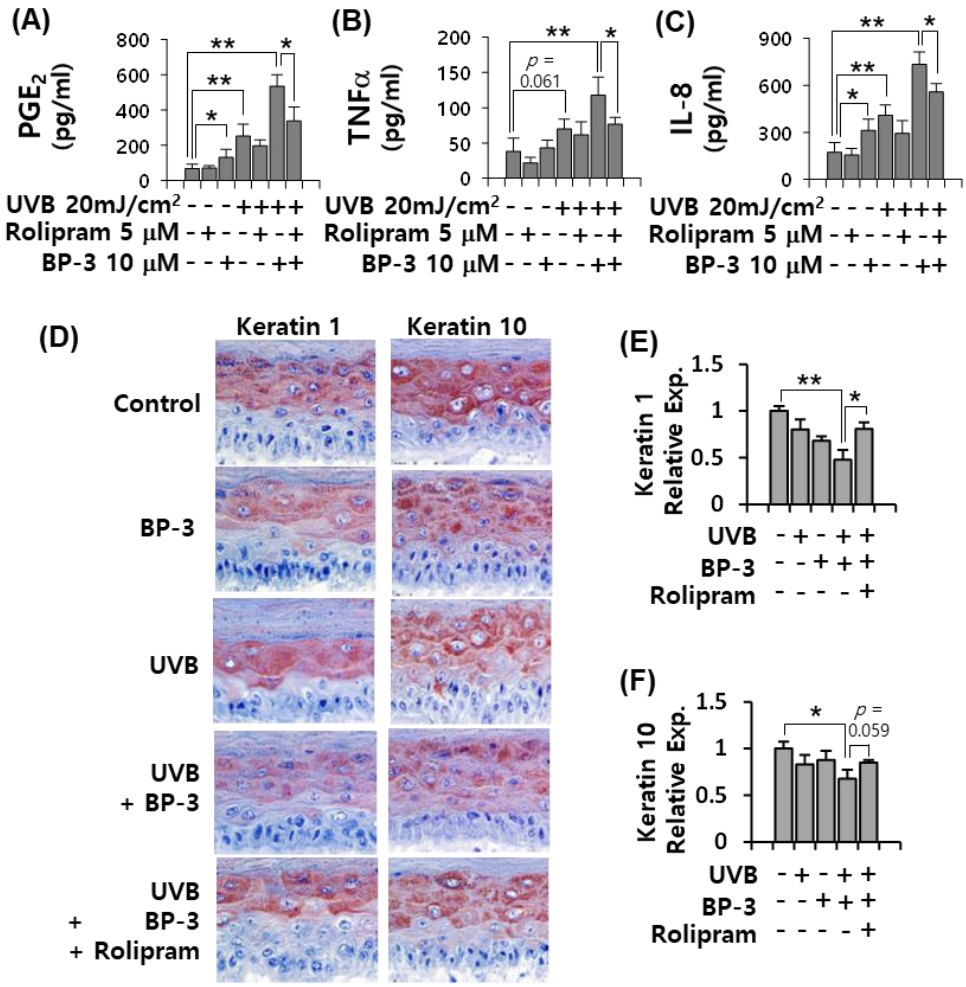

Fig. 25. Effects of PDE4B inhibitor rolipram in 3D reconstructed human epidermis model treated with both BP-3 and UVB irradiation. The protein levels of PGE_2 (A), TNFα (B) and IL-8 (C) in the culture supernatants using ELISA. (D) Red fluorescent dye-labeled antibodies against keratin 1 and keratin 10 by immunohistochemical staining. Results for keratin 1 (E) and keratin 10 (F) quantified using ImageJ software. Values represent the mean ± SD. (n = 3). $*p < 0.05$, $**p < 0.01$.

III. DISCUSSION

Chapter 1. Effects of formaldehyde on NHKs

In this study, we investigated formaldehyde concentrations that do not induce direct cell death in NHKs, to determine the effects of low levels as a daily condition of formaldehyde exposure. In total, 175 upregulated and 116 downregulated DEGs were selected for formaldehyde concentrations presenting no effect on cell viability. In GO BP enrichment analysis with the 175 upregulated DEGs, sub-cytotoxic formaldehyde simultaneously upregulated the transcription of both inflammatory and anti-inflammatory genes. Pro-inflammatory DEGs, including *MMP1*, *MMP3*, *prostaglandin-endoperoxide synthase 2 (PTGS2)*, and *CXCL8/IL8*, increased following the toxicological response to formaldehyde. Furthermore, it was first discovered that *CBS* and *CTH*, DEGs associated with the cellular detoxification pathway, increased after 24 h of formaldehyde treatment in parallel with the anti-inflammatory DEGs in NHKs. In time-course expression analysis, the immediate early inflammatory response-associated DEGs, *CXCL8/IL8* and *PTGS2*, were upregulated prior to the upregulation of *CBS* and *CTH* genes. GO BP enrichment analysis showed that ER-UPR was the topmost BP among upregulated DEGs. Under ER stress conditions, ER UPR was associated with the regulatory process, as well as the coordinated cellular response of cellular transcription and translation (Kaufman et al., 2002). In multicellular organisms, cell death responses, apoptosis or necrosis, can be stimulated under conditions regulating improperly unfolded protein levels (Kaufman et al., 2002). ER UPR plays a role in the modulation of normal cellular functions in the skin, including KC differentiation (Park et al.,

2019). Additionally, excessive ER stress levels are involved in the pathogenesis of certain skin diseases, including psoriasis, rosacea, vitiligo, and melanoma (Sugiura et al., 2009; Woo et al., 2016; Corazzari et al., 2017; Frisoli and Harris, 2017). In this study, the results suggest that sub-cytotoxic formaldehyde exposure can increase the ER stress response genes, especially *CTH*, in NHKs. The ER-UPR in mammalian cells affects cellular fates, apoptosis, or programmed homeostatic survival following toxic stress (Sano and Reed, 2013). In this regard, the upregulation of ER-UPR-associated DEGs such as *CTH*, *DDIT3*, *STC2*, *GFPT1*, *ASNS*, *PPP1R15A*, and *ERN1* may be important in cell death or survival induced by formaldehyde. Among the ER-UPR DEGs related to sub-cytotoxic formaldehyde exposure, *CTH* induced L-cysteine, the cytoprotective amino acid metabolite, and L-cysteine reduced the formaldehyde-induced inflammatory response. Inhibition of CTH leads to the induction of pro-inflammatory cytokines and an increase in the inflammatory response following kidney injury (Wang et al., 2014). Therefore, CTH activity may have important roles in the programmed recovery from toxic stressor-induced inflammation. Among the ER UPR DEGs, PPP1R15A, also known as growth arrest and DNA damage-inducible protein (GADD34), controls a programmed recovery from translational repression to ER stress-induced gene expression (Kojima et al., 2003; Novoa et al., 2003). Environmental or injury-induced toxicity responses are eliminated or neutralized through the movement of inflammatory reactions into the resolution phase (Gilroy et al., 2004; Medzhitov, 2010; Peeters et al., 2015). Cellular mechanisms associated with inflammation resolution influence cellular metabolic processes, resolution mediator production, and inflammatory cell repopulation (Alessandri et al., 2013). It has been reported that VEGF promotes the removal of activated macrophages, regarded as the resolution

of inflammation during wound healing (Petreaca et al., 2008). However, the mechanism of inflammation resolution in KCs has been poorly investigated. Furthermore, we demonstrated that VEGF was increased in formaldehyde-treated NHKs. In a previous study, VEGF was reportedly induced by various chemical allergens such as DNCB, nickel chloride, 4-phenylenediamine, and cinnamic alcohol. During the skin sensitization mechanism, VEGF production induced by chemical allergens may be regulated by the lymphangiogenic process (Bae et al., 2015a). However, it remains unclear whether VEGF promotes pathogenic inflammation or inflammatory resolution in the KCs. CBS and CTH, annotated as GO BP transsulfuration (GO:0019346), are associated with essential homocysteine-cysteine interconversions in sulfur amino acid metabolism (Vitvitsky et al., 2006). The metabolism of sulfur amino acid is linked to an important biochemical aspect, the transfer process of methyl groups to biomolecules or cellular metabolites (Brosnan and Brosnan, 2006). In human epithelial cells, the transsulfuration pathway connects glutathione synthesis to the metabolism of sulfur-containing amino acids (Belalcazar et al., 2014). During the inflammatory response, CBS and CTH directly regulate the production of glutathione and hydrogen sulfide (H_2S) (McBean, 2012). Therefore, metabolic pathways associated with CBS and CTH regulate the negative feedback process against pro-inflammatory responses. In this study, L-cysteine and L-cystathionine, amino acid biosynthetic metabolites of CBS and CTH, suppressed the production of pro-inflammatory mediators such as MMP1, PGE_2, and CXCL8/IL-8, in NHKs treated with low levels of formaldehyde. L-cysteine is known to function as a free radical scavenger via two pathways, either by binding with the radicals or by promoting the synthesis of the endogenous antioxidant, glutathione (Zhang and Forman, 2012). Alterations in cysteine homeostasis has been

associated with various human diseases (Kohl et al., 2019). Therefore, it is necessary to further investigate the association between the homeostatic control of cysteine in the cell and the inflammatory resolution process. In addition, we demonstrated that IFNγ and IL-4 upregulated *CBS* and *CTH* transcription, whereas their transcription was not affected by TNF-α, IL-17, and IL-22. IFNγ-secreting Th1 cells and IL4-secreting Th2 cells demonstrate a mutually antagonistic relationship (Nestle et al., 2009). These results suggest that CBS and CTH have specific roles in the immune response in the presence of T helper cells.

In conclusion, we showed that the genes associated with ER-UPR significantly increased in sub-cytotoxic formaldehyde-treated NHKs, indicating that ER-UPR plays an important role in the regulation of the inflammation resolution in human KCs after exposure to sub-cytotoxic formaldehyde. In the time-course profile study, the upregulation of CBS, CTH, and VEGF was preceded by pro-inflammatory mediators such as PTGS2, IL-8, and MMP1. In NHKs, CBS and CTH may contribute to maintaining cellular homeostasis through the negative feedback mechanism. Accordingly, CTH and CBS may have crucial roles during the inflammation resolution phase, indicating their contribution to inflammation resolution induced by toxic stimuli.

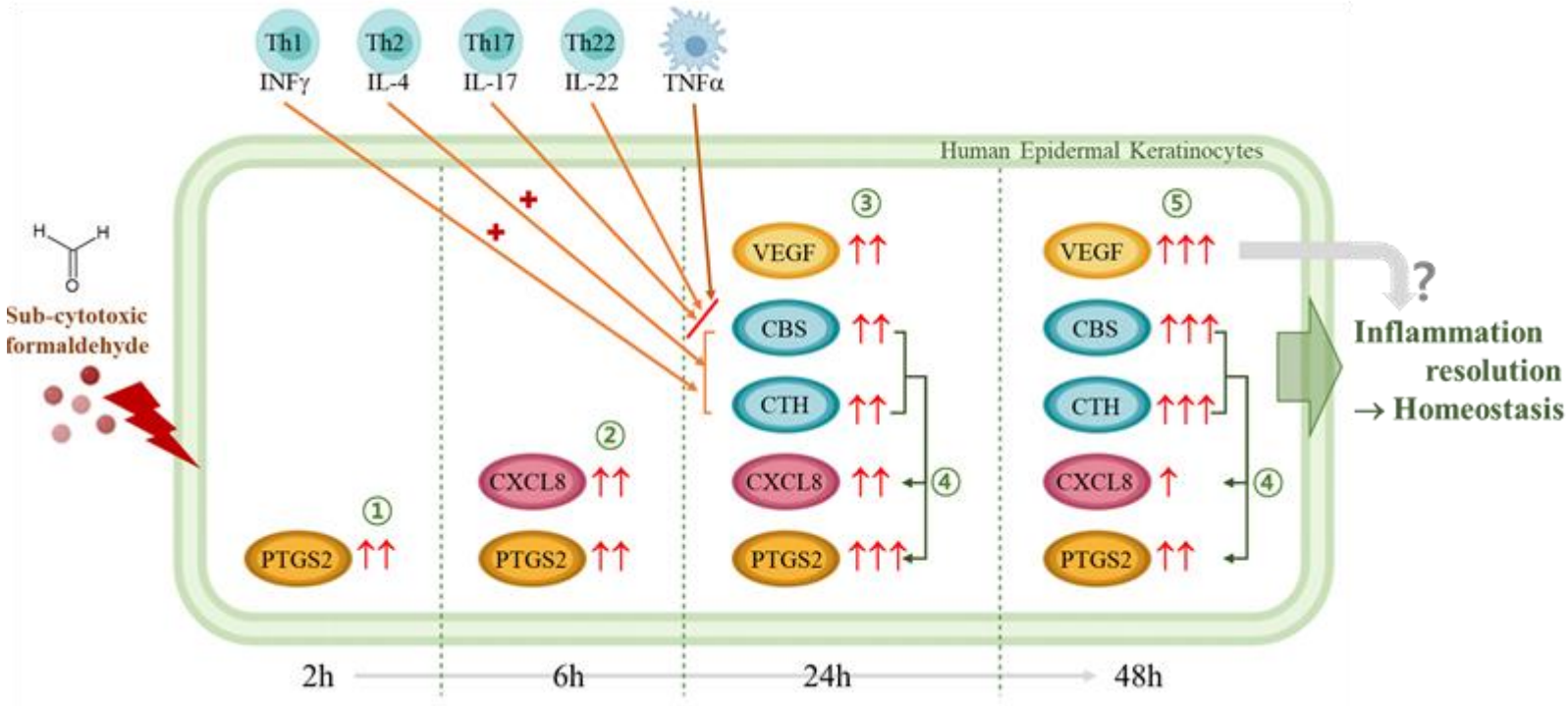

Fig. 26. Roles of CTH and CBS in inflammation resolution in NHKs

Chapter 2. Effects of sensitizers and non-sensitizers in NHKs

In the molecular pathogenesis of both ACD and ICD, KC-derived pro-inflammatory cytokines are well known as essential key mediators. Skin sensitizers and irritants produce various pro-inflammatory mediators in epidermal KCs (Coquette et al., 2003; Jin et al., 2014; Bae et al., 2015a). Genome-scale transcriptional analysis in SLS-treated or urushiol-treated NHKs was performed to identify the role of KCs in the molecular pathogenesis stimulated by a non-sensitizer and sensitizer. In the GO BP enrichment analyses, 259 SLS-treated and 173 urushiol-upregulated DEGs were mainly associated with the pro-inflammatory response and cutaneous differentiation processes in NHKs. Despite the similarities in functional signatures of GO BP terms in SLS- and urushiol-treated NHKs, the DEG sets for each GO BP term revealed differences between SLS and urushiol, suggesting that the two chemicals stimulated different toxicological pathways in human KCs. For example, SLS induced the gene transcription of cytoskeletal intermediate filament-associated proteins, KRTs and SPRR2G, whereas urushiol frequently increased the gene transcription levels of cell-to-cell adhesion-related proteins, DSG4 and CDSN. The GO BP analyses of 193 SLS-downregulated and 124 urushiol-downregulated DEGs showed that the cellular protein metabolic process was classified as a commonly downregulated DEG signature in response to both SLS and urushiol in NHKs. In NHKs, CXCL8/IL-8 was upregulated, but CXCL14 was downregulated by both SLS and urushiol. Moreover, cytokines and chemokines produced by epidermal KCs have been identified as predictive biomarkers for *in vitro* skin sensitization tests (Coquette et al., 2003; Bae et al., 2015a; Kim et al., 2018). The chemokine CXCL8/IL-8 is reportedly increased in KCs and DCs following exposure to

skin irritants and sensitizers (Coquette et al., 2003). However, the major physiological role of CXCL14 in human skin has been poorly investigated. CXCL14 is constitutively expressed in several human normal tissues such as the skin, lung, kidney, and intestines, and could be a chemotactic factor recruiting DCs in epithelial tissues (Shellenberger et al., 2004). Furthermore, it is expressed in several immune cell types, including immature DCs, activated B-cells, and activated isolated human monocytes (Frederick et al., 2000; Salogni et al., 2009). Additionally, CXCL14 may be an essential homeostatic chemokine (Banisadr et al., 2011; Lu et al., 2016). A recent study has shown that constitutively expressed CXCL14 participates in the recruitment of dendritic precursor cells (Kurth et al., 2001; Schaerli et al., 2005). Thus, CXCL14 is well known as an immune modulator (Lu et al., 2016). In addition to its direct immune-modulatory effects, CXCL14 inhibits the migration of endothelial cells, thus regulating angiogenic processes as an angiostatic chemokine (Shellenberger et al., 2004). In this study, the results suggest that the decrease in constitutively expressed CXCL14 may trigger the migration of sensitizer-activated DCs to the lymph nodes. Additionally, CXCL14, downregulated in DEGs, was proposed as a novel biomarker for the *in vitro* skin sensitization test using OECD TG429 reference chemicals, to improve the prediction accuracy of potential allergens. In NHKs, CXCL14 was significantly decreased in response to 10 of the 16 reference sensitizers, and CXCL8/IL-8 was upregulated by 10 sensitizers. Notably, 14 reference sensitizers significantly influenced the expression of both CXCL8/IL-8 and/or CXCL14 in NHKs. In our previous study, we have demonstrated that 14 reference sensitizers significantly influenced the expression of both CXCL8 and/or VEGF in NHKs (Bae et al., 2015a). Ethylene glycol dimethacrylate, classified as a sensitizer in the TG429 mouse LLNA test, has presented a false neg-

ative result in the altered expression levels of CXCL8/IL-8 and VEGF in NHKs (Bae et al., 2015a). Only one non-sensitizer, SLS, among six OECD TG429 reference non-sensitizers, downregulated the constitutive CXCL14 production in NHKs. The other non-sensitizers failed to affect CXCL14 expression. Nickel chloride, one of the OECD TG429 reference sensitizers, significantly decreased the expression level of CXCL14; however, nickel chloride is classified as a false negative chemical in the OECD TG429 mouse LLNA method (OECD, 2010). Additionally, in the OECD TG429 mouse LLNA method, SLS and xylene are considered false-positive chemicals. In this study, xylene failed to impact the expression levels of the CXCL14 in NHKs, but SLS downregulated CXCL14 expression. SLS affected both CXCL8/IL-8 and VEGF production in NHKs (Bae et al., 2015a). Although SLS is a known irritating non-sensitizer in the OECD TG429, SLS induced a weak positive response in skin sensitization tests with both LLNA and THP-1 cells, demonstrating similar allergic patch reactions (Bruynzeel et al., 1982; Lim et al., 2008; Ahn et al., 2016). In this regard, SLS as a reference non-sensitizer should be reconsidered in validation studies for novel *in vitro* skin sensitization tests. SLS is a false-positive irritating non-sensitizer in the OECD TG429 mouse LLNA method. However, CXCL14 downregulation in NHKs contributes to the enhanced accuracy of the novel in vitro sensitization tests for distinguishing between sensitizers and non-sensitizers. Furthermore, we showed that CXCL14 production was regulated through both the MAPK/ERK and JAK3/STAT6 pathways. CXCL14 was significantly upregulated in NHKs following treatment with either the MAPK/ERK inhibitor, PD98059, or the JAK3 inhibitor, WHI-P131, in a dose-dependent manner. These results suggest that both the MAPK/ERK and JAK3/STAT6 pathways co-regulate the maintenance of constitutive CXCL14 production in NHKs. The

MAPK/ERK pathway is related to an early and rapid inflammatory reaction (Kim and Choi, 2010). The JAK3/STAT6 pathway is associated with various cytokine signaling pathways in NHKs (Jin et al., 2014; O'Shea et al., 2015). The downregulation of CXCL14 by SLS is partially mediated through the STAT6 signal transduction pathway. In STAT6-deficient mice, the lung epithelia lack IgE-responses induced by allergens or Th2-type cytokine responses (Miyata et al., 1999). In our previous study, IL-4, a Th2-type cytokine related to various allergic reactions, has induced STAT6 phosphorylation in NHKs (Jin et al., 2014). Transgenic mice constitutively producing STAT6 are reportedly predisposed to allergic diseases such as ACD and atopic dermatitis (Sehra et al., 2008; Sehra et al., 2010). Therefore, based on the STAT6-dependent pathway regulating CXCL14 expression in human epidermal KCs, CXCL14 can be used as mechanism-based novel biomarker to improve the discrimination between allergenic non-sensitizers and sensitizers.

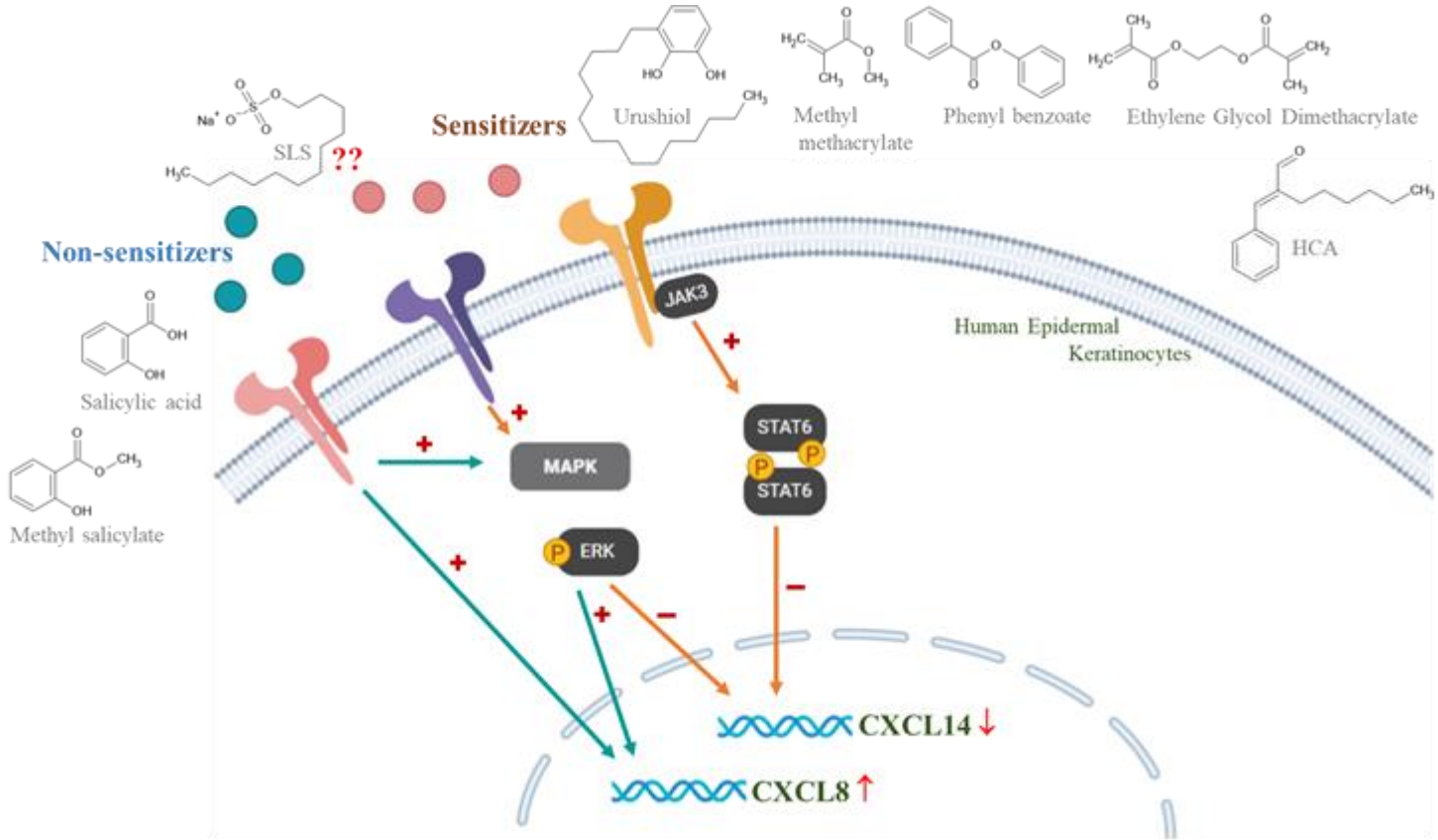

Fig. 27. CXCL14 downregulated-dependent pathway in skin sensitization.

Chapter 3. Effects of photoactivated BP-3 in NHKs

Phototoxicity is a toxic response requiring the combined effects of light exposure and various external chemicals such as drug, cosmetics and food additives (Onoue et al., 2017). For several years, BP-3 has been widely used as an organic sunscreen agent to protect from UVB irradiation (Rastogi, 2002) and has been known to cause a photo-allergenic reaction when applied topically to human skin (Lenique et al., 1992; Landers et al., 2003; Nedorost, 2003). To elucidate the mechanism of BP-3 phototoxicity, we investigated how the combination of BP-3 and UVB irradiation affected cellular and molecular responses in human epidermal KCs. UVB-induced intercellular cAMP levels, activating cAMP-dependent PKA to stimulate the phosphorylation of cAMP response element-binding protein (CREB) and activating transcription factor 1 (ATF-1) (Chun et al., 2007). The phosphorylation of H2AX and BRCA1, UV-induced DNA damage markers in mammalian cells, is induced by UVB irradiation (Podhorecka et al., 2010). First, we demonstrated that in NHKs, BP-3 and BP-8 significantly increased PDE4B among 17 organic sunscreen agents. Upregulation of the BP-3-induced PDE4B induced the phosphorylation of CREB and ATF-1, whereas BP-3 failed to impact the phosphorylation of H2AX and BRCA1. PDE4B possesses an essential role in the regulation of pro-inflammatory responses by degrading the secondary mediator cAMP in inflammatory cells, endothelial cells, and KCs (Chujor et al., 1998; Komatsu et al., 2013). In psoriasis and atopic dermatitis, reduced cAMP is associated with an increase in PDE4 activity (Kumar et al., 2013). Interestingly, the inhibition of cellular PDE4B activity downregulates inflammatory responses in animal models of atopic dermatitis and psoriasis, implying that the elevation of intercellular cAMP in the

epidermis inhibits pro-inflammatory responses (Akama et al., 2009). In our previous study, we have demonstrated that chemical allergens upregulate the transcription of pro-inflammatory mediators such as TNF-α, PTGS2, and IL-8 in NHKs (Bae et al., 2015a; Bae et al., 2015b). In this study, the combination of BP-3 and UVB, additively or synergistically, upregulated the expression of TNF-α, PTGS2, and VEGF-C. Therefore, PDE4B may regulate pro-inflammatory responses in NHKs, as well as the susceptibility to phototoxic dermatitis in the human skin. Human epidermal KCs differentiate for the generation of a skin permeability barrier, an important physical defense mechanism to protect against various environmental toxic stimuli. However, environmental stressors, including chemical allergens and physical stress, can affect the integrity of the epidermal permeability barrier (Proksch et al., 2008). The epidermal cornified envelope proteins are major components mediating the skin barrier functions. Genetic mutation and polymorphisms in cornified envelope proteins, including involucrin, filaggrin, loricrin, keratin 1, and keratin 10, are pathophysiologically associated with various inflammatory skin diseases such as atopic dermatitis (Candi et al., 2005; Agrawal and Woodfolk, 2014). Keratin 1 and keratin 10 play a role in inflammatory networks related with barrier function in inflammatory responses (Roth et al., 2012). We observed that BP-3 and UVB-induced downregulation of cornified envelope proteins, including keratin 1 and keratin 10, weakened the integrity of the epidermal permeability barrier, suggesting that this weakened integrity of the skin barrier would allow environmental toxic stimuli to more easily penetrate the skin than during homeostasis. Notably, BP-8, possessing a common 2-hydroxy-4-methoxyphenylmethanone moiety like BP-3, also significantly upregulated *PDE4B* gene transcription in NHKs. Although avobenzone, known as a photo-allergen and

contains a methoxyphenyl group like BP-3 and BP-8, failed to demonstrate statistical significance, it tended to increase the transcription of *PDE4B* in NHKs.

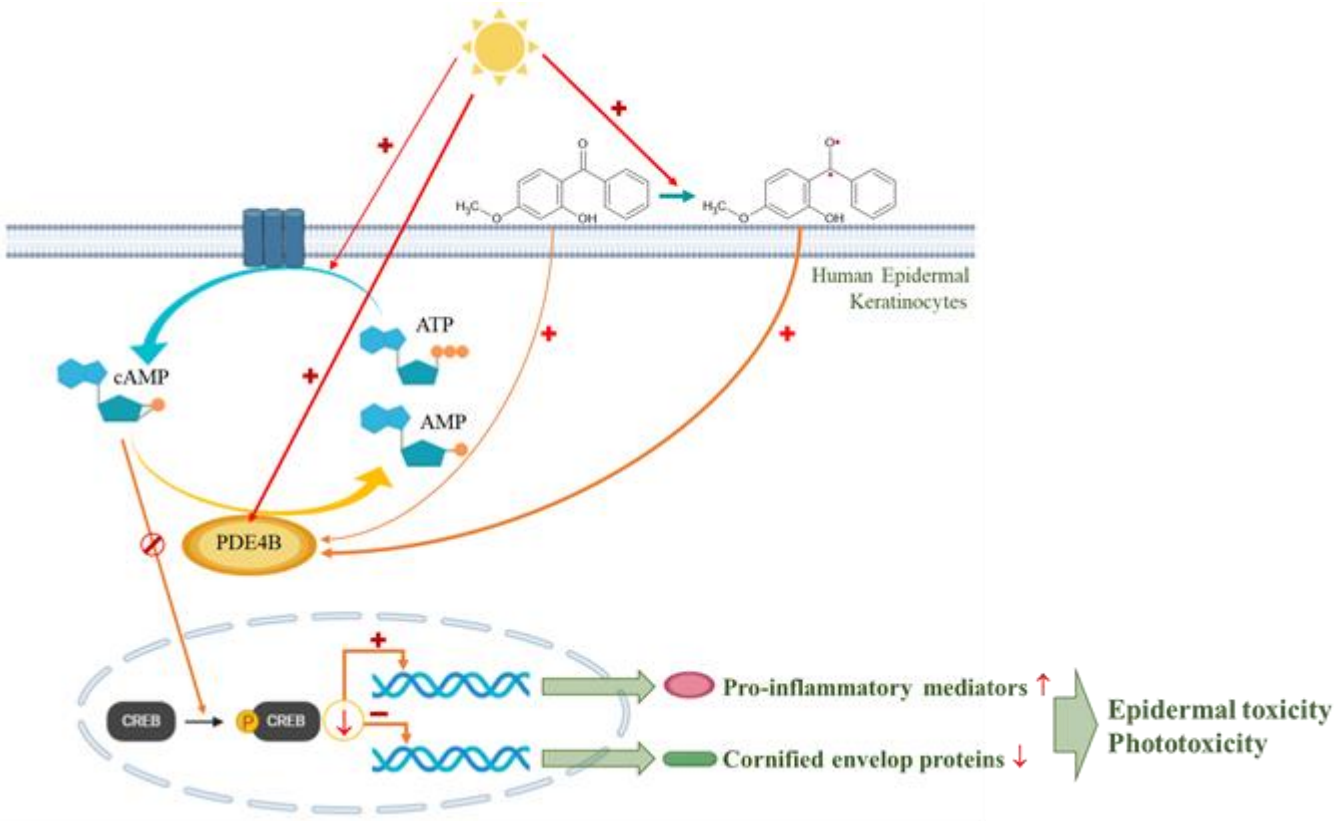

Fig. 28. Roles of PDE4B in photoactivated BP-3-induced phototoxicity.

IV. CONCLUSION

In this study, CTH and CBS, associated with ER-UPR, may play roles in the resolution of xenobiotic-induced inflammation by suppressing the early pro-inflammatory response in NHKs. Downregulation of CXCL14 is associated with the skin sensitization process in the JAK3/STATA6 signaling pathway and is proposed as a novel biomarker for the skin sensitization test. We showed that PDE4B has an important role in the BP-3-induced phototoxicity response, as well as the disruption of the skin permeability barrier through the cAMP-dependent signaling pathway. Furthermore, our previous studies have shown that lymphangiogenic VEGF-C has a role in inflammatory responses, VEGF may have a role in inflammatory resolution in the delayed inflammatory pathway, and BP-3 and BP-8 directly bind to peroxisome proliferator-activated receptor γ (PPARγ) (Shin et al., 2020). In this regard, future studies should investigate the relationship between VEGF-C and PPARγ in NHKs to elucidate the inflammatory mechanism induced by xenobiotics.

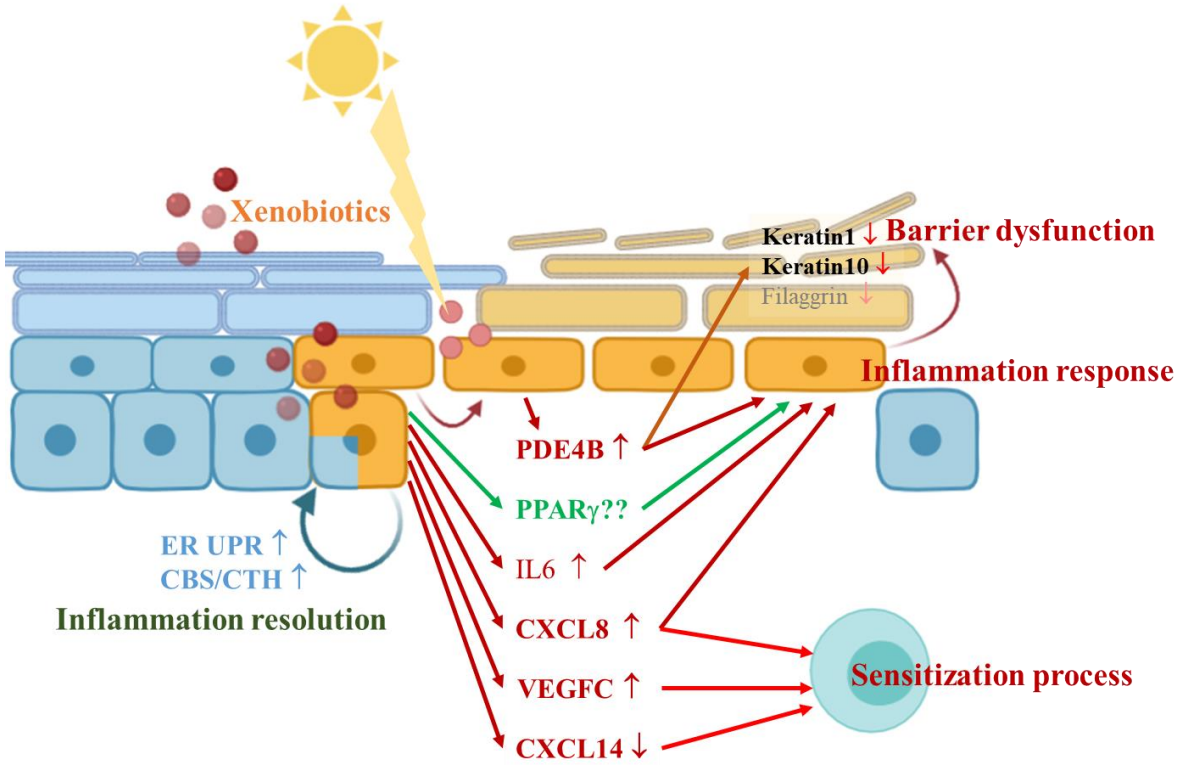

Fig. 29. Molecular mechanism of xenobiotic-induced inflammatory response and resolution in human epidermal KCs.

V. MATERIALS AND METHODS

1. Cell culture and cell viability test

Normal human keratinocytes (NHKs) form neonatal foreskins were obtained from Lonza (Basel, Switzerland) and cultured in Keratinocyte Basal Medium (KBM) medium with Keratinocyte Growth Medium-2 (KGM^{TM}-2) supplements containing insulin, human epidermal growth factor, bovine pituitary extract, hydrocortisone, epinephrine, transferrin, and gentamicin/amphotericin B (Lonza). Three independent NHKs batches prepared from different donors were used, and all experiments were performed in triplicates or quadruplicates. NHKs were subcultured at 80-90% confluence and the third passage of primary NHKs was used in this study. Cell viability was evaluated using a Cell counting Kit-8 assay (CCK-8, Dojindo, Kumamoto, Japan) according to the manufacture's method. Formaldehyde (Sigma-Aldrich, St. Louis, MO, USA), SLS (Sigma-Aldrich), urushiol (ChromaDex; Irvine, CA, USA) or the other human sensitizers and non-sensitizers listed in OECD TG429 was treated to NHKs cultured in 48-well plates up to 100% confluence immediately before experiments. All of OECD TG429 chemicals were purchased from Sigma-Aldrich except for 5-chloro-2-methyl-4-isothiazolin-3-one/2-methyl-4-isothiazolin-3-one (CMI/MI) which was prepared by mixing CMI (Sigma-Aldrich) and MI (Sigma-Aldrich) in a 3:1 ratio.

2. Microarray experiments

Total RNA was isolated using TRIzol (Invitrogen, Carlsbad, CA, USA). The

RNA purified using the RNeasy Mini Kit (Qiagen, Germantown, MD, USA). The quantity of the total RNA determined with the NanoDrop ND-1000 spectrophotometer (NanoDrop Technologies, INC., Montchanin, DE, USA). RNA integrity was verified with the Bioanalyzer 2100 (Agilent Technologies, Santa Clara, ca, USA). Affymetrix Human Genome U133 2.0 GeneChip arrays (Affymetrix, Santa Clara, CA, USA) were prepared, hybridized, and scanned by an authorized local Affymetrix service provider (DNA Link, Inc., Seoul, South Korea). RNA reverse transcribed to cDNA and transcribed into cRNA in the presence of biotinylated ribonucleotides. The hybridized probe array was stained and washed with GeneChip hybridization, stain and wash kit using Fluidics Station 450 (Affymetrix). The stained GeneChip probe array was scanned with a GeneChip Scanner 3000 + 7G (Affymetrix). The signal intensity of the gene expression level was calculated using the Expression Console Software, Version 1.1 (Affymetrix) based on the MAS 5.0 algorithm. The procedure used to select the DEGs was as follows: (i) selection of "present" Affymetrix probe sets as control or chemical-treated samples; (ii) selection of Affymetirx probe sets with comparison signal sample/control standard ratios as "upregulated" or "downregulated"; and (iii) selection of Affymetrix probe sets with simultaneously significant p-values (threshold, 0.05) in the Wilcoxon rank test when compared with vehicle-treated samples as control.

3. Gene Ontology enrichment analysis

Gene ontology (GO) enrichment analysis of DEGs was performed by comparing the frequency of GO BP terms assigned to each gene in a DEGs group with that in all the gene set in the Affymetrix Human 133 2.0 GeneChip array. The GO anno-

tation files were obtained from the Gene Ontology consortium webpage (http://www.geneontology.org). For the GO BP enrichment analysis, 2 × 2 contingency matrix for each GO BP term was constructed between the frequency of a specific GO BP term in the DEGs sets and that for the full set genes. The 2 × 2 contingency matrix data were analyzed by the fisher's exact test (frequency < 5) or chi-squared test (frequency ≥ 5) using SPSS 25.0 for windows (IBM corp., Armonk, NY, USA) to calculate the level of significance.

4. Quantitative real-time reverse transcription polymerase chain reaction (Q-RT-PCR)

Total RNA from each sample was transcribed with SuperScript™ reverse transcriptase (Invitrogen). The expression level of the target mRNAs was quantified by Q-RT-PCR using the Applied Biosystems 7500 Real Time PCR System (Applied Biosystems, Foster city, ca, USA). The TaqMan RT-PCR primer sets (Applied Biosystems) used in the Q-RT-PCR were: cystathionine-β-synthase (*CBS*), Hs00163925_m1; cystathionine-γ-lyase (*CTH*), Hs00542284_m1; asparagine synthetase (*ASNS*), Hs04186194_m1; matrix metalloproteinase 1 (*MMP1*), Hs00899658_m1; metalloproteinase 3 (*MMP3*), Hs00968305_m1; fibronectin, Hs01549937_m1; involucrin (*IVL*), Hs00846307_s1; small proline rich protein 4 (*SPRR4*), Hs01917405_s1; prostaglandin-endoperoxide synthase 2 (*PTGS2*), Hs00153133_m1; VEGF-A, Hs00900055_m1; interleukin (IL)-8 (*CXCL8*), Hs00174103_m1; phosphodiesterase 4B (*PDE4B*), Hs00277080_m1; interleukin 33 (*IL33*), Hs00369211_m1; solute carrier family 25, member 4 (*SLC25A4*), Hs00154037_m1; growth arrest-specific 1 (*GAS1*), Hs00266715_s1. annexin A1

(*ANXA1*), 00167549_ml; CC motif chemokine ligand 5 (*CCL5*), Hs00982282_ml; CXC Motif Chemokine Ligand 14 (*CXCL14*), Hs01557413_ml; desmoglein 4 (*DSG4*), Hs00698286_ml; FBJ murine osteosarcoma viral oncogene homolog (*FOS*), Hs04194186_s1; *H19*, Hs00399294_ml; jun B proto-oncogene (*JUNB*), Hs00357891_ml; suppressor of cytokine signaling 1 (*SOCS1*), Hs00705164_s1; SP100 nuclear antigen (*SP100*), Hs00162109_ml; small proline-rich protein 2G (*SPRR2G*), Hs00972901_s1; thrombospondin 1 (*THBS1*), Hs00962908_ml; and *TNF*, Hs00174128_m1Human *GAPDH* (4333764F, Applied Biosystems) was also amplified to normalize variations in cDNA levels across different samples. Quantification of relative expression levels was performed using a mathematical developed by Pfaffl (Pfaffl, 2001).

5. Western blot analysis and enzyme-linked immunosorbent assay (ELISA)

Protein expression levels of the selected genes were determined by western blotting and ELISA using three independent NHKs batches. NHKs were seeded to six-well culture plates and cultured up to 100% confluence. For inhibitory effects in Janus kinase (JAK) and mitogen-activated protein kinase (MAPK) pathway, MAPK signaling inhibitor (PD98059) and JAK inhibitors (Piceatannol, AG-490 and WHI-P131) were co-applied with SLS to the NHKs for 24 h. Piceatannol, AG-490 and WHI-P131 were purchased from Calbiochem (San Diego, CA, USA). NHKs were lysed in cell lysis buffer (RIPA buffer) containing protease inhibitors (Sigma-Aldrich). The lysate was then subjected to centrifugation a 15,000g for 10 min, and the supernatant was used for protein expression analysis. Proteins were

fractionated by SDS PAGE and transferred to nitrocellulose membranes. The membranes were blocked with 5% skim milk in TBST (10 mM Tris-HCL, pH 8.0, 150 mM NaCl, and 0.15% Tween-20) for 1h at 25 °C and subsequently probed overnight at 4 °C with anti-body of target proteins. Anti-CBS antibody (# PA5-22273, Thermo-Scientific, Rockford, IL, USA), anti-CTH (#PA5-29725, Thermo-Scientific), anti-fibronectin (#SC-9068, Santa Cruz Biotechnology), anti-phospho-ERK antibody (#4370; Cell Signaling Technology (CST), Beverly, MA, USA), anti-ERK (#4695; CST), anti-phospho-STAT6 (#9361; CST), anti-STAT6 (#9363; CST) and anti-β-actin (#A5441, Sigma-Aldrich) were used and detection was performed with an ECL system (Invitrogen). Protein concentrations in the supernatant were measured with enzyme immunoassay kits (R&D Systems, Minneapolis, MN, USA) according to the manufacture's instructions and was determined in pg/mg of total protein.

6. Statistical analysis

The data were expressed as means ± standard deviation (SD). Statistical analyses were performed with Student's *t*-test for comparison with control or one-way ANOVA followed by Bonferroni's post-test for multiple comparison. *P*-values < 0.05 indicated statistical significance. Statistical analysis was conducted using SPSS 25.0 for windows (IBM Corp.).

VI. REFERENCES

Agrawal, R., Woodfolk, J.A., 2014. Skin barrier defects in atopic dermatitis. Curr. Allergy Asthma Rep. 14, 433.

Ahn, I., Kim, T.S., Jung, E.S., Yi, J.S., Jang, W.H., Jung, K.M., Park, M., Jung, M.S., Jeon, E.Y., Yeo, K.U., Jo, J.H., Park, J.E., Kim, C.Y., Park, Y.C., Seong, W.K., Lee, A.Y., Chun, Y.J., Jeong, T.C., Jeung, E.B., Lim, K.M., Bae, S., Sohn, S., Heo, Y., 2016. Performance standard-based validation study for local lymph node assay: 5-bromo-2-deoxyuridine-flow cytometry method. Regul. Toxicol. Pharmacol. 80, 183-194.

Akama, T., Baker, S.J., Zhang, Y.K., Hernandez, V., Zhou, H., Sanders, V., Freund, Y., Kimura, R., Maples, K.R., Plattner, J.J., 2009. Discovery and structure-activity study of a novel benzoxaborole anti-inflammatory agent (AN2728) for the potential topical treatment of psoriasis and atopic dermatitis. Bioorg. Med. Chem. Lett. 19, 2129-2132.

Albanesi, C., Scarponi, C., Giustizieri, M.L., Girolomoni, G., 2005. Keratinocytes in inflammatory skin diseases. Curr. Drug Targets Inflamm. Allergy 4, 329-334.

Alessandri, A.L., Sousa, L.P., Lucas, C.D., Rossi, A.G., Pinho, V., Teixeira, M.M., 2013. Resolution of inflammation: mechanisms and opportunity for drug development. Pharmacol. Ther. 139, 189-212.

Bachand, A.M., Mundt, K.A., Mundt, D.J., Montgomery, R.R., 2010. Epidemiological studies of formaldehyde exposure and risk of leukemia and nasopharyngeal cancer: a meta-analysis. Crit. Rev. Toxicol. 40, 85-100.

Bae, O.N., Ahn, S., Jin, S.H., Hong, S.H., Lee, J., Kim, E.S., Jeong, T.C., Chun,

Y.J., Lee, A.Y., Noh, M., 2015a. Chemical allergens stimulate human epidermal keratinocytes to produce lymphangiogenic vascular endothelial growth factor. Toxicol. Appl. Pharmacol. 283, 147-155.

Bae, O.N., Noh, M., Chun, Y.J., Jeong, T.C., 2015b. Keratinocytic vascular endothelial growth factor as a novel biomarker for pathological skin condition. Biomol. Ther. 23, 12-18.

Banisadr, G., Bhattacharyya, B.J., Belmadani, A., Izen, S.C., Ren, D., Tran, P.B., Miller, R.J., 2011. The chemokine BRAK/CXCL14 regulates synaptic transmission in the adult mouse dentate gyrus stem cell niche. J. Neurochem. 119, 1173-1182.

Barker, J.N., Jones, M.L., Mitra, R.S., Crockett-Torabe, E., Fantone, J.C., Kunkel, S.L., Warren, J.S., Dixit, V.M., Nickoloff, B.J., 1991. Modulation of keratinocyte-derived interleukin-8 which is chemotactic for neutrophils and T lymphocytes. Am. J. Pathol. 139, 869-876.

Becher, B., Tugues, S., Greter, M., 2016. GM-CSF: From Growth Factor to Central Mediator of Tissue Inflammation. Immunity 45, 963-973.

Belalcazar, A.D., Ball, J.G., Frost, L.M., Valentovic, M.A., Wilkinson, J.t., 2014. Transsulfuration Is a Significant Source of Sulfur for Glutathione Production in Human Mammary Epithelial Cells. ISRN Biochem 2013, 637897.

Brosnan, J.T., Brosnan, M.E., 2006. The sulfur-containing amino acids: an overview. J. Nutr. 136, 1636S-1640S.

Bruynzeel, D.P., van Ketel, W.G., Scheper, R.J., von Blomberg-van der Flier, B.M., 1982. Delayed time course of irritation by sodium lauryl sulfate: observations on threshold reactions. Contact Dermatitis 8, 236-239.

Calafat, A.M., Wong, L.Y., Ye, X., Reidy, J.A., Needham, L.L., 2008. Concentra-

tions of the sunscreen agent benzophenone-3 in residents of the United States: National Health and Nutrition Examination Survey 2003--2004. Environ. Health Perspect. 116, 893-897.

Candi, E., Schmidt, R., Melino, G., 2005. The cornified envelope: a model of cell death in the skin. Nat. Rev. Mol. Cell Biol. 6, 328-340.

Choi, H., Shin, D.W., Kim, W., Doh, S.J., Lee, S.H., Noh, M., 2011. Asian dust storm particles induce a broad toxicological transcriptional program in human epidermal keratinocytes. Toxicol. Lett. 200, 92-99.

Chujor, C.S., Hammerschmid, F., Lam, C., 1998. Cyclic nucleotide phosphodiesterase 4 subtypes are differentially expressed by primary keratinocytes and human epidermoid cell lines. J. Invest. Dermatol. 110, 287-291.

Chun, K.S., Akunda, J.K., Langenbach, R., 2007. Cyclooxygenase-2 inhibits UVB-induced apoptosis in mouse skin by activating the prostaglandin E2 receptors, EP2 and EP4. Cancer Res. 67, 2015-2021.

Cogliano, V.J., Grosse, Y., Baan, R.A., Straif, K., Secretan, M.B., El Ghissassi, F., Working Group for, V., 2005. Meeting report: summary of IARC monographs on formaldehyde, 2-butoxyethanol, and 1-tert-butoxy-2-propanol. Environ. Health Perspect. 113, 1205-1208.

Coquette, A., Berna, N., Vandenbosch, A., Rosdy, M., De Wever, B., Poumay, Y., 2003. Analysis of interleukin-1alpha (IL-1alpha) and interleukin-8 (IL-8) expression and release in in vitro reconstructed human epidermis for the prediction of in vivo skin irritation and/or sensitization. Toxicol. In Vitro 17, 311-321.

Corazzari, M., Gagliardi, M., Fimia, G.M., Piacentini, M., 2017. Endoplasmic Reticulum Stress, Unfolded Protein Response, and Cancer Cell Fate. Front. On-

col. 7, 78.

de Groot, A., White, I.R., Flyvholm, M.A., Lensen, G., Coenraads, P.J., 2010. Formaldehyde-releasers in cosmetics: relationship to formaldehyde contact allergy. Part 2. Patch test relationship to formaldehyde contact allergy, experimental provocation tests, amount of formaldehyde released, and assessment of risk to consumers allergic to formaldehyde. Contact Dermatitis 62, 18-31.

De Jong, W.H., Arts, J.H., De Klerk, A., Schijf, M.A., Ezendam, J., Kuper, C.F., Van Loveren, H., 2009. Contact and respiratory sensitizers can be identified by cytokine profiles following inhalation exposure. Toxicology 261, 103-111.

ECHA, 2020. Registered Substances CAS 50-00-0. https://echa.europa.eu/registration- dossier/-/registered-dossier/15858.

Eyerich, K., Dimartino, V., Cavani, A., 2017. IL-17 and IL-22 in immunity: Driving protection and pathology. Eur. J. Immunol. 47, 607-614.

Eyerich, S., Eyerich, K., Pennino, D., Carbone, T., Nasorri, F., Pallotta, S., Cianfarani, F., Odorisio, T., Traidl-Hoffmann, C., Behrendt, H., Durham, S.R., Schmidt-Weber, C.B., Cavani, A., 2009. Th22 cells represent a distinct human T cell subset involved in epidermal immunity and remodeling. J. Clin. Invest. 119, 3573-3585.

Eyerich, S., Onken, A.T., Weidinger, S., Franke, A., Nasorri, F., Pennino, D., Grosber, M., Pfab, F., Schmidt-Weber, C.B., Mempel, M., Hein, R., Ring, J., Cavani, A., Eyerich, K., 2011. Mutual antagonism of T cells causing psoriasis and atopic eczema. N. Engl. J. Med. 365, 231-238.

Fasth, I.M., Ulrich, N.H., Johansen, J.D., 2018. Ten-year trends in contact allergy to formaldehyde and formaldehyde-releasers. Contact Dermatitis 79, 263-269.

Ferrara, N., Gerber, H.P., LeCouter, J., 2003. The biology of VEGF and its recep-

tors. Nat. Med. 9, 669-676.

Fluhr, J.W., Darlenski, R., Angelova-Fischer, I., Tsankov, N., Basketter, D., 2008. Skin irritation and sensitization: mechanisms and new approaches for risk assessment. 1. Skin irritation. Skin Pharmacol. Physiol. 21, 124-135.

Flyvholm, M.A., Andersen, P., 1993. Identification of formaldehyde releasers and occurrence of formaldehyde and formaldehyde releasers in registered chemical products. Am. J. Ind. Med. 24, 533-552.

Frederick, M.J., Henderson, Y., Xu, X., Deavers, M.T., Sahin, A.A., Wu, H., Lewis, D.E., El-Naggar, A.K., Clayman, G.L., 2000. In vivo expression of the novel CXC chemokine BRAK in normal and cancerous human tissue. Am. J. Pathol. 156, 1937-1950.

Frisoli, M.L., Harris, J.E., 2017. Vitiligo: Mechanistic insights lead to novel treatments. J. Allergy Clin. Immunol. 140, 654-662.

Garrett, M.H., Hooper, M.A., Hooper, B.M., Rayment, P.R., Abramson, M.J., 1999. Increased risk of allergy in children due to formaldehyde exposure in homes. Allergy 54, 330-337.

Gaspar, L.R., Tharmann, J., Maia Campos, P.M., Liebsch, M., 2013. Skin phototoxicity of cosmetic formulations containing photounstable and photostable UV-filters and vitamin A palmitate. Toxicol. In Vitro 27, 418-425.

Gilroy, D.W., Lawrence, T., Perretti, M., Rossi, A.G., 2004. Inflammatory resolution: new opportunities for drug discovery. Nat. Rev. Drug Discov. 3, 401-416.

Gustafson, P., Barregard, L., Lindahl, R., Sallsten, G., 2005. Formaldehyde levels in Sweden: personal exposure, indoor, and outdoor concentrations. J. Expo. Anal. Environ. Epidemiol. 15, 252-260.

Hanel, K.H., Cornelissen, C., Luscher, B., Baron, J.M., 2013. Cytokines and the

skin barrier. Int. J. Mol. Sci. 14, 6720-6745.

Hoste, E., Kemperman, P., Devos, M., Denecker, G., Kezic, S., Yau, N., Gilbert, B., Lippens, S., De Groote, P., Roelandt, R., Van Damme, P., Gevaert, K., Presland, R.B., Takahara, H., Puppels, G., Caspers, P., Vandenabeele, P., Declercq, W., 2011. Caspase-14 is required for filaggrin degradation to natural moisturizing factors in the skin. J. Invest. Dermatol. 131, 2233-2241.

Huggenberger, R., Detmar, M., 2011. The cutaneous vascular system in chronic skin inflammation. J. Investig. Dermatol. Symp. Proc. 15, 24-32.

Ichinose, T., Yoshida, S., Hiyoshi, K., Sadakane, K., Takano, H., Nishikawa, M., Mori, I., Yanagisawa, R., Kawazato, H., Yasuda, A., Shibamoto, T., 2008. The effects of microbial materials adhered to Asian sand dust on allergic lung inflammation. Arch. Environ. Contam. Toxicol. 55, 348-357.

Jeong, H.S., Chung, H., Song, S.H., Kim, C.I., Lee, J.G., Kim, Y.S., 2015. Validation and Determination of the Contents of Acetaldehyde and Formaldehyde in Foods. Toxicol. Res. 31, 273-278.

Jin, S.H., Choi, D., Chun, Y.J., Noh, M., 2014. Keratinocyte-derived IL-24 plays a role in the positive feedback regulation of epidermal inflammation in response to environmental and endogenous toxic stressors. Toxicol. Appl. Pharmacol. 280, 199-206.

Jux, B., Kadow, S., Esser, C., 2009. Langerhans cell maturation and contact hypersensitivity are impaired in aryl hydrocarbon receptor-null mice. J. Immunol. 182, 6709-6717.

Kaplan, D.H., Igyarto, B.Z., Gaspari, A.A., 2012. Early immune events in the induction of allergic contact dermatitis. Nat. Rev. Immunol. 12, 114-124.

Kaufman, R.J., Scheuner, D., Schroder, M., Shen, X., Lee, K., Liu, C.Y., Arnold,

S.M., 2002. The unfolded protein response in nutrient sensing and differentiation. Nat. Rev. Mol. Cell Biol. 3, 411-421. https://doi.org/10.1038/nrm829.

Kim, E.K., Choi, E.J., 2010. Pathological roles of MAPK signaling pathways in human diseases. Biochim. Biophys. Acta 1802, 396-405.

Kim, H.J., Lee, E., Lee, M., Ahn, S., Kim, J., Liu, J., Jin, S.H., Ha, J., Bae, I.H., Lee, T.R., Noh, M., 2018. Phosphodiesterase 4B plays a role in benzophenone-3-induced phototoxicity in normal human keratinocytes. Toxicol. Appl. Pharmacol. 338, 174-181.

Kim, K., Park, H., Lim, K.M., 2015. Phototoxicity: Its Mechanism and Animal Alternative Test Methods. Toxicol. Res. 31, 97-104.

Kimber, I., Maxwell, G., Gilmour, N., Dearman, R.J., Friedmann, P.S., Martin, S.F., 2012. Allergic contact dermatitis: a commentary on the relationship between T lymphocytes and skin sensitising potency. Toxicology 291, 18-24.

Kohl, J.B., Mellis, A.T., Schwarz, G., 2019. Homeostatic impact of sulfite and hydrogen sulfide on cysteine catabolism. Br. J. Pharmacol. 176, 554-570.

Kojima, E., Takeuchi, A., Haneda, M., Yagi, A., Hasegawa, T., Yamaki, K., Takeda, K., Akira, S., Shimokata, K., Isobe, K., 2003. The function of GADD34 is a recovery from a shutoff of protein synthesis induced by ER stress: elucidation by GADD34-deficient mice. FASEB J. 17, 1573-1575.

Komatsu, K., Lee, J.Y., Miyata, M., Hyang Lim, J., Jono, H., Koga, T., Xu, H., Yan, C., Kai, H., Li, J.D., 2013. Inhibition of PDE4B suppresses inflammation by increasing expression of the deubiquitinase CYLD. Nat. Commun. 4, 1684.

Kumar, N., Goldminz, A.M., Kim, N., Gottlieb, A.B., 2013. Phosphodiesterase 4-targeted treatments for autoimmune diseases. BMC Med. 11, 96.

Kurth, I., Willimann, K., Schaerli, P., Hunziker, T., Clark-Lewis, I., Moser, B.,

2001. Monocyte selectivity and tissue localization suggests a role for breast and kidney-expressed chemokine (BRAK) in macrophage development. J. Exp. Med. 194, 855-861.

Landers, M., Law, S., Storrs, F.J., 2003. Contact urticaria, allergic contact dermatitis, and photoallergic contact dermatitis from oxybenzone. Am. J. Contact Dermat. 14, 33-34.

Lefebvre, M.A., Meuling, W.J., Engel, R., Coroama, M.C., Renner, G., Pape, W., Nohynek, G.J., 2012. Consumer inhalation exposure to formaldehyde from the use of personal care products/cosmetics. Regul. Toxicol. Pharmacol. 63, 171-176.

Lenique, P., Machet, L., Vaillant, L., Bensaid, P., Muller, C., Khallouf, R., Lorette, G., 1992. Contact and photocontact allergy to oxybenzone. Contact Dermatitis 26, 177-181.

Li, G.Y., Lee, H.Y., Shin, H.S., Kim, H.Y., Lim, C.H., Lee, B.H., 2007. Identification of gene markers for formaldehyde exposure in humans. Environ. Health Perspect. 115, 1460-1466.

Lim, Y.M., Moon, S.J., An, S.S., Lee, S.J., Kim, S.Y., Chang, I.S., Park, K.L., Kim, H.A., Heo, Y., 2008. Suitability of macrophage inflammatory protein-1beta production by THP-1 cells in differentiating skin sensitizers from irritant chemicals. Contact Dermatitis 58, 193-198.

Lowes, M.A., Kikuchi, T., Fuentes-Duculan, J., Cardinale, I., Zaba, L.C., Haider, A.S., Bowman, E.P., Krueger, J.G., 2008. Psoriasis vulgaris lesions contain discrete populations of Th1 and Th17 T cells. J. Invest. Dermatol. 128, 1207-1211.

Lu, J., Chatterjee, M., Schmid, H., Beck, S., Gawaz, M., 2016. CXCL14 as an

emerging immune and inflammatory modulator. J. Inflamm. 13, 1.

Lundov, M.D., Johansen, J.D., Carlsen, B.C., Engkilde, K., Menne, T., Thyssen, J.P., 2010. Formaldehyde exposure and patterns of concomitant contact allergy to formaldehyde and formaldehyde-releasers. Contact Dermatitis 63, 31-36.

McBean, G.J., 2012. The transsulfuration pathway: a source of cysteine for glutathione in astrocytes. Amino Acids 42, 199-205.

McFadden, J.P., Puangpet, P., Basketter, D.A., Dearman, R.J., Kimber, I., 2013. Why does allergic contact dermatitis exist? Br. J. Dermatol. 168, 692-699.

Medzhitov, R., 2010. Inflammation 2010: new adventures of an old flame. Cell 140, 771-776.

Miyata, S., Matsuyama, T., Kodama, T., Nishioka, Y., Kuribayashi, K., Takeda, K., Akira, S., Sugita, M., 1999. STAT6 deficiency in a mouse model of allergen-induced airways inflammation abolishes eosinophilia but induces infiltration of CD8+ T cells. Clin. Exp. Allergy 29, 114-123.

Monk, S.A., Denison, M.S., Rice, R.H., 2003. Reversible stepwise negative regulation of CYP1A1 in cultured rat epidermal cells. Arch. Biochem. Biophys. 419, 158-169.

Nedorost, S.T., 2003. Facial erythema as a result of benzophenone allergy. J. Am. Acad. Dermatol. 49, S259-261.

Nestle, F.O., Di Meglio, P., Qin, J.Z., Nickoloff, B.J., 2009. Skin immune sentinels in health and disease. Nat. Rev. Immunol. 9, 679-691.

Neuss, S., Holzmann, K., Speit, G., 2010. Gene expression changes in primary human nasal epithelial cells exposed to formaldehyde in vitro. Toxicol. Lett. 198, 289-295.

Noske, K., 2018. Secreted immunoregulatory proteins in the skin. J. Dermatol. Sci.

89, 3-10.

Novoa, I., Zhang, Y., Zeng, H., Jungreis, R., Harding, H.P., Ron, D., 2003. Stress-induced gene expression requires programmed recovery from translational repression. EMBO J. 22, 1180-1187.

O'Shea, J.J., Schwartz, D.M., Villarino, A.V., Gadina, M., McInnes, I.B., Laurence, A., 2015. The JAK-STAT pathway: impact on human disease and therapeutic intervention. Annu. Rev. Med. 66, 311-328.

OECD, 2010. Test guideline 429. In: Skin Sensitisation: Local Lymph Node Assay,. https://read.oecd-ilibrary.org/environment/test-no-429-skin-sensitisation_9789264071100-en#page1 (accessed July 23, 2010).

Onoue, S., Seto, Y., Sato, H., Nishida, H., Hirota, M., Ashikaga, T., Api, A.M., Basketter, D., Tokura, Y., 2017. Chemical photoallergy: photobiochemical mechanisms, classification, and risk assessments. J. Dermatol. Sci. 85, 4-11.

Park, J., Lee, H., Park, K., 2018. Mixture Toxicity of Methylisothiazolinone and Propylene Glycol at a Maximum Concentration for Personal Care Products. Toxicol. Res. 34, 355-361.

Park, K., Lee, S.E., Shin, K.O., Uchida, Y., 2019. Insights into the role of endoplasmic reticulum stress in skin function and associated diseases. FEBS J. 286, 413-425.

Peeters, P.M., Wouters, E.F., Reynaert, N.L., 2015. Immune Homeostasis in Epithelial Cells: Evidence and Role of Inflammasome Signaling Reviewed. J. Immunol. Res. 2015, 828264.

Petreaca, M.L., Yao, M., Ware, C., Martins-Green, M.M., 2008. Vascular endothelial growth factor promotes macrophage apoptosis through stimulation of tumor necrosis factor superfamily member 14 (TNFSF14/LIGHT). Wound Re-

pair Regen. 16, 602-614.

Pfaffl, M.W., 2001. A new mathematical model for relative quantification in real-time RT-PCR. Nucleic Acids Res. 29, e45.

Podhorecka, M., Skladanowski, A., Bozko, P., 2010. H2AX Phosphorylation: Its Role in DNA Damage Response and Cancer Therapy. J. Nucleic Acids 2010.

Proksch, E., Brandner, J.M., Jensen, J.M., 2008. The skin: an indispensable barrier. Exp. Dermatol. 17, 1063-1072.

Rastogi, S.C., 2002. UV filters in sunscreen products--a survey. Contact Dermatitis 46, 348-351.

Reich, K., Westphal, G., Konig, I.R., Mossner, R., Schupp, P., Gutgesell, C., Hallier, E., Ziegler, A., Neumann, C., 2003. Cytokine gene polymorphisms in atopic dermatitis. Br. J. Dermatol. 148, 1237-1241.

Roth, W., Kumar, V., Beer, H.D., Richter, M., Wohlenberg, C., Reuter, U., Thiering, S., Staratschek-Jox, A., Hofmann, A., Kreusch, F., Schultze, J.L., Vogl, T., Roth, J., Reichelt, J., Hausser, I., Magin, T.M., 2012. Keratin 1 maintains skin integrity and participates in an inflammatory network in skin through interleukin-18. J. Cell Sci. 125, 5269-5279.

Rovira, J., Roig, N., Nadal, M., Schuhmacher, M., Domingo, J.L., 2016. Human health risks of formaldehyde indoor levels: An issue of concern. J. Environ. Sci. Health A Tox. Hazard. Subst. Environ. Eng. 51, 357-363.

Salogni, L., Musso, T., Bosisio, D., Mirolo, M., Jala, V.R., Haribabu, B., Locati, M., Sozzani, S., 2009. Activin A induces dendritic cell migration through the polarized release of CXC chemokine ligands 12 and 14. Blood 113, 5848-5856.

Sano, R., Reed, J.C., 2013. ER stress-induced cell death mechanisms. Biochim. Biophys. Acta 1833, 3460-3470.

Schaerli, P., Willimann, K., Ebert, L.M., Walz, A., Moser, B., 2005. Cutaneous CXCL14 targets blood precursors to epidermal niches for Langerhans cell differentiation. Immunity 23, 331-342.

Scheller, J., Chalaris, A., Schmidt-Arras, D., Rose-John, S., 2011. The pro- and anti-inflammatory properties of the cytokine interleukin-6. Biochim. Biophys. Acta 1813, 878-888.

Sehra, S., Bruns, H.A., Ahyi, A.N., Nguyen, E.T., Schmidt, N.W., Michels, E.G., von Bulow, G.U., Kaplan, M.H., 2008. IL-4 is a critical determinant in the generation of allergic inflammation initiated by a constitutively active Stat6. J. Immunol. 180, 3551-3559.

Sehra, S., Yao, Y., Howell, M.D., Nguyen, E.T., Kansas, G.S., Leung, D.Y., Travers, J.B., Kaplan, M.H., 2010. IL-4 regulates skin homeostasis and the predisposition toward allergic skin inflammation. J. Immunol. 184, 3186-3190.

Shellenberger, T.D., Wang, M., Gujrati, M., Jayakumar, A., Strieter, R.M., Burdick, M.D., Ioannides, C.G., Efferson, C.L., El-Naggar, A.K., Roberts, D., Clayman, G.L., Frederick, M.J., 2004. BRAK/CXCL14 is a potent inhibitor of angiogenesis and a chemotactic factor for immature dendritic cells. Cancer Res. 64, 8262-8270.

Shin, J.C., Lee, E., An, S., Jin, S.H., Ha, J., Choi, W.J., Noh, M., 2020. Benzophenone-3 and benzophenone-8 exhibit obesogenic activity via peroxisome proliferator-activated receptor gamma pathway. Toxicol. In Vitro 67, 104886.

Steinhoff, M., Brzoska, T., Luger, T.A., 2001. Keratinocytes in epidermal immune responses. Curr. Opin. Allergy Clin. Immunol. 1, 469-476.

Sugawara, T., Gallucci, R.M., Simeonova, P.P., Luster, M.I., 2001. Regulation and role of interleukin 6 in wounded human epithelial keratinocytes. Cytokine 15,

328-336.

Sugiura, K., Muro, Y., Futamura, K., Matsumoto, K., Hashimoto, N., Nishizawa, Y., Nagasaka, T., Saito, H., Tomita, Y., Usukura, J., 2009. The unfolded protein response is activated in differentiating epidermal keratinocytes. J. Invest. Dermatol. 129, 2126-2135.

Suter, M.M., Schulze, K., Bergman, W., Welle, M., Roosje, P., Muller, E.J., 2009. The keratinocyte in epidermal renewal and defence. Vet. Dermatol. 20, 515-532.

Szende, B., Tyihak, E., 2010. Effect of formaldehyde on cell proliferation and death. Cell Biol. Int. 34, 1273-1282.

Teixeira, L.K., Fonseca, B.P., Barboza, B.A., Viola, J.P., 2005. The role of interferon-gamma on immune and allergic responses. Mem. Inst. Oswaldo Cruz 100, 137-144.

Thairu, N., Kiriakidis, S., Dawson, P., Paleolog, E., 2011. Angiogenesis as a therapeutic target in arthritis in 2011: learning the lessons of the colorectal cancer experience. Angiogenesis 14, 223-234.

Thyssen, J.P., Johansen, J.D., Menne, T., 2007. Contact allergy epidemics and their controls. Contact Dermatitis 56, 185-195.

Vitvitsky, V., Thomas, M., Ghorpade, A., Gendelman, H.E., Banerjee, R., 2006. A functional transsulfuration pathway in the brain links to glutathione homeostasis. J. Biol. Chem. 281, 35785-35793.

Wang, P., Isaak, C.K., Siow, Y.L., O, K., 2014. Downregulation of cystathionine beta-synthase and cystathionine gamma-lyase expression stimulates inflammation in kidney ischemia-reperfusion injury. Physiol. Rep. 2, e12251.

Woo, Y.R., Lim, J.H., Cho, D.H., Park, H.J., 2016. Rosacea: Molecular Mecha-

nisms and Management of a Chronic Cutaneous Inflammatory Condition. Int. J. Mol. Sci. 17.

Zhang, H., Forman, H.J., 2012. Glutathione synthesis and its role in redox signaling. Semin. Cell Dev. Biol. 23, 722-728.

Zhang, Y., Matsuo, H., Morita, E., 2006. Increased production of vascular endothelial growth factor in the lesions of atopic dermatitis. Arch. Dermatol. Res. 297, 425-429.

요약(국문 초록)

Research on the functional role of epidermal keratinocytes in inflammatory responses to skin toxicants
피부독성물질에 대한 표피각질형성세포의 염증 반응 연구

이 은 영
서울대학교 대학원
약학과 천연물과학전공

피부는 자외선이나 미생물 침입, 외래물질 등 다양한 환경유해인자로부터 물리적, 면역학적 방법으로 인체를 보호하는 장벽 기능을 한다. 이러한 외부 유해인자로 인하여 피부를 보호하기 위하여 제약 및 화장품 산업에서는 피부의 가장 외각층인 각질형성세포에서의 다양한 환경 스트레스 요인에 의한 독성 기전 연구가 활발이 진행하고 있다. 그러나 외인성 자극원으로 유래된 피부 염증 반응에 대한 기전은 아직 완전하게 밝혀져 있지 않다. 본 연구에서는 다양한 외래물질에 의해 유도된 자극에 대한 사람 표피 각질형성세포 내 생체표지자를 발굴하고 작용 기전을 연구하였다. 대기오염이나 다양한 종류의 제품을 통하여 매우 낮은 농도로 인체에 노출되어 염증을 유발하는 formaldehyde, 피부염을 유도하는 대표 외래물질인 자극원과 항원, 화장품에서 여러가지 부작용을 유발하는 자외선 차단제를 이용하여 외래물질에 의한 각질형성세포의 독성 기전을 확인하고자 하였다.

저농도 formaldehyde에 의한 사람 표피 각질형성세포의 자극 반응에서 유전체 수준에서의 전사체를 이용한 온톨로지 기반 기능 정보 분석을 통해 소포체 미접힘 단백질 반응과 황전환작용 경로와 관련된 CTH와 CBS가 저농도 formaldehyde 처리 독성기전에서 염증유발 사이토카인을 조절하여 염증해소 반응에 중요한 역할을 한다는 것을 밝혔다. 또한 CTH와 CBS와 증가와 함께 감소하는 염증유발 사이토카인과 달리 함께 증가하는 VEGF가 염증 반응뿐만 아니라 염증

해소 반응에도 관여할 가능성이 있음을 보였다. 자극원 SLS와 항원 urushiol를 처리한 각질형성세포에서 온톨로지 기반 기능 정보 분석을 한 결과, 염증 조절과 표피 분화 과정에 관련된 DEGs가 증가하였고 세포내 단백질 대사과정과 관련된 DEGs가 유의하게 감소하였음을 확인하였다. 감소된 DEGs 중에서 CXCL14가 피부 감작성 시험에서 유의한 생체표지자임을 밝혔다. OECD TG429 참고 물질을 이용한 확인시험에서, 감작원의 62.5%가 CXCL14를 유의하게 감소시킴을 확인하였다. 염증반응 사이토카인으로 잘 알려져 있는 CXCL8(IL8)의 증가와 CXCL14의 감소를 함께 분석하면, 참고 감작원의 87.5%가 유의하게 CXCL8(IL8)을 증가시키거나 CXCL14를 감소시켰다. 또한 CXCL14의 감소는 각질형성세포에서 MAPK/ERK 경로와 JAK3/STAT6 경로를 통해 조절됨을 밝혔다. 자외선 차단제 중 BP-3와 BP-8는 PDE4B를 유의하게 증가시키지만, PDE4B의 광독성 기전은 잘 알려져 있지 않다. BP-3는 UVB가 조사된 각질성성세포에서 PGE_2, TNF α, IL8 등 염증유발 사이토카인을 유의하게 증가시켰고, 표피 장벽에 중요한 역할을 하는 각질외피 단백질의 생성을 영향을 준다는 것을 확인하였다. 이를 통하여 PDE4B가 BP-3에 의한 광독성 기전에서 중요한 역할을 할 것임을 확인하였다.

본 연구를 통하여 다양한 외래물질의 독성 반응에서 새로운 생체표지자인 CTH와 CBS의 독성 해소 기전에서의 역할을 발굴하였고, JAK3/STAT6 경로를 통한 CXCL14의 감소가 염증 반응 증가에 관여한다는 것을 밝혔다. 또한 PDE4B가 CREB 인산화 억제를 통하여 염증유발 사이토카인을 증가시키고 표피 장벽을 손상시켜 염증반응이 증가함을 보였다. 또한, 외인성 자극원으로 유래된 염증반응의 기전 연구를 심화하기 위하여 각질생성세포에서 PPARγ와 VEGFC, 염증 반응 기전의 연관성에 대한 추가적인 연구를 진행해야 할 것으로 생각된다.

주요어: Human keratinocytes, Gene Ontology (GO) enrichment analysis, Cystathionine γ-lyase (CTH), Cystathionine-β-synthase (CBS), CXCL14, Inflammation resolution, Allergic contact dermatitis (ACD)

학번: 2015-31191

Toxicology and Applied Pharmacology 310 (2016) 185–194

Contents lists available at ScienceDirect

Toxicology and Applied Pharmacology

journal homepage: www.elsevier.com/locate/ytaap

Cystathionine metabolic enzymes play a role in the inflammation resolution of human keratinocytes in response to sub-cytotoxic formaldehyde exposure

Eunyoung Lee [a,b,1], Hyoung-June Kim [c,1], Moonyoung Lee [a], Sun Hee Jin [a,b], Soo Hyun Hong [a,b], Seyeon Ahn [a,b], Sae On Kim [a,b], Dong Wook Shin [c], Seung-Taek Lee [d], Minsoo Noh [a,b,*]

[a] College of Pharmacy, Seoul National University, Seoul 08826, Republic of Korea
[b] Natural Products Research Institute, Seoul National University, Seoul 08826, Republic of Korea
[c] Basic Research and Innovation Division, AmorePacific Corporation R&D Center, Yongin, Gyeounggi-do 17074, Republic of Korea
[d] Department of Biochemistry, College of Life Science and Biotechnology, Yonsei University, Seoul 03722, Republic of Korea

ARTICLE INFO

Article history:
Received 24 June 2016
Revised 15 September 2016
Accepted 20 September 2016
Available online 21 September 2016

Keywords:
Formaldehyde
Human keratinocytes
Gene Ontology (GO) enrichment analysis
Cystathionine γ-lyase (CTH)
Cystathionine-β-synthase (CBS)
Inflammation resolution

ABSTRACT

Low-level formaldehyde exposure is inevitable in industrialized countries. Although daily-life formaldehyde exposure level is practically impossible to induce cell death, most of mechanistic studies related to formaldehyde toxicity have been performed in cytotoxic concentrations enough to trigger cell death mechanism. Currently, toxicological mechanisms underlying the sub-cytotoxic exposure to formaldehyde are not clearly elucidated in skin cells. In this study, the genome-scale transcriptional analysis in normal human keratinocytes (NHKs) was performed to investigate cutaneous biological pathways associated with daily life formaldehyde exposure. We selected the 175 upregulated differentially expressed genes (DEGs) and 116 downregulated DEGs in NHKs treated with 200 μM formaldehyde. In the Gene Ontology (GO) enrichment analysis of the 175 upregulated DEGs, the endoplasmic reticulum (ER) unfolded protein response (UPR) was identified as the most significant GO biological process in the formaldeyde-treated NHKs. Interestingly, the sub-cytotoxic formaldehyde affected NHKs to upregulate two enzymes important in the cellular transsulfuration pathway, cystathionine γ-lyase (CTH) and cystathionine-β-synthase (CBS). In the temporal expression analysis, the upregulation of the pro-inflammatory DEGs such as *MMP1* and *PTGS2* was detected earlier than that of *CTH*, *CBS* and other ER UPR genes. The metabolites of CTH and CBS, L-cystathionine and L-cysteine, attenuated the formaldehyde-induced upregulation of pro-inflammatory DEGs, *MMP1*, *PTGS2*, and *CXCL8*, suggesting that CTH and CBS play a role in the negative feedback regulation of formaldehyde-induced pro-inflammatory responses in NHKs. In this regard, the sub-cytotoxic formaldehyde-induced CBS and CTH may regulate inflammation fate decision to resolution by suppressing the early pro-inflammatory response.

1. Introduction

Formaldehyde exposure is one of the most common environmental hazards that threaten human health. It has been the focus of many toxicological and epidemiological investigations. Since the early 1900s, formaldehyde has been widely used in a variety of industrial products such as press-wood products, permanent-press fabrics, paper product coatings, insulation supports and general consumer products (Flyvholm and Andersen, 1993; Bostrom et al., 1994). Formaldehyde is also released from vehicle emissions, particle boards, carpets, paints and varnishes. Epidemiological studies have shown that formaldehyde is associated with an increased risk of sino-nasal cancer (Roush et al., 1987), nasopharyngeal cancer (Vaughan et al., 2000), childhood asthma (Garrett et al., 1999), and leukemia (Zhang et al., 2010). Toxicological studies have shown that formaldehyde causes squamous cell carcinoma in rodents (Swenberg et al., 1980; Brown, 1985). Formaldehyde is currently classified as a human carcinogen (Cogliano et al., 2005).

Formaldehyde exposure can result in various respiratory and dermatologic problems in humans, including irritation or allergic reactions in the eyes, skin and the respiratory system (De Jong et al., 2009; Hauksson et al., 2016). Therefore, formaldehyde-induced transcription profile studies have been performed in various kinds of mammalian cells including human nasal epithelial cells (Neuss et al., 2010) and human tracheal fibroblasts (Li et al., 2007). However, few studies have investigating their effects on human skin cells. Irritant and allergic contact dermatitis are common inflammatory human skin diseases induced by repeated exposure to chemicals (Nosbaum et al., 2009). The

* Corresponding author at: Natural Products Research Institute, College of Pharmacy, Seoul National University, 1 Gwanak-ro, Gwanak-gu, Seoul 08826, Republic of Korea.
E-mail addresses: minsoonoh@snu.ac.kr, minsoo@alum.mit.edu (M. Noh).
[1] These authors contributed equally to this work.

http://dx.doi.org/10.1016/j.taap.2016.09.017
0041-008X/

formaldehyde-induced contact allergy in cosmetics has been reported in industrialized countries since the 1960s (Thyssen et al., 2007). According to the FDA's Voluntary Cosmetic Registration Program database, 19.5% of cosmetic products in the USA contained formaldehyde or formaldehyde-releasing preservatives (de Groot and Veenstra, 2010) and formaldehyde is still categorized as a major contact allergen (Warshaw et al., 2015). Despite the causative association of formaldehyde exposure with both irritant and allergic contact dermatitis (Garrett et al., 1999), the molecular mechanism of formaldehyde-induced allergy in human skin is not comprehensively understood. In human skin, epidermal keratinocytes are the primary cells that are in direct contact with environmental chemicals and have an essential role in skin permeability barrier functions (Vandebriel et al., 2010). Human keratinocytes can sense toxic chemicals or organic materials and produce various pro-inflammatory autacoids, cytokines, and anti-microbial peptides (Jin et al., 2014; Bae et al., 2015a; Bae et al., 2015b). Recently, we reported that formaldehyde significantly increased the expression of interleukin-8 (IL-8), interleukin-24 (IL-24), and vascular endothelial growth factor (VEGF) in human keratinocytes (Bae et al., 2015a). However, it is still unclear how human epidermal keratinocytes respond to formaldehyde at a whole genome transcription level.

Genome-wide transcription profile studies to elucidate the molecular mechanisms underlying formaldehyde-induced toxicological outcomes such as allergy and carcinogenesis have mainly been performed in respiratory epithelial cells (Li et al., 2007; Neuss et al., 2010). Formaldehyde is normally present in both indoor and outdoor air at low levels (Gustafson et al., 2005; Rovira et al., 2016). Formaldehyde is usually present as a contaminant in foods, albeit at very low concentrations (Jeong et al., 2015). Many consumer products may contain small amounts of formaldehyde due to their use as fumigants, fertilizers, or preservatives. However, most transcriptional profile studies have been performed with high concentrations of formaldehyde that are cytotoxic to target cells as formaldehyde was determined to be a carcinogen in animal models using high-dose exposure. At cytotoxic concentrations, the formaldehyde-induced gene expression signature of target cells is associated with cell death-related biological pathways such as apoptosis (Szende and Tyihak, 2010). Currently, information on the toxicological response to sub-toxic concentrations of formaldehyde is limited in human cells. In addition, a direct cell death in human skin may not be a primary cellular mechanism to explain the pathophysiology of formaldehyde-induced cutaneous allergy in normal life conditions. However, the effects of sub-cytotoxic formaldehyde concentrations on human skin are not fully understood. To investigate the toxicological effect of low-dose formaldehyde exposure in the general environment, we performed a genome-wide transcription profile analysis on cultured human primary keratinocytes treated with sub-cytotoxic formaldehyde concentrations, which did not cause cell death.

2. Materials and methods

2.1. Cell culture and cell viability test

Normal human keratinocytes (NHKs) from neonatal foreskins were purchased from Lonza (first passage, Basel, Switzerland) and cultured in a KBM medium with KGM2 growth supplements containing insulin, human epidermal growth factor, bovine pituitary extract, hydrocortisone, epinephrine, transferrin, and gentamicin/amphotericin B, purchased from Lonza (KBM/KGM-2). We purchased three NHK batches prepared form different donors and performed all experiments in triplicates or quadruplicates. Cells were serially passaged at 80–90% confluence and the third passage of primary NHKs was used in the cytotoxicity and other experiments in this study. Cell viability was evaluated using a Cell Counting Kit-8 assay (CCK-8, Dojindo, Kumamoto, Japan) according to the manufacturer's instructions. 5×10^4 NHKs were seeded to each well in 48-well plates and cultured up to 100% confluence. The 200 μM solution of formaldehyde (#F8775, 37% solution, Sigma-Aldrich, St. Louis, MO, USA) was freshly prepared in KBM/KGM-2 media just before performing experiments. Formaldehyde in KBM/KGM-2 was treated at 24 h after KBM/KGM-2 media were exchanged in confluent NHKs. NHKs were exposed to formaldehyde for 24 h in a KBM/KGM-2 medium and washed with phosphate-buffered saline (PBS) three times. The CCK-8 solution, 2-(2-methoxy-4-nitrophenyl)-3-(4-nitrophenyl)-5-(2,4-disulfophenyl)-2H–tetrazolium, monosodium salt (WST-8) diluted in PBS, was used to treat the NHKs cells prior to further incubation for 2 h. The absorbance at 450 nm was measured using a microplate reader (BioTek, Winooski, VT, USA). Absolute optical density was expressed as a percentage of the control value.

2.2. Microarray experiments

Total RNA was isolated using TRIzol (Invitrogen, Carlsbad, CA, USA), per the manufacturer's instructions. RNA was further purified using the RNeasy Mini Kit (Qiagen, Germantown, MD, USA). The quantity of the total RNA was measured using the NanoDrop ND-1000 spectrophotometer (NanoDrop Technologies, Inc., Montchanin, DE, USA). RNA integrity was verified with the Bioanalyzer 2100 (Agilent Technologies, Santa Clara, CA, USA). Affymetrix Human Genome U133 2.0 GeneChip arrays (Affymetrix, Santa Clara, CA, USA) were prepared, hybridized and scanned by the local authorized Affymetrix service provider (DNA Link, Inc., Seoul, South Korea). RNA reverse transcribed to cDNA and transcribed into cRNA in the presence of biotinylated ribonucleotides, per standard Affymetrix protocols. The hybridized probe array was stained and washed with a GeneChip hybridization wash and stain kit using the Fluidics Station 450 (Affymetrix). The stained GeneChip probe array was scanned with a GeneChip Scanner 3000 + 7G (Affymetrix). The signal intensity of the gene expression level was calculated using Expression Console Software, Version 1.1 (Affymetrix) based on the MAS 5.0 algorithm. The procedure used to select the differentially expressed genes (DEGs) was as follows: (i) selection of "present" Affymetrix probe sets as control or formaldehyde-treated samples; (ii) selection of Affymetrix probe sets with comparison signal sample/control ratios greater than two as "up-regulated" and less than two as "down-regulated"; and (iii) selection of Affymetrix probe sets with simultaneously significant P values (threshold, 0.05) in the Wilcoxon rank test when compared with vehicle-treated samples.

2.3. Gene Ontology (GO) enrichment analysis

GO enrichment analysis was performed by comparing the frequency of GO biological process (BP) terms assigned for a specific gene included in a group of DEGs with that in all the genes set in Affymetrix Human 133 2.0 GeneChip arrays. The GO annotation files were downloaded from the Gene Ontology Consortium webpage (http://www.geneontology.org) and the August 2015 version of the GO BP terms, which are annotated to a specific gene in the whole genome, was used in the GO enrichment analysis. When redundant probe sets for the same gene in the Affymetrix Human 133 2.0 GeneChip were considered as a single gene unit in the GO enrichment analysis, 23, 624 probe sets were counted as the total number of genes in the analysis. A 2×2 contingency matrix was constructed to determine the frequency of a specific GO BP term in a group of DEGs compared with that in the 23,624 total gene set. The 2×2 contingency matrix data were analyzed by the Fisher's exact test (frequency ≤ 5) or χ^2 test (frequency ≥ 5) using SPSS® for Windows (SPSS Science, Chicago, USA) to calculate the level of significance.

2.4. Validation of microarray results using quantitative real-time PCR

Quantitative real-time PCR (Q-RT-PCR) was performed to validate the microarray data on selected genes from DEGs. Total RNA samples were prepared in independent experiments in the microarray study. cDNA samples were synthesized from the total RNA using SuperScript

™ reverse transcriptase (Invitrogen). The expression level of target mRNAs was quantified by Q-RT-PCR using the Applied Biosystems' 7500 Real Time PCR System (Applied Biosystems, Foster City, CA, USA). The TaqMan RT-PCR primer sets (Applied Biosystems) used in the RT-PCR were: cystathionine-β-synthase (*CBS*), Hs00163925_m1; cystathionine-γ-lyase (*CTH*), Hs00542284_m1; asparagine synthetase (*ASNS*), Hs04186194_m1; matrix metalloproteinase 1 (*MMP1*), Hs00899658_m1; metalloproteinase 3 (*MMP3*), Hs00968305_m1; fibronectin, Hs01549937_m1; involucrin (*IVL*), Hs00846307_s1; small proline rich protein 4 (*SPRR4*), Hs01917405_s1; prostaglandin-endoperoxide synthase 2 (*PTGS2*), Hs00153133_m1; VEGF-A, Hs00900055_m1; interleukin 8 (*CXCL8*), Hs00174103_m1; phosphodiesterase 4B (*PDE4B*), Hs00277080_m1; interleukin 33 (*IL33*), Hs00369211_m1; solute carrier family 25, member 4 (*SLC25A4*), Hs00154037_m1; growth arrest-specific 1 (*GAS1*), Hs00266715_s1. Human *GAPDH* (4333764F, Applied Biosystems) was also amplified to normalize variations in cDNA levels across different samples.

2.5. Western blot analysis and enzyme-linked immunosorbent assay (ELISA)

Protein expression of the selected genes was confirmed by western blot analysis and ELISA with three independent NHK batches. NHKs (Third passages, 2×10^5 cells/well) were seeded to 6-well plates and cultured up to 100% confluence. Confluently cultured NHKs in 6-well culture plates were treated with 200 μM formaldehyde for 24 h. Human CBS, CTH, and fibronectin were measured by western blot analysis. NHKs were lysed in cell lysis buffer (RIPA buffer) containing protease inhibitors (Sigma-Aldrich). The lysate was then subjected to centrifugation at 15, 000*g* for 10 min, and the supernatant was used for protein expression analysis. Proteins (40 μg/well) were fractionated by SDS-PAGE and transferred to nitrocellulose membranes. The membranes were blocked with 5% skimmed milk in TBST (10 mM Tris-HCl, pH 8.0, 150 mM NaCl, and 0.15% Tween-20) for 1 h at room temperature and were subsequently probed overnight at 4 °C with an anti-CBS antibody (#PA5-22273, Thermo-Scientific, Rockford, IL, USA), anti-CTH (#PA5-29725, Thermo-Scientific), anti-fibronectin (#SC-9068, Santa Cruz Biotechnology) and anti-β-actin (#A5441, Sigma-Aldrich). The blots were washed thrice with TBST and incubated with horseradish peroxidase-conjugated goat anti-rabbit IgG (Bio-Rad, Richmond, CA, USA) at room temperature for 1 h. Detection was performed using the ECL system (Invitrogen). Human MMP1, PTGS2, and IL-8 were measured by ELISA assay. The concentrations of MMP1, PGE_2, and IL-8 in the supernatant were measured using enzyme immunoassay kits (MMP1 and IL-8 EIA kits, R&D systems; PGE_2 EIA kit, Cayman Chemical Co., MI, USA), per the manufacturer's instructions.

2.6. Statistical analysis

Statistical analysis was conducted using SPSS® for Windows (SPSS Science). The data are expressed as means ± standard deviation (SD). Statistical analyses were performed using Student's *t*-test for comparison with the control or by one-way ANOVA followed by Bonferroni's post-test for multiple comparison. *P*-values < 0.05 indicated statistical significance.

3. Results

3.1. Genome-wide transcription profile of NHKs to sub-cytotoxic formaldehyde exposure

To investigate a genome-wide transcription profile of NHKs after exposure to formaldehyde at sub-cytotoxic concentrations as the level of formaldehyde exposure in daily life conditions may not cause significant cell death, we first determined the formaldehyde concentration that caused no apparent phenotypic cell death. Cell viability of NHKs was evaluated at 24 h after the formaldehyde treatment by the WST-8-based cytotoxicity test (Supplementary Fig. 1). The cell viability of the 300 μM formaldehyde-treated NHKs was 44% lower than that of the vehicle-treated control. No difference in cell viability was detected in NHKs treated with 200 μM formaldehyde for 24 h in culture compared to that of the control. Therefore, the whole genome-scale transcription profile study was performed in NHKs treated with 200 μM formaldehyde. The raw data used in the Affymetrix oligonucleotide microarrays in this study can be accessed from the National Center for

Table 1
Top 20 upregulated and downregulated DEGs in the sub-cytotoxic formaldehyde-treated NHKs.

Probe set ID	Gene title	Gene symbol	Mean fold change
Up regulated genes			
204475_at	Matrix metallopeptidase 1 (interstitial collagenase)	MMP1	8.19
205828_at	Matrix metallopeptidase 3 (stromelysin 1, progelatinase)	MMP3	7.98
221565_s_at	Calcium homeostasis modulator 2	CALHM2	6.65
219563_at	Long intergenic non-protein coding RNA 341	LINC00341	5.89
209114_at	Tetraspanin 1	TSPAN1	5.48
203234_at	Uridine phosphorylase 1	UPP1	5.36
218843_at	Fibronectin type III domain containing 4	FNDC4	5.11
217127_at	Cystathionine gamma-lyase	CTH	4.93
212419_at	zinc finger, CCHC domain containing 24	ZCCHC24	4.62
209611_s_at	Solute carrier family 1, member 4	SLC1A4	4.56
218000_s_at	Pleckstrin homology-like domain, family A, member 1	PHLDA1	4.38
208161_s_at	ATP-binding cassette, sub-family C (CFTR/MRP), member 3	ABCC3	4.33
212816_s_at	Cystathionine-beta-synthase	CBS	4.28
226028_at	Roundabout, axon guidance receptor, homolog 4 (Drosophila)	ROBO4	4.25
226769_at	Fin bud initiation factor homolog (zebrafish)	FIBIN	4.09
241994_at	Xanthine dehydrogenase	XDH	4.07
212190_at	Serpin peptidase inhibitor, clade E member 2	SERPINE2	4.03
234699_at	Ribonuclease, RNase A family, 7	RNASE7	4.00
209949_at	Neutrophil cytosolic factor 2	NCF2	3.97
1555788_a_at	Tribbles pseudokinase 3	TRIB3	3.85
Down regulated genes			
203708_at	Phosphodiesterase 4B, cAMP-specific	PDE4B	0.11
209821_at	Interleukin 33	IL33	0.21
214821_at	Solute carrier family 25, member 4	SLC25A4	0.24
204457_s_at	Growth arrest-specific 1	GAS1	0.26
228262_at	MAP7 domain containing 2	MAP7D2	0.26
206149_at	Calcineurin-like EF-hand protein 2	CHP2	0.27
219893_at	Coiled-coil domain containing 71	CCDC71	0.27
230560_at	Syntaxin binding protein 6 (amisyn)	STXBP6	0.27
241416_at	Uncharacterized LOC101928806	LOC101928806	0.28
214598_at	Claudin 8	CLDN8	0.30
1560305_x_at	FK506 binding protein 4, 59 kDa	FKBP4	0.30
229390_at	Family with sequence similarity 26, member F	FAM26F	0.32
220263_at	SMAD5 antisense RNA 1	SMAD5-AS1	0.33
204519_s_at	Plasmolipin	PLLP	0.35
235006_at	CDKN2A interacting protein N-terminal like	CDKN2AIPNL	0.36
226539_s_at	Coiled-coil domain containing 42B	CCDC42B	0.36
228062_at	Nucleosome assembly protein 1-like 5	NAP1L5	0.37
237386_at	Chromosome X open reading frame 69-like	LOC100129361	0.37
229290_at	Death associated protein-like 1	DAPL1	0.38
1553111_a_at	Kelch repeat and BTB (POZ) domain containing 6	KBTBD6	0.38

Values represent the ratio of formaldehyde-treated to vehicle-treated control expression values.

Biotechnology Information Gene Expression Omnibus (NCBI GEO) database using the accession number GSE76446. DEGs were identified based on data variability among samples, fold expression change, and statistical *p*-value for each probe set in the Affymetrix MAS 5.0 algorithm. In terms of these three criteria, we selected 175 genes as up-regulated DEGs in the formaldehyde-treated NHKs and 116 genes as down-regulated DEGs (Supplementary Table 1). Based on the fold change, the top 20 genes were listed in the Table 1. Notably, the up-regulated DEGs in the formaldehyde-treated NHKs included *MMP1*, *MMP3*, and *SERPINE2*, which are major protein-encoding genes important in skin inflammation (Herouy et al., 2001; Boivin et al., 2006).

3.2. Gene Ontology Biological Process enrichment analysis for DEGs

Next, in order to determine statistically significant biological phenotypes in the formaldehyde-treated NHKs, we compared the frequency of Gene Ontology Biological Process (GO BP) terms in the DEGs with that in the total gene set in the Affymetrix human genome array platform as described in the Materials and methods section (Table 2). By using the Fisher's exact test- or the χ^2 test-based statistics, the frequencies of all GO BP terms annotated for the 175 up-regulated DEGs were compared with those in the total gene set. The topmost GO BP term that was significantly enriched in the up-regulated DEGs was the endoplasmic reticulum (ER) unfolded protein response (UPR) (GO:0030968). For the ER UPR analysis, a contingency table was generated from which seven genes in the 175 up-regulated DEGs were annotated as the GO BP term ER UPR compared with 99 genes in a total of 23,624 genes on the genome array platform. The *p*-value of the ER UPR enrichment was 0.000009, which was calculated by χ^2 test using the contingency table. The other GO BP terms listed in the 175 up-regulated DEGs were analyzed using the same procedure and the top 20 GO BP terms enriched in the up-regulated DEGs are listed in Table 2.

The biological ER UPR phenotype is associated with cell death mechanisms (Sano and Reed, 2013). Although we chose the formaldehyde concentration that did not phenotypically affect cell viability, the GO BP enrichment analysis showed that the cellular pathway associated with cell death was transcriptionally activated in NHKs treated with sub-cytotoxic formaldehyde. As expected, cellular pathways related to inflammation were significantly enriched in the up-regulated DEGs, such as positive regulation of the nitric oxide biosynthetic process (GO:0045429), cell migration (GO:0016477), positive regulation of fever generation (GO:0031622), positive regulation of the prostaglandin biosynthetic process (GO:0031394), and positive regulation of interleukin (IL)-8 production (GO:0032757). Notably, there were two up-regulated DEGs encoding enzymes associated with cellular detoxification responses such as transsulfuration (GO:0019346) and the hydrogen sulfide biosynthetic process (GO:0070814) (Vitvitsky et al., 2006). The GO BP enrichment analysis suggests that cellular mechanisms regulating both inflammation and detoxification were simultaneously triggered in NHKs by the sub-cytotoxic formaldehyde treatment.

In the 116 down-regulated DEGs, GO BPs such as cellular response to bacterial lipopeptide (GO:0071221), neutrophil chemotaxis (GO:0030593), and negative regulation of the growth of symbiont in host (GO:0044130) were significantly suppressed biological phenotypes in the formaldehyde-treated NHKs, which are associated with innate immunity (Supplementary Table 2). The down-regulated DEGs, *GAS1*, *MITF*, *TNFSF11*, and *WNT4*, may contribute to phenotypic changes associated with cellular proliferation and differentiation (GO:0045670, GO:0002053, GO:0045165, GO:0043010, etc.).

3.3. Validation of DEGs in formaldehyde-treated NHKs

DEGs determined from microarray results require experimental validation by independent measurements such as Q-RT-PCR and Western blotting. In this study, the microarray expression was validated for the up-regulated DEGs listed in both Tables 1 and 2. First, the transcription of *MMP1* and *MMP3*, the top two up-regulated DEGs (Table 1), was confirmed by Q-RT-PCR in the independently prepared formaldehyde-treated NHKs (Fig. 1A and B). Next, we measured the mRNA levels of CBS and CTH, not only because they were ranked in the top 20 up-regulated DEG list (Table 1), but also many top listed GO BP terms such as GO:0030968, GO:0008652, GO:0019346, and GO:0070814, included these two genes (Table 2). The mRNA levels of CBS and CTH were significantly up-regulated in a concentration-dependent manner (Fig. 1C and D). The gene transcription of asparagine synthetase (ASNS), an enzyme functionally related to CBS and CTH as GO:0008652, was also

Table 2
Top 20 Gene Ontology (GO) biological process (BP) terms in the formaldehyde-induced upregulated DEGs.

GO code	Up DEGs	Total	Gene ontology biological process term	p Value	Gene symbol (fold change)
GO:0030968	7	99	Endoplasmic reticulum unfolded protein response	0.000009	CTH (4.93), DDIT3 (3.85), STC2 (3.04), GFPT1 (2.73), ASNS (2.66), PPP1R15A (2.6), ERN1 (2.2)
GO:0008652	5	41	Cellular amino acid biosynthetic process	0.000012	CTH (4.93), CBS (4.28), BCAT1 (3.61), ASNS (2.66), ASS1 (2.12)
GO:0018149	4	23	Peptide cross-linking	0.000023	ANXA1 (3.25), FN1 (3.06), IVL (2.17), SPRR4 (2.13)
GO:0008360	7	116	Regulation of cell shape	0.000026	LINC00341 (5.89), BAMBI (3.57), EPB41L3 (3.27), FN1 (3.06), SH3KBP1 (2.72), FERMT2 (2.17), VEGFA (2.04)
GO:0019346	2	2	Transsulfuration	0.000054	CTH (4.93), CBS (4.28)
GO:0045429	4	35	Positive regulation of nitric oxide biosynthetic process	0.000125	PTGS2 (3.07), P2RX4 (2.4), ASS1 (2.12), IL1B (2.02)
GO:0070814	2	3	Hydrogen sulfide biosynthetic process	0.000161	CTH (4.93), CBS (4.28)
GO:0030949	3	16	Positive regulation of vascular endothelial growth factor receptor signaling pathway	0.000208	GRB10 (2.42), IL1B (2.02), VEGFA (2.04)
GO:0016477	7	174	Cell migration	0.000326	TSPAN1 (5.48), BAMBI (3.57), FN1 (3.06), SH3KBP1 (2.72), HBEGF (2.53), CCDC88A (2.16), VEGFA (2.04)
GO:0007179	6	136	Transforming growth factor beta receptor signaling pathway	0.000522	BAMBI (3.57), ID1 (3.19), PPP1R15A (2.6), SERPINE1 (2.41), FERMT2 (2.17), TGIF1 (2.14)
GO:0010757	2	5	Negative regulation of plasminogen activation	0.000532	SERPINE2 (4.03), SERPINE1 (2.41)
GO:0031622	2	5	Positive regulation of fever generation	0.000532	PTGS2 (3.07), IL1B (2.02)
GO:0031394	2	5	Positive regulation of prostaglandin biosynthetic process	0.000532	ANXA1 (3.25), PTGS2 (3.07)
GO:0046882	2	5	Negative regulation of follicle-stimulating hormone secretion	0.000532	INHBA (3.38), FST (3.36)
GO:0032757	3	23	Positive regulation of interleukin-8 production	0.000624	DDIT3 (3.85), SERPINE1 (2.41), IL1B (2.02)
GO:0042346	3	24	Positive regulation of NF-kappaB import into nucleus	0.000709	PTGS2 (3.07), EDA (2.92), IL1B (2.02)
GO:0006801	3	24	Superoxide metabolic process	0.000709	CBS (4.28), NCF2 (3.97), NOX4 (2.24)
GO:0030198	9	325	Extracellular matrix organization	0.000711	MMP1 (8.19), MMP3 (7.98), CRISPLD2 (3.66), ECM2 (3.22), FN1 (3.06), LAMC2 (2.81), SMOC2 (2.47), SERPINE1 (2.41), NTN4 (2.08)
GO:0034976	4	55	Response to endoplasmic reticulum stress	0.000723	TRIB3 (3.85), DDIT3 (3.85), STC2 (3.04), FAM129A (2.61)
GO:0050667	2	6	Homocysteine metabolic process	0.000794	CBS (4.28), NOX4 (2.24)

upregulated in the formaldehyde-treated NHKs when it was measured by Q-RT-PCR (Fig. 1E). The DEGs annotated as peptide cross-linking (GO:0018149), fibronectin, involucrin (IVL), and small proline rich protein 4 (SPRR4) were up-regulated in the 200 μM formaldehyde-treated NHKs than in that of the control (Fig. 1F-H). In addition, the microarray results of the DEGs associated with the production of major pro-inflammatory mediators such as *PTGS2*, *VEGFA*, and *CXCL8/IL8* were validated by Q-RT-PCR (Fig. 1I-K). In the downregulated DEGs in the formaldehyde-treated NHKs, the gene transcription of *PDE4B*, *IL33*, *SLC25A* and *GAS1* was also confirmed by independent measurements (Fig. 1L-O).

Among the validated DEGs in the Q-RT-PCR analysis, the protein expression levels of CBS, CTH, and fibronectin were further confirmed by Western blotting (Fig. 2A). Protein expression of CBS, CTH, and fibronectin was significantly up-regulated in NHKs treated with 100 and 200 μM of formaldehyde (Fig. 2B-D). In the cell culture supernatants, the concentrations of MMP1, prostaglandin E_2 (PGE2, a metabolite of PTGS2), VEGFA, and CXCL8/IL8 were determined by ELISA (Fig. 2E-H). Like their gene transcription, the cellular products of MMP1, PTGS2, VEGFA, and CXCL8/IL8 were significantly increased in NHKs in response to formaldehyde in a concentration-dependent manner. These results supported the finding that the microarray expression of the up-regulated DEGs was related to the significantly enriched GO BPs we validated in the sub-cytotoxic formaldehyde-treated NHKs.

3.4. Temporal expression profile of pro-inflammatory factors, CBS and CTH, in NHKs

The low-level exposure of formaldehyde affected NHKs to not only increase pro-inflammatory DEGs such as PTGS2 and CXCL8/IL8, but also to upregulate DEGs with cytoprotective or anti-inflammatory potentials such as CBS and CTH (Wang et al., 2014), suggesting that these two opposing biological reactions existed simultaneously. In the microarray study, transcriptional changes of NHKs were determined only at 24 h after formaldehyde exposure. As toxic stimuli trigger and

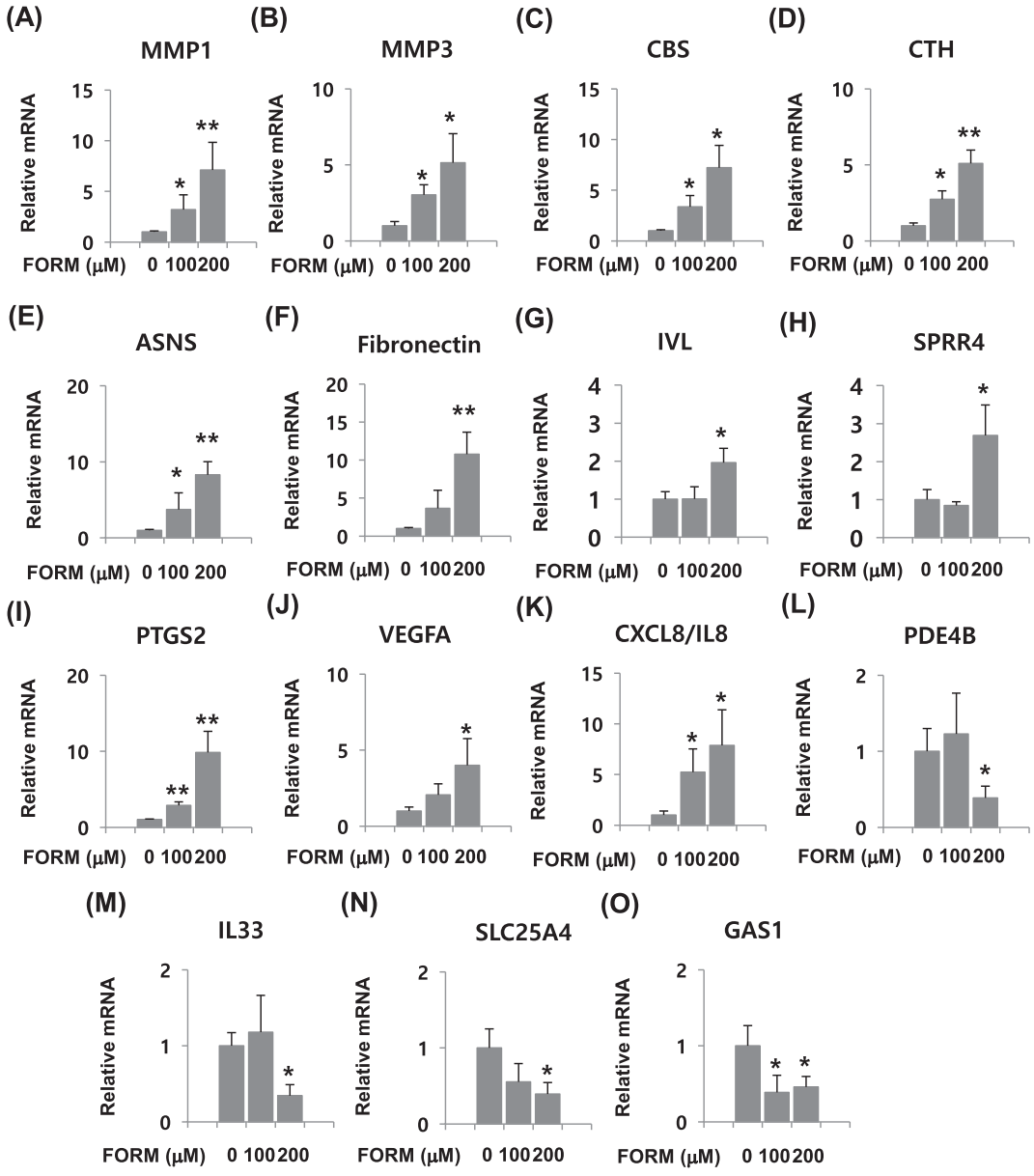

Fig. 1. Validation of the microarray results by Q-RT-PCR. To determine the mRNA levels of MMP1 (A), MMP3 (B), CBS (C), CTH (D), ASNS (E), Fibronectin (F), IVL (G), SPRR4 (H), PTGS2 (I), VEGFA (J), CXCL8/IL8 (K), PDE4B (L), IL33 (M), SLC25A4 (N) and GAS1 (O), total RNA samples were extracted from confluently cultured NHKs treated with formaldehyde (FORM) for 24 h. Values represent the mean expression ± SD of the mRNA of the various genes relative to human GAPDH expression. Error bars represent SD of three independent measurements (n = 3). *$p \le 0.05$ and ** $p \le 0.01$.

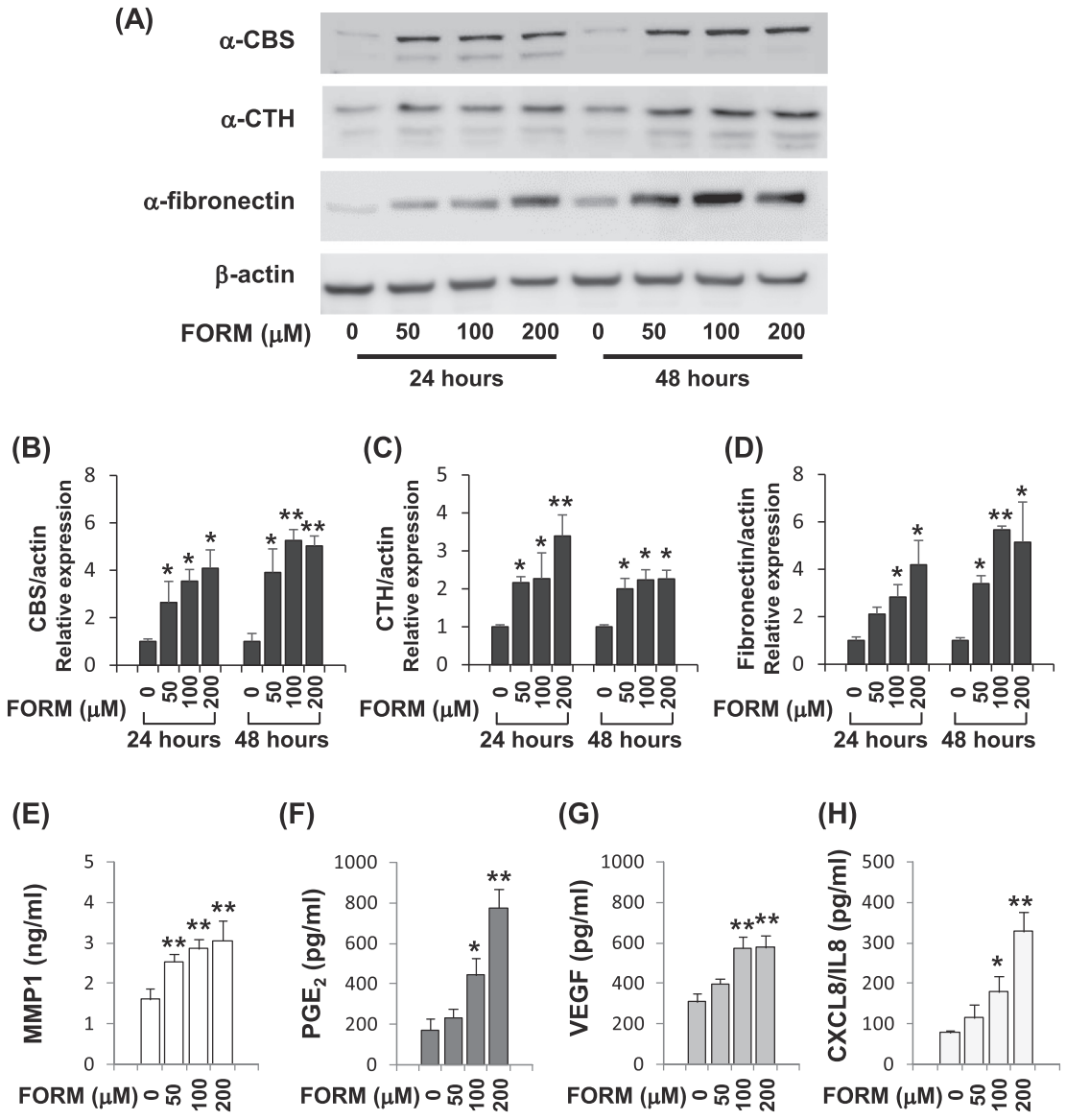

Fig. 2. The effects of formaldehyde on the protein expression of validated DEGs in NHKs. Formaldehyde (FORM) was treated for 24 h in confluently cultured NHKs and protein samples were prepared for western blotting analysis of CBS, CTH and fibronectin (A). Three independent Western blotting results were quantified against β-actin level for CBS (B), CTH (C) and fibronectin (D). The protein levels of MMP1 (E), PGE_2 (F), VEGF (G), and CXCL8/IL8 (H) in the culture supernatants of NHKs were measured by ELISA. Values represent the mean expression ± SD (n = 3). $^{*}p \le 0.05$ and $^{**}p \le 0.01$.

promote inflammatory reactions in a biological system, various inflammatory mediators show a differential and sequential expression pattern (Mozes et al., 1991; Klosterhalfen et al., 1992; Srinivasan et al., 2010). Therefore, the temporal expression profile of DEGs with opposing functions was determined in the formaldehyde-treated NHKs. In the time-course study, the upregulation of *PTGS2* mRNA was detected in NHKs at 2 h after the formaldehyde treatment (Fig. 3A), which was associated with an increase in PGE_2 levels in cell culture supernatants. IL-8 mRNA levels were significantly up-regulated from the sixth hour after the treatment (Fig. 3B). In contrast, significant changes in gene transcription of *VEGF*, *CBS*, and *CTH* were detected at the 24th hour (Fig. 3C-E). The up-regulation of *PTGS2* and *CXCL8/IL8* gene transcription preceded the increase in that of *VEGF*, *CBS*, and *CTH*. *PTGS2* and *CXCL8/IL8* play a role in the acute phase of inflammation, whereas *VEGF* is known to participate in the transitional or resolving phase of inflammation (Kataru et al., 2009). It was reported that CBS and CTH play an important role in regulating the cellular production of glutathione and H_2S, which have anti-inflammatory functions (Wang et al., 2014).

3.5. Roles of CBS and CTH in the formaldehyde-induced inflammation in NHKs

We hypothesized that CBS and CTH are associated with the attenuation of severe inflammatory responses, which is essential to the resolution of inflammation. If primary inflammatory mediators such as PGE_2, CXCL8/IL8, and MMP1 increased significantly during the immediate-early phase of inflammation and were not removed, pathological inflammatory reactions develop. Therefore, we investigated whether metabolites of CBS and CTH attenuate formaldehyde-induced pro-inflammatory responses in NHKs. CBS is the first enzyme in the transsulfuration pathway, catalyzing the conversion of homocysteine into cystathionine. The enzyme CTH breaks down cystathionine into cysteine (Fig. 4A). CBS and CTH, two enzymes in the transsulfuration pathway, regulate glutathione synthesis in the cellular metabolic pathway and glutathione functions as the most important endogenously-produced antioxidant (Belalcazar et al., 2014). Cellular glutathione activity is critical for normal detoxification and defense mechanisms in

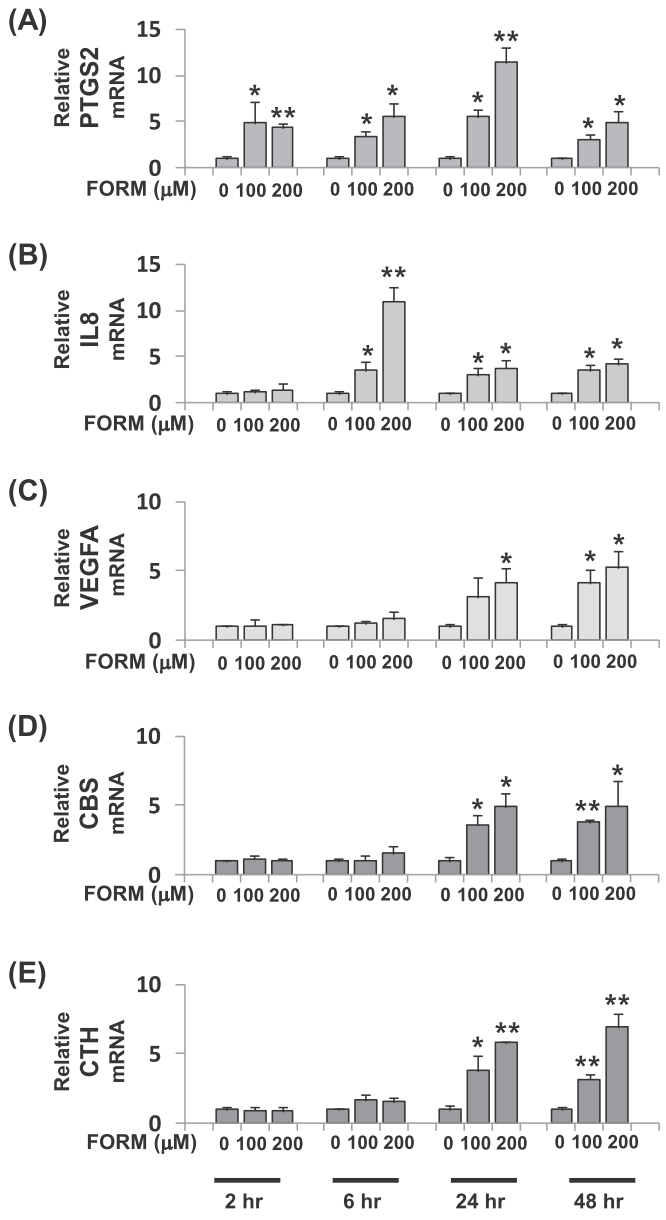

Fig. 3. Temporal expression profile in the formaldehyde-treated NHKs. NHKs (2×10^5 cells/well) were seeded to 6-well plates and cultured up to 100% confluence. Formaldehyde (FORM) was treated in confluent NHKs for 2, 6, 24 or 48 h. Total RNA was extracted at given times after the formaldehyde treatment. Q-RT-PCR was performed for PTGS2 (A), CXCL8/IL8 (B), VEGFA (C), CBS (D), and CTH (E). Values represent the mean expression ± SD of the mRNA of the various genes relative to human GAPDH expression (n = 3). $^{*}p \le 0.05$ and $^{**}p \le 0.01$.

mammalian cells. Therefore, we evaluated whether L-cystathionine and L-cysteine, key intermediates in the CBS/CTH-mediated metabolic pathways, affected the cellular production of MMP1, PGE_2, CXCL8/IL8, and VEGF in NHKs treated with 100 μM formaldehyde. As shown in Fig. 4B-D, L-cystathionine and L-cysteine significantly antagonized the formaldehyde-induced upregulation of MMP1, PEG_2 and CXCL8/IL8 in NHKs. Formaldehyde-induced VEGF up-regulation was significantly inhibited by treatment with L-cysteine (Fig. 4E). In the 200 μM formaldehyde-treated NHKs, both L-cystathionine and L-cysteine attenuated the formaldehyde-induced upregulation of MMP1, PGE_2 and CXCL8/IL8 by 25.9%, 35.2% and 27.5% respectively, however, these effects were not statistically significant (data not shown).

3.6. Effects of pro-inflammatory cytokines on CBS and CTH transcription

Next, we investigated whether formaldehyde-induced upregulation of CBS and CTH in NHKs is valid in other cutaneous inflammatory responses. We treated NHKs with major pro-inflammatory cytokines important in acute or chronic cutaneous inflammation (Jin et al., 2014). Tumor necrosis factor α (TNFα) was chosen to evaluate the change of CBS and CTH in acute inflammation states while T helper (Th) cell cytokines, interferon γ (IFNγ), IL4, IL17, and IL22, were chosen for chronic states. TNFα did not significantly change the gene transcription of both CBS and CTH at the sub-cytotoxic levels. Among the major T helper cell cytokines, IFNγ and IL4 significantly increased *CBS* and *CTH* gene transcription in NHKs (Fig. 5). Interestingly, IFNγ significantly increased *CBS* and *CTH* genes transcriptions at 6 h after treatment, which was an earlier response compared to that of formaldehyde. These results suggested that CBS and CTH may have specific roles in general cutaneous inflammation.

4. Discussion

Genome-scale transcription profiles of NHKs in response to exposure to sub-cytotoxic formaldehyde concentrations can provide mechanistic insights into skin toxicity in real-life conditions. In this study, formaldehyde exposure conditions did not cause direct cell deaths in NHKs, which was determined by the NADH/NADPH dehydrogenase activity-based WST-8 assay. The 175 upregulated and 116 down-regulated DEGs were identified under conditions in which formaldehyde had no effect on the cell viability of NHKs. The GO BP enrichment analysis with the 175 upregulated DEGs suggested that NHKs simultaneously increased the transcription of both pro-inflammatory and anti-inflammatory genes (Tables 1 and 2). The upregulation of pro-inflammatory DEGs such as *MMP1*, *MMP3*, *PTGS2*, and *CXCL8*/*IL8* was expected due to the well-known toxicological outcomes of formaldehyde. Notably, it was first discovered that the cellular detoxification pathway-associated DEGs such as *CBS* and *CTH* in NHKs were upregulated after 24 h of formaldehyde treatment in parallel with those of the anti-inflammatory DEGs. Temporal expression analysis showed that DEGs associated with the immediate early inflammatory response such as *PTGS2* and *CXCL8*/*IL8* were upregulated before an increase in *CBS* and *CTH* gene transcription (Fig. 3). In the χ^2 test-based GO enrichment analysis, ER UPR (GO:0030968) was the most significant biological process in the upregulated DEGs. ER UPR represents molecular events associated with the coordinated regulation of cellular transcription and translation under ER stress conditions (Kaufman et al., 2002) (Table 2). In multicellular organisms, if the unfolded protein level is not properly controlled, cell-death responses such as apoptosis or necrosis can occur (Kaufman et al., 2002). This result suggests that low-level exposure to formaldehyde, which does not cause phenotypic cell deaths, can induce the ER-stress response genes, especially *CTH*, in NHKs. When intracellular unfolded proteins are properly regulated by the ER UPR mechanism, cells restore homeostasis. The ER UPR is important in deciding the fate of the cell: either death or survival. In this regard, the upregulation of ER UPR-related DEGs, *CTH*, *DDIT3*, *STC2*, *GFPT1*, *ASNS*, *PPP1R15A*, and *ERN1* may play a role in the formaldehyde-induced cell death or survival. The molecular mechanism associated with the roles of the unfolded protein response genes in human epidermal keratinocytes may provide important toxicological insights for understanding formaldehyde toxicity in human skin.

Under toxic stresses, the ER UPR of mammalian cells has an impact on the fate of the cell viz. apoptosis, death, or programmed homeostatic survival (Sano and Reed, 2013). Among the ER UPR DEGs discovered in this study, CTH increases the cytoprotective amino acid metabolite, L-cysteine, which attenuated the formaldehyde-induced inflammation (Fig. 4). The inhibition of CTH results in the upregulation of pro-inflammatory cytokines and increases inflammatory responses in kidney injury (Wang et al., 2014). Therefore, the activity of CTH may be important

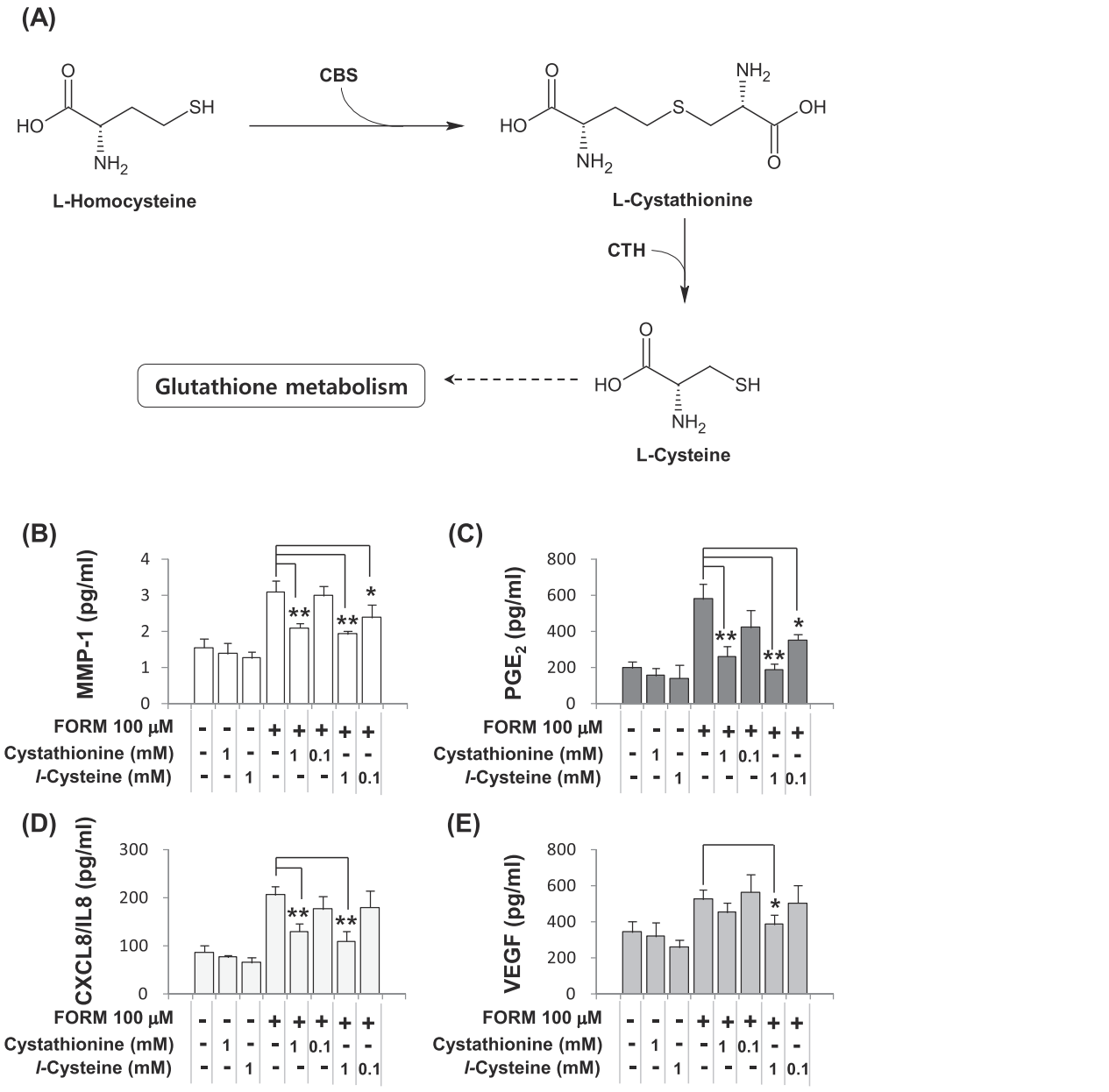

Fig. 4. The effects of L-cystathionine and L-cysteine on pro-inflammatory responses of NHKs. L-cystathionine and L-cysteine were key intermediates in the CBS and CTH-mediated transsulfuration pathway (A). NHKs (2×10^5 cells/well) were seeded to 6-well plates and cultured up to 100% confluence. Formaldehyde (FORM) was treated in confluent NHKs. The levels of MMP1 (B), PGE_2 (C), CXCL8/IL8 (D) and VEGF (E) in the culture supernatants were measured by ELISA. Values represent the mean expression ± SD (n = 3). $^*p \le 0.05$ and $^{**}p \le 0.01$.

in the programmed recovery from toxic stimulus-induced inflammation. In the ER UPR DEGs, protein phosphatase 1 regulatory subunit 15A (PPP1R15A), also known as GADD34, plays a role in the programmed recovery from the ER stress-induced translational repression (Kojima et al., 2003; Novoa et al., 2003). Interestingly, PPP1R15A can positively or negatively affect cellular genotoxic apoptosis depending on its interaction(s) with other cellular proteins (Grishin et al., 2001). The other ER UPR DEGs, similar to CTH and PPP1R15A, may regulate the resolution process of inflammation. However, more studies are needed to elucidate the role(s) of the ER UPR DEGs in deciding whether the formaldehyde-exposed human keratinocytes may end-up in a pathogenic inflammation or resolution.

Environmental toxic stimuli induce inflammatory responses in epithelial tissues such as the skin and respiratory tract. Epithelial inflammation has protective roles in physiological homeostasis from the standpoint of removing or neutralizing various toxicants that can initiate cellular injury reactions (Peeters et al., 2015). When the injury-inducing toxic stimuli are removed or neutralized, the inflammatory reactions move towards a resolution phase (Gilroy et al., 2004; Medzhitov, 2010). If the toxic stimuli are not eliminated, chronic inflammation leads to various pathological conditions where the pro-inflammatory mediators and cytokines are persistently increased. In this regard, the resolution of inflammation is an active biological process to initiate the cellular response that attenuates the effects of pro-inflammatory mediators or inflammatory cells (Alessandri et al., 2013). Cellular responses associated with inflammation resolution include changes in cellular metabolic profiles, production of resolution mediators, and repopulation of inflammatory cells (Alessandri et al., 2013). Recently, it was reported that VEGF plays a role in the removal of activated macrophages, which is regarded as a resolution response during wound healing (Petreaca et al., 2008). Human epidermal keratinocytes can also produce pro-inflammatory mediators and cytokines in response

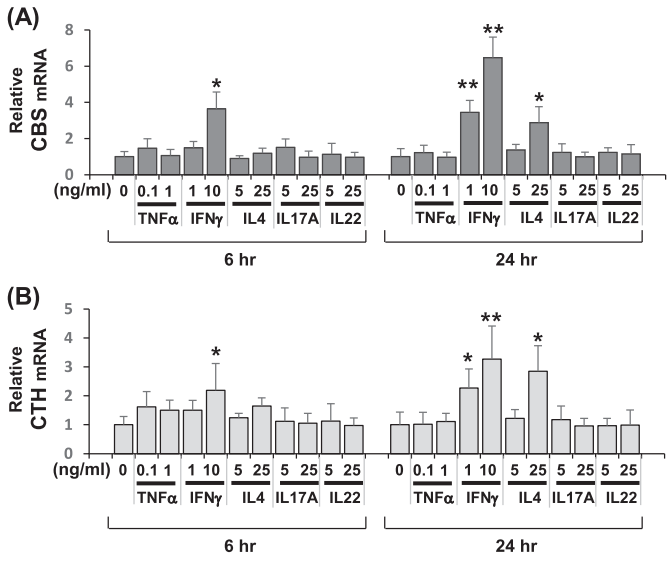

Fig. 5. The effects of immune cytokines on the gene transcription of CBS and CTH in NHKs. NHKs (2×10^5 cells/well) were seeded to 6-well plates and cultured up to 100% confluence. Confluent NHKs were stimulated with TNFα, IFNγ, IL4, IL17A, or IL22. At 6 h and 24 h after the treatment, total RNA samples were extracted and Q-RT-PCR was performed for determining the CBS (A) and CTH (B) mRNA levels. Values represent the mean expression ± SD (n = 3). $^{*}p \le 0.05$ and $^{**}p \le 0.01$.

to exogenous or endogenous noxious stimuli (Nestle et al., 2009). However, the keratinocyte-dependent inflammation resolution has not been well studied. In this study, we observed that VEGF was upregulated in the formaldehyde-treated NHKs. We previously reported that NHKs produce VEGF in response to various chemical allergens such as 1-chloro-2,4-dinitrobenzene (DNCB), nickel chloride, 4-phenylenediamine, 2-mercaptobenzothiazole, imidazolidinyl urea, and cinnamic alcohol, etc. The chemical allergen-induced upregulation of VEGF may be involved in the pathogenic mechanism of skin sensitization, possibly lymphangiogenesis (Bae et al., 2015a, 2015b). In the keratinocyte context, it is still unclear whether VEGF promotes progression into pathogenic inflammation or into inflammation resolution. As formaldehyde elicits allergic reactions in human skin, it is highly probable that the upregulation of VEGF contributes to the pathogenesis of formaldehyde-related toxicological outcomes in the skin. However, the possible role of VEGF in the resolution process of cutaneous inflammation induced by other toxic stimuli cannot be excluded.

CBS and CTH, annotated as GO BP transsulfuration (GO:0019346), are related to homocysteine-cysteine interconversions that are essential in sulfur amino acid metabolism (Vitvitsky et al., 2006). Sulfur amino acid metabolism is important in the biochemical process that transfers methyl groups to biomolecules or cellular metabolites (Brosnan and Brosnan, 2006). Moreover, L-cysteine is the functional amino acid constituent of the major cellular antioxidant components, which include glutathione, glutaredoxins, thioredoxins, and peroxiredoxins (Bauchart-Thevret et al., 2009; McBean, 2012). The transsulfuration pathway participates in glutathione synthesis in human epithelial cells (Belalcazar et al., 2014). It was reported that CBS and CTH directly regulate glutathione and hydrogen sulfide (H_2S) production during inflammatory responses (McBean, 2012). Therefore, metabolic pathways including both CBS and CTH, regulate negative feedback mechanisms against excessive pro-inflammatory responses. In fact, L-cysteine and L-cystathionine, metabolites of the amino acid biosynthetic process with CBS and CTH, inhibited the upregulation of pro-inflammatory mediators, MMP1, PGE_2, and CXCL8/IL8, in NHKs treated with sub-cytotoxic formaldehyde (Fig. 4). The change in CBS and CTH is not limited to the formaldehyde response in NHKs. In addition, we found that IFNγ and IL4 increased the mRNA levels of CBS and CTH whereas the gene transcription of these enzymes was not affected by TNFα, IL17 and IL22. In immune system, IFNγ-producing Th1 cells and IL4-producing Th2 cells have mutually antagonistic relationships in general (Nestle et al., 2009). In contrast, CBS and CTH gene transcription was upregulated by both IFNγ and IL4 (Fig. 5), suggesting that pro-inflammatory cytokines affect human keratinocytes by different mechanisms from that of immune system. These results revealed that CBS and CTH have specific roles in the immune reaction of somatic tissue cells in the presence of T helper cells. To verify our hypothesis, further studies should be directed to elucidate the molecular pathway(s) regulated by CBS and CTH in different toxicological conditions.

5. Conclusion

This genome-scale transcription profile study showed that the ER UPR-associated genes were significantly upregulated in NHKs treated with sub-cytotoxic formaldehyde. ER UPR is important in regulating the inflammation fate of human keratinocytes after a sub-cytotoxic formaldehyde exposure. In the temporal profile study, the upregulation of CBS and CTH was preceded by those of pro-inflammatory DEGs such as PTGS2, IL-8, and MMP1. Importantly, CBS and CTH in NHKs may contribute to the maintenance of cellular homeostasis by the negative feedback mechanism. In this regard, CTH and CBS play a role in the resolution phase of inflammation, suggesting their contribution to the fate of inflammation in response to toxic stimuli.

Conflict of interest

Authors, Hyoung-June Kim and Dong Wook Shin, are employees of AmorePacific Co. The other authors have no conflict of interest.

Transparency document

The Transparency document associated with this article can be found, in online version.

Acknowledgments

This study was partly supported by a National Research Foundation of Korea (NRF) grant funded by the Ministry of Science, ICT and Future Planning (Grant No. 2014M3C9A2064603), by a grant (HN14C0088) from the Korea Healthcare Technology R&D Project, Ministry of Health & Welfare and by Promising-Pioneering Researcher Program through the Seoul National University (SNU) in 2015.

Appendix A. Supplementary data

Supplementary data to this article can be found online at http://dx.doi.org/10.1016/j.taap.2016.09.017.

References

Alessandri, A.L., Sousa, L.P., Lucas, C.D., Rossi, A.G., Pinho, V., Teixeira, M.M., 2013. Resolution of inflammation: mechanisms and opportunity for drug development. Pharmacol. Ther. 139, 189–212.

Bae, O.N., Ahn, S., Jin, S.H., Hong, S.H., Lee, J., Kim, E.S., Jeong, T.C., Chun, Y.J., Lee, A.Y., Noh, M., 2015a. Chemical allergens stimulate human epidermal keratinocytes to produce lymphangiogenic vascular endothelial growth factor. Toxicol. Appl. Pharmacol. 283, 147–155.

Bae, O.N., Noh, M., Chun, Y.J., Jeong, T.C., 2015b. Keratinocytic vascular endothelial growth factor as a novel biomarker for pathological skin condition. Biomol. Ther. 23, 12–18.

Bauchart-Thevret, C., Stoll, B., Burrin, D.G., 2009. Intestinal metabolism of sulfur amino acids. Nutr. Res. Rev. 22, 175–187.

Belalcazar, A.D., Ball, J.G., Frost, L.M., Valentovic, M.A., Wilkinson, J.t., 2014. Transsulfuration is a significant source of sulfur for glutathione production in human mammary epithelial cells. ISRN Biochem. 2013, 637897.

Boivin, W.A., Jiang, H., Utting, O.B., Hunt, D.W., 2006. Influence of interleukin-1alpha on androgen receptor expression and cytokine secretion by cultured human dermal papilla cells. Exp. Dermatol. 15, 784–793.

Bostrom, C.E., Almen, J., Steen, B., Westerholm, R., 1994. Human exposure to urban air pollution. Environ. Health Perspect. 102 (Suppl. 4), 39–47.
Brosnan, J.T., Brosnan, M.E., 2006. The sulfur-containing amino acids: an overview. J. Nutr. 136, 1636S–1640S.
Brown, K.G., 1985. Risk assessment of laboratory rats and mice chronically exposed to formaldehyde vapors. Risk Anal. 5, 171–180.
Cogliano, V.J., Grosse, Y., Baan, R.A., Straif, K., Secretan, M.B., El Ghissassi, F., Working Group for V., 2005. Meeting report: summary of IARC monographs on formaldehyde, 2-butoxyethanol, and 1-tert-butoxy-2-propanol. Environ. Health Perspect. 113, 1205–1208.
de Groot, A.C., Veenstra, M., 2010. Formaldehyde-releasers in cosmetics in the USA and in Europe. Contact Dermatitis 62, 221–224.
De Jong, W.H., Arts, J.H., De Klerk, A., Schijf, M.A., Ezendam, J., Kuper, C.F., Van Loveren, H., 2009. Contact and respiratory sensitizers can be identified by cytokine profiles following inhalation exposure. Toxicology 261, 103–111.
Flyvholm, M.A., Andersen, P., 1993. Identification of formaldehyde releasers and occurrence of formaldehyde and formaldehyde releasers in registered chemical products. Am. J. Ind. Med. 24, 533–552.
Garrett, M.H., Hooper, M.A., Hooper, B.M., Rayment, P.R., Abramson, M.J., 1999. Increased risk of allergy in children due to formaldehyde exposure in homes. Allergy 54, 330–337.
Gilroy, D.W., Lawrence, T., Perretti, M., Rossi, A.G., 2004. Inflammatory resolution: new opportunities for drug discovery. Nat. Rev. Drug Discov. 3, 401–416.
Grishin, A.V., Azhipa, O., Semenov, I., Corey, S.J., 2001. Interaction between growth arrest-DNA damage protein 34 and Src kinase Lyn negatively regulates genotoxic apoptosis. Proc. Natl. Acad. Sci. U. S. A. 98, 10172–10177.
Gustafson, P., Barregard, L., Lindahl, R., Sallsten, G., 2005. Formaldehyde levels in Sweden: personal exposure, indoor, and outdoor concentrations. J. Expo. Anal. Environ. Epidemiol. 15, 252–260.
Hauksson, I., Ponten, A., Isaksson, M., Hamada, H., Engfeldt, M., Bruze, M., 2016. Formaldehyde in cosmetics in patch tested dermatitis patients with and without contact allergy to formaldehyde. Contact Dermatitis 74, 145–151.
Herouy, Y., Mellios, P., Bandemir, E., Dichmann, S., Nockowski, P., Schopf, E., Norgauer, J., 2001. Inflammation in stasis dermatitis upregulates MMP-1, MMP-2 and MMP-13 expression. J. Dermatol. Sci. 25, 198–205.
Jeong, H.S., Chung, H., Song, S.H., Kim, C.I., Lee, J.G., Kim, Y.S., 2015. Validation and determination of the contents of acetaldehyde and formaldehyde in foods. Toxicol. Res. 31, 273–278.
Jin, S.H., Choi, D., Chun, Y.J., Noh, M., 2014. Keratinocyte-derived IL-24 plays a role in the positive feedback regulation of epidermal inflammation in response to environmental and endogenous toxic stressors. Toxicol. Appl. Pharmacol. 280, 199–206.
Kataru, R.P., Jung, K., Jang, C., Yang, H., Schwendener, R.A., Baik, J.E., Han, S.H., Alitalo, K., Koh, G.Y., 2009. Critical role of CD11b + macrophages and VEGF in inflammatory lymphangiogenesis, antigen clearance, and inflammation resolution. Blood 113, 5650–5659.
Kaufman, R.J., Scheuner, D., Schroder, M., Shen, X., Lee, K., Liu, C.Y., Arnold, S.M., 2002. The unfolded protein response in nutrient sensing and differentiation. Nat. Rev. Mol. Cell Biol. 3, 411–421.
Klosterhalfen, B., Horstmann-Jungemann, K., Vogel, P., Flohe, S., Offner, F., Kirkpatrick, C.J., Heinrich, P.C., 1992. Time course of various inflammatory mediators during recurrent endotoxemia. Biochem. Pharmacol. 43, 2103–2109.
Kojima, E., Takeuchi, A., Haneda, M., Yagi, A., Hasegawa, T., Yamaki, K., Takeda, K., Akira, S., Shimokata, K., Isobe, K., 2003. The function of GADD34 is a recovery from a shutoff of protein synthesis induced by ER stress: elucidation by GADD34-deficient mice. FASEB J. 17, 1573–1575.
Li, G.Y., Lee, H.Y., Shin, H.S., Kim, H.Y., Lim, C.H., Lee, B.H., 2007. Identification of gene markers for formaldehyde exposure in humans. Environ. Health Perspect. 115, 1460–1466.
McBean, G.J., 2012. The transsulfuration pathway: a source of cysteine for glutathione in astrocytes. Amino Acids 42, 199–205.
Medzhitov, R., 2010. Inflammation 2010: new adventures of an old flame. Cell 140, 771–776.
Mozes, T., Zijlstra, F.J., Heiligers, J.P., Tak, C.J., Ben-Efraim, S., Bonta, I.L., Saxena, P.R., 1991. Sequential release of tumour necrosis factor, platelet activating factor and eicosanoids during endotoxin shock in anaesthetized pigs: protective effects of indomethacin. Br. J. Pharmacol. 104, 691–699.
Nestle, F.O., Di Meglio, P., Qin, J.Z., Nickoloff, B.J., 2009. Skin immune sentinels in health and disease. Nat. Rev. Immunol. 9, 679–691.
Neuss, S., Holzmann, K., Speit, G., 2010. Gene expression changes in primary human nasal epithelial cells exposed to formaldehyde in vitro. Toxicol. Lett. 198, 289–295.
Nosbaum, A., Vocanson, M., Rozieres, A., Hennino, A., Nicolas, J.F., 2009. Allergic and irritant contact dermatitis. Eur. J. Dermatol. 19, 325–332.
Novoa, I., Zhang, Y., Zeng, H., Jungreis, R., Harding, H.P., Ron, D., 2003. Stress-induced gene expression requires programmed recovery from translational repression. EMBO J. 22, 1180–1187.
Peeters, P.M., Wouters, E.F., Reynaert, N.L., 2015. Immune homeostasis in epithelial cells: evidence and role of Inflammasome signaling reviewed. J. Immunol. Res. 2015, 828264.
Petreaca, M.L., Yao, M., Ware, C., Martins-Green, M.M., 2008. Vascular endothelial growth factor promotes macrophage apoptosis through stimulation of tumor necrosis factor superfamily member 14 (TNFSF14/LIGHT). Wound Repair Regen. 16, 602–614.
Roush, G.C., Walrath, J., Stayner, L.T., Kaplan, S.A., Flannery, J.T., Blair, A., 1987. Nasopharyngeal cancer, sinonasal cancer, and occupations related to formaldehyde: a case-control study. J. Natl. Cancer Inst. 79, 1221–1224.
Rovira, J., Roig, N., Nadal, M., Schuhmacher, M., Domingo, J.L., 2016. Human health risks of formaldehyde indoor levels: an issue of concern. J. Environ. Sci. Health, Part A: Tox. Hazard. Subst. Environ. Eng. 51, 357–363.
Sano, R., Reed, J.C., 2013. ER stress-induced cell death mechanisms. Biochim. Biophys. Acta 1833, 3460–3470.
Srinivasan, S., Leeman, S.E., Amar, S., 2010. Beneficial dysregulation of the time course of inflammatory mediators in lipopolysaccharide-induced tumor necrosis factor alpha factor-deficient mice. Clin. Vaccine Immunol. 17, 699–704.
Swenberg, J.A., Kerns, W.D., Mitchell, R.I., Gralla, E.J., Pavkov, K.L., 1980. Induction of squamous cell carcinomas of the rat nasal cavity by inhalation exposure to formaldehyde vapor. Cancer Res. 40, 3398–3402.
Szende, B., Tyihak, E., 2010. Effect of formaldehyde on cell proliferation and death. Cell Biol. Int. 34, 1273–1282.
Thyssen, J.P., Johansen, J.D., Menne, T., 2007. Contact allergy epidemics and their controls. Contact Dermatitis 56, 185–195.
Vandebriel, R.J., Pennings, J.L., Baken, K.A., Pronk, T.E., Boorsma, A., Gottschalk, R., Van Loveren, H., 2010. Keratinocyte gene expression profiles discriminate sensitizing and irritating compounds. Toxicol. Sci. 117, 81–89.
Vaughan, T.L., Stewart, P.A., Teschke, K., Lynch, C.F., Swanson, G.M., Lyon, J.L., Berwick, M., 2000. Occupational exposure to formaldehyde and wood dust and nasopharyngeal carcinoma. Occup. Environ. Med. 57, 376–384.
Vitvitsky, V., Thomas, M., Ghorpade, A., Gendelman, H.E., Banerjee, R., 2006. A functional transsulfuration pathway in the brain links to glutathione homeostasis. J. Biol. Chem. 281, 35785–35793.
Wang, P., Isaak, C.K., Siow, Y.L., O, K., 2014. Downregulation of cystathionine beta-synthase and cystathionine gamma-lyase expression stimulates inflammation in kidney ischemia-reperfusion injury. Phys. Rep. 2, e12251.
Warshaw, E.M., Maibach, H.I., Taylor, J.S., Sasseville, D., DeKoven, J.G., Zirwas, M.J., Fransway, A.F., Mathias, C.G., Zug, K.A., DeLeo, V.A., Fowler Jr., J.F., Marks, J.G., Pratt, M.D., Storrs, F.J., Belsito, D.V., 2015. North American contact dermatitis group patch test results: 2011-2012. Dermatitis 26, 49–59.
Zhang, L., Freeman, L.E., Nakamura, J., Hecht, S.S., Vandenberg, J.J., Smith, M.T., Sonawane, B.R., 2010. Formaldehyde and leukemia: epidemiology, potential mechanisms, and implications for risk assessment. Environ. Mol. Mutagen. 51, 181–191.

Toxicology and Applied Pharmacology 386 (2020) 114828

Contents lists available at ScienceDirect

Toxicology and Applied Pharmacology

journal homepage: www.elsevier.com/locate/taap

CXCL14 downregulation in human keratinocytes is a potential biomarker for a novel *in vitro* skin sensitization test

Eunyoung Lee[a,b], Sungjin Ahn[a,b], Sun Hee Jin[a,b], Moonyoung Lee[a,b], Jeong Joo Pyo[a,b], Jeayoung C. Shin[a,b], Seungchan An[a,b], Jaehyoun Ha[c], Minsoo Noh[a,b,*]

[a] College of Pharmacy, Seoul National University, Seoul 08826, Republic of Korea
[b] Natural Products Research Institute, Seoul National University, Seoul 08826, Republic of Korea
[c] Toxicology Division, IEC Korea Inc., Suwon 17074, Republic of Korea

ARTICLE INFO

Keywords:
Human keratinocytes
CXCL14
Allergic contact dermatitis
Sensitizers
OECD TG429

ABSTRACT

To elucidate the roles of epidermal keratinocytes in the toxicological outcomes of chemically induced contact dermatitis, genome-scale transcriptional analyses were performed using normal human keratinocytes (NHKCs) treated with 10 μM sodium lauryl sulfate (SLS) or 5 μM urushiol. In Gene Ontology (GO) enrichment analyses, SLS- and urushiol-induced upregulated DEGs are commonly associated with the regulation of pro-inflammatory responses and epidermal differentiation processes in NHKCs whereas cellular protein metabolic process was also identified as a commonly downregulated DEG signature. Among the downregulated DEGs, CXCL14 was investigated as a potential biomarker for a new *in vitro* skin sensitization test using OECD TG429 reference chemicals. CXCL14 was significantly downregulated in NHKCs in response to 62.5% of the OECD TG429 sensitizers in a concentration-dependent manner. When the sensitizer-induced upregulation of chemokine CXCL8 was included in the analysis, 87.5% of the OECD TG429 reference sensitizing chemicals significantly induced either CXCL8 upregulation or CXCL14 downregulation in NHKCs. Only one OECD TG429 reference non-sensitizer changed the constitutive CXCL14 expression in NHKCs whereas five out of six non-sensitizers altered CXCL8 production. The reference irritating non-sensitizer SLS caused a false-positive outcome. The downregulation of constitutively expressed CXCL14 was regulated by both the MAPK/ERK and JAK3/STAT6 pathways in NHKCs. CXCL14 can be used as a mechanism-based biomarker in the development of *in vitro* skin sensitization tests and may help improve the distinction between allergenic sensitizers and non-sensitizers.

1. Introduction

Allergic contact dermatitis (ACD) and irritant contact dermatitis (ICD) are two major forms of contact dermatitis, which can be classified by their immunological characteristics. Despite differences in their pathogenesis, ACD and ICD induce similar clinical symptoms such as erythema, edema, itching, and pain. It was reported that irritant dermatitis predisposes to the development of ACD (Willis et al., 1986; English, 2001). However, molecular pathways have not yet been elucidated to discriminate between irritation and allergenic sensitization. Certain irritants show weak allergen-like outcomes and may activate molecular and cellular profiles similar to those induced by allergens (Fluhr et al., 2008; Park et al., 2018a).

The epidermis is the interface between the environment and human skin. The stratum corneum, the outermost layer of the epidermis, consists mainly of differentiated keratinocytes (KCs), also called as corneocytes. Epidermal KCs are in direct contact with toxic stimuli in the environment. They form physical and immunological barriers against the penetration of toxic stimuli such as foreign matter and infectious agents (Suter et al., 2009). They are also regarded as immunologically active skin cells because they produce proinflammatory autacoids, cytokines, and chemotactic factors in response to toxic stimuli which, in turn, transmit innate and adaptive immune signals to other cells (Albanesi et al., 2005; Proksch et al., 2008; Choi et al., 2011). Once stimulated, KCs modulate the immune response by recruiting immune cells in the skin and function as nonprofessional antigen-presenting cells (Nestle et al., 2009). All of these cellular events occur after specific or nonspecific ligands bind to the biomolecules that are found primarily in the cell membranes of KCs (Santinha et al., 2013).

Keratinocyte-derived cytokines, their regulatory networks, and their temporal expression profiles participate in the immunological function

* Corresponding author at:College of Pharmacy, Seoul National University, Seoul 08826, Republic of Korea.
E-mail addresses: minsoonoh@snu.ac.kr, minsoo@alum.mit.edu (M. Noh).

https://doi.org/10.1016/j.taap.2019.114828
Received 30 June 2019; Received in revised form 13 November 2019; Accepted 13 November 2019
Available online 14 November 2019
0041-008X/

of the skin barrier (Suter et al., 2009). Various skin irritants and sensitizers stimulate KCs to produce proinflammatory cytokines such as interleukin (IL)-1α, tumor necrosis factor (TNF)-α, IFNγ, CXCL8, and VEGF (Coquette et al., 2003; Bae et al., 2015; Kim et al., 2018). Therefore, the identification and characterization of keratinocyte-derived cytokines are necessary to understand the cellular and molecular mechanisms responsible for the pathogenesis of ACD or ICD.

Various biological effects of skin irritants and sensitizers have been investigated to develop new *in vitro* irritation and/or sensitization tests to replace animal experiments. Keratinocyte-derived cytokines such as IL-1α and CXCL8 have been evaluated as biomarkers to predict skin irritation and/or sensitization (Coquette et al., 2003; Park et al., 2018b). In our previous study, we found that 14 of the 16 human sensitizers listed in OECD Test Guideline (TG) 429 significantly upregulated either CXCL8 or VEGF in KCs (Bae et al., 2015). However, chemical non-sensitizers also induced the upregulation of CXCL8 or VEGF. At present, there are no cytokine biomarkers available to distinguish between primary irritation and sensitization. To understand the molecular mechanisms of chemical-induced sensitization associated with KCs, we analyzed genome-wide transcription profile data of normal human epidermal KCs (NHKCs) treated with subcytotoxic concentrations of sodium lauryl sulfate (SLS) and urushiol. CXCL14 was downregulated in NHKCs in response to both SLS and urushiol. Therefore, we evaluated it as a downregulated biomarker for skin sensitizers using the reference chemicals in OECD TG 429 (Ehling et al., 2005; OECD, 2010).

2. Materials and methods

2.1. Cell culture and treatment with contact allergens and OECD TG 429 references chemicals

NHKCs from neonatal foreskins were obtained from Lonza (Basel, Switzerland) and maintained in keratinocyte growth medium (KGM) consisting of bovine pituitary extract, insulin, human epidermal growth factor, transferrin, epinephrine, hydrocortisone, amphotericin B, and gentamicin (KGM-2; Lonza). Cells were subcultured at 80–90% confluence to the next passage. The third passage of primary NHKCs was used in this study. NHKCs at 100% confluence were treated with sodium lauryl sulfate (SLS; Sigma-Aldrich Corp., St. Louis, MO, USA), urushiol (ChromaDex; Irvine, CA, USA) or the other human sensitizers and non-sensitizers listed in OECD TG429. All of these chemicals were purchased from Sigma-Aldrich except for 5-chloro-2-methyl-4-isothiazolin-3-one/2-methyl-4-isothiazolin-3-one (CMI/MI) which was prepared by mixing CMI (Sigma-Aldrich Corp.) and MI (Sigma-Aldrich Corp.) in a 3:1 ratio.

2.2. Total RNA sample preparation

Total RNA was isolated using TRIzol reagent (Invitrogen, Carlsbad, CA, USA). The RNA was purified with the RNeasy Mini Kit (Qiagen, Germantown, MD, USA). The total RNA concentration was determined with a NanoDrop ND-1000 spectrophotometer (NanoDrop Technologies, Inc., Montchanin, DE, USA). RNA integrity was verified with a Bioanalyzer 2100 (Agilent Technologies, Santa Clara, CA, USA).

2.3. Microarray experiments

Affymetrix Human Genome U133 2.0 GeneChip arrays (Affymetrix, Santa Clara, CA, USA) were prepared, hybridized, and scanned by an authorized local Affymetrix service provider (DNA Link Inc., Seoul, South Korea). RNA was reverse-transcribed to cDNA in the presence of biotinylated ribonucleotides according to standard Affymetrix protocols. Microarray experiments were performed and the differentially expressed genes (DEGs) were selected as follows: (1) the selection of Affymetrix probe sets determined as “present”; (2) the selection of probe sets with sample/control ratios of expression values > 1.8 as “up-regulated” and < 1.8 as “down-regulated”; and (3) the selection of probe sets with significant p values ($p < 0.05$) in the Wilcoxon rank test when the values of sample treated samples were compared with those of vehicle-treated samples (Lee et al., 2016). A gene ontology (GO) enrichment analysis of SLS- or urushiol-induced DEGs was performed by comparing the frequencies of the GO biological process (BP) terms assigned to each gene in a DEGs group to that of the entire gene set in the Affymetrix Human 133 2.0 GeneChip array. The GO annotation files were obtained from the Gene Ontology Consortium webpage (http://www.geneontology.org; May 2017 version). In the Affymetrix 133 2.0 GeneChip, the total number of genes was 23,517 because there were redundant probe sets for the same genes in the microarray. For the GO BP enrichment analysis (GOBPEA), a 2×2 contingency matrix for each GO BP term was constructed between the frequency of a specific GO BP term in the DEGs sets and that for the 23,517 genes. The 2×2 contingency matrix was analyzed by Fisher's exact test (frequency < 5) or a χ^2 test (frequency ≥ 5) using SPSS 25.0 for Windows® (IBM Corp., Armonk, NY, USA) to calculate the level of significance.

2.4. Validation of microarray data by quantitative real-time reverse transcription polymerase chain reaction (Q-RT-PCR)

Total RNA (1 μg) from each sample was transcribed with SuperScript™ reverse transcriptase (Invitrogen). Samples were extracted from confluently cultured NHKCs treated with SLS (5 and 10 μM) or urushiol (1 and 5 μM) for 24 h. The expression level of the target mRNAs was quantified by Q-RT-PCR using the Applied Biosystems 7500 Real Time PCR System (Applied Biosystems, Foster City, CA, USA). The TaqMan RT-PCR primer sets (Applied Biosystems) used in the Q-RT-PCR were: annexin A1 (*ANXA1*), 00167549_ml; CC motif chemokine ligand 5 (*CCL5*), Hs00982282_ml; CXC Motif Chemokine Ligand 14 (*CXCL14*), Hs01557413_ml; desmoglein 4 (*DSG4*), Hs00698286_ml; FBJ murine osteosarcoma viral oncogene homolog (FOS), Hs04194186_s1; *H19*, Hs00399294_ml; interleukin (IL)-8 (*CXCL8*), Hs00174103_m1; jun B proto-oncogene (*JUNB*), Hs00357891_ml; suppressor of cytokine signaling 1 (*SOCS1*), Hs00705164_s1; SP100 nuclear antigen (*SP100*), Hs00162109_ml; small proline-rich protein 2G (*SPRR2G*), Hs00972901_s1; thrombospondin 1 (*THBS1*), Hs00962908_ml; and *TNF*, Hs00174128_m1. Human *GAPDH* (4333764F, Applied Biosystems) was also amplified to normalize the variations in cDNA level across different samples. Quantification of the relative expression levels was performed using equations from a mathematical model developed by Pfaffl (Pfaffl, 2001).

2.5. Enzyme-linked immunosorbent assay (ELISA) and western blot analysis

Protein expression levels were determined by western blotting and ELISA with three independent NHKC batches. NHKCs were confluently cultured in six-well culture plates. Mitogen-activated protein kinase (MAPK) signaling inhibitor (PD98059) and Janus kinase (JAK) inhibitors (Piceatannol, AG-490 and WHI-P131) were co-applied with SLS to the NHKCs for 24 h. Piceatannol, AG-490 and WHI-P131 were purchased from Calbiochem (San Diego, CA, USA). The CXCL14 concentrations in the supernatant were measured with enzyme immunoassay kits (R&D Systems, Minneapolis, MN, USA) according to the manufacturer's instructions and was determined in pg/mg of total protein. NHKCs were lysed in cell lysis buffer (RIPA buffer; Invitrogen) containing a protease inhibitor cocktail (Sigma-Aldrich Corp.). The lysate was centrifuged at 15,000 $\times g$ for 10 min and the supernatant was used in protein expression analysis. Proteins (20 μg/well) were fractionated by SDS-PAGE and transferred to nitrocellulose membranes. The membranes were blocked with 5% skim milk in TBST (10 mM Tris-HCl (pH 8.0), 150 mM NaCl, and 0.15% Tween-20) for 1 h at 25 °C and

probed overnight at 4 °C with anti-phospho-ERK antibody (#4370; Cell Signaling Technology (CST), Beverly, MA, USA), anti-ERK (#4695; CST), anti-phospho-STAT6 (#9361; CST), anti-STAT6 (#9363; CST) and anti-β-actin (sc-47,778; Santa Cruz Biotechnology Inc., Dallas, TX, USA). The blots were washed thrice with TBST and incubated with horseradish peroxidase-conjugated goat anti-rabbit IgG (Bio-Rad Laboratories, Richmond, CA, USA) at 25 °C for 1 h. Detection was performed with an ECL system (Invitrogen).

2.6. Statistical analysis

Statistical analysis was conducted using SPSS 25.0 for Windows® (IBM Corp.). Data were expressed as means ± standard deviation (SD). The group means were compared to the control by Student's *t*-test for comparison. $p < 0.05$ indicated statistical significance.

3. Results

3.1. Genome-wide transcription profile of NHKCs in response to SLS or urushiol

To obtain genome-wide transcription data for the SLS- or urushiol-treated NHKCs, we first determined noncytotoxic concentrations of these agents to rule out the possibility that the genes associated with cell death were predominantly identified as DEGs. NHKCs viability was assessed by a WST-8-based cytotoxicity test 24 h after chemical treatment (Supplementary Fig. 1). Compared to the control, 10 μM SLS and 5 μM urushiol were determined as the highest concentrations which did not affect NHKC viability. Therefore, whole genome-scale transcription data were obtained for NHKCs treated with 10 μM SLS or 5 μM urushiol for 24 h. The raw microarray data can be accessed from the National Center for Biotechnology Information Gene Expression Omnibus (NCBI GEO) database under accession number GSE126354. According to three selection criteria, data variability among samples, fold expression changes, and statistical *P* for each probe set, 259 upregulated and 193 downregulated DEGs were chosen in the SLS-treated NHKCs (Supplementary Table 1). For the urushiol-treated NHKCs, 173 upregulated and 124 downregulated DEGs were identified (Supplementary Table 2). We constructed Venn diagrams showing the DEGs overlapping in response to both SLS and urushiol (Fig. 1A and B). In the NHKCs, 9 DEGs were commonly upregulated in response to SLS and urushiol, *ATP12A*, *CXCL8*, *DEFB103A*, *MAP3K8*, *MMP10*, *SNORA68*, *TAC1*, *TM4SF1* and *UCA1* (Fig. 1A). Commonly downregulated DEGs in NHKCs by both SLS and urushiol were *ARFGAP2*, *CLK3*, *CXCL14*, *H19*, *HERC6* and *MIR302B* (Fig. 1B).

3.2. GO BP enrichment analysis of SLS- or urushiol-induced DEGs

To identify statistically significant biological phenotypes among the SLS- and urushiol-induced DEGs, the probability of the frequency of each GO BP term in the DEG set was calculated by setting the frequency in the total gene set as the null condition (Table 1 and Supplementary Table 3). The significantly enriched GO BP terms in the upregulated SLS-induced DEGs were proinflammatory biological processes such as the inflammatory response (GO:0006954), cellular response to calcium ion (GO:0071277), immune response (GO:0006955), and cellular response to lipopolysaccharide (GO:0071222). Upregulated urushiol-induced DEGs were also enriched in proinflammatory biological processes such as cytokine-mediated signaling pathway (GO:0019221) and inflammatory response (GO:0006954). In the NHKCs, SLS and urushiol both affected the transcription of epidermal differentiation-associated genes. Epidermal differentiation-associated GO BP terms in the SLS-upregulated DEGs were cornification (GO:0070268) and peptide cross-linking (GO:0018149). A significant proportion of the urushiol-upregulated DEGs were annotated as keratinocyte differentiation (GO:0030216) and epidermis development (GO:0008544). The gene expression signature of the SLS-downregulated DEGs was characterized by chemotaxis (GO:0006935), oxidation-reduction process (GO:0055114), cornification (GO:0070268), G1/S transition of the mitotic cell cycle (GO:0000082), keratinization (GO:0031424), and cellular protein metabolic process (GO:0044267). Only three GO biological processes, nervous system development (GO:0007399), positive regulation of cell proliferation (GO:0008284), and cellular protein metabolic process (GO:0044267), showed significant *P* when the urushiol-downregulated DEGs were statistically analyzed. Notably, the cellular protein metabolic process was the commonly downregulated biological phenotype in the SLS- and urushiol-downregulated DEGs of the NHKCs. SLS downregulated mitotic cell cycle-associated genes and urushiol also affected the cell proliferation-associated genes, suggesting that epidermal keratinocytes may temporarily inhibit cell cycle progression during proinflammatory responses to toxic stimuli such as SLS and urushiol.

3.3. Validation of DEG expression in SLS- and urushiol-treated NHKCs

The microarray expression of DEGs should be validated by measuring transcriptional changes using alternative methods (Lee et al., 2016). For the SLS-upregulated DEGs, the mRNA levels of *CXCL8, TNF, CCL5, JUNB*, *FOS,* and *SPRR2G* were measured with independently prepared NHKC samples (Fig. 2). In Q-RT-PCR, the transcriptional upregulation of the proinflammatory cytokine genes, *CXCL8*, *TNF*, and *CCL5*, was validated in the SLS-treated NHKCs. SLS increased the mRNA levels of the AP1 transcription factor superfamily, *JUNB* and *FOS*,

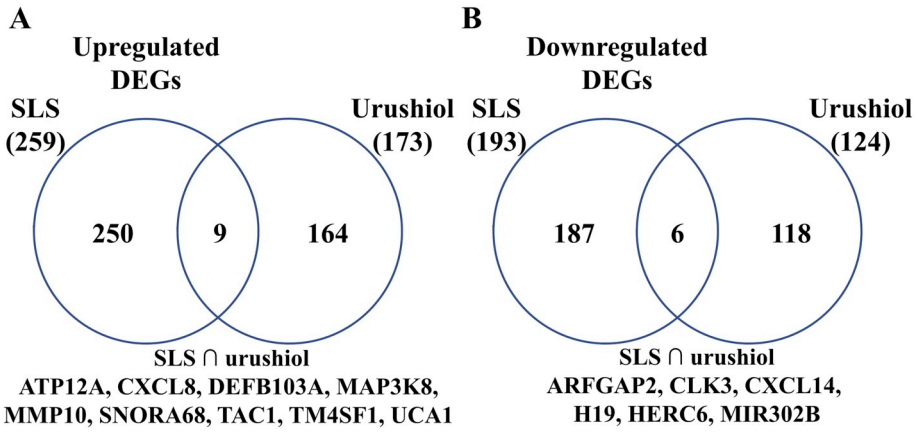

Fig. 1. Venn diagrams for DEGs in NHKCs in response to SLS and Urushiol. The Venn diagrams show numbers of selected DEGs in SLS- or urushiol-treated NHKCs. Commonly upregulated (A) and downregulated (B) DEGs were shown in Gene Symbol. The microarray raw data can be accessed from the NCBI GEO database under accession number GSE126354.

Table 1
Enriched Gene Ontology biological processes in the SLS- or urushiol-induced DEGs in NHKCs.

		GO term id	GO BP terms	P value (*chi* test)	# of GO BP in DEGs	# of GO BP in the microarray (Total 23,517)	Gene symbol (fold change)
Up	SLS-enriched GO BPs in 259 DEGs	GO:0006954	Inflammatory response	< 0.0001	16	378	CXCL8 (6.21), TNF (3.81), FOS (3.03), CXCL1 (2.84), CCL20 (2.80), CCL5 (2.75), PTX3 (2.7), GAL (2.33), IL36G (2.25), CD97 (2.14), TNFRSF10D (2.12), IL36RN (1.95), TNFAIP3 (1.88), TAC1 (1.86), CXCL10 (1.85), LYN (1.82)
		GO:0070268	Cornification	< 0.0001	9	96	KRT37 (2.93), KRT18 (2.17), SPRR2G (2.04), SPINK6 (1.99), PRSS8 (1.94), PCSK6 (1.9), LCE3D (1.88), PI3 (1.83), KRT2 (1.8)
		GO:0018149	Peptide cross-linking	< 0.0001	7	37	LCE2B (3.65), SPRR2G (2.04), CRCT1 (1.92), LCE3D (1.88), PRR9 (1.85), PI3 (1.83), KRT2 (1.80)
		GO:0071277	Cellular response to calcium ion	< 0.0001	6	52	FOS (3.03), ALOX5AP (2.61), EDN1 (2.44), JUNB (1.94), SLC25A24 (1.86), PPIF (1.83)
		GO:0006955	Immune response	< 0.0001	13	356	CXCL8 (6.21), TNF (3.81), CXCL1 (2.84), CCL20 (2.8), CCL5 (2.75), GEM (2.54), CD97 (2.14), TNFRSF10D (2.12), MICB (2.04), PXDN (1.88), TNFAIP3 (1.88), CXCL10 (1.85), IL1RL1 (1.84)
		GO:0071222	Cellular response to lipopolysaccharide	< 0.0001	8	129	CXCL8 (6.21), CCL20 (2.8), CCL5 (2.75), LCN2 (2.04), ABCC2 (2.02), TNFAIP3 (1.88), CXCL10 (1.85), SERPINE1 (1.81)
		GO:0032868	Response to insulin	< 0.0001	6	73	FABP3 (3.07), CCL5 (2.75), GAL (2.33), EGR1 (2.06), SLC27A1 (1.95), LYN (1.82)
	Urushiol- enriched GO BPs in 173 DEGs	GO:0043434	Response to peptide hormone	0.0002	4	58	AREG (2.3), SOCS1 (2.02), IRS1 (1.94) ANXA1 (1.8)
		GO:0030216	Keratinocyte differentiation	0.0003	4	60	DSG4 (2.62), SCEL (2.55), CDSN (2.12), ANXA1 (1.8)
		GO:0008544	Epidermis development	0.0007	4	78	SCEL (2.55), CDSN (2.12), CST6 (1.91), PTHLH (1.89)
		GO:0019221	Cytokine-mediated signaling pathway	0.0008	7	292	SP100 (2.38), SH2B2 (2.24), PTPN2 (2.23), SOCS1 (2.02), IFNE (1.94), F3 (1.88), IL1F10 (1.87)
		GO:0006928	Movement of cell or subcellular component	0.0011	4	8	CALD1 (2.42), CXCL8 (2.12), TPM4 (1.84), ANXA1 (1.8)
		GO:0055086	Nucleobase-containing small molecule metabolic process		4	89	TYMP (2.01), GLRX (1.92), ADK (1.88), NT5E (1.86)
		GO:0007565	Female pregnancy	0.0019	4	102	PSG1 (2.44), ADRB2 (2.26), PTHLH (1.89), PSG6 (1.85)
		GO:0006954	Inflammatory response	0.0131	7	378	SP100 (2.38), THBS1 (2.15), CXCL8 (2.12), IL18 (1.89), IL1F10 (1.87), TAC1 (1.83), ANXA1 (1.8)
Down	SLS-enriched GO BPs in 193 DEGs	GO:0006935	Chemotaxis	0.0001	6	118	CXCL14 (0.04), ACKR3 (0.40), TYMP (0.41), PLD1 (0.41), PLGRKT (0.5), CMTM8 (0.52)
		GO:0055114	Oxidation-reduction process	0.0001	13	624	ALDH3B2 (0.12), IMPDH2 (0.32), AKR1C3 (0.37), PIR (0.43), RDH12 (0.46), MSRB2 (0.47), F8 (0.48), DCXR (0.52), DEGS1 (0.52), CYB561A3 (0.54), BLVRB (0.54), CYP4F12 (0.54), CYB5R4 (0.55)
		GO:0070268	Cornification	0.0003	5	96	RPTN (0.25), DSC1 (0.27), DSG1 (0.31), KRT80 (0.4), KRT1 (0.46)
		GO:0000082	G1/S transition of mitotic cell cycle	0.0030	5	161	PSMB9 (0.46), RB1 (0.5), FBXO5 (0.51), PSMB10 (0.53), RHOU (0.55)
		GO:0031424	Keratinization	0.0054	4	116	DSC1 (0.27), DSG1 (0.31), KRT80 (0.4), KRT1 (0.46)
		GO:0044267	Cellular protein metabolic process	0.0137	11	801	COX19 (0.29), DDIT3 (0.3), CTSH (0.34), ST6GALNAC2 (0.36), BCHE (0.36), MSRB2 (0.47), F8 (0.48), RFT1 (0.49), ARFGAP2 (0.52), ASNS (0.54), MUC15 (0.56)
	Urushiol- enriched GO BPs in 127 DEGs	GO:0007399	Nervous system development	0.0384	4	307	NAB2 (0.48), ENC1 (0.53), MAFB (0.54), GLIS2 (0.54)
		GO:0008284	Positive regulation of cell proliferation	0.0425	5	462	CTGF (0.24), HOXC10 (0.51), SERTAD1 (0.54), ZNF703 (0.56), FOSL1 (0.56)
		GO:0044267	Cellular protein metabolic process	0.0478	7	801	ARFGAP2 (0.44), MSRA (0.46), GSPT2 (0.47), TIMM17B (0.53), ALG2 (0.53), NUP62 (0.54), MDC1 (0.55)

* '#' denotes 'number'.

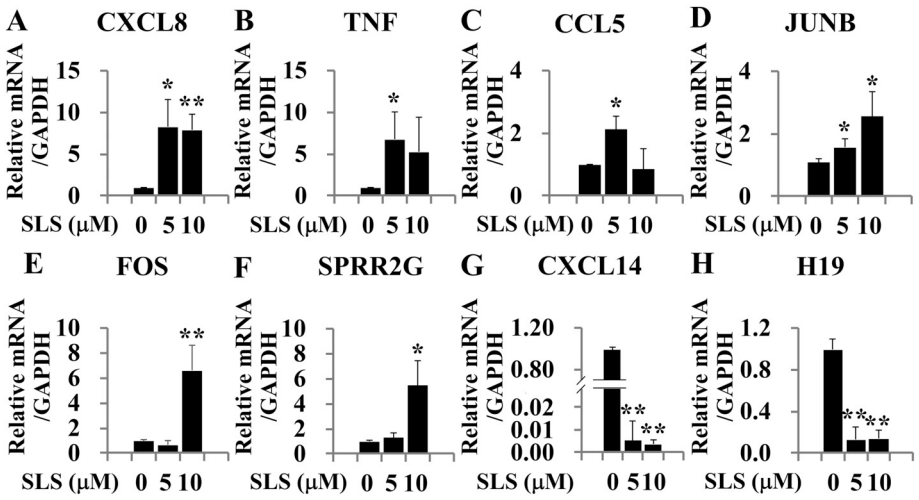

Fig. 2. Validation of the microarray results by Q-RT-PCR in response to SLS. To determine the mRNA levels of CXCL8 (A), TNF (B), CCL5 (C), JUNB (D), FOS (E), SPRR2G (F), CXCL14 (G) and H19 (H), total RNA samples were extracted from confluently cultured NHKCs treated with SLS for 24 h. Values represent the mean expression ± SD of the mRNA of the various genes relative to human GAPDH expression (n = 3). $^{*}p < 0.05$ and $^{**}p < 0.01$ were considered statistically significant compared to the controls.

which are called as cellular immediate-early response genes against various extracellular stimuli (Healy et al., 2013). Upregulation of the epidermal differentiation-associated gene *SPRR2G* was also confirmed in SLS-treated NHKCs. Microarray expression of the downregulated DEGs, *CXCL14* and *H19*, was validated by Q-RT-PCR in SLS-treated NHKCs (Fig. 2).

To validate the urushiol-induced DEGs, the mRNA levels of *CXCL8*, *SP100*, *SOCS1*, *THBS1, ANXA1,* and *DSG4* were measured by Q-RT-PCR because they were significantly associated with enriched GO BPs (Fig. 3). Among the inflammatory response-associated DEGs, the urushiol-induced upregulation of *CXCL8*, *SOCS1,* and *THBS1* was validated in NHKCs but microarray expression of *SP100* was not confirmed by Q-RT-PCR (Fig. 3B). Urushiol upregulated the gene transcription of keratinocyte differentiation-associated DEGs, *ANXA1* and *DSG4* in independently prepared NHKC samples (Fig. 3E and F). The downregulation of *CXCL14* and *H19* gene transcription was also confirmed by Q-RT-PCR in urushiol-treated NHKCs (Fig. 3G and H). Although *SP100* gene transcription was not validated in urushiol-treated NHKCs, the microarray expression of DEGs associated with inflammation and epidermal differentiation was validated for both SLS- and urushiol-treated NHKCs.

3.4. Temporal expression profile of DEGs in NHKCs treated with irritant or sensitizers

The transcription of two chemokine DEGs, *CXCL8* and *CXCL14*, was changed in NHKCs treated with either SLS or urushiol. CXCL8 upregulation in epidermal KCs or dendritic cells has been extensively studied as a potential biomarker for the development of skin sensitization tests (Coquette et al., 2003; Bae et al., 2015). In contrast, CXCL14 has not been investigated as an *in vitro* toxicity test. To investigate a potential biomarker for animal alternative tests, NHKCs were treated with the primary irritant methyl salicylate or the skin sensitizer 2-mercaptobenzothiazole in addition to SLS or urushiol (Fig. 4). *CXCL8* was significantly upregulated in NHKCs in response to SLS, methyl salicylate, urushiol, and 2-mercaptobenzothiazole (Fig. 4A–D). In contrast, SLS, urushiol, and 2-mercaptobenzothiazole significantly downregulated *CXCL14* in NHKCs. However, methyl salicylate had no effect on *CXCL14* gene transcription (Fig. 4E–H). In the NHKCs, IFNγ, IL-4, and IL-22 downregulated the constitutively expressed CXCL14 (Jin et al., 2014). CXCL14 downregulation plays a pivotal role in the immunological process of NHKCs during cutaneous immune responses such as allergenic sensitization.

3.5. Effects of OECD TG429 sensitizers and non-sensitizers on CXCL8 and CXCL14 production in NHKCs

To evaluate CXCL14 as a biomarker for the development of a novel *in vitro* toxicity test, the expression of CXCL14 protein was measured in NHKCs treated with skin allergenic sensitizers and non-sensitizers listed in the OECD TG429. The OECD TG429, known as the mouse *in vivo* local lymph node assay (LLNA), is the method to identify and characterize potential human skin sensitizers (Ehling et al., 2005; OECD, 2010). The OECD TG429 provides the reference chemical list consisting

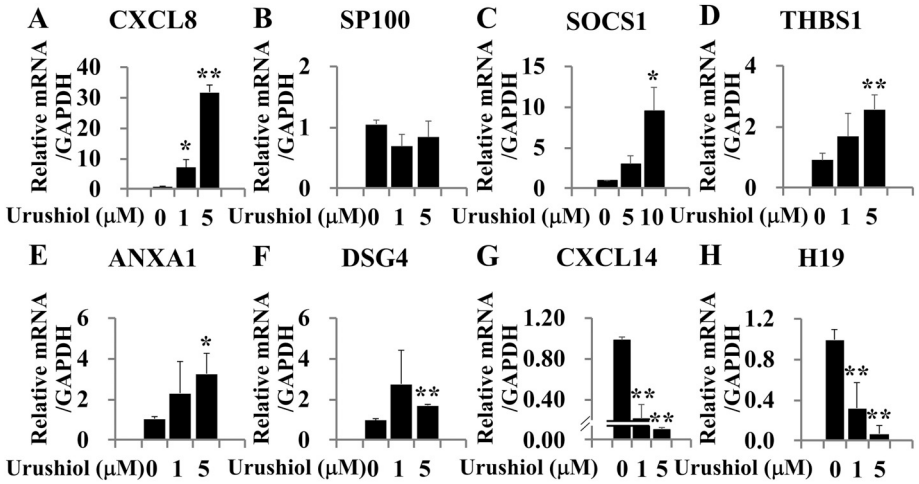

Fig. 3. Validation of the microarray results by Q-RT-PCR in response to Urushiol. To determine the mRNA levels of CXCL8 (A), SP100 (B), SOCS1 (C), THBS1 (D), ANXA1 (E), DSG4 (F), CXCL14 (G) and H19 (H), total RNA samples were extracted from confluently cultured NHKCs treated with urushiol for 24 h. Values represent the mean expression ± SD of the mRNA of the various genes relative to human GAPDH expression (n = 3). $^{*}p < 0.05$ and $^{**}p < 0.01$ were considered statistically significant compared to the controls.

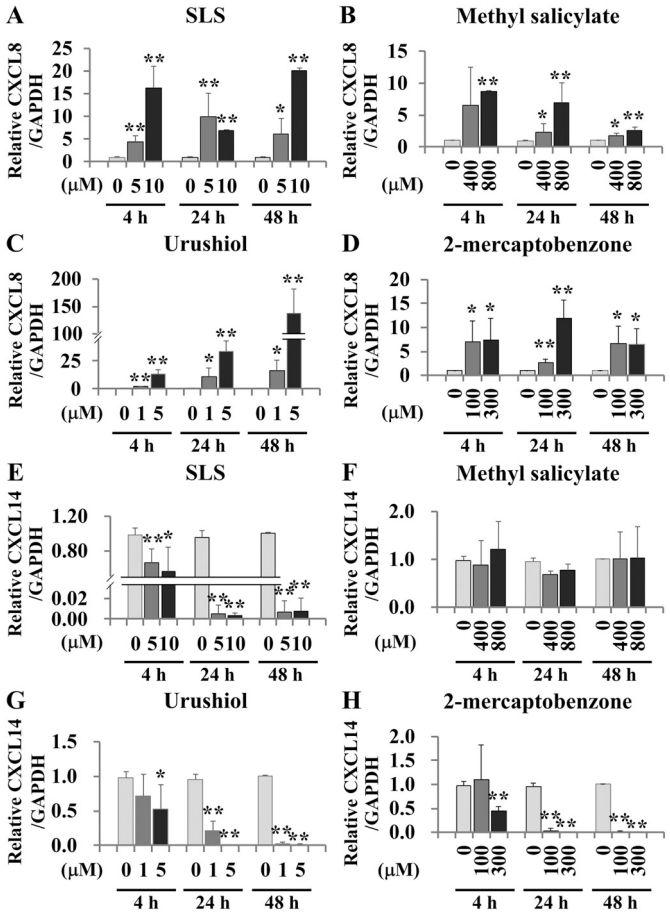

Fig. 4. Temporal expression profile in irritant- or allergen-treated NHKCs. Total RNA was extracted at given times after the treatment for 4, 24 or 48 h. Q-RT-PCR was performed for the measurement of CXCL8 mRNA in NHKCs treated with SLS (A), methyl salicylate (B), urushiol (C) and 2-mercaptobenzothiazole (D). CXCL14 mRNA levels were measured in NHKCs treated with SLS (E), methyl salicylate (F), urushiol (G) and 2-mercaptobenzothiazole (H). Values represent the mean expression ± SD of the mRNA of the various genes relative to human GAPDH expression ($n = 3$). $^{*}p < 0.05$ and $^{**}p < 0.01$ were considered statistically significant compared to the controls.

of 16 human skin sensitizers and 6 non-sensitizers. The OECD TG429 non-sensitizers can induce irritation reactions in human skin. NHKCs were treated with the 22 reference chemicals for 24 h and the CXCL14 levels were measured in the culture supernatants by enzyme-linked immunosorbent assay (ELISA). Changes in CXCL8 expression were simultaneously measured because it has been studied as a predictive biomarker for numerous *in vitro* skin sensitization assays based on keratinocytes and dendritic cells (Hitzler et al., 2013). CXCL8 also plays a crucial role in ACD pathogenesis (Griffiths et al., 1991; Jia et al., 2012). Among 16 reference sensitizers, 10 TG429 reference sensitizers including CMI/MI, cobalt chloride, DNCB, ethylene glycol dimethacrylate, HCA, 2-mercaptobenzothiazole, methyl methacrylate, nickel chloride, phenyl benzoate, and 4-phenylene diamine significantly downregulated CXCL14 protein expression in NHKCs at concentrations wherein cell viability was > 70% (Table 2). In contrast, 10 reference sensitizers, cinnamic alcohol, citral, cobalt chloride, DNCB, imidazolidinyl urea, isoeugenol, 2-mercaptobenzothiazole, methyl methacrylate, phenyl benzoate, and 4-phenylene diamine significantly upregulated CXCL8 protein expression in NHKCs (Table 2; Fig. 5A). The 6 sensitizers, cobalt chloride, DNCB, 4-phenylene diamine, 2-mercaptobenzothiazole, methyl methacrylate, and phenyl benzoate significantly changed the protein expression of both CXCL8 and CXCL14 in NHKCs (Table 2; Fig. 5A). The sensitizers CMI/MI, ethylene glycol dimethacrylate, HCA, and nickel chloride significantly downregulated CXCL14 in NHKCs but they did not affect CXCL8 production (Table 2; Fig. 5A). In contrast, cinnamic alcohol, citral, imidazolidinyl urea, and isoeugenol upregulated CXCL8 in NHKCs but had no effect on CXCL14 expression. The two sensitizers, eugenol and isopropanol, had no effect on the expression of either CXCL8 or CXCL14 compared to the vehicle-treated control (Table 2

When the TG429 reference non-sensitizers were treated in NHKCs, only SLS significantly downregulated CXCL14 compared with the control (Table 3; Fig. 5B). In contrast, 5 OECD TG429 non-sensitizers, chlorobenzene, methyl salicylate, salicylic acid, SLS, and xylene, significantly upregulated CXCL8 production (Table 3; Fig. 5B). Only SLS changed the CXCL14 level whereas 5 out of the 6 non-sensitizers significantly affected CXCL8 production. The use of CXCL14 as a biomarker increased the specificity and accuracy for the predictive performance (Fig. 5C). Therefore, CXCL14 may be a more selective biomarker than CXCL8 to distinguish human sensitizers from human skin non-sensitizers.

3.6. CXCL14 downregulation is associated with the JAK/STAT and MAPK signal transduction pathways in NHKCs

To investigate the intracellular signaling mechanisms associated with changes in the downregulation of CXCL14 in NHKCs, we evaluated the pharmacological signaling inhibitors affecting Janus kinase (JAK), the signal transducer and activator of the transcription (STAT) pathway, and the mitogen-activated protein kinase/extracellular signal-regulated kinase (MAPK/ERK) pathway in SLS-treated NHKCs (Fig. 6). The SLS-induced CXCL14 downregulation in NHKCs was significantly inhibited by the treatment with the MAPK/ERK inhibitor PD98059 or the JAK3 inhibitor WHI-P131 (Fig. 6A). The JAK1 inhibitor piceatannol and the JAK2 inhibitor AG490 did not affect the SLS-induced CXCL14 downregulation (Fig. 6A). Notably, PD98059 and WHI-P131 significantly upregulated CXCL14 in NHKCs compared to the expression level in the vehicle-treated control. Both PD98059 and WHI-P131 upregulated CXCL14 in NHKCs in a concentration-dependent manner (Fig. 6B). SLS increased the phosphorylation in both the MAPK/ERK and STAT6 pathways in NHKCs (Fig. 6C–F). The phosphorylation of the other STAT subtypes was not detected in the SLS-treated NHKCs (data not shown). The MAPK/ERK inhibitor PD98059 significantly suppressed the ERK phosphorylation by SLS (Fig. 6C and D). The JAK3 inhibitor WHI-P131 significantly suppressed the SLS-induced STAT6 phosphorylation (Fig. 6E and F). These results suggest that SLS-induced CXCL14 downregulation was mediated by both the MAPK/ERK and JAK3/STAT6 pathways in NHKCs. Moreover, the constitutive CXCL14 expression in NHKCs is regulated by these signaling mechanisms.

4. Discussion

Keratinocyte-derived proinflammatory cytokines play important roles in the molecular pathogenesis of both ICD and ACD. Skin irritants and sensitizers stimulate human epidermal KCs to produce various cytokines and chemokines (Coquette et al., 2003; Natsch and Emter, 2008; Jin et al., 2014; Bae et al., 2015). In the present study, the whole genome-scale transcriptional profiles of SLS- or urushiol-treated NHKCs were analyzed to elucidate the role of epidermal KCs in the molecular pathogenesis of chemically induced ICD and ACD. The GO BP enrichment analyses of 259 SLS- and 173 urushiol-upregulated DEGs showed that both of these agents induced proinflammatory responses and epidermal differentiation processes in NHKCs. Despite the similarity in the functional signatures of the GO BP terms, the DEG sets for each GO BP term differed between SLS and urushiol, suggesting that two chemicals induce different toxicological signaling pathways in human KCs. Regarding to the epidermal differentiation, for example, SLS affected the gene transcription of cytoskeletal intermediate filament-associated proteins such as KRTs and SPRR2G whereas urushiol primarily changed

Table 2
Effects of human skin allergen in NHKCs.

OECD TG429 substances (CAS number)					
CMI/MI (26172–55-4) /	Chemical concentration (μm)	0 (vehicle)	50	10	2
Human sensitizer (+), LLNA (+)	Cell survival (%)	100 ± 9	37 ± 12**	103 ± 8	95 ± 7
	CXCL14 (pg/ml)	130 ± 19	9 ± 5**	30 ± 24**	52 ± 34**
	IL-8 (pg/ml)	12 ± 8	20 ± 17	15 ± 5	22 ± 12*
DNCB (97–00-7)	Chemical concentration (μm)	0 (vehicle)	10	2	0.4
Human sensitizer (+), LLNA (+)	Cell survival (%)	100 ± 7	6 ± 4**	61 ± 18**	84 ± 6*
	CXCL14 (pg/ml)	146 ± 33	55 ± 14**	25 ± 24**	136 ± 67
	IL-8 (pg/ml)	15 ± 1	26 ± 10	13 ± 1	16 ± 4
4-phenylene diamine (106–50-3)	Chemical concentration (μm)	0 (vehicle)	10	2	0.4
Human sensitizer (+), LLNA (+)	Cell survival (%)	100 ± 8	22 ± 7**	68 ± 18*	98 ± 8
	CXCL14 (pg/ml)	141 ± 17	23 ± 5**	18 ± 18**	135 ± 36
	IL-8 (pg/ml)	16 ± 8	87 ± 26**	81 ± 36*	15 ± 13
Cobalt chloride (7646-79-9)	Chemical concentration (μm)	0 (vehicle)	50	10	2
Human sensitizer (+), LLNA (+)	Cell survival (%)	100 ± 8	56 ± 18**	90 ± 6	97 ± 2
	CXCL14 (pg/ml)	117 ± 42	41 ± 15*	48 ± 21*	105 ± 38
	IL-8 (pg/ml)	13 ± 11	386 ± 27**	88 ± 33**	13 ± 5
Nickel chloride (7718-54-9)	Chemical concentration (μm)	0 (vehicle)	50	10	2
Human sensitizer (+), LLNA (−)	Cell survival (%)	100 ± 8	26 ± 8**	100 ± 8	102 ± 8
	CXCL14 (pg/ml)	139 ± 19	36 ± 8**	76 ± 16**	93 ± 28*
	IL-8 (pg/ml)	15 ± 3	14 ± 2	13 ± 2	15 ± 3
Isoeugenol (97–54-1)	Chemical concentration (μm)	0 (vehicle)	10	2	0.4
Human sensitizer (+), LLNA (+)	Cell survival (%)	100 ± 8	16 ± 8**	59 ± 19**	92 ± 8
	CXCL14 (pg/ml)	130 ± 32	180 ± 39	104 ± 39	143 ± 59
	IL-8 (pg/ml)	17 ± 8	45 ± 18*	5 ± 4	7 ± 2
2-Mercaptobenzothiazole (149–30-4)	Chemical concentration (μm)	0 (vehicle)	50	10	2
Human sensitizer (+), LLNA (+)	Cell survival (%)	100 ± 8	99 ± 8	102 ± 8	99 ± 7
	CXCL14 (pg/ml)	128 ± 22	15 ± 5**	50 ± 20**	138 ± 29
	IL-8 (pg/ml)	12 ± 11	749 ± 45**	576 ± 174**	35 ± 11*
Citral (5392-40-5)	Chemical concentration (μm)	0 (vehicle)	10	2	0.4
Human sensitizer (+), LLNA (+)	Cell survival (%)	100 ± 8	11 ± 5**	91 ± 8	98 ± 3
	CXCL14 (pg/ml)	133 ± 16	194 ± 18**	133 ± 22	133 ± 20
	IL-8 (pg/ml)	16 ± 4	130 ± 27**	15 ± 4	15 ± 3
HCA (101–86-0)	Chemical concentration (μm)	0 (vehicle)	10	2	0.4
Human sensitizer (+), LLNA (+)	Cell survival (%)	100 ± 10	50 ± 18**	103 ± 9	106 ± 11
	CXCL14 (pg/ml)	126 ± 24	80 ± 14*	102 ± 42	119 ± 22
	IL-8 (pg/ml)	16 ± 3	14 ± 1	13 ± 2	14 ± 2
Eugenol (97–53-0)	Chemical concentration (μm)	0 (vehicle)	10	2	0.4
Human sensitizer (+), LLNA (+)	Cell survival (%)	100 ± 8	9 ± 1**	76 ± 6**	96 ± 8
	CXCL14 (pg/ml)	137 ± 18	111 ± 44	105 ± 29	119 ± 30
	IL-8 (pg/ml)	15 ± 2	19 ± 3	12 ± 2	13 ± 2
Phenyl benzoate (93–99-2)	Chemical concentration (μm)	0 (vehicle)	50	10	2
Human sensitizer (+), LLNA (+)	Cell survival (%)	100 ± 10	86 ± 9	106 ± 8	105 ± 7
	CXCL14 (pg/ml)	130 ± 23	96 ± 16	97 ± 10*	120 ± 36
	IL-8 (pg/ml)	14 ± 6	23 ± 8	13 ± 1	13 ± 2
Cinnamic alcohol (104–54-1)	Chemical concentration (μm)	0 (vehicle)	10	2	0.4
Human sensitizer (+), LLNA (+)	Cell survival (%)	100 ± 10	51 ± 5**	104 ± 8	107 ± 10
	CXCL14 (pg/ml)	135 ± 22	157 ± 16	112 ± 14	114 ± 21
	IL-8 (pg/ml)	15 ± 1	176 ± 33**	16 ± 2	17 ± 1*
Imidazolidinyl urea (39236–46-9)	Chemical concentration (μm)	0 (vehicle)	10	2	0.4
Human sensitizer (+), LLNA (+)	Cell survival (%)	100 ± 8	34 ± 13**	100 ± 8	98 ± 8
	CXCL14 (pg/ml)	128 ± 25	115 ± 27	116 ± 26	137 ± 33
	IL-8 (pg/ml)	15 ± 3	169 ± 15**	18 ± 3	16 ± 2
Methyl methacrylate (80–62-6)	Chemical concentration (μm)	0 (vehicle)	50	10	2
Human sensitizer (+), LLNA (+)	Cell survival (%)	100 ± 10	69 ± 5**	106 ± 9	103 ± 12
	CXCL14 (pg/ml)	127 ± 17	68 ± 14**	80 ± 8**	120 ± 39
	IL-8 (pg/ml)	14 ± 7	34 ± 8*	16 ± 10	14 ± 10
Isopropanol (67–63-0)	Chemical concentration (μm)	0 (vehicle)	50	10	2
Human sensitizer (+), LLNA (−)	Cell survival (%)	100 ± 8	99 ± 7	95 ± 7	100 ± 8
	CXCL14 (pg/ml)	144 ± 25	176 ± 35	158 ± 23	147 ± 22
	IL-8 (pg/ml)	14 ± 6	17 ± 4	23 ± 14	16 ± 4
Ethylene glycol dimethacrylate (97-90-54)	Chemical concentration (μm)	0 (vehicle)	50	10	2
Human sensitizer (+), LLNA (+)	Cell survival (%)	100 ± 7	17 ± 3**	82 ± 8*	99 ± 7
	CXCL14 (pg/ml)	127 ± 12	30 ± 17**	51 ± 4**	114 ± 12
	IL-8 (pg/ml)	15 ± 3	20 ± 5	8 ± 5*	7 ± 1**

CMI/MI = 5-chloro-2-methyl-4-isothiazolin-3-one/2-methyl-4-isothiazolin-3-one, DNCB = 2,4dinitrochlorobenzene, HCA = hexyl cinnamic alcohol.
* Denotes $p < .05$ ($n = 3$).
** Denotes $p < .01$ ($n = 3$), when compared to the values of vehicle-treated samples.

the gene transcription of cell-to-cell adhesion-related proteins such as DSG4 and CDSN (Table 1). In the analyses of 193 SLS- and 124 urushiol-downregulated DEGs, cellular protein metabolic process (GO:0044267) was identified in NHKCs as a downregulated gene expression signature of NHKCs in response to both SLS and urushiol. A future study should be directed to elucidate the pathological contribution of downregulated metabolic processes to toxicological outcomes to toxic chemicals.

In NHKCs, two chemokines, CXCL8 and CXCL14, were commonly changed by both SLS and urushiol. In the present study, we

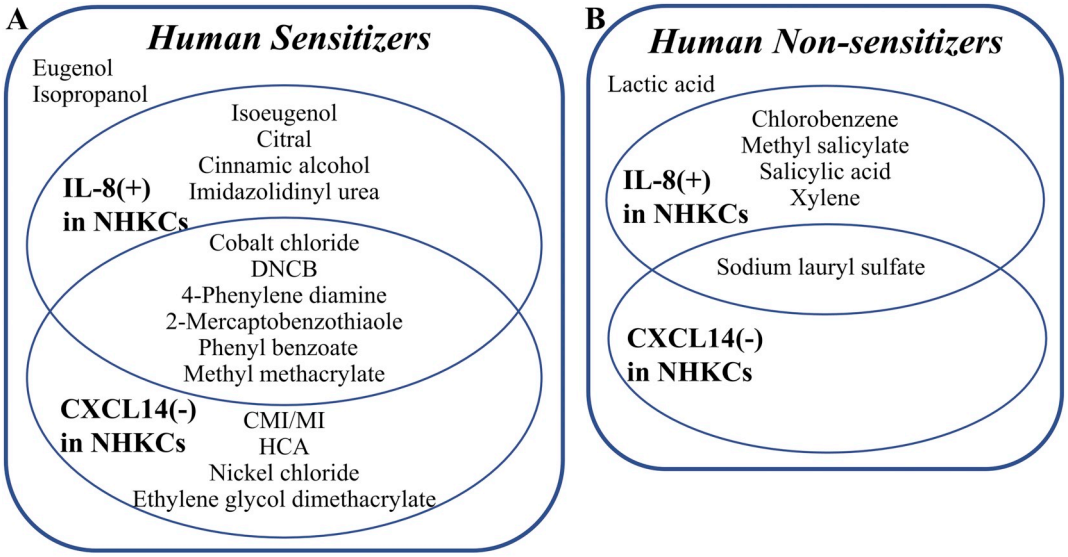

C

Human	CXCL8		CXCL14	
	Positive	Negative	Positive	Negative
16 sensitizers	10	6	10	6
6 non-sensitizers	5	1	1	5
Sensitivity (%)	62.5		62.5	
Specificity (%)	16.7		83.3	
Accuracy (%)	66.7		90.9	

Fig. 5. Venn diagram representing the effect of OECD TG429 sensitizers and non-sensitizers on CXCL8 and/or CXCL14 production in NHKCs. The effects of 16 OECD TG429 sensitizers (A) in Table 2 and 6 OECD TG429 non-sensitizers (B) in Table 3 were classified in the Venn diagram according to the significant upregulation of CXCL8 or the downregulation of CXCL14 in NHKCs. The predictive performance was calculated as sensitivity, specificity and accuracy (C).

Table 3
Effects of human skin non-sensitizers in NHKCs.

OECD TG429 substances (CAS number)					
Chlorobenzene (108–90-7)	Chemical concentration (μm)	0 (vehicle)	50	10	2
Human sensitizer (−), LLNA (−)	Cell survival (%)	100 ± 7	100 ± 7	95 ± 8	95 ± 7
	CXCL14 (pg/ml)	118 ± 36	100 ± 8	100 ± 9	114 ± 10
	IL-8 (pg/ml)	15 ± 2	44 ± 17*	24 ± 4**	36 ± 8**
Lactic acid (50–21-5)	Chemical concentration (μm)	0 (vehicle)	50	10	2
Human sensitizer (−), LLNA (−)	Cell survival (%)	100 ± 10	23 ± 4**	97 ± 12	100 ± 11
	CXCL14 (pg/ml)	127 ± 12	136 ± 31	118 ± 36	126 ± 23
	IL-8 (pg/ml)	15 ± 6	9 ± 1	16 ± 6	19 ± 2
Methyl salicylate (119–36-8)	Chemical concentration (μm)	0 (vehicle)	50	10	2
Human sensitizer (−), LLNA (−)	Cell survival (%)	100 ± 9	17 ± 4**	93 ± 9	99 ± 9
	CXCL14 (pg/ml)	126 ± 26	113 ± 37	100 ± 46	121 ± 45
	IL-8 (pg/ml)	16 ± 4	26 ± 10	93 ± 25**	26 ± 6*
Salicylic acid (69–72-7)	Chemical concentration (μm)	0 (vehicle)	50	10	2
Human sensitizer (−), LLNA (−)	Cell survival (%)	100 ± 7	23 ± 2**	92 ± 7	98 ± 8
	CXCL14 (pg/ml)	130 ± 21	144 ± 49	146 ± 39	145 ± 42
	IL-8 (pg/ml)	15 ± 1	94 ± 26**	40 ± 8**	29 ± 3**
Sodium lauryl sulfate (151–21-3)	Chemical concentration (μm)	0 (vehicle)	10	2	0.4
Human sensitizer (−), LLNA (+)	Cell survival (%)	100 ± 7	18 ± 3**	85 ± 10	103 ± 8
	CXCL14 (pg/ml)	140 ± 18	29 ± 3**	55 ± 8**	139 ± 21
	IL-8 (pg/ml)	21 ± 3	278 ± 55**	2 ± 2**	4 ± 1**
Xylene (1330-20-7)	Chemical concentration (μm)	0 (vehicle)	50	10	2
Human sensitizer (−), LLNA (+)	Cell survival (%)	100 ± 8	18 ± 3**	98 ± 7	104 ± 7
	CXCL14 (pg/ml)	135 ± 34	166 ± 56	133 ± 15	133 ± 20
	IL-8 (pg/ml)	15 ± 1	25 ± 9	24 ± 5**	28 ± 5**

* Denotes $p < .05$ ($n = 3$).
** Denotes $p < .01$ ($n = 3$), when compared to the values of vehicle-treated samples.

demonstrated that SLS and urushiol upregulated CXCL8 but downregulated CXCL14 in NHKCs. Epidermal keratinocyte-derived cytokines and chemokines have been investigated as predictive biomarkers for *in vitro* skin sensitization tests (Coquette et al., 2003; Bae et al., 2015; Kim et al., 2018). It is well known that the chemokine CXCL8 is upregulated in keratinocytes and dendritic cells by skin sensitizers and irritants (Coquette et al., 2003). In contrast, the physiological function of CXCL14 in human skin is poorly understood. CXCL14 is constitutively expressed in the human epithelial tissues of the skin, lung, kidney, and intestine. A previous study showed that fibroblasts in prostate tumor microenvironments produced CXCL14 and promoted cancer cell growth (Augsten et al., 2009). CXCL14 may be a chemotactic factor which

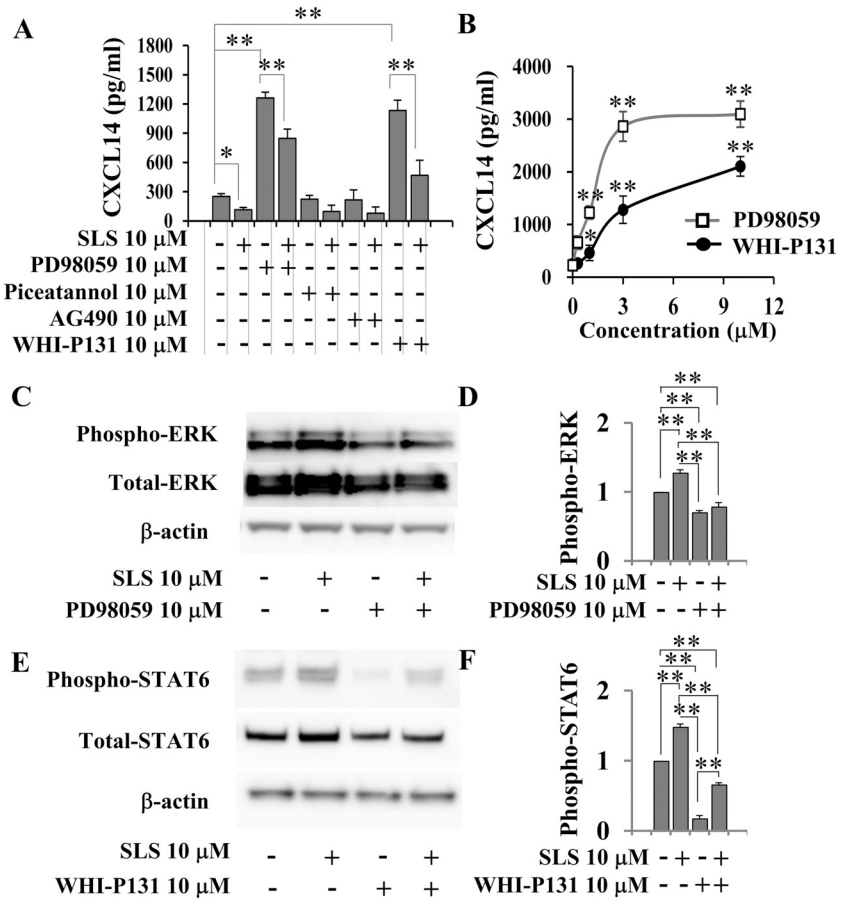

Fig. 6. Effects of SLS on STAT6 and MAPK signaling pathways in NHKCs. MAPK signaling inhibitor (PD98059) and JAK inhibitors (Piceatannol, AG-490 and WHI-P131) were co-treated with SLS for 24 hs in NHKCs. At 24 h after treatment, cell culture supernatants were harvested and evaluated to measure concentration of CXCL14 in NHKCs (A). The effect of PD98059 and WHI-P131 on CXCL14 protein expression was determined by ELISA (B). Results for phospho-ERK by PD98059 (C and D), phosphor-STAT6 by WHI-P131 (E and F) in SLS-treated NHKCs were quantified relative to β-actin levels using ImageJ software ($n = 3$, independent experiments). Values represent the mean expression ± SD. $^{*}p < 0.05$ and $^{**}p < 0.01$.

recruits dendritic cells (DCs) in epithelial tissues (Shellenberger et al., 2004). It may also be an important homeostatic chemokine (Banisadr et al., 2011; Lu et al., 2016). Interestingly, CXCL14-knockout mice did not exhibit any specific phenotype associated with monocyte migration or immune function, suggesting that CXCL14 may affect various target cells in health and disease (Meuter et al., 2007). Despite the association of CXCL14 with epithelial tumorigenesis, its role in keratinocyte-mediated cutaneous inflammation and its potential as a toxicity biomarker for various *in vitro* skin toxicity tests remain unknown. It was recently suggested that constitutively expressed CXCL14 participates in the recruitment of dendritic precursor cells (Kurth et al., 2001; Schaerli et al., 2005). Therefore, the downregulation of constitutively expressed CXCL14 could trigger the migration of sensitizer-activated dendritic cells to the lymph nodes. This mechanism might be the basis for CXCL14 downregulation in NHKCs and serve as a novel biomarker for *in vitro* skin sensitization tests.

The simultaneous measurement of multiple cytokines has been proposed to develop *in vitro* methods to determine skin sensitization potential in keratinocyte and dendritic cell lines (Coquette et al., 2003; Nukada et al., 2008; Takahashi et al., 2011; Hitzler et al., 2013; Son et al., 2013; Bae et al., 2015). Despite continuous efforts to validate various cytokine biomarkers for *in vitro* tests, most of the currently available skin sensitization assays focus on the co-measurement of upregulated cytokines such as CCL2, CXCL8, IL-1, TNFα, and VEGF in allergen- or irritant-exposed mammalian cells (Coquette et al., 2003; Natsch and Emter, 2008; Son et al., 2013; Bae et al., 2015). Co-measurement of upregulated and downregulated biomarkers may provide a more comprehensive mechanistic coverage of the sensitization process in response to toxic stimuli and could improve prediction accuracy of potential allergens. When the OECD TG429 reference chemicals were tested on NHKCs, 10 of the 16 reference sensitizers significantly downregulated CXCL14 and 10 sensitizers also upregulated CXCL8 in the NHKCs. Considering both CXCL8 and CXCL14, 14 reference sensitizers significantly changed the expression level of either CXCL8 or CXCL14 in NHKCs. In an earlier study, we reported that 14 reference sensitizers significantly changed the expression of both CXCL8 and/or VEGF in NHKCs (Bae et al., 2015). Ethylene glycol dimethacrylate, a positive sensitizer in the TG429 mouse LLNA test, yielded a false negative outcome when the expression levels of CXCL8 and VEGF were measured (Bae et al., 2015). However, significant CXCL14 downregulation was detected in NHKCs treated with ethylene glycol dimethacrylate. In the present study, eugenol only slightly increased CXCL8 production in NHKCs. However, it was determined that CXCL8 was positively affected by eugenol or isoeugenol treatment in NHKCs (Bae et al., 2015). This discrepancy may be explained by the genetic and epigenetic variations in primary human keratinocytes originating from different donors. For the development of novel *in vitro* skin sensitization tests using primary human keratinocytes, new statistical methods should be designed to normalize the biological variations inherent in donor genetics and epigenetics.

Five out of the six OECD TG429 reference non-sensitizers did not affect CXCL14 production in NHKCs. Only SLS significantly downregulated CXCL14 relative to the vehicle-treated control. In contrast, five out of six reference non-sensitizers significantly altered CXCL8 production. Nickle chloride, one of the OECD TG429 sensitizers, significantly downregulated CXCL14. Nickle chloride is considered as a false negative chemical in the OECD TG429 mouse LLNA method (OECD, 2010). In this regard, CXCL14 downregulation may increase the predictive power of an *in vitro* skin sensitization test. SLS and Xylene are classified as false-positive chemicals in the OECD TG429 mouse LLNA method (OECD, 2010). Xylene did not affect the constitutive CXCL14 expression in NHKCs but SLS changed. SLS also affected both CXCL8 and VEGF expression in NHKCs (Bae et al., 2015). Although SLS was recommended as an irritating non-sensitizer in the OECD TG429, it

induced a week positive response in both LLNA and THP-1 cell based skin sensitization tests, similar to allergic patch reactions (Bruynzeel et al., 1982; Lim et al., 2008; Ahn et al., 2016). Moreover, the combination of SLS and a weak skin allergen in human dermal patch testing improved the predictive power of weaker allergens as sensitizers or irritants (Geier et al., 2003). In this regard, the use of SLS as a reference irritant chemical should be reconsidered for future validation studies to develop novel *in vitro* skin sensitization tests. As SLS is a false-positive irritating non-sensitizer in the OECD TG429 mouse LLNA method (OECD, 2010), the investigation of CXCL14 downregulation in NHKCs enhances the distinction between allergenic sensitizers and non-sensitizers in novel *in vitro* sensitization tests. Future studies should be directed to validate CXCL14 downregulation by testing more extensive reference sensitizers and non-sensitizers.

In the present study, we demonstrated that CXCL14 expression in NHKCs was regulated by both the MAPK/ERK and JAK3/STAT6 pathways. Treatment with either the MAPK/ERK inhibitor PD98059 or the JAK3 inhibitor WHI-P131 significantly upregulated CXCL14 in NHKCs in a concentration-dependent manner. These results suggest that both the MAPK/ERK and JAK3/STAT6 pathways suppressively co-regulate to maintain constitutive CXCL14 expression in NHKCs. The MAPK/ERK pathway is associated with an early and rapid inflammatory response (Kim and Choi, 2010). The JAK/STAT pathway mediates various cytokine signals in NHKCs (Jin et al., 2014; O'Shea et al., 2015). CXCL14 downregulation by SLS is partially mediated by the STAT6 signaling pathway. The lung epithelia of STAT6-deficient mice lack allergen-induced IgE-responses or Th2 cytokine responses (Miyata et al., 1999). Previously, we reported that IL-4, a Th2 cytokine associated with various allergic reactions, increased STAT6 phosphorylation in NHKCs (Jin et al., 2014). Transgenic mice constitutively expressing STAT6 are predisposed to allergic diseases such as atopic dermatitis and allergic skin inflammation (Sehra et al., 2008; Sehra et al., 2010). Therefore, STAT6-dependent regulation of CXCL14 production in human KCs supports that CXCL14 might serve as a mechanism-based biomarker for novel *in vitro* skin sensitization and allergen tests.

Author statement

Eunyoung Lee: Conceptualization, Methodology, Formal analysis, Investigation, Writing - Original Draft. **Sungjin Ahn**: Methodology, Formal analysis, Investigation. **Sun Hee Jin**: Methodology, Formal analysis, Investigation. **Moonyoung Lee:** Software, Data Curation **Jeong Joo Pyo**: Validation, Data Curation. **Jeayoung C. Shin:** Validation, Data Curation. **Seungchan An:** Software, Data Curation. **Jaehyoun Ha**: Validation, Data Curation. **Minsoo Noh:** Conceptualization, Investigation, Data Curation, Writing - Original Draft, Writing - Review & Editing, Project administration, Funding acquisition.

Declaration of Competing Interest

Jaehyoun Ha is an employee of IEC Korea Inc. The other authors have no conflicts of interest.

Acknowledgements

This study was partly supported by the MRC grant of the National Research Foundation in Korea [NRF-2018R1A5A2024425] and a National Research Foundation of Korea (NRF) grant [2019R1A2C2085749].

Appendix A. Supplementary data

Supplementary data to this article can be found online at https://doi.org/10.1016/j.taap.2019.114828.

References

Ahn, I., Kim, T.S., Jung, E.S., Yi, J.S., Jang, W.H., Jung, K.M., Park, M., Jung, M.S., Jeon, E.Y., Yeo, K.U., Jo, J.H., Park, J.E., Kim, C.Y., Park, Y.C., Seong, W.K., Lee, A.Y., Chun, Y.J., Jeong, T.C., Jeung, E.B., Lim, K.M., Bae, S., Sohn, S., Heo, Y., 2016. Performance standard-based validation study for local lymph node assay: 5-bromo-2-deoxyuridine-flow cytometry method. Regul. Toxicol. Pharmacol. 80, 183–194. https://doi.org/10.1016/j.yrtph.2016.06.009.

Albanesi, C., Scarponi, C., Giustizieri, M.L., Girolomoni, G., 2005. Keratinocytes in inflammatory skin diseases. Curr. Drug Targets Inflamm. Allergy 4, 329–334. https://doi.org/10.2174/1568010054022033.

Augsten, M., Hagglof, C., Olsson, E., Stolz, C., Tsagozis, P., Levchenko, T., Frederick, M.J., Borg, A., Micke, P., Egevad, L., Ostman, A., 2009. CXCL14 is an autocrine growth factor for fibroblasts and acts as a multi-modal stimulator of prostate tumor growth. Proc. Natl. Acad. Sci. U. S. A. 106, 3414–3419. https://doi.org/10.1073/pnas.0813144106.

Bae, O.N., Ahn, S., Jin, S.H., Hong, S.H., Lee, J., Kim, E.S., Jeong, T.C., Chun, Y.J., Lee, A.Y., Noh, M., 2015. Chemical allergens stimulate human epidermal keratinocytes to produce lymphangiogenic vascular endothelial growth factor. Toxicol. Appl. Pharmacol. 283, 147–155. https://doi.org/10.1016/j.taap.2015.01.008.

Banisadr, G., Bhattacharyya, B.J., Belmadani, A., Izen, S.C., Ren, D., Tran, P.B., Miller, R.J., 2011. The chemokine BRAK/CXCL14 regulates synaptic transmission in the adult mouse dentate gyrus stem cell niche. J. Neurochem. 119, 1173–1182. https://doi.org/10.1111/j.1471-4159.2011.07509.x.

Bruynzeel, D.P., van Ketel, W.G., Scheper, R.J., von Blomberg-van der Flier, B.M., 1982. Delayed time course of irritation by sodium lauryl sulfate: observations on threshold reactions. Contact Dermatitis 8, 236–239. https://doi.org/10.1111/j.1600-0536.1982.tb04205.x.

Choi, H., Shin, D.W., Kim, W., Doh, S.J., Lee, S.H., Noh, M., 2011. Asian dust storm particles induce a broad toxicological transcriptional program in human epidermal keratinocytes. Toxicol. Lett. 200, 92–99. https://doi.org/10.1016/j.toxlet.2010.10.019.

Coquette, A., Berna, N., Vandenbosch, A., Rosdy, M., De Wever, B., Poumay, Y., 2003. Analysis of interleukin-1alpha (IL-1alpha) and interleukin-8 (IL-8) expression and release in in vitro reconstructed human epidermis for the prediction of in vivo skin irritation and/or sensitization. Toxicol. in Vitro 17, 311–321. https://doi.org/10.1016/S0887-2333(03)00019-5.

Ehling, G., Hecht, M., Heusener, A., Huesler, J., Gamer, A.O., van Loveren, H., Maurer, T., Riecke, K., Ullmann, L., Ulrich, P., Vandebriel, R., Vohr, H.W., 2005. An European inter-laboratory validation of alternative endpoints of the murine local lymph node assay: first round. Toxicology 212, 60–68. https://doi.org/10.1016/j.tox.2005.04.010.

English, J., 2001. Current concepts in contact dermatitis. Br. J. Dermatol. 145, 527–529. https://doi.org/10.1136/oem.2003.010710.

Fluhr, J.W., Darlenski, R., Angelova-Fischer, I., Tsankov, N., Basketter, D., 2008. Skin irritation and sensitization: mechanisms and new approaches for risk assessment 1. Skin Irrit. Skin Pharmacol. Physiol. 21, 124–135. https://doi.org/10.1159/000131077.

Geier, J., Uter, W., Pirker, C., Frosch, P.J., 2003. Patch testing with the irritant sodium lauryl sulfate (SLS) is useful in interpreting weak reactions to contact allergens as allergic or irritant. Contact Dermatitis 48, 99–107. https://doi.org/10.1034/j.1600-0536.2003.480209.x.

Griffiths, C.E., Barker, J.N., Kunkel, S., Nickoloff, B.J., 1991. Modulation of leucocyte adhesion molecules, a T-cell chemotaxin (IL-8) and a regulatory cytokine (TNF-alpha) in allergic contact dermatitis (rhus dermatitis). Br. J. Dermatol. 124, 519–526. https://doi.org/10.1111/j.1365-2133.1991.tb04943.x.

Healy, S., Khan, P., Davie, J.R., 2013. Immediate early response genes and cell transformation. Pharmacol. Ther. 137, 64–77. https://doi.org/10.1016/j.pharmthera.2012.09.001.

Hitzler, M., Bergert, A., Luch, A., Peiser, M., 2013. Evaluation of selected biomarkers for the detection of chemical sensitization in human skin: a comparative study applying THP-1, MUTZ-3 and primary dendritic cells in culture. Toxicol. in Vitro 27, 1659–1669. https://doi.org/10.1016/j.tiv.2013.04.009.

Jia, Q., Zang, D., Yi, J., Dong, H., Niu, Y., Zhai, Q., Teng, Y., Bin, P., Zhou, W., Huang, X., Li, H., Zheng, Y., Dai, Y., 2012. Cytokine expression in trichloroethylene-induced hypersensitivity dermatitis: an in vivo and in vitro study. Toxicol. Lett. 215, 31–39. https://doi.org/10.1016/j.toxlet.2012.09.018.

Jin, S.H., Choi, D., Chun, Y.J., Noh, M., 2014. Keratinocyte-derived IL-24 plays a role in the positive feedback regulation of epidermal inflammation in response to environmental and endogenous toxic stressors. Toxicol. Appl. Pharmacol. 280, 199–206. https://doi.org/10.1016/j.taap.2014.08.019.

Kim, E.K., Choi, E.J., 2010. Pathological roles of MAPK signaling pathways in human diseases. Biochim. Biophys. Acta 1802, 396–405. https://doi.org/10.1016/j.bbadis.2009.12.009.

Kim, H.J., Lee, E., Lee, M., Ahn, S., Kim, J., Liu, J., Jin, S.H., Ha, J., Bae, I.H., Lee, T.R., Noh, M., 2018. Phosphodiesterase 4B plays a role in benzophenone-3-induced phototoxicity in normal human keratinocytes. Toxicol. Appl. Pharmacol. 338, 174–181. https://doi.org/10.1016/j.taap.2017.11.021.

Kurth, I., Willimann, K., Schaerli, P., Hunziker, T., Clark-Lewis, I., Moser, B., 2001. Monocyte selectivity and tissue localization suggests a role for breast and kidney-expressed chemokine (BRAK) in macrophage development. J. Exp. Med. 194, 855–861. https://doi.org/10.1084/jem.194.6.855.

Lee, E., Kim, H.J., Lee, M., Jin, S.H., Hong, S.H., Ahn, S., Kim, S.O., Shin, D.W., Lee, S.T., Noh, M., 2016. Cystathionine metabolic enzymes play a role in the inflammation resolution of human keratinocytes in response to sub-cytotoxic formaldehyde

exposure. Toxicol. Appl. Pharmacol. 310, 185–194. https://doi.org/10.1016/j.taap.2016.09.017.
Lim, Y.M., Moon, S.J., An, S.S., Lee, S.J., Kim, S.Y., Chang, I.S., Park, K.L., Kim, H.A., Heo, Y., 2008. Suitability of macrophage inflammatory protein-1beta production by THP-1 cells in differentiating skin sensitizers from irritant chemicals. Contact Dermatitis 58, 193–198. https://doi.org/10.1111/j.1600-0536.2007.01311.x.
Lu, J., Chatterjee, M., Schmid, H., Beck, S., Gawaz, M., 2016. CXCL14 as an emerging immune and inflammatory modulator. J. Inflamm. 13, 1. https://doi.org/10.1186/s12950-015-0109-9.
Meuter, S., Schaerli, P., Roos, R.S., Brandau, O., Bosl, M.R., von Andrian, U.H., Moser, B., 2007. Murine CXCL14 is dispensable for dendritic cell function and localization within peripheral tissues. Mol. Cell. Biol. 27, 983–992. https://doi.org/10.1128/MCB.01648-06.
Miyata, S., Matsuyama, T., Kodama, T., Nishioka, Y., Kuribayashi, K., Takeda, K., Akira, S., Sugita, M., 1999. STAT6 deficiency in a mouse model of allergen-induced airways inflammation abolishes eosinophilia but induces infiltration of CD8+ T cells. Clin. Exp. Allergy 29, 114–123. https://doi.org/10.1046/j.1365-2222.1999.00405.x.
Natsch, A., Emter, R., 2008. Skin sensitizers induce antioxidant response element dependent genes: application to the in vitro testing of the sensitization potential of chemicals. Toxicol. Sci. 102, 110–119. https://doi.org/10.1093/toxsci/kfm259.
Nestle, F.O., Di Meglio, P., Qin, J.Z., Nickoloff, B.J., 2009. Skin immune sentinels in health and disease. Nat. Rev. Immunol. 9, 679–691. https://doi.org/10.1038/nri2622.
Nukada, Y., Miyazawa, M., Kosaka, N., Ito, Y., Sakaguchi, H., Nishiyama, N., 2008. Production of IL-8 in THP-1 cells following contact allergen stimulation via mitogen-activated protein kinase activation or tumor necrosis factor-alpha production. J. Toxicol. Sci. 33, 175–185. https://doi.org/10.2131/jts.33.175.
OECD, 2010. Test guideline 429. In: Skin Sensitisation: Local Lymph Node Assay, . https://read.oecd-ilibrary.org/environment/test-no-429-skin-sensitisation_9789264071100-en#page1 (accessed July 23, 2010).
O'Shea, J.J., Schwartz, D.M., Villarino, A.V., Gadina, M., McInnes, I.B., Laurence, A., 2015. The JAK-STAT pathway: impact on human disease and therapeutic intervention. Annu. Rev. Med. 66, 311–328. https://doi.org/10.1146/annurev-med-051113-024537.
Park, H., Hwang, J.H., Han, J.S., Lee, B.S., Kim, Y.B., Joo, K.M., Choi, M.S., Cho, S.A., Kim, B.H., Lim, K.M., 2018a. Skin irritation and sensitization potential of oxidative hair dye substances evaluated with in vitro, in chemico and in silico test methods. Food Chem. Toxicol. 121, 360–366. https://doi.org/10.1016/j.fct.2018.09.017.
Park, J., Lee, H., Park, K., 2018b. Mixture toxicity of Methylisothiazolinone and propylene glycol at a maximum concentration for personal care products. Toxicol. Res. 34, 355–361. https://doi.org/10.5487/TR.2018.34.4.355.
Pfaffl, M.W., 2001. A new mathematical model for relative quantification in real-time RT-PCR. Nucleic Acids Res. 29, e45. https://doi.org/10.1093/nar/29.9.e45.
Proksch, E., Brandner, J.M., Jensen, J.M., 2008. The skin: an indispensable barrier. Exp. Dermatol. 17, 1063–1072. https://doi.org/10.1111/j.1600-0625.2008.00786.x.
Santinha, D.R., Doria, M.L., Neves, B.M., Maciel, E.A., Martins, J., Helguero, L., Domingues, P., Cruz, M.T., Domingues, M.R., 2013. Prospective phospholipid markers for skin sensitization prediction in keratinocytes: a phospholipidomic approach. Arch. Biochem. Biophys. 533, 33–41. https://doi.org/10.1016/j.abb.2013.02.012.
Schaerli, P., Willimann, K., Ebert, L.M., Walz, A., Moser, B., 2005. Cutaneous CXCL14 targets blood precursors to epidermal niches for Langerhans cell differentiation. Immunity 23, 331–342. https://doi.org/10.1016/j.immuni.2005.08.012.
Sehra, S., Bruns, H.A., Ahyi, A.N., Nguyen, E.T., Schmidt, N.W., Michels, E.G., von Bulow, G.U., Kaplan, M.H., 2008. IL-4 is a critical determinant in the generation of allergic inflammation initiated by a constitutively active Stat6. J. Immunol. 180, 3551–3559. https://doi.org/10.4049/jimmunol.180.5.3551.
Sehra, S., Yao, Y., Howell, M.D., Nguyen, E.T., Kansas, G.S., Leung, D.Y., Travers, J.B., Kaplan, M.H., 2010. IL-4 regulates skin homeostasis and the predisposition toward allergic skin inflammation. J. Immunol. 184, 3186–3190. https://doi.org/10.4049/jimmunol.0901860.
Shellenberger, T.D., Wang, M., Gujrati, M., Jayakumar, A., Strieter, R.M., Burdick, M.D., Ioannides, C.G., Efferson, C.L., El-Naggar, A.K., Roberts, D., Clayman, G.L., Frederick, M.J., 2004. BRAK/CXCL14 is a potent inhibitor of angiogenesis and a chemotactic factor for immature dendritic cells. Cancer Res. 64, 8262–8270. https://doi.org/10.1158/0008-5472.CAN-04-2056.
Son, D., Na, Y., Cho, W.S., Lee, B.H., Heo, Y., Park, J.H., Seok, S.H., 2013. Differentiation of skin sensitizers from irritant chemicals by interleukin-1alpha and macrophage inflammatory protein-2 in murine keratinocytes. Toxicol. Lett. 216, 65–71. https://doi.org/10.1016/j.toxlet.2012.10.017.
Suter, M.M., Schulze, K., Bergman, W., Welle, M., Roosje, P., Muller, E.J., 2009. The keratinocyte in epidermal renewal and defence. Vet. Dermatol. 20, 515–532. https://doi.org/10.1111/j.1365-3164.2009.00819.x.
Takahashi, T., Kimura, Y., Saito, R., Nakajima, Y., Ohmiya, Y., Yamasaki, K., Aiba, S., 2011. An in vitro test to screen skin sensitizers using a stable THP-1-derived IL-8 reporter cell line, THP-G8. Toxicol. Sci. 124, 359–369. https://doi.org/10.1093/toxsci/kfr237.
Willis, C.M., Young, E., Brandon, D.R., Wilkinson, J.D., 1986. Immunopathological and ultrastructural findings in human allergic and irritant contact dermatitis. Br. J. Dermatol. 115, 305–316. https://doi.org/10.1111/j.1365-2133.1986.tb05745.x.

Toxicology and Applied Pharmacology 338 (2018) 174–181

Contents lists available at ScienceDirect

Toxicology and Applied Pharmacology

journal homepage: www.elsevier.com/locate/taap

Phosphodiesterase 4B plays a role in benzophenone-3-induced phototoxicity in normal human keratinocytes

Hyoung-June Kim[a,1], Eunyoung Lee[b,c,1], Moonyoung Lee[b,c], Sungjin Ahn[b,c], Jungmin Kim[b,c], Jingjing Liu[b,c], Sun Hee Jin[b,c], Jaehyoun Ha[d], Il Hong Bae[a], Tae Ryong Lee[a], Minsoo Noh[b,c,*]

[a] Basic Research and Innovation Division, AmorePacific Corporation R&D Center, Yongin, Gyeounggi-do 17074, Republic of Korea
[b] College of Pharmacy, Seoul National University, Seoul 08826, Republic of Korea
[c] Natural Products Research Institute, Seoul National University, Seoul 08826, Republic of Korea
[d] Toxicology Division, IEC Korea, Suwon 17074, Republic of Korea

ARTICLE INFO

Keywords:
Phosphodiesterase 4B
Benzophenone-3
Phototoxicity
Normal human keratinocytes

ABSTRACT

Benzophenone-3 (BP-3), which is extensively used in organic sunscreen, has phototoxic potential in human skin. Phosphodiesterase 4B (PDE4B) has a well-established role in inflammatory responses in immune cells. Currently, it is unknown if PDE4B is associated with BP-3-induced phototoxicity in normal human keratinocytes (NHKs). We found that BP-3 significantly increased PDE4B expression in ultraviolet B (UVB)-irradiated NHKs. Notably, BP-8, a sunscreen agent that shares the 2-hydroxy-4-methoxyphenyl methanone moiety with BP-3, also upregulated PDE4B expression in NHKs. Upon UVB irradiation, BP-3 upregulated the expression of pro-inflammatory factors, such as prostaglandin endoperoxide synthase 2, tumor necrosis factor α, interleukin 8, and S100A7, and downregulated the level of cornified envelope associated proteins, which are important in the development of the epidermal permeability barrier. The additive effects of UVB-activated BP-3 on the expression of both pro-inflammatory mediators and cornified envelope associated proteins were antagonized by treatment with the PDE4 inhibitor rolipram. The BP-3 and UVB co-stimulation-induced PDE4B upregulation and its association with the upregulation of pro-inflammatory mediators and the downregulation of epidermal differentiation markers were confirmed in a reconstituted three dimensional human epidermis model. Therefore, PDE4B has a role in the mechanism of BP-3-induced phototoxicity.

1. Introduction

The broad spectrum ultraviolet (UV) absorber benzophenone-3 (BP-3), also known as oxybenzone or 2-hydroxy-4-methoxybenzophenone, is widely used in organic sunscreen to protect skin from sun-induced damage (Calafat et al., 2008). BP-3 is approved in most countries as a sunscreen ingredient for use in medicine, cosmetics, industry, and agriculture (Okereke et al., 1995). The US Food and Drug Administration (FDA) allows up to 6% BP-3 in over-the-counter sunscreen products (Wang and Lim, 2011). In 2008, the Scientific Committee on Consumer Safety of the European Commission concluded that up to 6% BP-3 is allowed in sunscreens (SCCP/1201/08, 2008). However, BP-3 is known to cause skin irritation and phototoxicity in the susceptible population (Collins and Ferguson, 1994; Landers et al., 2003).

Phototoxicity is defined as a toxic response to a substance that is elicited or increased after application to the body in response to apparently low dose UV or light exposure (Gaspar et al., 2013). A phototoxic substance absorbs excessive solar radiation energy, adpots a photoactivated state, and triggers pro-inflammatory responses in tissues causing direct cellular damage (Kim et al., 2015). UVB is the most harmful solar radiation that directly affects human skin (Afaq et al., 2009; Madduma Hewage et al., 2016). In human skin, epidermal keratinocytes have a pivotal role in the generation of a primary defensive barrier against environmental toxic stressors like UVB irradiation. Keratinocytes in the basal layer of the epidermis move upward and, ultimately, differentiate into cornified cells in the epidermal stratum corneum, thereby forming the epidermal permeability barrier (Elias et al., 2002; Feingold et al., 2007). Notably, various toxic stressors stimulate epidermal keratinocytes to produce pro-inflammatory mediators and cytokines that can affect the integrity of the epidermal permeability barrier (Proksch et al., 2008; Choi et al., 2011). Thus, epidermal keratinocytes are the major cellular target of the UVB-induced toxic effects of various contact irritants and allergens in human skin (Bernerd and Asselineau, 1997; Moravcova et al., 2013). Currently, the

* Corresponding author at: Natural Products Research Institute, College of Pharmacy, Seoul National University, 1 Gwanak-ro, Gwanak-gu, Seoul 08826, Republic of Korea.
E-mail addresses: minsoonoh@snu.ac.kr, minsoo@alum.mit.edu (M. Noh).
[1] These authors contributed equally to this work.

https://doi.org/10.1016/j.taap.2017.11.021
Received 6 October 2017; Received in revised form 23 November 2017; Accepted 24 November 2017
Available online 26 November 2017
0041-008X/

molecular and cellular mechanisms driving the phototoxic potential of BP-3 in human epidermal keratinocytes have not yet been fully elucidated.

Phosphodiesterase 4B (PDE4B) is highly expressed in immune cells and airway smooth muscle cells, and is known to regulate inflammatory responses (Wang et al., 1999; Jin and Conti, 2002; Jin et al., 2010). PDE4B inhibition results in accumulation of the intracellular second messenger cyclic adenosine monophosphate (cAMP), activation of protein kinase A (PKA), and the subsequent phosphorylation of transcription factors, such as cAMP-response element binding protein (CREB) (Wen et al., 2010; Komatsu et al., 2013) and activating transcription factor 1 (ATF1) (Mayr and Montminy, 2001). cAMP induces the phosphorylation of CREB and ATF1 (Gupta and Prywes, 2002; Wen et al., 2010). CREB and ATF1 are the phosphorylation-dependent transcription factors that regulate cell proliferation, differentiation and immune responses. UVB irradiation upregulates phosphorylation of CREB at serine 133 and ATR1 at serine 63 through a cAMP-dependent signaling pathway (Tang et al., 2001). In mammalian cells, UV irradiation also increased phosphorylation of histone H2AX and BRCA1 in response to UV-induced DNA damage (Ouchi, 2006; Oh et al., 2011). The human S100 calcium-binding protein A7 (*S100A7*, psoriasin) gene has been implicated in inflammation (Webb et al., 2005) and S100A7 mRNA and protein were upregulated in skin of volunteers exposed to UVB (Di Nuzzo et al., 2000).

In human epidermal keratinocytes, the role of PDE4B in the regulation of cutaneous inflammation is unknown. In the present study, we investigated if PDE4B was associated with the phototoxic mechanism of BP-3 in human epidermal keratinocytes. We evaluated if BP-3 affected PDE4B function in normal human keratinocytes (NHKs). In addition, we determined if BP-3-regulated PDE4B expression was associated with phototoxic responses in NHKs.

2. Materials and methods

2.1. Culture of NHKs and an artificial epidermis model

First-passage NHKs from neonatal foreskins were purchased and cultured in Keratinocyte Basal Medium (KBM) medium with Keratinocyte Growth Medium-2 (KGM™-2) supplements containing insulin, human epidermal growth factor, bovine pituitary extract, hydrocortisone, epinephrine, transferrin, and gentamicin/amphotericin B (Lonza, Basel, Switzerland). We used 3 NHK batches prepared from different donors and performed all experiments in triplicate. NHKs were serially passaged at 90% confluence, and third passage primary NHKs were used in the study. We used the reconstituted human epidermis model, EpiDerm™ (MatTek Corporation, Ashland, MA, USA). The EpiDerm™ samples were transferred to 6-well plates and maintained according to the manufacturer's recommendations (MatTek Corporation). After overnight culture at 37 °C in 5% CO_2, the samples were transferred to fresh medium and directly used in experiments. All sunscreen agents including BP-3 and rolipram were purchased from Sigma-Aldrich (St. Louis, MO, USA).

2.2. Cell viability test

To investigate the molecular mechanism of BP-3 and UVB co-treatment-induced effects on NHKs, sub-cytotoxic BP-3 and UVB conditions were determined. Cell viability was evaluated using a Cell Counting Kit-8 assay (CCK-8, Dojindo, Kumamoto, Japan) according to the manufacturer's instructions. NHKs cultured in 24-well plates up to 100% confluence were pretreated with BP-3 in KBM/KGM™-2 media immediately before experiments. UVB irradiation was performed with a Vilber Lourmat Bio-Sun instrument (Vilber Lourmat, Marne-la-Vallée, France). The UVB irradiation conditions were determined by the instrumental programmed software (Vilber Lourmat). The UVB spectral peak was set at 312 nm. In order to measure their viability, NHKs were incubated for the indicated times in KBM/KGM™-2 medium and washed 3 times with phosphate-buffered saline (PBS). The NHK cells were treated with 2-(2-methoxy-4-nitrophenyl)-3-(4-nitrophenyl)-5-(2,4-disulfophenyl)-2H-tetrazolium, monosodium salt (WST-8) solution from the CCK-8 assay (in PBS) and incubate for an additional 2 h. We measured the absorbance at 450 nm using a microplate reader (BioTek, Winooski, VT, USA).

2.3. Quantitative real-time reverse transcription-polymerase chain reaction

Total RNA was isolated using a TRIzol® reagent (Invitrogen, Carlsbad, CA, USA). RNA was further purified using the RNeasy Mini Kit (Qiagen, Germantown, MD, USA). The amount of total RNA was measured using a NanoDrop® ND-1000 spectrophotometer (NanoDrop Technologies, Montchanin, DE, USA). RNA integrity was verified with the Agilent 2100 Bioanalyzer (Agilent Technologies, Santa Clara, CA, USA). Total RNA (1 μg) from each sample was transcribed using SuperScript™ reverse transcriptase (Invitrogen). The expression levels of target mRNAs were quantified by quantitative real-time reverse transcription-polymerase chain reaction (qRT-PCR) using the Applied Biosystems®' 7500 Real Time PCR System (Applied Biosystems, Foster City, CA, USA). The TaqMan RT-PCR primer sets (Applied Biosystems) used in the RT-PCR were: PDE4B, Hs00963543_m1; prostaglandin-endoperoxide synthase 2 (*PTGS2*) Hs00153133_m1; tumor necrosis factor α (TNFα, *TNFA*) Hs00174128_m1; interleukin (IL)-8 (*IL8/CXCL8*), Hs00174103_m1; and vascular endothelial growth factor C (*VEGFC*), Hs00153458_ml. Human *GAPDH* (4333764F, Applied Biosystems) and *RPL14A* (Hs04194366_g1, Applied Biosystems) were used as control genes against which to normalize variations in the cDNA levels across different samples for the determination of mRNA levels in NHKs after treatment with commonly used sunscreen agents (Fig. 1A). Because *GAPDH* or *RPL14A* gene transcription levels were not affected by BP-3 treatment in NHKs, GAPDH mRNA level was used as a normalizer in other qRT-PCR measurements. Quantification of relative expression levels was performed using a mathematical model developed by Pfaffl (Pfaffl, 2001).

2.4. Enzyme-linked immunosorbent assay

The concentration of prostaglandin(PG) E_2, TNFα, IL-8, and VEGF in supernatants were measured using enzyme-linked immunosorbent assay (ELISA) kits (PGE_2 ELISA kit, Cayman Chemical, Ann Arbor, MI, USA; TNFα, IL-8 and VEGF ELISA kits, R&D Systems, Minneapolis, MN, USA). Conditioned medium samples from BP-3-treated NHKs were centrifuged for 5 min at 1000*g*, and the supernatants were diluted for use in the ELISAs.

2.5. Western blot analysis

Cells were lysed in RIPA buffer containing protease inhibitor cocktails (Sigma-Aldrich). The lysates were then subjected to centrifugation at 15,000*g* for 10 min, and the supernatants were used for protein expression analysis. Proteins (40 μg/well) were fractionated by sodium dodecyl sulfate-polyacrylamide gel electrophoresis (SDS-PAGE) and transferred to nitrocellulose membranes. The membranes were blocked with 5% skim milk in 10 mM Tris-HCl (pH 8.0), 150 mM NaCl, and 0.15% Tween®-20 (TBST) for 1 h at 24 °C, then probed overnight at 4 °C with anti-PDE4B (#PA1-31134, Thermo Fisher Scientific, Waltham, MA, USA), anti-phospho-CREB (#9198, Thermo Fisher Scientific), anti-CREB (#9197, Thermo Fisher Scientific), anti-keratin 1 (#PRB-149P, Covance, Dedham, MA, USA), anti-keratin 10 (#PRB-159P, Covance), anti-loricrin (#PRB-145P, Covance), anti-involucrin (#PRB-140C, Covance), anti-psoriasin (#47C1068, Abcam, Cambridge, UK), or anti-β-actin (sc-47,778, Santa Cruz Biotechnology, Dallas, TX, USA). The blots were washed thrice with TBST and incubated with horseradish peroxidase-conjugated goat anti-rabbit IgG (Bio-Rad, Richmond, CA,

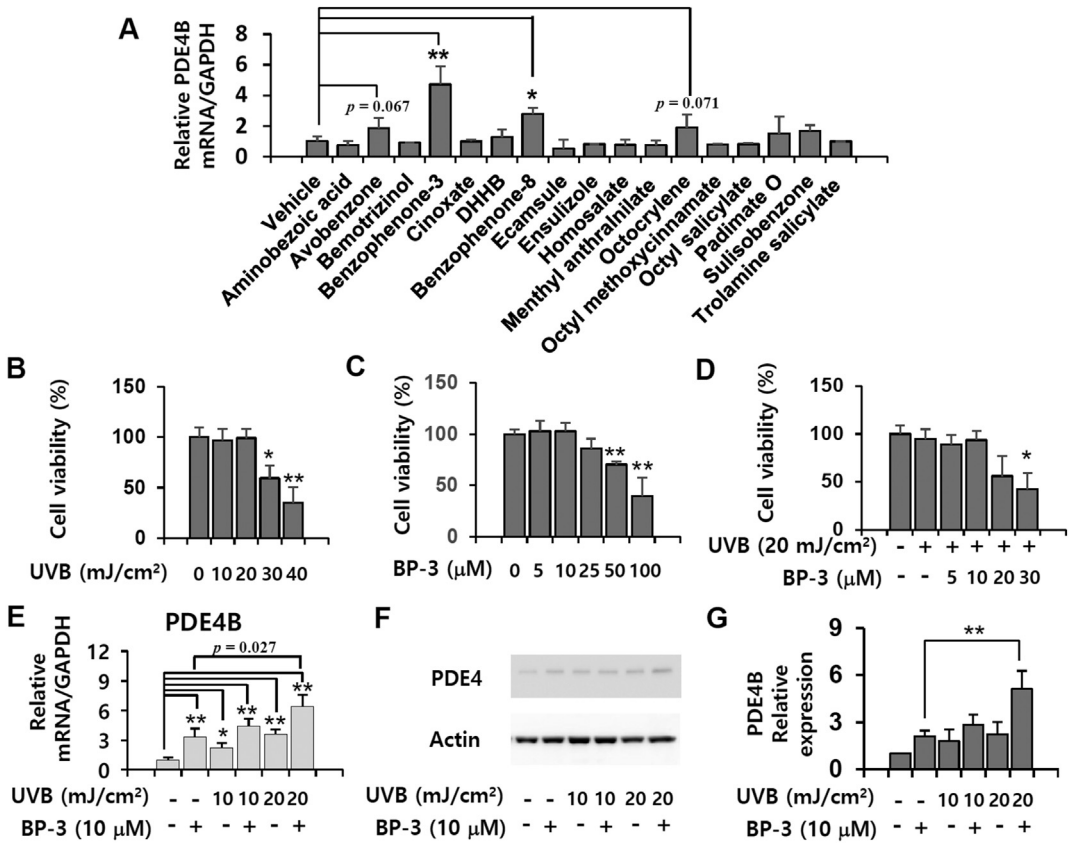

Fig. 1. Effects of UVB, BP-3 or UVB-activated BP-3 on PDE4B expression in NHKs. (A) To determine the mRNA levels of *PDE4B* in NHKs after treatment with commonly used sunscreen agents by qRT-PCR, total RNA samples were extracted from confluently cultured NHKs treated with test materials for 24 h. Cell viability was evaluated 24 h after treating NHKs with UVB (B), BP-3 (C), or both UVB and BP-3 (D) using a WST-8-based cytotoxicity assay. PDE4B mRNA (E) and protein levels (F) were measured by qRT-PCR and Western blotting, respectively, 24 h after NHKs were treated individually or with a combination of BP-3 and UVB. (G) Three independent PDE4 Western blotting results were quantified against β-actin using ImageJ software. Values represent the mean expression level ± SD (n = 3). $*p < 0.05$; $**p < 0.01$.

USA) at room temperature for 1 h. Detection was performed using the enhanced chemiluminescence (ECL) system (Invitrogen).

2.6. Immunohistochemical staining

To determine the effects of BP-3 in a 3-dimensional (3D) epidermis model, chemicals were topically applied to EpiDerm™ (MatTek Corporation) 30 min before UVB exposure. Twenty four hours after UVB irradiation, epidermal-equivalent specimens were cryopreserved (FSC 221, Leica Microsystems, Buffalo Grove, IL, USA) for frozen sectioning and sliced at a 6 μm thickness with a cryo-microtome (CM1950, Leica Instruments, Nussloch, Germany). Samples were incubated with primary antibodies against keratin-1 and keratin-10 (Novus Biologicals, Littleton, CO, USA) for 1 h at room temperature, then incubated with secondary rabbit AlexaFluor®488-conjugated secondary antibody (Abcam, Cambridge, UK) for 1 h at room temperature. All images were taken with a digital camera (DP72, Olympus, Tokyo, Japan).

2.7. Statistical analysis

Statistical analysis was conducted using SPSS® for Windows (SPSS Science, Chicago, IL, USA). The data were expressed as mean ± standard deviation (SD). Statistical analyses were performed using Student's *t*-test for comparison with the control. For multiple comparisons, statistical analysis was performed using one-way analysis of variance followed by Tukey's *post hoc* tests. *P*-values < 0.05 indicated statistical significance.

3. Results

3.1. BP-3 and UVB additively upregulated PDE4B gene transcription in NHKs

We first screened if commercially available sunscreen agents affected the transcription of *PDE4B* in NHKs (Fig. 1A). When NHKs were treated with 10 μM of each sunscreen agent for 24 h, BP-3 and BP-8 significantly upregulated *PDE4B* transcription by 4.71 and 2.27 fold, respectively, over the vehicle control. Avobenzone and octocrylene increased *PDE4B* expression by 1.85- and 1.88-fold, although the increases were not statistically significant. Therefore, we selected BP-3 to study the role of PDE4B in the phototoxic responses in NHKs caused by organic sunscreen agents. In order to study the toxicological mechanisms of BP-3-induced phototoxicity in NHKs, we determined the cell culture conditions under which there was no apparent cell death. The viability of UVB-treated NHKs was 56% and 42% in response to 30 and 40 mJ/cm^2, respectively (Fig. 1B). No apparent cytotoxicity was observed in NHKs irradiated with 20 mJ/cm^2 UVB. In the BP-3 treated NHKs, viability remained unaffected compared to the control for 24 h in culture up to a dose of 25 μM BP-3 (Fig. 1C). To study the combined effects of UVB and BP-3 under non-cytotoxic conditions, we evaluated the concentration-dependent cytotoxic effects of BP-3 on NHKs under a fixed dose of UVB irradiation (Fig. 1D). After 20 mJ/cm^2 UVB, 20 μM BP-3 decreased the viability of NHKs compared to the vehicle treatment. Therefore, we selected 20 mJ/cm^2 UVB and 10 μM BP-3 as the maximum treatment doses to investigate their combined effects on phototoxicity in NHKs. We found that the treatment with UVB alone upregulated the mRNA levels of *PDE4B* in NHKs in a dose-dependent

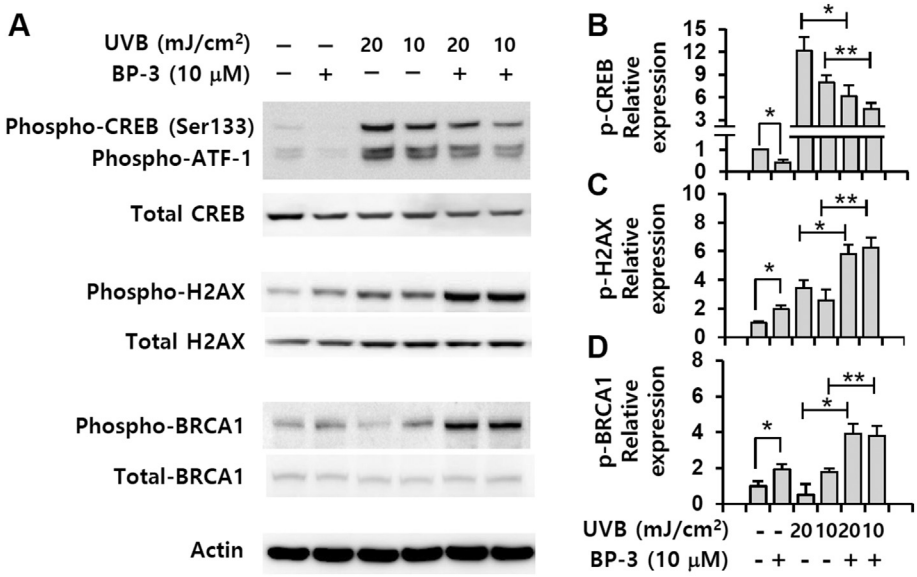

Fig. 2. Comparative phosphorylation profiles of cAMP-dependent transcription factors and UVB-dependent DNA damage biomarker proteins after BP-3 and/or UVB exposure. (A) Protein samples were prepared for Western blotting for phospho-CREB, phospho-ATF-1, total CREB, phospho-H2AX, total H2AX, phospho-BRCA1, and total BRCA1. Results for phospho-CREB (B), phospho-H2AX (C), and phospho-BRCA1 (D) were quantified relative to β-actin levels using ImageJ software (n = 3, independent experiments). Values represent the mean expression level ± SD. $^{*}p < 0.05$; $^{**}p < 0.01$.

manner (Fig. 1E). Importantly, we observed additive upregulation of *PDE4B* gene transcription in NHKs co-treated with UVB and BP-3 (Fig. 1E). In addition, PDE4B protein levels were synergistically upregulated in NHKs by co-treatment with both 10 μM BP-3 and 20 mJ/cm^2 UVB irradiation (Fig. 1F and G).

3.2. BP-3 downregulated intracellular cAMP signaling in UVB-irradiated NHKs

To investigate if the BP-3-induced PDE4B upregulation affected the cAMP intracellular signaling pathway, we compared the phosphorylation levels of CREB, H2AX, and BRCA1 in UVB-irradiated NHKs (Fig. 2). UVB-irradiation increased the levels of phospho-CREB and phospho-ATF1 over the levels in non-irradiated NHKs (Fig. 2A and B). In contrast, BP-3 decreased the phosphorylation of both CREB and ATF1 in NHKs regardless of UVB treatment, suggesting that the BP-3-induced PDE4B upregulation decreases the activation of cAMP-dependent transcription factors. Notably, UVB irradiation increased the levels of phospho-H2AX and phospho-BRCA1, which play a role in the major DNA damage responses induced by UV. Single treatment of BP-3 increased the phosphorylation of H2AX and BRCA1, which was different from the effect on phospho-CREB (Fig. 2C and D). BP-3 and UVB co-treatment did not change the level of either phospho-H2AX or phospho-BRCA1 in NHKs compared to those of UVB single treatments (Fig. 2C and D). These results suggested that BP-3 directly affected cAMP-dependent cellular pathways in NHKs, perhaps through PDE4B upregulation.

3.3. BP-3 and UVB increased PGE_2, TNFα, and IL-8 expression in NHKs

To investigate the combined effect of BP-3 and UVB-irradiation on NHKs, we measured the mRNA levels of major UVB-dependent pro-inflammatory factors such as *PTGS2*, *TNFA*, *IL8/CXCL8* and lymphangiogenic *VEGFC* (Fig. 3). Twenty-four hours after stimulation, treatment with 10 μM BP-3 alone significantly upregulated the transcription of *PTGS2*, *IL8/CXCL8*, and *VEGFC*. *TNFA* gene was not affected by the 10 μM BP-3 single treatment (Fig. 3B). When BP-3 was combined with UVB irradiation, the mRNA level of *PTGS2* was additively upregulated in NHKs treated with 10 and 20 mJ/cm^2 UVB-irradiation. The BP-3-dependent synergistic upregulation of *TNFA* and *IL8/CXCL8* transcription was observed in NHKs that received 20 mJ/cm^2 UVB-irradiation (Fig. 3C). We did not observe additive or synergistic upregulation of *VEGFC* transcription (Fig. 3D). Next, we measured the PGE_2, TNFα, IL-8, and VEGF accumulated in the cell culture supernatants over 24 h after stimulation with BP-3 and UVB. PGE_2, which is generated by PTGS2, was significantly increased by individual or co-treatment with BP-3 and UVB in NHKs (Fig. 3E). The protein concentrations of TNFα, IL-8, and VEGF in NHKs that received 20 mJ/cm^2 UVB-irradiation were significantly higher than those in the non-treated control (Fig. 3F–3H). BP-3-induced synergistic upregulation of TNFα and IL-8 was observed in the culture supernatants of NHKs that received 20 mJ/cm^2 UVB-irradiation whereas the effect on PGE_2 was additive by BP-3 and UVB. However, BP-3 did not additively increase VEGF production in UVB-irradiated NHKs (Fig. 3H). We sequentially profiled the expression of pro-inflammatory mediators in NHKs in response to various toxic stimuli, and found that PTGS2, TNFα, and IL-8 were expressed within 8 h of stimulation, whereas VEGFC expression was detectable approximately 24 h after stimulation (Bae et al., 2015a). BP-3 may differentially affect the UVB-irradiated NHKs in the early and delayed stages of inflammatory response. Taken together, these findings indicate that BP-3 increased PGE_2, TNFα, and IL-8 expression in UVB-irradiated NHKs.

3.4. BP-3 and UVB irradiation regulated the expression of epidermal differentiation markers in NHKs

Next, we investigated if BP-3 altered the expression of epidermal differentiation markers in UVB-irradiated NHKs (Fig. 4). In NHKs that received 20 mJ/cm^2 UVB-irradiation, the epidermal permeability barrier-associated proteins, keratin 1, keratin 10, loricrin and involucrin, were down-regulated in response to BP-3 (Fig. 4B–4E), indicating that BP-3 and UVB changed skin barrier integrity. Although 10 μM BP-3 alone did not change S100A7 protein expression in NHKs, BP-3 and UVB co-treatment synergistically increased S100A7 protein levels in NHKs compared to only UVB treatment (Fig. 4F). Notably, BP-3 and UVB irradiation synergistically downregulated the expression of loricrin and involucrin, major cornified envelope-associated proteins. In parallel, we also confirmed the additive upregulation of PDE4B protein expression by BP-3 and UVB stimulation (Fig. 4G) and the phosphorylation of both CREB and ATF-1.

3.5. The effects of BP-3 in UVB-irradiated NHKs were mediated by PDE4B

We used a pharmacological inhibitor of PDE4B, rolipram, to investigate if BP-3-induced PDE4B upregulation was associated with the regulation of pro-inflammatory factors and epidermal differentiation

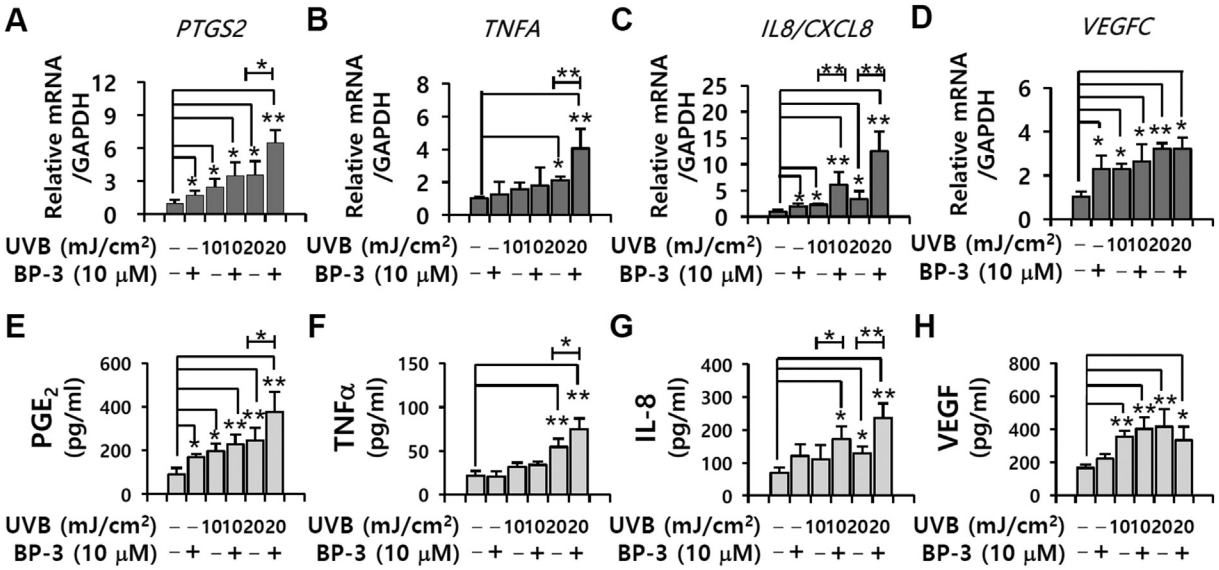

Fig. 3. The effects of UVB and BP-3 on NHK pro-inflammatory cytokine responses. Total RNA samples were prepared for qRT-PCR measurements of the mRNA levels of *PTGS2* (A), *TNFA* (B), *IL8/CXCL8* (C) and *VEGFC* (D). Values represent the mean expression level ± SD of the genes of interest relative to that of human GAPDH. In parallel, the concentrations of PGE_2 (E), TNFα (F), IL-8 (G) and VEGF (H) were measured by ELISA in the cell culture supernatants of NHKs treated with UVB and BP-3 for 24 h. Values represent the mean concentrations ± SD (n = 3). $*p < 0.05$; $**p < 0.01$.

markers. Rolipram treatment significantly attenuated the BP-3-induced downregulation of the skin barrier function-related epidermal differentiation markers, keratin 1, keratin 10, and loricrin in UVB-irradiated NHKs (Fig. 5A–5D). The BP-3-dependent upregulation of S100A7 in UVB-irradiated NHKs was also antagonized by rolipram (Fig. 5A and E). Furthermore, we confirmed the association of PDE4B with the effects of BP-3 and UVB on both the upregulation of pro-inflammatory mediators and the downregulation of epidermal differentiation markers, using a reconstituted 3D human epidermis model, EpiDerm™. In reconstituted 3D human epidermis (Lee et al., 2017), the pro-inflammatory mediators, PGE_2, TNFα, and IL-8, were additively upregulated by BP-3 and UVB co-treatment, and the upregulation was inhibited by the PDE4 inhibitor rolipram (Fig. 6A–6C). We observed additive downregulation of keratin 1 and keratin 10 by BP-3 and UVB co-treatment using immunohistochemistry (Fig. 6D). Rolipram also attenuated the decrease in keratin 1 and keratin 10 in the 3D human epidermis co-treated with BP-3 and UVB (Fig. 6E and F). We concluded that BP-3 induced PDE4B upregulation was associated with changes in the expression of pro-inflammatory and epidermal differentiation markers in NHKs.

4. Discussion

Phototoxicity is an undesirable skin response caused by the combined effects of light exposure and various external factors, such as

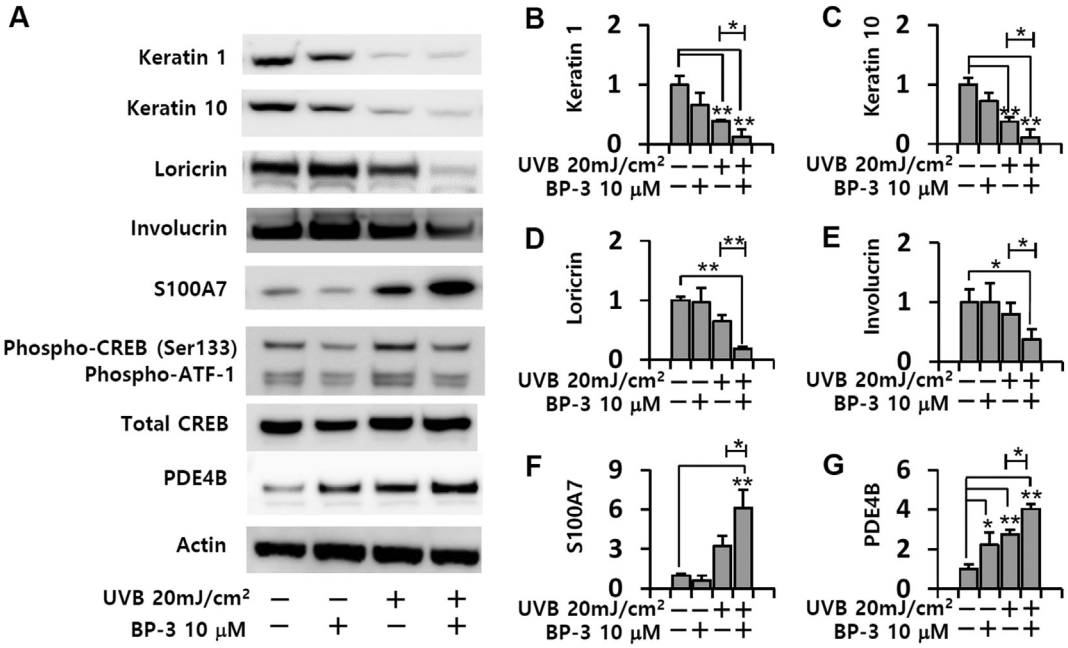

Fig. 4. The expression of cornified envelope-associated proteins in NHKs treated with UVB and BP-3. (A) Twenty four hours after treatment of NHKs with BP-3 and UVB, protein samples were prepared for Western blotting for keratin 1, keratin 10, loricrin, involucrin, S100A7, phospho-CREB, phospho-ATF-1, total CREB and PDE4B. Three independent results for keratin 1 (B), keratin 10 (C), loricrin (D), involucrin (E), S100A7 (F) and PDE4B (G) were quantified relative to β-actin levels by using ImageJ software. Values represent the mean expression level ± SD (n = 3). $*p < 0.05$; $** p < 0.01$.

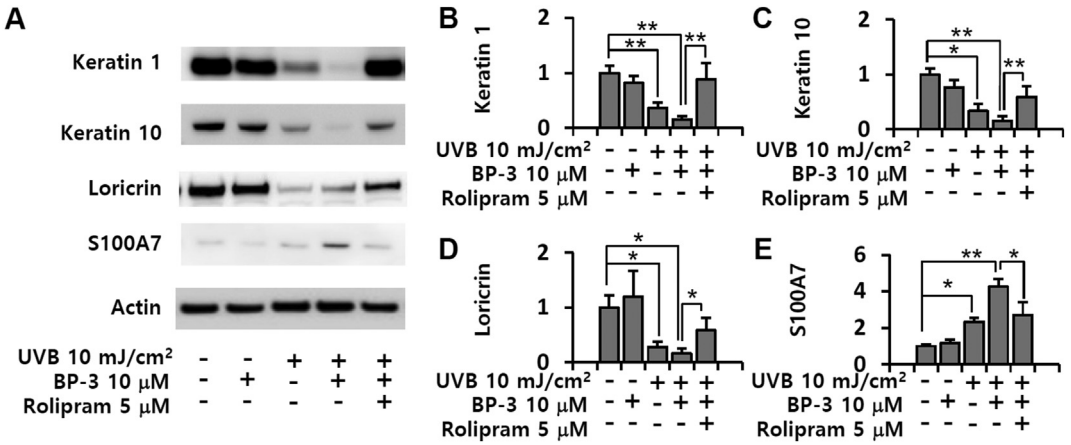

Fig. 5. The effect of PDE4 inhibitor rolipram on UVB-stimulated BP-3-induced responses in NHKs. NHKs were pre-treated with rolipram for 30 min before combined BP-3 and UVB treatment. Cells were treated or co-treated with UVB and BP-3 for 24 h. (A) Protein samples were prepared for Western blotting for keratin 1, keratin 10, loricrin, and S100A7. Three independent results for keratin 1 (B), keratin 10 (C), loricrin (D) and S100A7 (E) were quantified relative to β-actin levels by using ImageJ software. Values represent the mean expression level ± SD (n = 3). $*p < 0.05$; $**p < 0.01$.

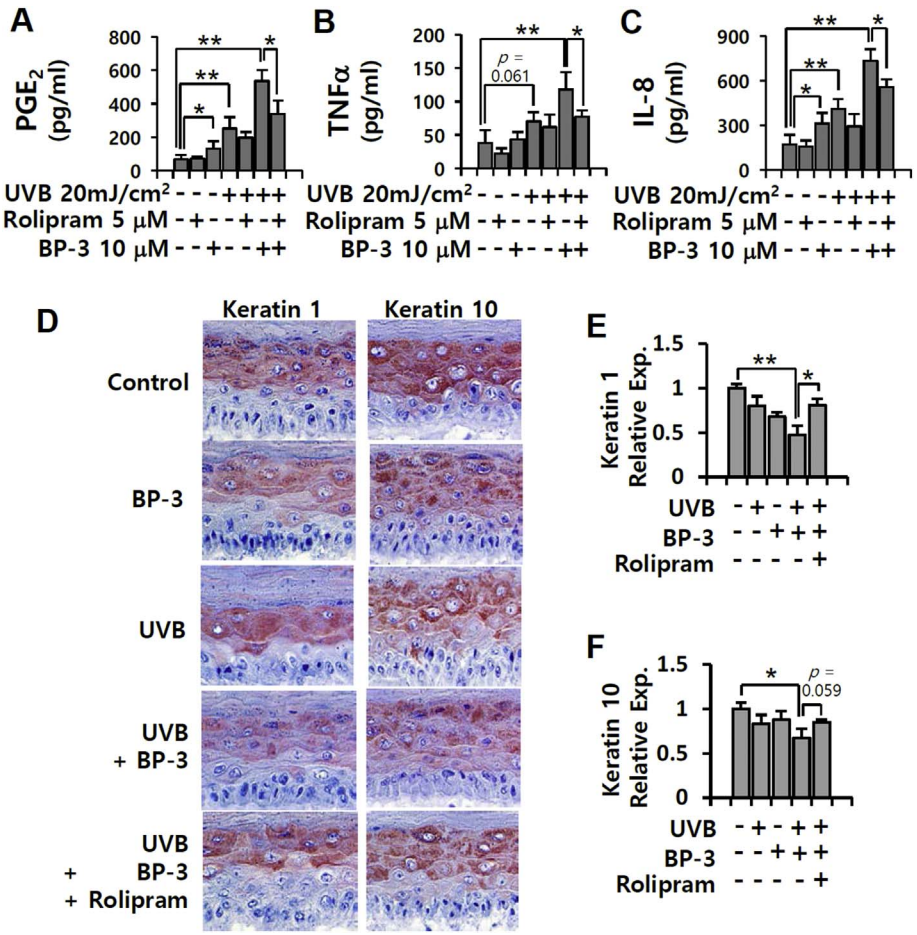

Fig. 6. Effects of PDE4 inhibitor rolipram on UVB-stimulated, BP-3-induced responses in a 3D reconstructed human epidermis model. BP-3 was topically applied to EpiDerm™ 30 min before UVB exposure. Twenty four hours after UVB irradiation, epidermal equivalent specimens and culture supernatants were analyzed. The levels of PGE_2 (A), TNFα (B) and IL8 (C) in the culture supernatants were measured by ELISA. (D) Red fluorescent dye-labeled antibodies against keratin 1 and keratin 10 were used for immunohistochemical staining. Results for keratin 1 (E) and keratin 10 (F) were quantified relative to β-actin levels using ImageJ software. Values represent the mean expression level ± SD. (n = 3). $*p < 0.05$; $**p < 0.01$. (For interpretation of the references to colour in this figure legend, the reader is referred to the web version of this article.)

drugs, cosmetics, and food components (Onoue et al., 2017). Although some phototoxic compounds are not intrinsically toxic without light exposure, photoactivation can trigger their toxicity. Among all phototoxic responses caused by topical personal care products, photoirritation and photoallergy are of the greatest toxicological interest. BP-3 has been widely used in sunscreen cosmetic products for many years to protect human skin against UVB irradiation (Rastogi, 2002). Topically applied BP-3 has photoallergenic potential in a portion of the human population (Lenique et al., 1992; Landers et al., 2003; Nedorost, 2003). Thus, in order to understand BP-3 phototoxicity, it is essential to elucidate how the combination of BP-3 and UVB irradiation affects the molecular and cellular processes of human epidermal keratinocytes.

UVB irradiation increased the intracellular cAMP levels and, subsequently, activated cAMP-dependent PKA promotes the phosphorylation of CREB and ATF-1 (Chun et al., 2007). UVB irradiation enhances the phosphorylation of H2AX and BRCA1, which are UV-induced DNA damage markers in mammalian cells (Podhorecka et al., 2010). We found that the BP-3-induced upregulation of PDE4B specifically

upregulated the phosphorylation of CREB and ATF-1 whereas it did not affect the phosphorylation of H2AX and BRCA1. PDE4B plays an important role in the regulation of pro-inflammatory responses by degrading the second messenger cAMP in inflammatory cells, endothelial cells, and keratinocytes (Chujor et al., 1998; Komatsu et al., 2013). In skin diseases like atopic dermatitis and psoriasis, cAMP responsiveness to adenylate cyclase-activating stimuli, such as epinephrine, histamine and PGE_2, is low (Mui et al., 1975; Hanifin, 1990; Hanifin et al., 1996). Reduced cAMP responsiveness is known to be associated with the upregulation of PDE4 activity in atopic dermatitis and psoriasis (Kumar et al., 2013). Notably, the pharmacological inhibition of cellular PDE4 activity decreases inflammatory responses in animal models for psoriasis and atopic dermatitis, suggesting that the elevation of intracellular cAMP in the epidermis inhibits pro-inflammatory pathways in skin (Akama et al., 2009). We previously reported that chemical allergens induced the transcriptional upregulation of pro-inflammatory mediators, such as PTGS2, TNFα, and IL-8 in NHKs (Bae et al., 2015a; Bae et al., 2015b). In combination with UVB irradiation, BP-3 additively or synergistically upregulated the expression of PTGS2, TNFα, and VEGFC; this effect was attenuated by treatment with the PDE4 inhibitor rolipram. Therefore, PDE4B appears to modulate pro-inflammatory responses in NHKs and human susceptibility to phototoxic dermatitis.

In human skin, environmental stresses, like chemical allergens and physical stresses, can affect the integrity of the epidermal permeability barrier (Proksch et al., 2008). Human epidermal keratinocytes differentiate to generate a skin permeability barrier, which is important as a physical defense mechanism to inhibit the penetration of various environmental toxic stimuli. Cornified envelope proteins are major components of this epidermal permeability barrier. Genetic mutations or polymorphisms in cornified envelope proteins such as filaggrin, loricrin, involucrin, keratin 1, and keratin 10 have pathophysiological associations with various inflammatory skin diseases like atopic dermatitis (Candi et al., 2005; Agrawal and Woodfolk, 2014). In addition, keratin 1 and keratin 10 participate in an inflammatory network that links barrier function to inflammation (Roth et al., 2012). The BP-3/UVB-induced additive or synergistic downregulation of major cornified envelope proteins that we observed may weaken the integrity of the epidermal permeability barrier, which would allow environmental toxins to more readily penetrate the epidermis than in homeostatic condition. Given that rolipram antagonized BP-3/UVB-mediated effects on epidermal differentiation markers essential to the epidermal barrier integrity, PDE4B also appears to play a pivotal role in this element of BP-3-induced phototoxicity.

Notably, BP-8 also significantly increased the gene transcription of PDE4B. BP-3 and BP-8 have a common 2-hydroxy-4-methoxyphenyl methanone moiety in their chemical structures. Although it did not reach statistical significance, avobenzone, reported as a photoallergen in various sunscreen agents (Scheuer and Warshaw, 2006), tended to increase PDE4B gene transcription in NHKs. Avobenzone, like BP-3 and BP-8, contains a methoxyphenyl group. In the future, we will investigate the role of the methoxyphenyl group in PDE4B-related phototoxicity in the standpoint of the structure-toxicity relationship.

Conflict of interest

Hyoung-June Kim, Il-Hong Bae and Tae Ryong Lee are employees of AmorePacific. Jaehyoun Ha is employee of IEC Korea Inc. The other authors have no conflicts of interest.

Acknowledgments

This study was partly supported by the Collaborative Genome Program for Fostering New Post-Genome Industry of the National Research Foundation (NRF) funded by the Ministry of Science and ICT (MSIT) (No. 2014M3C9A2064603), by NRF grant (2015R1A2A2A01008408), by a grant from the Korea Healthcare Technology R&D Project, Ministry of Health & Welfare (HN14C0088) and by the Promising-Pioneering Researcher Program through the Seoul National University in 2015.

References

Afaq, F., Zaid, M.A., Khan, N., Dreher, M., Mukhtar, H., 2009. Protective effect of pomegranate-derived products on UVB-mediated damage in human reconstituted skin. Exp. Dermatol. 18, 553–561.
Agrawal, R., Woodfolk, J.A., 2014. Skin barrier defects in atopic dermatitis. Curr Allergy Asthma Rep 14, 433.
Akama, T., Baker, S.J., Zhang, Y.K., Hernandez, V., Zhou, H., Sanders, V., Freund, Y., Kimura, R., Maples, K.R., Plattner, J.J., 2009. Discovery and structure-activity study of a novel benzoxaborole anti-inflammatory agent (AN2728) for the potential topical treatment of psoriasis and atopic dermatitis. Bioorg. Med. Chem. Lett. 19, 2129–2132.
Bae, O.N., Ahn, S., Jin, S.H., Hong, S.H., Lee, J., Kim, E.S., Jeong, T.C., Chun, Y.J., Lee, A.Y., Noh, M., 2015a. Chemical allergens stimulate human epidermal keratinocytes to produce lymphangiogenic vascular endothelial growth factor. Toxicol. Appl. Pharmacol. 283, 147–155.
Bae, O.N., Noh, M., Chun, Y.J., Jeong, T.C., 2015b. Keratinocytic vascular endothelial growth factor as a novel biomarker for pathological skin condition. Biomol. Ther. 23, 12–18.
Bernerd, F., Asselineau, D., 1997. Successive alteration and recovery of epidermal differentiation and morphogenesis after specific UVB-damages in skin reconstructed in vitro. Dev. Biol. 183, 123–138.
Calafat, A.M., Wong, L.Y., Ye, X., Reidy, J.A., Needham, L.L., 2008. Concentrations of the sunscreen agent benzophenone-3 in residents of the United States: National Health and Nutrition Examination Survey 2003–2004. Environ. Health Perspect. 116, 893–897.
Candi, E., Schmidt, R., Melino, G., 2005. The cornified envelope: a model of cell death in the skin. Nat. Rev. Mol. Cell Biol. 6, 328–340.
Choi, H., Shin, D.W., Kim, W., Doh, S.J., Lee, S.H., Noh, M., 2011. Asian dust storm particles induce a broad toxicological transcriptional program in human epidermal keratinocytes. Toxicol. Lett. 200, 92–99.
Chujor, C.S., Hammerschmid, F., Lam, C., 1998. Cyclic nucleotide phosphodiesterase 4 subtypes are differentially expressed by primary keratinocytes and human epidermoid cell lines. J. Invest. Dermatol. 110, 287–291.
Chun, K.S., Akunda, J.K., Langenbach, R., 2007. Cyclooxygenase-2 inhibits UVB-induced apoptosis in mouse skin by activating the prostaglandin E2 receptors, EP2 and EP4. Cancer Res. 67, 2015–2021.
Collins, P., Ferguson, J., 1994. Photoallergic contact dermatitis to oxybenzone. Br. J. Dermatol. 131, 124–129.
Di Nuzzo, S., Sylva-Steenland, R.M., Koomen, C.W., de Rie, M.A., Das, P.K., Bos, J.D., Teunissen, M.B., 2000. Exposure to UVB induces accumulation of LFA-1 + T cells and enhanced expression of the chemokine psoriasin in normal human skin. Photochem. Photobiol. 72, 374–382.
Elias, P.M., Ahn, S.K., Denda, M., Brown, B.E., Crumrine, D., Kimutai, L.K., Komuves, L., Lee, S.H., Feingold, K.R., 2002. Modulations in epidermal calcium regulate the expression of differentiation-specific markers. J. Invest. Dermatol. 119, 1128–1136.
Feingold, K.R., Schmuth, M., Elias, P.M., 2007. The regulation of permeability barrier homeostasis. J. Invest. Dermatol. 127, 1574–1576.
Gaspar, L.R., Tharmann, J., Maia Campos, P.M., Liebsch, M., 2013. Skin phototoxicity of cosmetic formulations containing photounstable and photostable UV-filters and vitamin A palmitate. Toxicol. in Vitro 27, 418–425.
Gupta, P., Prywes, R., 2002. ATF1 phosphorylation by the ERK MAPK pathway is required for epidermal growth factor-induced c-jun expression. J. Biol. Chem. 277, 50550–50556.
Hanifin, J.M., 1990. Phosphodiesterase and immune dysfunction in atopic dermatitis. J. Dermatol. Sci. 1, 1–6.
Hanifin, J.M., Chan, S.C., Cheng, J.B., Tofte, S.J., Henderson Jr., W.R., Kirby, D.S., Weiner, E.S., 1996. Type 4 phosphodiesterase inhibitors have clinical and in vitro anti-inflammatory effects in atopic dermatitis. J. Invest. Dermatol. 107, 51–56.
Jin, S.L., Conti, M., 2002. Induction of the cyclic nucleotide phosphodiesterase PDE4B is essential for LPS-activated TNF-alpha responses. Proc. Natl. Acad. Sci. U. S. A. 99, 7628–7633.
Jin, S.L., Goya, S., Nakae, S., Wang, D., Bruss, M., Hou, C., Umetsu, D., Conti, M., 2010. Phosphodiesterase 4B is essential for T(H)2-cell function and development of airway hyperresponsiveness in allergic asthma. J. Allergy Clin. Immunol. 126, 1252–1259.
Kim, K., Park, H., Lim, K.M., 2015. Phototoxicity: its mechanism and animal alternative test methods. Toxicol. Res. 31, 97–104.
Komatsu, K., Lee, J.Y., Miyata, M., Hyang Lim, J., Jono, H., Koga, T., Xu, H., Yan, C., Kai, H., Li, J.D., 2013. Inhibition of PDE4B suppresses inflammation by increasing expression of the deubiquitinase CYLD. Nat. Commun. 4, 1684.
Kumar, N., Goldminz, A.M., Kim, N., Gottlieb, A.B., 2013. Phosphodiesterase 4-targeted treatments for autoimmune diseases. BMC Med. 11, 96.
Landers, M., Law, S., Storrs, F.J., 2003. Contact urticaria, allergic contact dermatitis, and photoallergic contact dermatitis from oxybenzone. Am. J. Contact Dermat. 14, 33–34.
Lee, M., Hwang, J.H., Lim, K.M., 2017. Alternatives to in vivo draize rabbit eye and skin irritation tests with a focus on 3D reconstructed human cornea-like epithelium and epidermis models. Toxicol. Res. 33, 191–203.
Lenique, P., Machet, L., Vaillant, L., Bensaid, P., Muller, C., Khallouf, R., Lorette, G., 1992. Contact and photocontact allergy to oxybenzone. Contact Dermatitis 26, 177–181.
Madduma Hewage, S.R., Piao, M.J., Kang, K.A., Ryu, Y.S., Han, X., Oh, M.C., Jung, U.,

Kim, I.G., Hyun, J.W., 2016. Hesperidin attenuates ultraviolet B-induced apoptosis by mitigating oxidative stress in human keratinocytes. Biomol. Ther. 24, 312–319.
Mayr, B., Montminy, M., 2001. Transcriptional regulation by the phosphorylation-dependent factor CREB. Nat. Rev. Mol. Cell Biol. 2, 599–609.
Moravcova, M., Libra, A., Dvorakova, J., Viskova, A., Muthny, T., Velebny, V., Kubala, L., 2013. Modulation of keratin 1, 10 and involucrin expression as part of the complex response of the human keratinocyte cell line HaCaT to ultraviolet radiation. Interdiscip. Toxicol. 6, 203–208.
Mui, M.M., Hsia, S.L., Halprin, K.M., 1975. Further studies on adenyl cyclase in psoriasis. Br. J. Dermatol. 92, 255–262.
Nedorost, S.T., 2003. Facial erythema as a result of benzophenone allergy. J. Am. Acad. Dermatol. 49, S259–261.
Oh, K.S., Bustin, M., Mazur, S.J., Appella, E., Kraemer, K.H., 2011. UV-induced histone H2AX phosphorylation and DNA damage related proteins accumulate and persist in nucleotide excision repair-deficient XP-B cells. DNA Repair (Amst) 10, 5–15.
Okereke, C.S., Barat, S.A., Abdel-Rahman, M.S., 1995. Safety evaluation of benzophenone-3 after dermal administration in rats. Toxicol. Lett. 80, 61–67.
Onoue, S., Seto, Y., Sato, H., Nishida, H., Hirota, M., Ashikaga, T., Api, A.M., Basketter, D., Tokura, Y., 2017. Chemical photoallergy: photobiochemical mechanisms, classification, and risk assessments. J. Dermatol. Sci. 85, 4–11.
Ouchi, T., 2006. BRCA1 phosphorylation: biological consequences. Cancer Biol. Ther. 5, 470–475.
Pfaffl, M.W., 2001. A new mathematical model for relative quantification in real-time RT-PCR. Nucleic Acids Res. 29, e45.
Podhorecka, M., Skladanowski, A., Bozko, P., 2010. H2AX phosphorylation: its role in DNA damage response and cancer therapy. J. Nucleic Acids 2010. http://dx.doi.org/10.4061/2010/920161.
Proksch, E., Brandner, J.M., Jensen, J.M., 2008. The skin: an indispensable barrier. Exp. Dermatol. 17, 1063–1072.
Rastogi, S.C., 2002. UV filters in sunscreen products—a survey. Contact Dermatitis 46, 348–351.
Roth, W., Kumar, V., Beer, H.D., Richter, M., Wohlenberg, C., Reuter, U., Thiering, S., Staratschek-Jox, A., Hofmann, A., Kreusch, F., Schultze, J.L., Vogl, T., Roth, J., Reichelt, J., Hausser, I., Magin, T.M., 2012. Keratin 1 maintains skin integrity and participates in an inflammatory network in skin through interleukin-18. J. Cell Sci. 125, 5269–5279.
SCCP/1201/08, Scientific Committee on Consumer Safety, 2008. Opinion on Benzophenone-3. SCCP/1201/08, pp. 1e15. Available online at: http://ec.europa.eu/health/phrisk/committees/04_sccp/docs/sccp_o_159.pdf.
Scheuer, E., Warshaw, E., 2006. Sunscreen allergy: a review of epidemiology, clinical characteristics, and responsible allergens. Dermatitis 17, 3–11.
Tang, Q., Chen, W., Gonzales, M.S., Finch, J., Inoue, H., Bowden, G.T., 2001. Role of cyclic AMP responsive element in the UVB induction of cyclooxygenase-2 transcription in human keratinocytes. Oncogene 20, 5164–5172.
Wang, S.Q., Lim, H.W., 2011. Current status of the sunscreen regulation in the United States: 2011 Food and Drug Administration's final rule on labeling and effectiveness testing. J. Am. Acad. Dermatol. 65, 863–869.
Wang, P., Wu, P., Ohleth, K.M., Egan, R.W., Billah, M.M., 1999. Phosphodiesterase 4B2 is the predominant phosphodiesterase species and undergoes differential regulation of gene expression in human monocytes and neutrophils. Mol. Pharmacol. 56, 170–174.
Webb, M., Emberley, E.D., Lizardo, M., Alowami, S., Qing, G., Alfia'ar, A., Snell-Curtis, L.J., Niu, Y., Civetta, A., Myal, Y., Shiu, R., Murphy, L.C., Watson, P.H., 2005. Expression analysis of the mouse S100A7/psoriasin gene in skin inflammation and mammary tumorigenesis. BMC Cancer 5, 17.
Wen, A.Y., Sakamoto, K.M., Miller, L.S., 2010. The role of the transcription factor CREB in immune function. J. Immunol. 185, 6413–6419.